DESIGN OF NOVEL BIOLOGICALLY ACTIVE POLYMERS TO ENHANCE DRUG DELIVERY ACROSS EPITHELIAL BARRIERS

PHD THESIS

Karen Phelps, Bsc (Hons) Molecular Biology

The Centre for Polymer Therapeutics
Welsh School of Pharmacy,
King Edward VII Avenue,
Cardiff,
CF10 3XF.

This work is funded by the BBSRC

ProQuest LLC
789 East Eisenhower Parkway
P.O. Box 1346
Ann Arbor, MI 48106-1346

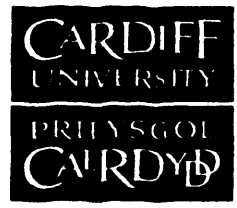

BINDING SERVICES
Tel +44 (0)29 2087 4949
Fax +44 (0)29 20371921
e-mail bindery@cardiff.ac.uk

To my Family!

ACKNOWLEDGEMENTS

To quote my writing-up buddy Siani 'you don't do a PhD you survive it', and it would have been hard to if it wasn't for the support of my friend's family and my supervisor Professor Ruth Duncan.

First of all I'd like to acknowledge my family, most notably parents, for all the laughs, cwtches and financial support, especially over the past year. Thanks dad 'Saint Chris' you're the greatest! Thanks mum for all the chats and Starbucks! Thanks Gadget for being the sweetest brother ever!

I'd like to thank my friends especially my 'sister' Ali, the Prothero's Abi and James, my Portsmouth sweetie Kerry, my 'schoolies' Sponna, Helen, Lyd, and 'the boys', especially my traveling buddy Marshy, Gremo, the best cwtcher in the world Big Tom, Shyam and Matthius for all the fun and nights out around Cardiff.

A huge thank you goes to my CPT colleagues, past and present. Sweet Vivian, Tina and Michelle for support with the animal work, Saly for the chats about anything and everything, Neal for making me laugh on a daily basis, Philipp and Dot for all the chats and for making me smile. Thanks to Myrto for being an inspiration in the lab, KaWai, and the ever hard-working, sweet Maria. Thanks to Sioned, Wendy and Alison for all the pistacio fights, glasses of vino and brilliant times in bar HAHA, always-efficient, sweet little feather-head Elaine, Kerri, the most fashionable girl ever Lucile, Lorella, Jing, Helena, Sam and the visiting students Sooze, Verena, Mari and vampire Jacopo. Thanks also to the lecturers in our group: Maya, Arwyn and Dirk, for always being approachable and so friendly. A massive thanks to Siani and Fran, the most thoughtful and generous people I've ever known - I hope I never lose touch with either of you! Thanks also to Fran's other-half Gian-luigi for the silly banter. Thanks to Tom for the useful advice when it came to lab, and for being a good friend over the years, and thanks to Zeena my super intelligent little warrior princess, who always gives good advice. I'd also like to thank Jan, the CPT lab manager, for advice with chemistry, for being a real people person, and for managing to sort out the problem out no matter how great. Thanks to Dr And and my neighbour Marieh for being my running buddies, and fantastic friends.

Finally thanks to Ruth for the advice, support and guidance, especially over the past few months. A big thanks also goes to my kind deputy supervisor Dr Mark Gumbleton, and once again to Wend for proof reading this thesis.

ABSTRACT

Numerous linear, water-soluble polymers (particularly polyanions) are biologically active and can induce cytokines such as tumour necrosis factor-alpha (TNF-α), interferon-gamma (IFN-γ) and interleukin-2 (IL-2) from cells depending on their molecular weight (MW), and composition. The proinflammatory cytokines TNF-α and IFN-γ are able to permeabilise epithelial barriers by affecting the protein composition of the tight junctions (TJ) (Walsh *et al.*, 2000). The aim of this work was to identify polymers that would promote enhanced drug delivery due to their inherent ability to stimulate TNF-α, IFN-γ and IL-2 release, and therefore transiently permeabilise epithelial barriers. Several linear polyanions already used as excipients, including alginate, hyaluronic acid (HA), and polyacrylic acids (PAcA; MW 30,000, 100,000, or 450,000 Da), were chosen as the first polymer library to investigate. Branched polymers including polyamidoamine (PAMAM) generation 3.5 dendrimers and the polycation polyethylenimine, PEI (MW 750,000 Da), were also studied.

Polyanions showed little cytotoxicity towards B16F10 cells and ECV304 cells at 72 h except PAcA of MW 100,000 Da in both cell lines, and 450,000 Da in B16F10. PEI was cytotoxic at low concentrations. Decreasing the incubation time to 1 h reduced polymer cytotoxicity (IC_{50} > 1 mg/mL) with the exception of PEI. Highest amounts of TNF-α, IL-2 and IFN-γ release from B16F10 and RAW 246.7 cells were seen with PEI (1 mg/mL). HA and HA sodium salt induced TNF-α release from DU937 cells in concentration-dependant manner. In transport studies, FITC-dextran transfer was greatest in the Ap→Bas direction, and in the absence of Peyer's patches. Cytokines had no significant effect on FITC-dextran transport, at either physiological or ng/mL concentrations. Polymers appeared to inhibit FITC-dextran transport in all directions and tissue types, though apically applied PAcA (MW 30,000 Da) and HA (1 mg/mL), showed some increase. This data was not significant. Lastly, PAcA (MW 30,000 Da) and PAMAM generation 3.5 dendrimers were labelled with OG cadaverine (OG_{cad}) to monitor their transport across rat intestinal tissue (with or without Peyer's patches) also using the vertical diffusion system. The uptake of the polymers into Caco-2_{BBe} cells (chosen as an enterocyte model) was investigated using flow cytometry. Fluorescently-labelled PAcA- (MW = 30,000 Da) and PAMAM-OG conjugates showed a greater rate of transport in the Bas→Ap direction. The conjugates did not appear to be taken up by Caco-2_{BBe} cells.

Although the scientific literature had suggested that certain polymers promote cytokine release, and that specific cytokines increase gastrointestinal permeability, it proved difficult here to validate the hypothesis that polymers might be designed to enhance transport in a reproducible and safe manner.

INDEX **PAGE**

Abstract i
List of Figures vi
List of Tables x
List of abbreviations xi
Appendix: List of publications

CHAPTER 1: General Introduction

1.1 Introduction 1
1.1.1 Biologically active polymers 4
1.2 The immune system 8
1.2.1 Innate immunity 8
1.2.2 Acquired immunity 9
1.3 Cytokines 11
1.3.1 Aberrant cytokine expression and disease 12
1.3.2 Cytokine therapy 14
1.4 Biologically active polymers as modulators for cytokine therapy 14
1.5 Biologically active polymers and cytokines as permeability enhancers 15
1.5.1 Structure and function of tight junctions (TJ) 18
1.5.2 Small intestine as a model epithelial barrier 21
1.5.3 Mucosal immune system 24
1.6 Rationale for the choice of polymers selected for these studies 25
1.61 Alginates 25
1.6.2 Hyaluronic acid 29
1.6.3 Polyacrylic acid (PAcA) 31
1.6.4 Polyamidoamine generation 3.5 dendrimers (PAMAM 3.5) 34
1.7 Biological rationale for the cytokines chosen for this work 35
1.7.1 Interferon-gamma (IFN-γ) 35
1.7.2 Interleukin-2 (IL-2) 38
1.7.3 Tumour necrosis factor-alpha (TNF-α) 40
1.8 Aims of this thesis 41

CHAPTER 2: Materials and General Methods

2.1 Materials 43

2.1.1 General chemicals 43

2.1.2 Polymers 43

2.1.3 Animals and cell lines 43

2.1.4 Reagents for tissue and cell culture 44

2.1.5 Cytokines and sandwich-ELISA kits 44

2.2 Equipment 44

2.2.1 General equipment 46

2.2.2 Analytical equipment 46

2.3 General methods 47

2.3.1 Cell culture 47

2.3.2 Measurement of cell growth curves using the MTT assay 49

2.3.4 Measuring polymer cytotoxicity using the MTT assay 54

2.3.5 Measuring cytokine release with sandwich- ELISA kits 56

2.3.6 Use of the vertical diffusion system to study transport across rat intestinal tissue 60

2.3.7 Measurement of tissue viability using the lactate dehydrogenase assay (LDH) 67

2.3.8 Gel permeation chromatography 68

2.3.9 Determination of lipopolysaccharide (LPS) contamination of polymer solutions 69

2.4 Statistics 69

CHAPTER 3: Investigating Polymer Cytotoxicity and Ability to Induce Cytokine Release from B16F10, RAW 246.7 and DU937 Cells

3.1 Introduction 71

3.2 Methods 75

3.2.1 Setting up MTT assays 77

3.2.2 Use of ELISA assays to monitor cytokine release 77

3.3 Results 79

3.3.1 Evaluation of polymer cytotoxicity by MTT assay 79

3.3.2 Establishing ELISA assays 79

3.3.3 Cytokine release from DU937 cells 87

3.3.4 Cytokine release from B16F10 and RAW 246.7 cells 87
3.4 Discussion 99

CHAPTER 4: Effect of TNF-α, IFN-γ and IL-2 on FITC-dextran Transport Across Rat Intestinal Tissue
4.1 Introduction 107
4.2 Methods 112
4.2.1 Characterisation of FITC-dextran 113
4.2.2 Evaluation of FITC-dextran transport in the presence of cytokines using the vertical diffusion system 114
4.2.3 FITC-dextran stability during incubation in the vertical diffusion system 115
4.2.4 Use of the LDH assay to measure tissue viability 115
4.3 Results 116
4.3.1 Properties of FITC-dextran batches and their stability 116
4.3.2 Establishment of the vertical diffusion system 116
4.3.3 Transport of FITC-dextran across rat intestinal tissue in the vertical diffusion system 116
4.3.4 Stability of FITC-dextran during incubation 124
4.3.5 Effect of cytokines on FITC-dextran transport across rat intestinal tissue with or without Peyer's patches 128
4.3.6 Effect of high concentrations of rTNF-α and IFN-γ on FITC-dextran transport 132
4.4 Discussion 137

CHAPTER 5: Effect of Polymers on FITC-dextran Transport Across Rat Intestinal Tissue
5.1 Introduction 145
5.2 Methods 150
5.2.1 Effect of polymers on the pH of tissue culture media 150
5.2.2 Effect of pH on FITC-dextran flourescence 151
5.2.3 Effect of polymers on FITC-dextran transport across rat intestinal tissue using the vertical diffusion system 152
5.3 Results 152

5.3.1 Effect of polymers on MEM pH 152
5.3.2 Effect of pH on FITC-dextran fluorescence 152
5.3.3 Effect of polymers on FITC-dextran transport across rat intestinal tissue 155
5.4 Discussion 161

CHAPTER 6: Synthesis and Characterisation of $PAcA_{30}$–OG and PAMAM 3.5-OG Conjugates, and Studies on their Transport Across Rat Intestinal Tissue and Uptake by Caco-2_{BBe} Cells
6.1 Introduction 170
6.2 Methods 174
6.2.1 Conjugation of Oregon green-cadaverine to polymers 174
6.2.2 TLC method 175
6.2.3 Purification and lyophilisation of polymer-OG conjugates 175
6.2.4 Characterisation of polymer-OG conjugates 176
6.2.5 Analysis of polymer-OG_{cad} transport across rat intestinal tissue using the vertical diffusion system 177
6.2.6 Flow cytometry of polymer-OG uptake by Caco-2_{BBe} cells 177
6.3 Results 179
6.3.1 Synthesis and characterisation of polymer-OG conjugates 179
6.3.2 Polymer-OG transport across rat intestinal tissue in the vertical diffusion system 179
6.3.3 $PAcA_{30}$-OG_{cad} uptake by Caco-2_{BBe} cells 191
6.4 Discussion 191

CHAPTER 7: General Discussion
7.1 General comments 199
7.2 Thoughts regarding the methods used and future experiments 203
7.3 Will the use of biologically active polymers ever be safe enough?? 204
7.4 Final thoughts 205

BIBLIOGRAPHY 207

LIST OF FIGURES

CHAPTER 1

Figure 1.1 Time-scale tracking the development of polymers as nanomedicines
Figure 1.2 Schematic showing the EPR effect within tumour tissue
Figure 1.3 Immune response
Figure 1.4 Cytokines & epithelial permeability
Figure 1.5 Protein components of the TJ
Figure 1.6 Physiology of the rat gastrointestinal tract
Figure 1.7 Histology of the small intestine
Figure 1.8 A Peyer's patch in the small intestine
Figure 1.9 Chemical structure & conformation of alginates
Figure 1.10 Hyaluronic acid
Figure 1.11 Chemical structure of PAcA
Figure 1.12 Molecular structure of the PAMAM generation 3.5 dendrimer

CHAPTER 2

Figure 2.1 Structure of MTT before & after reduction by respiring cells
Figure 2.2 Growth curves: B16F10, ECV304, RAW 246.7, Caco-2_{BBe}, U937 cells
Figure 2.3 Protocol for ELISA
Figure 2.4 Calibration curves observed for hTNF-α & hIL-2
Figure 2.5 Calibration curves observed for mTNF-α, mIFN-γ & mIL-2
Figure 2.6 Vertical diffusion cell & the vertical diffusion system
Figure 2.7 Preparation of tissue for the vertical diffusion system
Figure 2.8 Chromatogram & calibration curve for polysaccharide standards

CHAPTER 3

Figure 3.1 Chemical structures of PEI & dextran
Figure 3.2 Effects of LPS on macrophage cells
Figure 3.3 Effect of sHA on DU937 cell viability (24 h)
Figure 3.4 Effect of PEI & dextran on B16F10 & ECV304 cell viability (72h)
Figure 3.5 Effect of polysaccharides on B16F10 & ECV304 cell viability (72 h)
Figure 3.6 Effect of PAcAs on B16F10 & ECV304 cell viability (72 h)
Figure 3.7 Effect of PAMAM 3.5 on B16F10 & ECV304 cell viability (72 h)

Figure 3.8 Effect of polymers on the recovery of mTNF-α from culture media

Figure 3.9 Effect of PEI on the calibration curve observed for the mTNF-α

Figure 3.10 Effect of HA concentration & incubation time on hTNF-α release from DU937 cells

Figure 3.11 Effect of alginate on hTNF-α rlease from DU937 cells (24 h)

Figure 3.12 Effect of $sPAcA_{30}$ on hTNF-α rlease from DU937 cells (24 h)

Figure 3.13 Effect of PAMAM 3.5 on hTNF-α from DU937 cells (24 h)

Figure 3.14 Effect of polymers on mTNF-α release from B16F10 & RAW 246.7 cells (1 h)

Figure 3.15 Effect of polymers on mIFN-γ release from B16F10 & RAW 246.7 cells (1 h)

Figure 3.16 Effect of polymers on mIL-2 release from B16F10 & RAW 246.7 cells (1 h)

Figure 3.17 Effect of HA on mTNF-α release from RAW 246.7 cells (0 - 24 h)

CHAPTER 4

Figure 4.1 Chemical structure of FITC-dextran

Figure 4.2 Molecular weight and polydispersity of FITC-dextran batches

Figure 4.2 Molecular weight and polydispersity of FITC-dextran after storage

Figure 4.3 Fluorescence output of different FITC-dextran batches

Figure 4.4 Fluorescence output of FITC-dextran after storage

Figure 4.5 Photomicrographs of rat intestinal tissue

Figure 4.6 LDH release from rat intestinal tissue in the vertical diffusion system

Figure 4.7 FITC-dextran transport across rat intestinal Peyer's patch tissue

Figure 4.8 FITC-dextran transport across rat intestinal tissue with Peyer's patches

Figure 4.9 Elution profile of FITC-dextran fractions from a PD-10 column

Figure 4.10 Effect of rTNF-α on FITC-dextran transport across rat intestinal tissue

Figure 4.11 Effect of rIFN-γ on FITC-dextran transport across rat intestinal tissue

Figure 4.12 LDH release from rat intestinal tissue

Figure 4.13 Effect of rIL-2 on FITC-dextran transport across rat intestinal tissue

Figure 4.14 Effect of rTNF-α (ng/mL) on FITC-dextran transport across rat intestinal tissue

Figure 4.15 Effect of rIFN-γ (ng/mL) on FITC-dextran transport across rat

intestinal tissue

Figure 4.16 Effect of rTNF-α & rIFN-γ (ng/mL) on FITC-dextran transport across rat intestinal tissue

Figure 4.17 Levels of FITC-dextran transported across rat intestinal tissue at t = 60 min

CHAPTER 5

Figure 5.1 Fluorescence output of FITC-dextran in different pH buffers

Figure 5.2 FITC-dextran transport across rat intestinal tissue with or without Peyer's patches

Figure 5.3 Effect of alginate, HA & sHA on Ap→Bas FITC-dextran transport across rat intestinal tissue

Figure 5.3 Effect of PAcAs on Ap→Bas FITC-dextran transport across rat intestinal tissue

Figure 5.3 Effect of PAMAM 3.5 on Ap→Bas FITC-dextran transport across rat intestinal tissue

Figure 5.4 Effect of alginate, HA & PAcA on Bas→Ap FITC-dextran transport across rat intestinal tissue with Peyer's patches (PP)

Figure 5.5 Effect of alginate, HA & $sPAcA_{30}$ on Ap→Bas FITC-dextran transport across rat intestinal tissue with PPs

Figure 5.6 Effect of alginate, HA & PAcA on Bas→Ap FITC-dextran transport across rat intestinal tissue with PPs

Figure 5.7 Possible effects of polymers on FITC-dextran transport across rat intestinal tissue

CHAPTER

Figure 6.1 Reaction scheme for polymer conjugation to OG_{cad} using EDC & sulfo-NHS coupling reagents

Figure 6.2 TLC plates showing $PAcA_{30}$-OG conjugation

Figure 6.3 PD-10 elution profile of $PAcA_{30}$-OG before & after dialysis

Figure 6.4 TLC plates showing PAMAM 3.5-OG conjugation

Figure 6.5 PD-10 elution profile of PAMAM 3.5-OG before & after dialysis

Figure 6.6 UV/Vis spectra for $PAcA_{30}$-OG & PAMAM 3.5-OG

Figure 6.7 Fluorescence spectrums of $PAcA_{30}$-OG & PAMAM 3.5-OG

Figure 6.8 $PAcA_{30}$-OG transport across rat intestinal tissue with or without PP

Figure 6.9 PAMAM 3.5-OG transport across rat intestinal tissue with or without PP

Figure 6.10 PD-10 elution profile: $PAcA_{30}$-OG stock solution, donor & recipient chambers at t = 60 min

Figure 6.11 PD-10 elution profiles: PAMAM 3.5-OG stock solution, donor & recipient chambers at t = 60 min

Figure 6.12 $PAcA_{30}$-OG & FITC-dextran uptake by Caco-2_{BBe} cells over 60 min

Figure 6.13 Possible transport mechanisms of polymer-OG conjugates

LIST OF TABLES

CHAPTER 1

Table 1.1 Polymers with immunomodulatory or other biological properties

Table 1.2 Immunological properties of the polymers chosen for this work

CHAPTER 2

Table 2.1 Tissue culture media and passage numbers of each cell line used

Table 2.2 Dilutions made to establish polymer cytotoxcity

Table 2.3 Protocol for R&D Systems human ELISA kits

Table 2.4 Protocol for R&D Systems murine ELISA kits

CHAPTER 3

Table 3.1 Effect of polymers on the pH of medium

Table 3.2 Summary of the IC_{50} values observed

Table 3.3 Summary of IC_{50} values from literature

Table 3.4 Cytokines produced by the cells chosen for this work

CHAPTER 4

Table 4.1 Papp values of paracellular markers across the rat intestine

CHAPTER 5

Table 5.1 Recipe for citric acid-sodium citrate buffer

Table 5.2 Effect of polymers on tissue culture media pH

Table 5.3 Effect of polymers on FITC-dextran transport across rat intestinal tissue

CHAPTER 6

Table 6.1 Characteristics of polymer-OG conjugates

ABBREVIATIONS

AIDS:	Acquired immunodeficiency syndrome
ANOVA:	Analysis of variance
Ap→Bas:	Apical to basal
AP-1:	Activation protein-1
AP-6:	Activation protein-6
APC:	Antigen presenting cell
ATP:	Adenosine triphosphate
Bas→Ap:	Basal to apical
B-cells:	B-lymphocytes
BPI:	Bactericidal/ permeability increasing protein
BSA:	Bovine serum albumin
Ca^{2+}:	Calcium ions
CAR:	Coxsackievirus and adenovirus receptor
CD:	Crohn's disease
CD14:	Cluster designation 14
CD28:	Cluster designation 28
CD4:	Cluster designation 4
$CD4^{+}$:	Cluster designation 4 positive cells
CD44:	Cluster designation 44
CD8:	Cluster designation 8
$CD8^{+}$:	Cluster designation 8 positive cells
CMC:	Cyclohexyl-3-(2-morpholinoethyl) carbodiimide
c-Met:	Proto-oncogene that encodes for a tyrosine kinase receptor
CpG:	Cystosine and guanine nucleotides
CSF:	Colony stimulatory factor
C-terminal:	Carboxy terminal
CYP3A:	Cytochrome P450 3A
d:	Days
Da:	Daltons
DCC:	Dicyclohexy carodiimide
DIVEMA:	Divinyl ether malic anhydride
DMEM:	Dulbecco's minimal essential media
DMSO:	Dimethyl sulphoxide

DNA:	Deoxyribonucleic acid
EDC:	1-Ethyl-3-(3-dimethylaminopropyl)-carbodiimide
EDTA:	Ethylenediaminetetraaceticacid
EGF:	Epidermal growth factor
EI:	Endocytic index
ELISA:	Enzyme-linked immunosorbent assay
EPO:	Erythroprotein
EPR:	Enhanced permeability and retention effect
EU:	Endotoxin units
F-actin:	Filamentous actin
FBS:	Foetal bovine serum
FDA:	Food and drug agency
FITC:	Fluorescien isothiocyanate
G:	α-L-guluronate monomer
GALT:	Gut-associated lymphoid tissue
G-CSF:	Granulocyte-colony stimulating factor
GI:	Gastrointestinal
GK:	Guanylate kinase
GPC:	Gel permeation chromatography
h:	Hours
HA:	Hyaluronic acid
HAS:	Hyaluronic acid synthases
HBSS:	Hank's balanced salt solution
HCI:	Hydrochloric acid
HEPES:	N-(-2-hydroxyethyl)piperazine-N'-(2-ethanesulfonic acid)
HGF:	Hepatocyte growth factor
hIL-2	Human interleukin-2
HIV1:	Human immunodeficiency virus type 1
HPMA:	N-(2-hydroxypropyl)methycrylamide
HPV:	Human papiloma virus
hTNF-α:	Human tumour necrosis factor-alpha
IBD:	Inflammatory bowel disease
IC_{50}:	Inhibitory concentration 50
ICAM:	Intercellular adhesion molecule

IFN-β	Interferon-beta
IFN-γ:	Interferon-gamma
IFN-α:	Interferon-alpha
Ig:	Immunoglobulin (synonym for antibody)
IGF:	Insulin-like growth factor
IgG:	Immunoglobulin G
Ig-HRP	Immunoglobulin-horse radish peroxidase
IL10:	Interleukin-10
IL-12:	Interleukin-12
IL-13:	Interleukin-13
IL-15:	Interleukin-15
IL-2:	Interleukin-2
IL-2R:	Interleukin-2 receptor
IL-4:	Interleukin-4
IL-6:	Interleukin-6
IL-8:	Interleukin-8
IRE:	Interferon response element
IRS:	Interferon response sequences
ISRE:	Interferon-stimulated response elements
JAK/STAT:	Janus kinase/signal activators of transcription
JAM:	Junctional adhesion molecule
JAM-A:	Junctional adhesion molecule-A
LAL:	Limulus amoebocyte lysate
LBP:	LPS-binding protein
LDH:	Lactate dehydrogenase
LPS:	Lipopolysaccharide
M:	β-D-mannuronate monomer
MAGUK:	Membrane associated guanylate kinase homologues
M-CAF:	Monocyte-chemotactic and activating factor
M-cells:	Membranous cells
M-CSF:	Macrophage-colony stimulating factor
MEM:	Minimal essential media
mg/mL:	Miligrams per mililitre
MHC:	Major histocompatibility complex

MHRA:	Medical and health care regulatory agency
mIFN-γ:	Murine interferon-gamma
mTNF-α:	Murine tumour necrosis factor-alpha
MTT:	3-[4,5-Dimethylthiazol-2-yl]-2,5-diphenyl-tetrazolium bromide
MUPP1:	Multi-PDZ-domain protein
MW:	Weight average molecular weight
NAD:	Nicotimanamide adenine dinucleotide
NADH:	Nicotimanamide adenine dinucleotide (reduced form)
NADPH:	Nicotimanamide adenine dinucleotide phosphate (reduced form)
NaOH:	Sodium hydroxide
ND:	Not determined
NES:	Nuclear export signals
NFAT:	Nuclear factor for activated T-cells
NF-kB:	Nuclear factor kappa B
ng:	Nanogram
ng/mL:	Nanogram/militre
NK:	Natural killer cell
nm:	Nanometre
NS:	Non significant
OG:	Oregon green
OG_{cad}:	Oregon green-cadaverine
PAcA:	Polyacrylic acid
$PAcA_{100}$:	Polyacrylic acid (MW = 100,000 Da)
$PAcA_{450}$:	Polyacrylic acid (MW = 450,000 Da)
PAMAM 3.5:	Polyamidoamine generation 3.5 dendrimers
PAMAM:	Polyamidoamine dendrimers
Papp	Apparent permeability coefficient
PATJ:	PALS1-associated tight junction protein
PBS:	Phosphate buffered saline
PD-10:	Protein desalting column 10
PDI:	Polydispersity index
PDZ:	PSD95/disc large/ZO-1
PEG:	Polyethyleneglycol
PEI:	Polyethylenimine

pg:	Picogram
pg/mL:	Picograms per mililitre
P-gp:	P-glycoprotein
pH:	Measure of acidity or alkalinity of a solution
PK1:	Prague-Keele 1
PK2:	Prague-Keele 2
pKa:	Negative logarithum of the acid dissociation constant, Ka
PMA:	Phorbol 12-myristate 13-acetate
PVP:	Polyvinylpyrrolidone
RHAMM:	Receptor for hyaluronic acid mediated motility
RI:	Refractive index
rIFN-γ:	Rat interferon-gamma
rIL-2:	Rat interleukin-2
RNA:	Ribonucleic acid
RPMI:	Rose Park Memorial Institute
rTNF-α:	Rat tumour necrosis factor-alpha
SCF:	Stem cell factor
SD:	Standard deviation
SEC:	Size exclusion chromatography
SEM:	Standard error of the mean
SH3:	Src homology 3 domain
sHA:	Hyaluronic acid, sodium salt
$sPAcA_{30}$:	PAcA (MW = 30,000 Da), sodium salt
sulfo-NHS:	N-hydroxysulfosuccinimide
T-cells:	T-lymphocytes
TCF-8:	Transcription factor 8 (represses IL-2 expression)
TEER:	Transepithelial electrical resistance
TGF-β:	Transforming growth factor-beta
TJ:	Tight junctions
TLC:	Thin layer chromatography
TLR 2:	Toll like receptor 2
TLR 4:	Toll like receptor 4
TNF-β:	Tumour necrosis factor-beta
TNF-α:	Tumour necrosis factor-alpha

TNF-R1:	Tumour necrosis factor receptor-1
TNF-R2:	Tumour necrosis factor receptor-2
TRAFs:	Tumour necrosis factor receptor associated transcription factors
Tris:	Tris(hydroxymethyl)aminomethane
U:	Units
UC:	Ulcerative colitis
UDP:	Urdine diphosphate
UV:	Ultraviolet
UV-Vis:	Ultraviolet-visible spectroscopy
XTT:	Sodium 3,3'-[1[(phenylamino)carbonyl]-3,4-tetrazolim]-bis-(4-methoxy-6-nitro) benzene sulfonic acid hydrate
ZAK:	Zipper sterile alpha motif kinase
ZO-1:	Zonulae occludens - 1
ZO-2:	Zonulae occludens - 2
ZO-3:	Zonulae occludens - 3
ZONAB:	ZO-1-associated nucleic acid binding proteins

CHAPTER 1:

General Introduction

1.1 INTRODUCTION

The idea of using 'nanomedicines' as contemporary therapeutics has been the subject of much debate over recent years, and is often stigmatised as science fiction (The Lancet, 2003). However, research into the development of nano-sized, water-soluble polymers and polymer-constructs to use as drugs and pro-drugs rather than drug delivery systems, has a well-established history (Figure 1.1).

Natural polymers have unknowingly been used in herbal remedies for several millennia. Hermann Staudinger first discovered polymers in the 1920's (reviewed in Mülhaupt, 2004). Synthetic polymers (i.e. polyvinylprrolidone) first appeared in medicine as plasma expanders during World War II, and were later developed into polymer-drug conjugates in the 1950's (Jatzkewitz 1954). Later still, a rapid advancement in polymer chemistry in the 1960's and particularly 1970's, brought the concepts of block copolymer micelles (Gros *et al.*, 1981) and PEGylated proteins (reviewed by Davis, 2002) into light, and fuelled the synthesis of new polymeric drugs. Around this time increased attention was also paid to the biological properties of both natural and synthetic polymers (reviewed in section 1.1.1).

In the mid-1970's it was noted that endocytosis (process by which materials enter a cell without passing the membrane) could be used for lysomotropic drug delivery (DeDuve, 1974), and that soluble, synthetic polymer-drug conjugates could be tailor-made into targeted drug carriers (Ringsdorf, 1975). These ideas inspired Duncan, Kopecek and their co-workers to produce Prague-Keele 1 (PK1), the first polymer-anticancer drug conjugate to enter clinical trials (Vasey *et al.*, 1999), and later PK2, the only targeted polymer-anticancer drug conjugate to enter clinical trial to-date (Seymour *et al.*, 2002).

Next, research towards the molecular basis of disease in the 1980's and 1990's saw increased interest in polycationic non-viral vectors to deliver genetic material (Wagner, 1990; Boussif *et al.*, 1995). It was also the time that Maeda and colleagues discovered the enhanced permeability and retention (EPR) effect within tumours (Matsumara and Maeda, 1986), a phenomenon which is now used to passively target "polymer therapeutics" into tumours from the vasculature (Figure 1.2).

Polymer therapeutics is a descriptor founded by Duncan (1997), to encompass the wide range of polymeric nanomedicines previously described, and has now grown to include new polymers with increasingly intricate structures, tailored surface multi-valences and defined architectures (reviewed in Duncan, 2003).

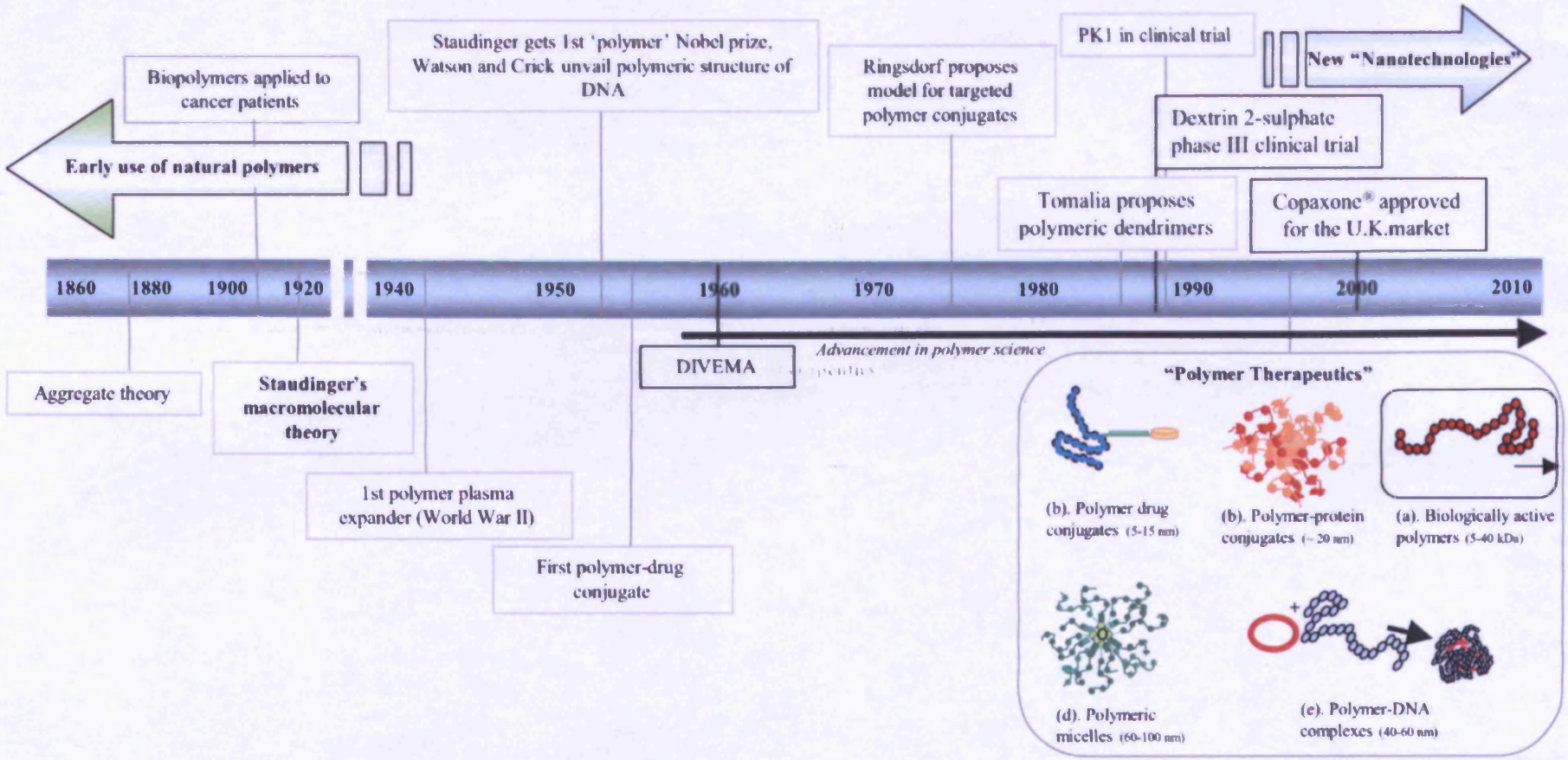

Figure 1.1 Time-scale tracking the development of polymers as nanomedicines

The idea for this picture was taken from http://www.chemheritage.org/explore/poly-time10.html (accessed 16/3/2005)

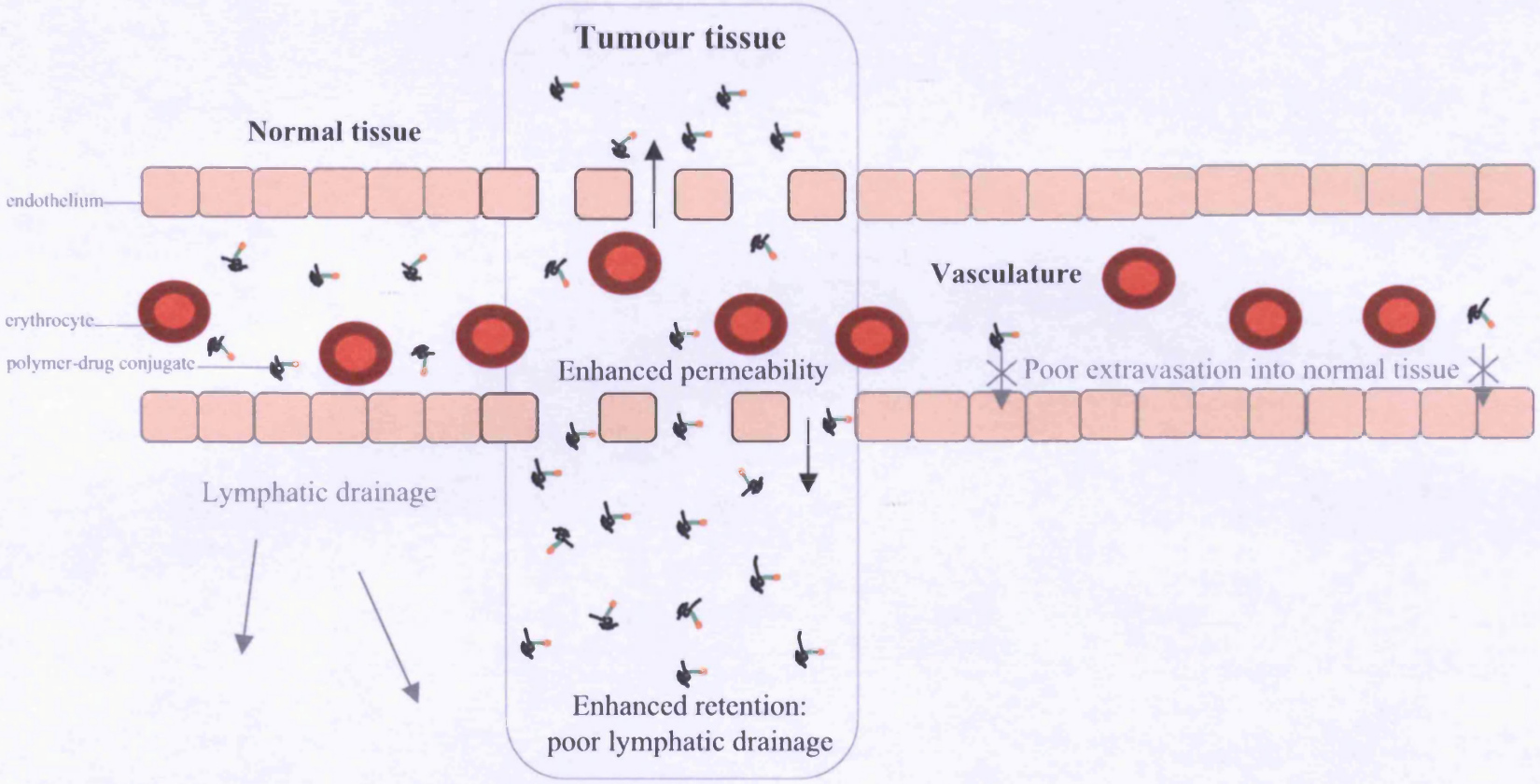

Figure 1.2 Schematic showing the EPR effect within tumour tissue

The idea for this picture came from Duncan, (2003)

However, as the new millennium progresses, current polymer research is turning once again to biologically active molecules, focusing on the relationship between their structure and properties, in an attempt to understand the structure-activity relationships that govern their behaviour. In light of this trend, biologically active polymers were investigated here as potential tools to enhance barrier permeability.

The overall aim of this project was to identify polymers capable of transiently permeabilising biological barriers such as the epithelial mucosa of the gastrointestinal tract, or endothelial barriers of the vasculature. Polymers capable of promoting drug transfer across these tissues, either directly, or through their ability to induce cytokine release (discussed below), could then be used to enhance the delivery of poorly absorbed drugs and macromolecules. In addition, they could also be used to increase drug accumulation in tumours by exaggerating the EPR effect (see Figure 1.2), and at the same time, initiate a local immune response towards it.

More specifically, rat intestinal tissue was chosen as an epithelial model for these studies, and the vertical diffusion system was used to measure the effects of cytokines or polymers on the transport of a fluorescent marker across this barrier. The polymers and cytokines chosen for this project are described in detail in the following sections, and as this work encompasses several disciplines, biologically active polymers, the immune system, cytokines and the intestine are also described. The specific aims of the project will be discussed at the end of this Chapter.

1.1.1 Biologically active polymers

Unlike the chemically inert polymers that have been chosen for conjugation to proteins and drugs (such as N-(2-hydroxypropyl)methacrylamide (HPMA) copolymers, which are non-immunogenic and non-toxic in the body at doses of up to 20 g/patient (Vasey *et al.*, 1999)), biologically active polymers elicit pronounced effects in living systems and can be thought of as polymeric drugs (reviewed by Liao and Ottenbrite, 1997). In a broad sense, the term biologically active can include a number of inherent activities such as the ability to mediate an immune response, and/or to inhibit enzymes, bacteria and viruses, or to act as antitumour agents (De Somer, 1968). Examples of biologically active polymers are shown in Table 1.1.

Table 1.1 Biologically active polymers with immunomodulatory or other biological properties.

Polymer	Type	Charge	Activity	References
Acetyl lignin	Polysaccharide	Anionic	Induce cytokines from macrophage	(Sorimachi *et al.*, 1999)
Bacteroides fragilis polymers A and B	Polysaccharide	Zwitterionic	Induces IL-2, and activates T-cells	(Stingele *et al.*, 2004)
Calcium spirualn	Polysaccharide	Anionic	Anticancer activity	(Mishima *et al.*, 1998)
Carbetimer	Synthetic	Anionic	Anticancer activity	(Hanauske *et al.*, 1988)
			Activates T cells	
Chitosan	Polysaccharide	Cationic	Induces cytokines from macrophage	(Zhijun *et al.*, 2004)
CT-1	Polysaccharide	Anionic	Anticancer activity	(Fernandez *et al.*, 1989)
Dextran carboxylate	Polysaccharide	Anionic	Inhibit tumour metastasis	(Bastias, 2002)
Dextran sulphate	Polysaccharide	Anionic	Block intracellular virus replication	(Takemoto and Fabish, 1963)
			Antiangiogenic activity	(Thornton *et al.*, 1999)
Ethylene maleic anhydride copolymers	Synthetic	Anionic	Block intracellular virus replication	(Feltz *et al.*, 1962)
Ginsan	Polysaccharide	Anionic	Activates immune system	(Lee *et al.*, 1997)
			Anticancer activity	(Song *et al.*, 2003)
Grifolan	Polysaccharide	Anionic	Induces cytokines from macrophage	(Ishibashi *et al.*, 2001)

Table 1.1 continued

Polymer	Type	Charge	Activity	References
Heparan sulphate	Polysaccharide	Anionic	Generate primary immune responses	(Kodaira *et al.*, 2000)
Lentinan	Polysaccharide		Induce cytokines & antitumour activity	(Ng, 2002)
Lysine polypeptide	Peptide	Cationic	Inhibit virus infectivity	(Burger *et al.*, 1951); (Green *et al.*, 1953); (Rubini *et al.*, 1951)
Maleic anhydride divinyl ether	Synthetic	Anionic	Enhances natural killer cell and macrophage response towards tumours	(Piccoli *et al.*, 1984)
Novispirin G-10	Peptide	Cationic	Antimicrobial activity	(Yasin *et al.*, 2003)
Polyacrylamide	Synthetic	Amphiphilic	Antimicrobial activity	(Tew *et al.*, 2002)
PolyETCA-co-VAc	Synthetic	-	Anticancer activity	(Neung-Ju *et al.*, 2001)
Polymethacrylic acid	Synthetic	Anionic	Induce IFN in animals	(De Somer, 1968)
Polysodium acrylate	Synthetic	Anionic	Slows tumour cell growth	(Hodnett and Tai, 1974)
Polystyrene sulphonate	Synthetic	Anionic	Block intracellular virus replication	(Christensen, 2001)
Schizophyllan	Polysaccharide	Neutral	Induces cytokines from leukocytes	(Kubala *et al.*, 2003)
Sulphated glucan	Polysaccharide	Anionic	Anticancer activity	(Zhang *et al.*, 2000)
Yam mucopolysaccharide	Polysaccharide	-	Induce cytokines from macrophage	(Choi *et al.*, 2002)

The activity they elicit is highly dependant on chemical composition and characteristics including tacticity, molecular weight and cross linking (reviewed in Donaruma, 1975). The ability of polymers to induce cytokines is generally dependent on polymer molecular weight (Breslow *et al.*, 1973), conformation, and ionic charge distribution (Hunt *et al.*, 1996).

Polyanions have been used clinically and have a wide spectrum of effects on the immune system and have shown great clinical potential in the areas of oncology, virology and immunology (reviewed in Liao and Ottenbrite, 1997). In 1910, Oestreich was the first to clinically apply polyanions (chondritin sulphate connective tissue extracts) as a treatment for cancer (cited in Liao and Ottenbritte, 1997). Since then, a large number of polyanions including polymaleic anhydride (Goodell *et al.*, 1978) and carbetimer (Fields *et al.*, 1982) have shown antitumour effects. This activity is probably due to their ability to modulate the immune system.

Several polyanions such as polyacrylic acids (PAcA) (De Somer, 1968), polyacetal carboxylic acids (Claes, 1970), and many polysaccharides (Artursson *et al.*, 1987; Tzianabos, 2000) including alginates (Son *et al.*, 2001) and hyaluronic acid (HA) (Boyce *et al.*, 1997) have shown an ability to induce cytokine release.

Pyran copolymer of ethylene maleic anhydride and divinyl ether (DIVEMA) was the first polyanion to enter clinical trials as an anticancer agent (Butler, 1960). DIVEMA is an inducer of interferon–gamma (IFN-γ) in mice, and displays antineoplastic, antibacterial and antiviral activity. However, the clinical trials involving DIVEMA were stopped due to toxic effects that were later found to be associated with a higher molecular weight fraction in the preparation (Breslow, 1976). Nevertheless, a number of new biologically active polyanions including copolymer-1 (Ampligen®, Hemispherx Biopharma) (Fellay, 2001) dextrin 2-sulphate (Shaunak *et al.*, 1998) and the cationic poly(lysine) dendrimer VivaGel™ (Starpharma) have successfully entered clinical trials for the prevention (VivaGel™) or treatment (dextrin 2-sulphate) of human immunodeficiency virus type 1 (HIV-1), or chronic fatigue syndrome (Ampligen®).

Some polyanions also appear to behave similarly to specific proteins, glycoproteins and polynucleotides that modulate biological responses (Liao and Ottenbritte, 1997). Polymers formed from poly(N-acryl amino acids) for example, have shown potential use in the inhibition of heparanase-mediated degranulation of basement membranes associated with tumour metastasis, inflammation and

autoimmunity (Bentolila *et al.*, 2000). Another example is Copaxone® (Teva Pharmaceuticals), an amphoteric polypeptide used to treat multiple sclerosis, which inhibits neuron degradation through its ability to mimick myelin-1 basic protein (Fridkis-Hareli *et al.*, 2002).

Unlike polyanions, polycations have shown direct antitumour activity. It has been suggested that they neutralise the enhanced negative charge on the tumour cell membrane, but it is clear they also have a number of other toxic effects (James *et al.*, 1956). Because polycations would also bind to other negatively charged mammalian cells (causing cell distortion, lysis and agglutination), the clinical use of these molecules is limited due to their extreme toxicity. In addition, it should be noted that polycationic amino acids such as poly(lysine) (PLL) can induce IFN-γ (Wild *et al.*, 1994; Giantonio *et al.*, 2001).

The chemical structure of polyelectrolytes is thought to determine the mechanism of cytokine induction. Naturally occurring anionic polyelectrolytes (and their synthetic analogues) often exhibit antigenic properties. As one aspect of this study was to determine the ability of polymers to initiate cytokine release, the following sections aim to briefly review the immune system.

1.2 The immune system

Multicellular organisms possess an innate immune system to protect them against pathogenic invasion, and all vertebrates also possess more specific and specialised defence mechanisms (termed adaptive immunity) that are superimposed on innate immunity to improve host defence against infection. Both types of immunity are briefly described below.

1.2.1 Innate immunity

Innate immunity (reviewed in Roitt *et al.*, 2001) is the first line of defence against microbes and the underlying mechanisms are present from birth. It relies on epithelial (epidermal and mucosal) barriers to protect against microbial entry, circulating leukocytes, specific proteins (expressed in the blood and tissues; see below), and cytokines (reviewed in Abbas *et al.*, 2000). Phagocytic (neutrophil and mononuclear phagocyte) and natural killer (NK) cells are the principal effector cells of this system, and attack microbes that have entered the circulation from breached

epithelia. Each cell type plays a distinct role. Phagocytes ingest and destroy microbes, whilst NK cells kill microbe-infected cells by direct lytic mechanisms (reviewed in Abbas *et al.*, 2000; reviewed in Roitt *et al.*, 2001). Macrophage and NK cells also secrete cytokines that activate phagocytes and stimulate the cellular reaction of innate immunity called inflammation. This involves the recruitment of leukocytes into a site of infection, and activation of the leukocytes to eliminate the infectious agent (reviewed in Oppenheim *et al.*, 2001).

Circulating microbes are also bound by plasma proteins (complement proteins, mannose-binding lectin, C-reactive protein, collectins, pentraxins and coagulation factors) that recognise specific binding sites shared by particular classes of infective agent, but that are not present on mammalian cells. These recognition sites include chemically distinct carbohydrates (e.g. lipopolysaccharide (LPS), mannans) lipids (e.g. lipoteichoic acid) and nucleic acids (double stranded RNA from certain viruses or DNA with unmethylated cystosine and guanine nucleotides (CpG) from bacteria) (reviewed in Abbas *et al.*, 2000; reviewed in Roitt *et al.*, 2001).

1.2.2 Acquired immunity

The acquired immune system is complex, intricately regulated and is mediated by lymphocytes. It is able to discriminate between self and non-self proteins (expressed by foreign organisms tissues or cells) and also has memory, so that resistance that is weak or absent on first exposure to an immunogen, gives a more effective response on repeated exposure (reviewed in Abbas *et al.*, 2000). Contemporary usage of the terms 'immunology' and 'immune response' refers primarily to this type of immunity, thus an overview of this process is given below.

Immune response

The immune response (reviewed in Abbas *et al.*, 2000; reviewed in Roitt *et al.*, 2001) involves several cell types and is triggered when a foreign agent enters the body (see Figure 1.3). The first cells to recognise 'foreign' material are the antigen presenting cells (APC) such as macrophages and dendritic cells that constantly patrol their environment. These cells phagocytose foreign material and display the digested peptide fragments (antigens) on their cell-surface via the major histocompatibility complex (MHC) to be presented to T-lymphocytes (T-cells). Only lymphocytes

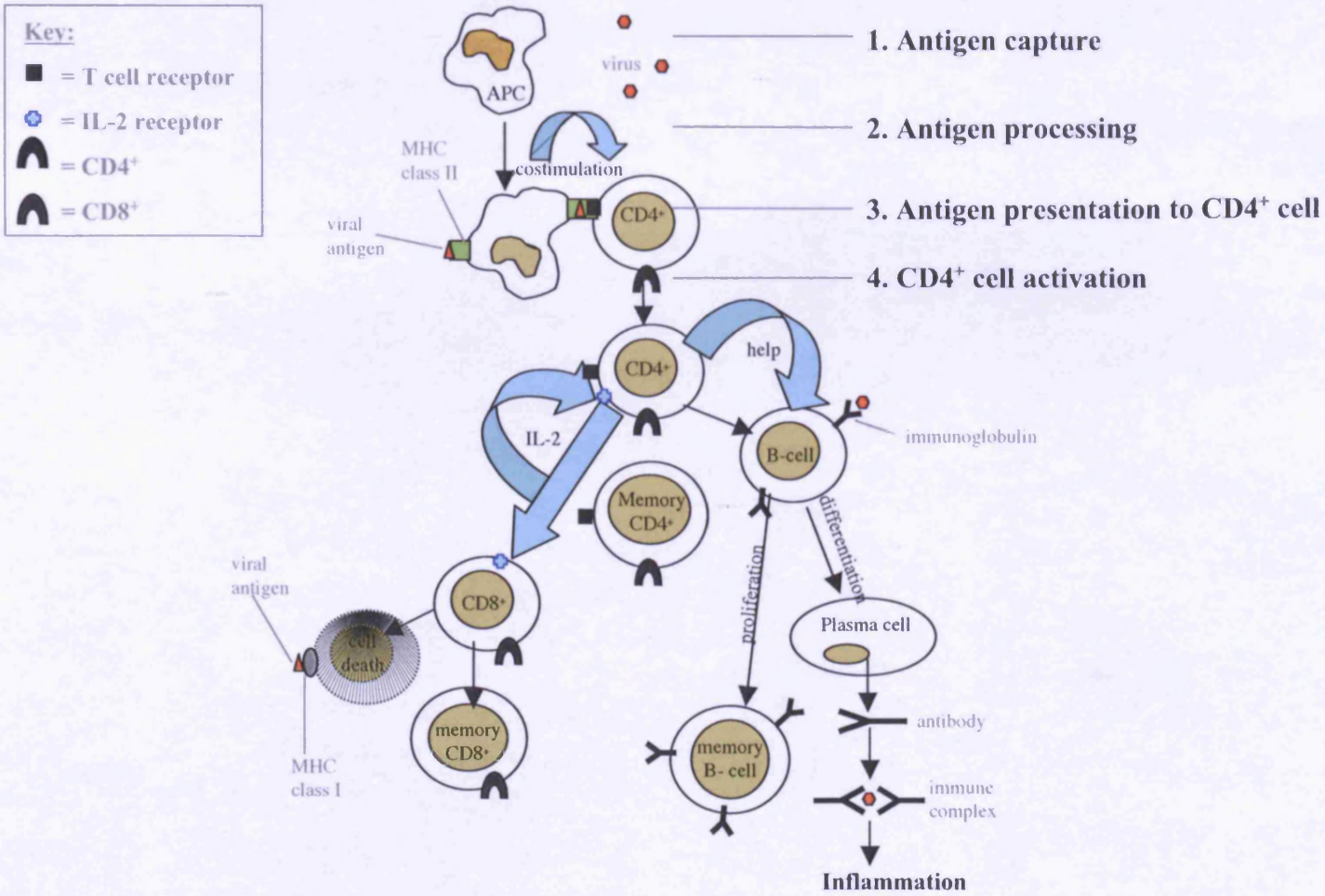

Figure 1.3 Sequence of events in a prototypical immune response

Picture adopted from Parslow et al. (2001)

carrying the extracellular-membrane receptors specific to the antigen will bind the APC and proliferate to mount an immune response, and this is dependent on the type of T-cell activated (reviewed in Abbas *et al.*, 2000; reviewed in Roitt *et al.*, 2001).

There are two major subsets of T-cell, and each recognises one of two different classes of MHC proteins. Cytotoxic cluster designation-8 positive ($CD8^+$), T-cells recognise class I MHC proteins that are expressed by virtually all somatic cells. Class II MHC proteins are only expressed by macrophages, dendritic cells and B-lymphocytes (B-cells), that endocytose antigens bound to their surface immunoglobulins or other receptors. These cells present antigens to $CD4^+$ T-cells that are necessary for virtually all immune responses. However, in addition to MHC class II activation, co-stimulatory signals are also required by $CD4^+$ T-cells in order to achieve activation. This is provided through the close contact of the $CD4^+$ T-cell and APC, and through the binding of the CD28 protein on the $CD4^+$ T-cell surface, with the B7 proteins on the surface of the APC. Together these signals cause the T-cell to begin secreting a cytokine called interleukin-2 (IL-2; see section 1.7.2), and to begin expressing specific high affinity IL-2 receptors on its surface.

Activated $CD4^+$ T-cells also secrete other cytokines that promote the growth, differentiation and functions of B-cells, macrophages and other cell types (reviewed in Abbas *et al.*, 2000; reviewed in Roitt *et al.*, 2001).

The following sections introduce cytokines and discuss their role in disease and disease therapy. The cytokines explored in detail in this study are described later.

1.3 Cytokines

Cytokines are a diverse group of intercellular signalling peptides and glycoproteins with a molecular weight of 6,000 - 60,000 daltons (Da) (reviewed in Oppenheim *et al.*, 2001). They are produced by all nucleated cells in response to various (mainly inflammatory or antigenic) stimuli. In man, several hundred types of genetically and structurally unrelated cytokines (interleukins, interferons, tumour necrosis factors, growth factors, colony stimulating factors and chemokines) have been identified (reviewed in Roitt *et al.*, 2001).

The biological properties of cytokines include the ability to mediate cell growth, division, differentiation, and apoptosis. They also mediate inflammation, immunity (reviewed in Abbas *et al.*, 2000), wound repair (reviewed in Werner and

Grose, 2002; Boniface *et al.*, 2005) and fibrosis (Oh *et al.*, 2005). Cytokines activate cells through specific, high-affinity cell surface receptors at micromolar, picomolar or femtomolar concentrations in either a paracrine or an autocrine way. Transforming growth factor-beta (TGF-β), erythropoietin (EPO), stem cell factor (SCF) and monocyte-colony stimulating factor (M-CSF), affect distant target cells (reviewed in Oppenheim *et al.*, 2001).

Most cytokine receptors belong to a family of proteins called the hematopoietin receptor family that share an extracellular domain, with a similar three-dimensional structure, that has common amino acid residues at key positions (reviewed in Oppenheim *et al.*, 2001). Each receptor that is a multiprotein complex comprising two or more integral membrane polypeptide subunits has different ligand specificities. Each subunit also has an extracellular domain that participates in cytokine binding, a transmembrane domain, and a cytoplasmic tail involved in signal transduction. An α- and β-subunit are found in all cytokine receptors, though trimeric receptors (such as the IL-2 receptor) may also have a γ-subunit. The sharing of subunits between different cytokine receptors is thought to explain their pleotropic actions upon cells, by enabling them to trigger identical signalling events inside the cell (reviewed in Abbas *et al.*, 2000; reviewed in Roitt *et al.*, 2001; reviewed in Oppenheim *et al.*, 2001).

Normally cytokines are not stored pre-formed in cells (except in mast cells and platelets which release cytokines during degranulation), but they are synthesised by transient gene transcription following cell activation. The messenger RNA encoding most cytokines is also unstable, so cytokine production is transient. In addition, cytokine release from cells is also subject to tight regulation, and it often involves cleavage of a pro-form (reviewed in Abbas *et al.*, 2000).

The production cycle of a given cytokine lasts only a few hours to a few days in a normal state, and the deregulation of this process is the cause of many diseases. Some of these diseases are discussed in the next section.

1.3.1 Aberrant cytokine expression and disease

The deregulation of cytokines and/or their receptors within biological systems

is a common cause of many inflammatory diseases, which often appear as sites of cell activation, with an inflammatory and/or immune response. In normal physiology, cytokine cascades are key mediators of disease, and the cytokines released are diverse. They can be pathogenic or act merely as innocent bystanders. A stimulus can cause prolonged cytokine production, altering local cell behaviour (reviewed in Feldmann *et al.*, 1996). For example, Crohn's disease and rheumatoid arthritis are associated with a persistent up-regulation of tumour necrosis factor-α (TNF-α). In Crohn's disease this causes chronic inflammation and a high infiltrate of inflammatory cells (reviewed in Aggarwal, 2000), which results in hyperpermeable epithelia and granulomas in the intestine. In arthritis, high levels of TNF-α cause increased degradation of bone and cartilage in rheumatic joints (Zwerina *et al.*, 2004).

Overproduction of IL-6 has also been observed in rheumatoid arthritis, and this leads to Castleman's disease (Kishimoto, 2005). High levels of IL-6 cause several other pathological conditions such as multiple myeloma (Xiao *et al.*, 2004), histiocytic lymphoma (reviewed in Knowles and Eriksson, 2001), cardiac myxomas (Mendoza *et al.*, 2001) and liver cirrhosis (Eriksson *et al.*, 2004).

Aberrant expression of IL-2 or its receptors has been associated with Hodgkin's disease, graft-versus-host reaction, multiple sclerosis, rheumatoid arthritis, systemic lupus erythematosis, type-1 diabetes, lepromatous leprosy, acquired immunodeficiency syndrome (AIDS), severe burn traumas and allogenic bone marrow transplantation (reviewed in Thorpe, 1998). Current research is focusing on the identification of mechanisms able to correct the deviant expression of these cytokines and/or their receptors to allow development of new therapies.

Monoclonal antibodies (e.g. Infliximab®) have been developed to neutralise cytokines in relation to specific disease conditions. Infliximab® binds TNF-α and it has been approved for the treatment of Crohn's disease (Agnholt *et al.*, 2003) and rheumatoid arthritis (reviewed in Schottelius *et al.*, 2004). Enbrel® (known as etanercept) is a soluble TNF-α receptor-fusion protein that has also shown promise as a treatment of these diseases (Agnholt *et al.*, 2003; reviewed in Schottelius *et al.*, 2004). Anti-IL-2-receptor monoclonal antibodies specific for the IL-2 receptor α-subunit, unmodified or bound to toxins, have been used for the treatment of Hodgkin's lymphoma (Engert *et al.*, 1991) and T-cell leukemia (Kreitman *et al.*, 1992).

Although cytokines can play an important role in causing diseases, they have also been used to treat viral infections and certain types of cancer. As biologically active polymers have been shown to induce cytokines, the role of cytokines and biologically active polymers in therapy are therefore discussed in the following sections.

1.3.2 Cytokine therapy

Several cytokines have undergone clinical trials. TNF-α has been used for the treatment of sarcoma and melanoma when given locally by isolated limb perfusion (Eggermont *et al.*, 1997; DiFilippo *et al.*, 2004). IFN-γ has been used for the treatment of warts caused by the human papiloma virus (HPV), and IL-2 (Proleukin®) for the treatment of renal and colon cancer (Emery *et al.*, 2002). Interleukin-12 is currently in phase II clinical trails as a treatment for non-Hodgkin's lymphoma and Hodgkins disease. However, the clinical application of these, and other cytokines, is often limited by their short half-life and toxic side effects. High concentrations of TNF-α can cause septic shock syndrome (Tracey, 2004), IFN-γ can give rise to malaise, weakness and lethargy (Oppenheim *et al.*, 2001), IL-2 can cause vascular leak, shock and pulmonary odema (reviewed in Vial, 1995), and IL-12 can give rise to abnormal liver function (reviewed in Abbas *et al.*, 2000).

Since low concentrations, or locally administered cytokines have a beneficial role towards disease and tumour regression (see following section), attempts to prolong the half-life of some cytokines have been made. IL-2, TNF-α and IFN-α for example, have been "PEGylated" by covalently linking the proteins to polyethylene glycol (PEG) chains (Harris, 2003). However, although PEG is non-immunogenic itself (Chinol *et al.*, 1998), high doses of PEGylated cytokines still have significant toxicity. Recent reports have also shown that cytokines can be stabilised and designed to become bioactive fusion proteins, such as Hyper-IL-6. This protein consists of IL-6 and a soluble IL-6 receptor, and synergises with murine stromal elements to promote the long-term survival of primitive human hematopoietic progenator cells (Gotze *et al.*, 2001).

1.4 Biologically active polymers as modulators for cytokine therapy

Normally, the ability of tumour cells to trigger an effective immune response is

limited due to their weak expression of MHC antigens, adhesion molecules and costimulatory signals. Some tumours may also secrete immunosuppressive cytokines such as IL-10 (Monti *et al.*, 2004), TGF-β (Kao *et al.*, 2003; Blanchere *et al.*, 2002), and platelet-derived growth factor 2 (Zhou *et al.*, 2005), or fail to express the cytokines that activate local immune responses. However, these evasive strategies can be overcome by directly introducing cytokines or other immunomodulatory molecules (e.g. biologically active polymers) into the tumour milieu, or through tumour cell transfection. Biologically active polymers (particularly polyanions) capable of increasing the local production of therapeutic cytokines can therefore be used to initiate acquired immunity, enabling identification and destruction of tumour cells, and eliciting a long-lasting memory of this interaction. It has been proposed that this can also be used to treat local viral or bacterial infections, or immune-deprived conditions e.g. chronic non-healing leg ulcers, which respond to treatment with TNF-α. Here it was postulated that as a result of local cytokine release, biologically active polymers might also be exploited as a means to permeabilise epithelial and/or endothelial barriers.

1.5 Biologically active polymers and cytokines as permeability enhancers

Several polyanions are known to induce the production of TNF-α and IFN-γ *in vitro* and *in vivo*. Besides their role in the immune response, these cytokines can mediate the permeability of epithelial and endothelial cells, by permeabilising their tight junctions (Walsh *et al.*, 2000; Nusrat *et al.*, 2000) (Figure 1.4). Tight junctions (TJ) are highly regulated, apical, multiprotein complexes (Figure 1.5) that act as a dynamic physical barrier to prevent the diffusion of fluids with different molecular compositions (e.g. urine, milk, gastric juice, blood) through the paracellular pathway into surrounding tissues (see Figure. 1.4). This is referred to as the gate property of TJ and is commonly affected by a variety of exogenous agents such as calcium ions (Ca^{2+}) bacterial toxins, and glucose. Permanent disruption of TJ function drastically alters permeability and is the hallmark of many pathologic states (Walsh *et al.*, 2000). However, changes in permeability caused by TNF-α, IFN-γ, and hepatocyte growth factor (HGF), are transient, reversible (unless the cytokine persists as in disease), and involve alterations in the distribution of individual TJ proteins, or the actin cytoskeleton. The structure of the TJ is discussed in the following section.

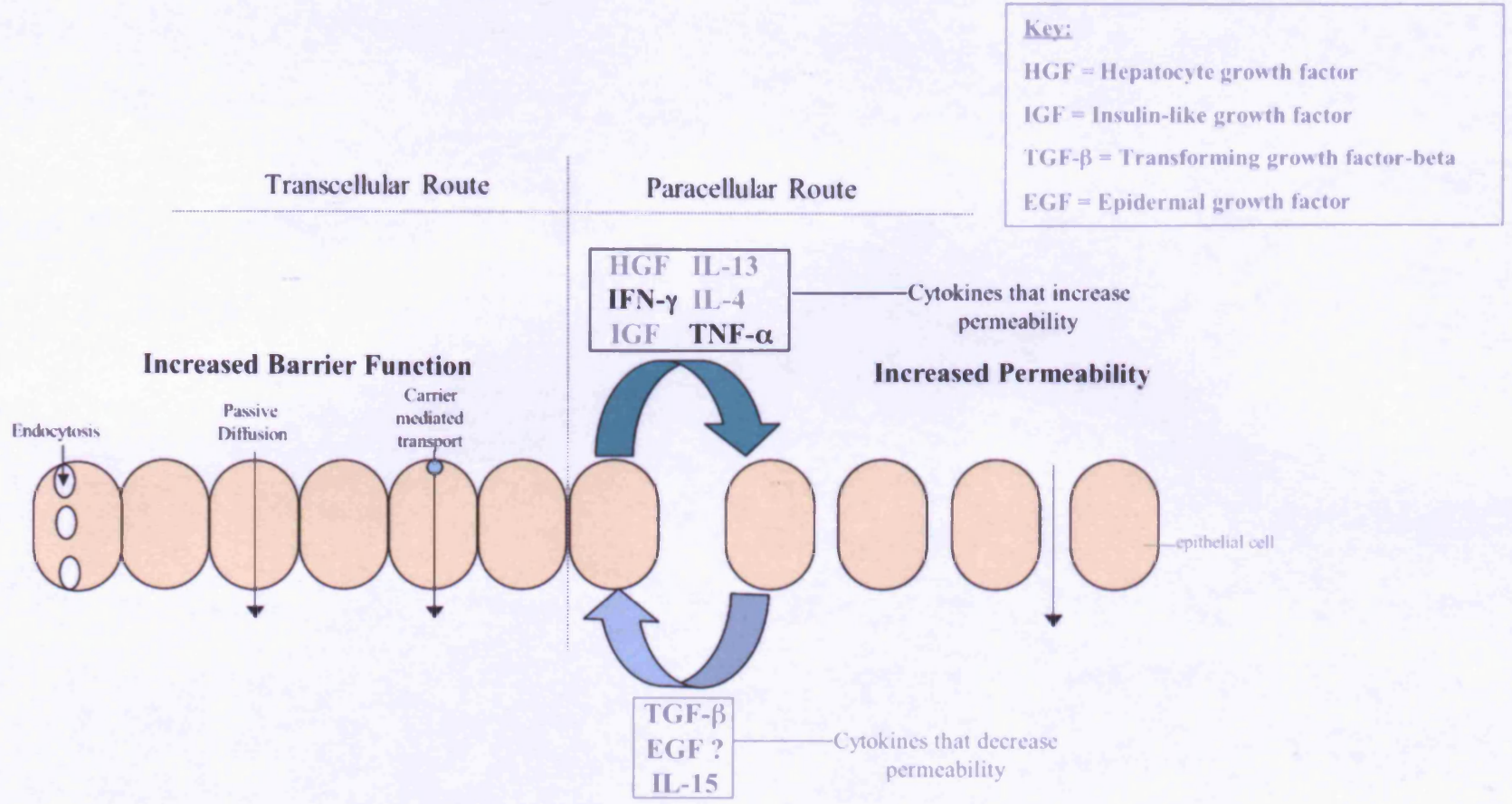

Figure 1.4 Cytokines and epithelial permeability

The idea for this picture was taken from Hillery et al. (2001) and Walsh et al. (2000)

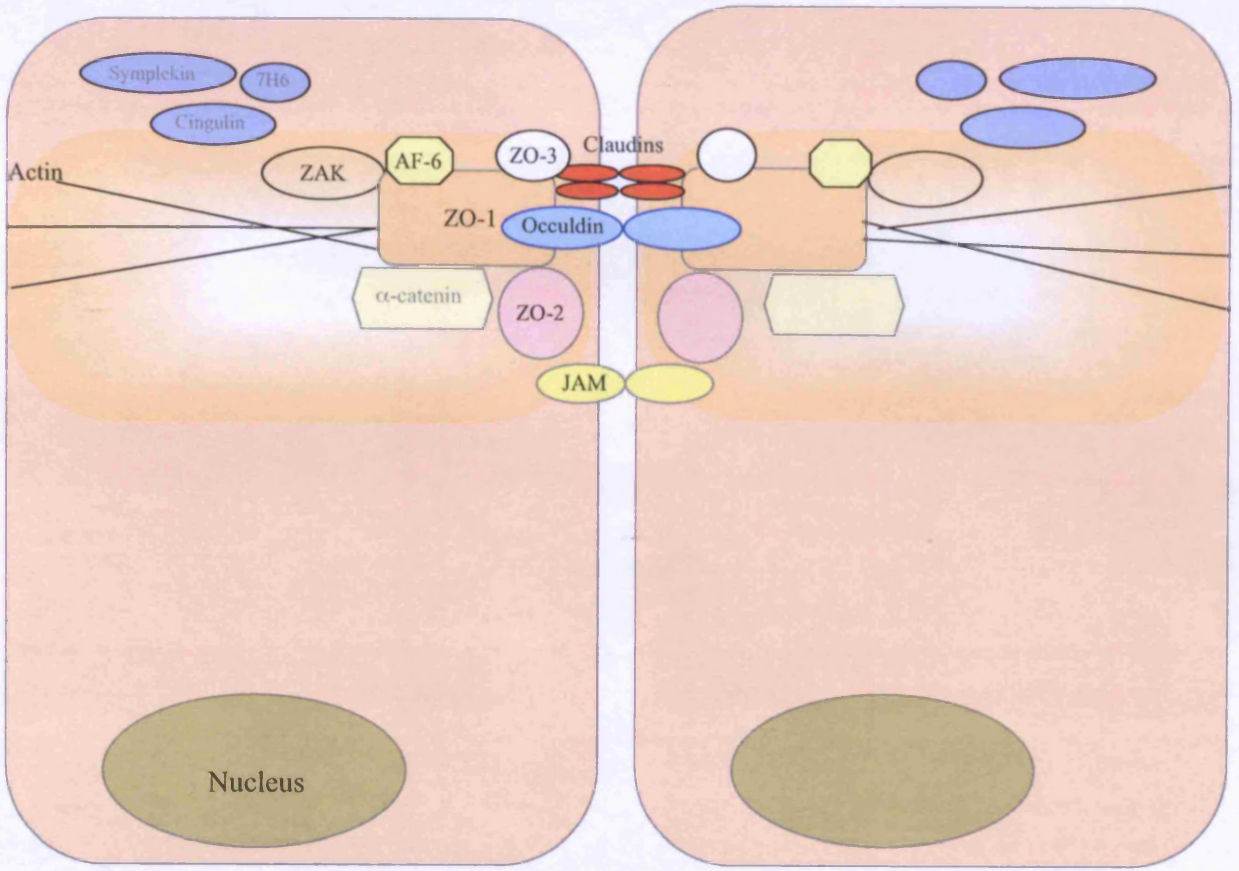

Figure 1.5 Protein components of the tight junction

Picture adopted from Fanning et al. (2001)

1.5.1 Structure and function of tight junctions

Formation of the TJ requires the assembly of several proteins that are anchored directly or indirectly to the actin cytoskeleton (Han *et al.*, 2002), or intracellular proteins (e.g. zonulae occludins proteins, catenins and cytoskeletal proteins (microtubules and microfilaments)). Recent work has uncovered a constellation of molecules, several of which comprise three unique families of transmembrane proteins (see Figure. 1.5). Each family is described below.

Occludin

The first TJ integral protein to be characterised was occludin. It is 65,000 Da in size, possesses two extracellular loops, four transmembrane domains, three cytoplasmic regions and a large cytosolic C-terminal (Furuse *et al.*, 1993). Both extracellular loops of this protein are of similar size, and are enriched in glycine (one loop is also rich in tyrosine). Unlike other TJ integral proteins, occludin possesses a conserved 150 amino acid sequence in its carboxyl tail domain, which allows it to bind directly to filamentous (F)-actin (Wittchen *et al.*, 1999), and not rely upon scaffolding proteins for association. Moreover, the same carboxyl segment of occludin is also capable of binding to other TJ related proteins such as the membrane associated guanylate kinase homologues (MAGUK) proteins, zonulae occludins-1 (ZO-1) (Furuse *et al.*, 1994), ZO-2 (Itoh *et al.*, 1999), and ZO-3 (Haskins *et al.*, 1998).

The role of occludin in TJs seems to be an important one, as over expression of mutant forms of the protein leads to changes in the gate function of epithelia (Balda *et al.*, 1996; McCarthy *et al.*, 1996). Occludin also has the ability to form TJ filaments in L-fibroblasts (which lack TJ) when transfected (Furuse *et al.*, 1998). However, the precise role of occludin in the TJ is unclear, especially since the discovery that occludin knockout mice still display well developed TJ (Saitou *et al.*, 2000).

Claudin

Claudins are a family of 17,000 - 27,000 Da integral TJ proteins, with four transmembrane domains, short carboxyl intracellular tails and two extracellular loops, one of-which is larger than the other. Like occludins, the amino acid tails of these proteins are highly conserved within the family and constitute PSD95/disc large/ZO-1

homology domain (PDZ) binding motifs (Furuse *et al.*, 1998), which connect to the PDZ containing proteins ZO-1, ZO-2, ZO-3, PALS1-associated TJ protein (PATJ) (Roh *et al.*, 2002) and the scaffolding protein, multiple PDZ domain protein (MUPP1) (reviewed in Mrsny, 2005). The PDZ binding motifs are 80 - 90 amino acid modules that bind to specific motifs found at the carboxyl terminal ends of several proteins, and are crucial for the clustering and anchoring of transmembrane proteins (reviewed in Mrsny, 2005).

Claudins appear to help constitute the backbone of TJ strands, as cells that are devoid of TJ (murine L-fibroblasts) can generate intramembrane strands following claudin addition (Furuse *et al.*, 1998; Morita *et al.*, 1999). Down-regulation of claudin proteins is often a contributory factor for various disease conditions and cancers. Different species of claudin are found in different epi- and endothelia, and are responsible for the ample variety in electrical resistance and paracellular ionic selectivity (reviewed in Gonzalez-Mariscal *et al.*, 2003). This is because the different species of claudins are capable of generating different intramembrane strand patterns (Furuse *et al.*, 1999; Morita *et al.*, 1999).

Junctional adhesion molecule and coxsackievirus and adenovirus receptor

The third transmembrane protein involved in the TJ complex of epithelial and endothelial cells, is a 43,000 Da, glycosylated protein termed, junctional adhesion molecule (JAM). Like the coxsackievirus and adenovirus receptor (CAR), this protein belongs to the immunoglobulin superfamily. Both proteins have only one transmembrane domain, possess a large extracellular region with two immunoglobulin (Ig) domains and share similar function.

CAR is a 46,000 Da integral membrane protein with a long cytoplasmic tail that increases transepithelial electrical resistance (TEER) when over expressed in epithelial cells (Cohen *et al.*, 2001). It is also believed to be involved in diapedesis, and is over expressed at sites of inflammation (Ito *et al.*, 2000; reviewed in Gonzalez-Mariscal *et al.*, 2003).

Compared to CAR, JAM possesses a short intracellular tail featuring a PDZ binding motif that interacts with a number of TJ proteins such as ZO-1 (Bazzoni *et al.*, 2000) AF6 (Ebnet *et al.*, 2000) and cingulin (Bazzoni *et al.*, 2000; Ebnet *et al.*,

2000). Freeze-fracture immunoreplicas have shown this protein to reside near the TJ strands, and it is thought to associate laterally as homodimers, which may interact with occludin and claudin (reviewed in Gonzelez-Mariscal *et al.*, 2003). Fresh evidence also suggests that JAM is involved in the closure of the TJ, as antibodies against the protein prevent the recovery of the gate function of epithelia transiently deprived of calcium (Liu *et al.*, 2000). The presence of JAM is also known to be required for leukocyte migration across vascular endothelia (Lechner *et al.*, 2000).

Plaque proteins

Plaque proteins are cytosolic proteins associated with the TJ. The MAGUK proteins are a family recognised for having structurally conserved PDZ, src homolgy 3 (SH3) and guanylate kinase (GK) domains. Of these proteins ZO-1 is most important.

ZO-1 is a phosphoprotein found at the submembranous domain in the TJ. It is linked to several other proteins including claudins (Itoh *et al.*, 1999), JAM (Ebnet *et al.*, 2000), occludin (via its GK module) and CAR. It independently associates with ZO-2 and ZO-3, and is also linked with the actin-binding protein 4.1, and the actin cytoskeleton (Fanning *et al.*, 1998; Itoh *et al.*, 1997). Interestingly, it is thought to shuttle between the nucleus and plasma membrane (Islas *et al.*, 2002).

Sequencing of ZO-1 has recently revealed its possession of reputed nuclear export signals (NES) (Gonzalez-Mariscal *et al.*, 1999). In mechanically injured cells (with decreased TJ), ZO-1 is located in the nucleus (Gottardi *et al.*, 1996), where it interacts with a transcription factor termed ZONAB (Balda *et al.*, 2003). The interaction of ZO-1 with ZONAB regulates paracellular permeability and gene expression in reporter assays (Balda and Matter, 2000). Therefore, the function of ZO-1 can be thought of as a protein that establishes a cross talk between the nucleus and the TJ that balances epithelial cell differentiation and growth. High levels of ZO-1 are associated with an increase in barrier function, and are seen in intestinal epithelia after IL-15 treatment (Nishiyama *et al.*, 2001). Low levels of ZO-1 and occludin are found in lung epithelia following the addition of IL-4 and IL-13, though this can be reversed with IFN-γ (Ahdieh *et al.*, 2001).

As TJ play an important role in the intestine, which was chosen as a model epithelial barrier for these studies, the following section aims to introduce this tissue.

1.5.2 Small intestine as a model epithelial barrier

The small intestine presents one of the most complex biological barriers for drug delivery, and can loosely be divided into three regions stretching from the stomach to the anus that are: the duodenum, jejunum and ileum (see Figure 1.6). The wall of the small intestine has a basic arrangement of tissues that from the inside out are: the mucosa (see below), submucosa (dense connective tissue and submucosal plexus), muscularis (two sheets of thin muscle) and serosa (connective tissue) (reviewed in Tortora and Grabowski, 2003) (Figure 1.7a).

The small intestinal mucosa is covered by villi (Figure 1.7b), which increase the surface area for absorption. The core of each villus is an extension of the lamina propria, (connective tissue layer of the mucosa), and its surface is covered with simple columnar epithelial cells. Opening into the luminal surface at the bases of the villi are intestinal glands termed the crypts of Lieberkuhn, which extend downward toward the muscularis mucosae (a thin layer of muscle that supports the laminar propria). The simple columnar epithelial lining them is continuous with that covering the villi. This cell layer comprises diffuse neuroendocrine cells (paracrine and autocrine hormone-producing cells that form approximately 1 % of the total cell population), goblet cells and surface absorptive cells (reviewed in Tortora and Grabowski, 2003). Goblet cells are unicellular glands that secrete mucinogen, which hydrates to form mucin (mucus), and acts as a viscoelastic barrier to reduce shear stresses on epithelia. Mucus also binds bacteria to prevent epithelial colocalisation, and from a drug delivery perspective, has important implications as a physical barrier through which drug molecules must diffuse before reaching the absorbing surface.

The most numerous cell-type in the small intestinal mucosa are the surface absorptive cells, termed enterocytes (reviewed in Hillery *et al.*, 2001; reviewed in Tortora and Grabowski, 2003), which are responsible for the terminal digestion and absorption of nutrients and water (mentioned above). These cells are responsible for transporting the bulk of the absorbed nutrients into the lamina propria to be distributed throughout the body. Their apical surface presents a brush border of microvilli (approximately 1 μm long), whose tips contain a glycocaylx coat to protect against auto-digestion, and to hold enzymes that digest dipeptides and disaccharides (into their monomers), and re-esterify fatty acids (into triglycerides from chylomicrons). Drug metabolising enzymes such as cytochrome P450 3A (CYP3A),

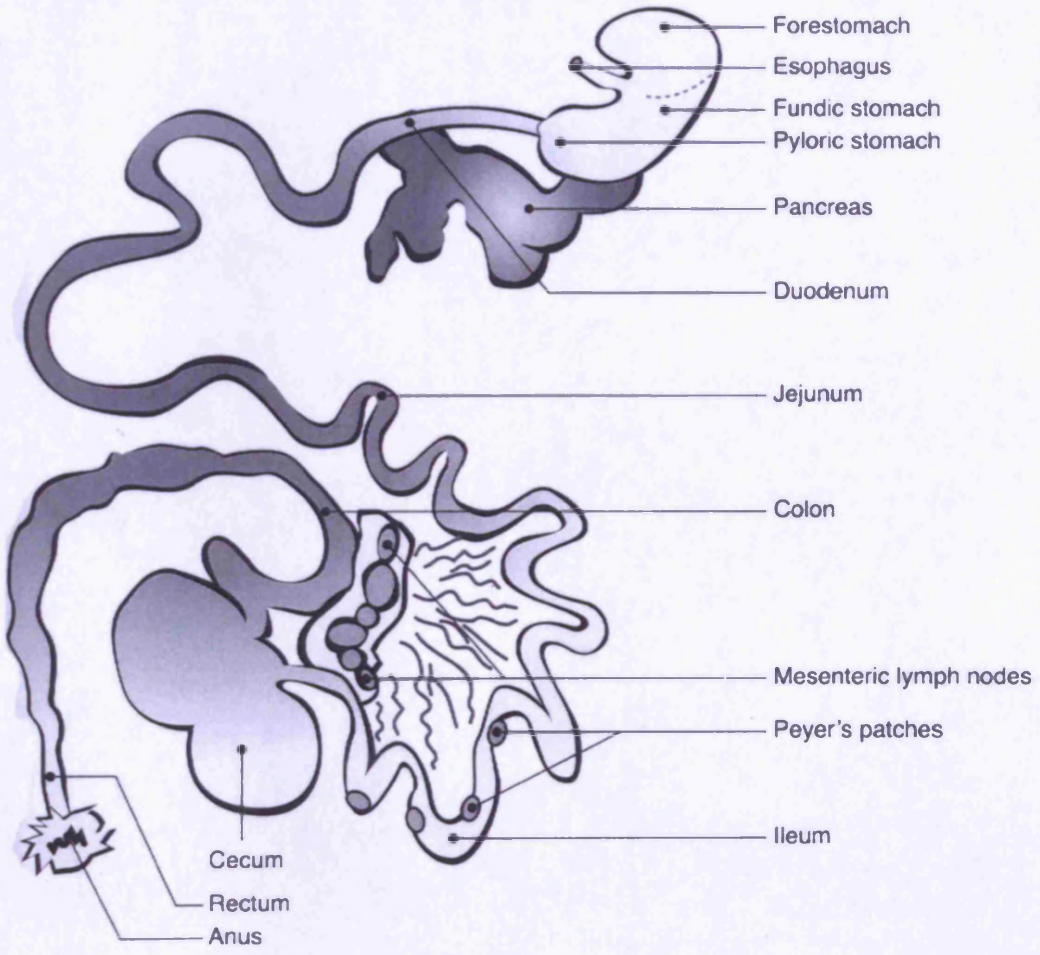

Figure 1.6 An illustration showing the physiology of the rat gastrointestinal tract *Picture taken from Remie, (2000)*

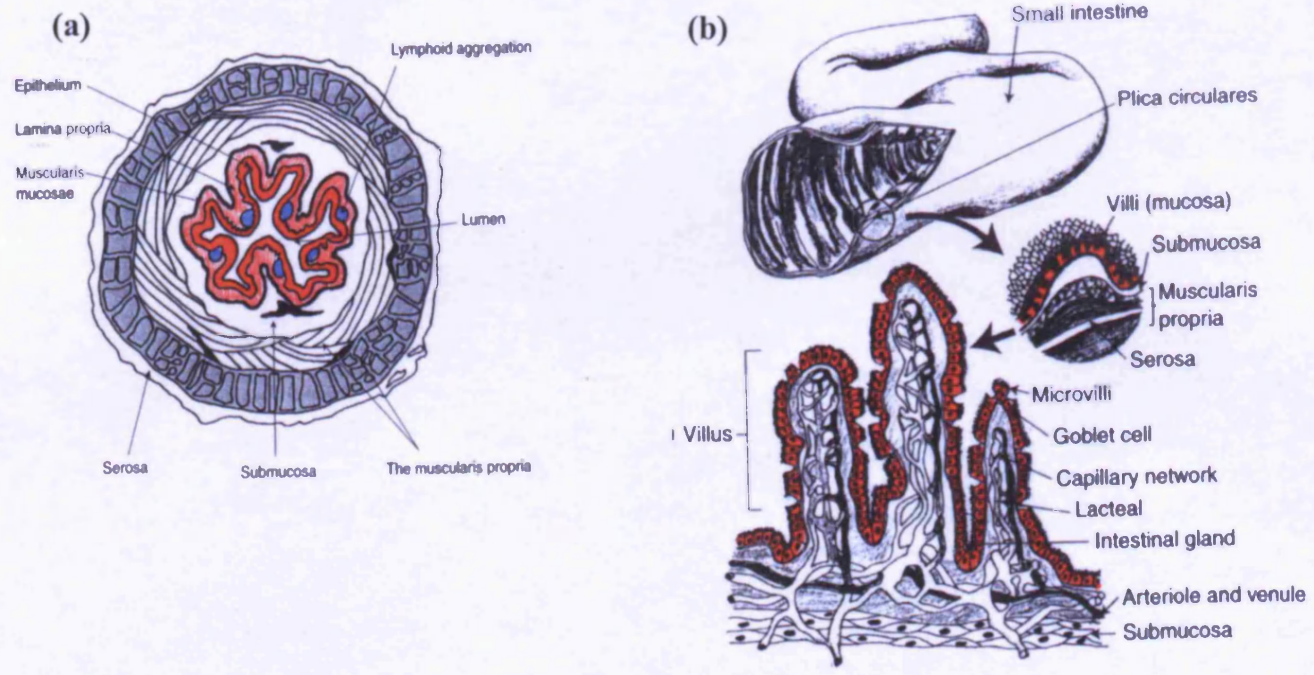

Figure 1.7 Histology of the small intestine

Picture taken from Hillery et al. (2001)

urdine diphosphate (UDP)-glucuronyl transferases, sulphotransferases, glutathione S-transferases, N-acetyl transferases, are also found on the apical surface of these cells, along with the efflux transporter P-glycoprotein (P-gp) (reviewed in Hillery *et al.*, 2001). P-gp confers multi-drug resistance by acting as an ATP-dependant efflux pump that reduces intracellular accumulation and/or transcellular flux of several drugs and some peptides (reviewed in Oude-Elferink and Paulusma, 2006).

Drugs that are not affected by the above cross the mucosal barrier (enterocytes) via (1) transcellular mechanisms that involve transport across the plasma membrane e.g. passive diffusion, or active processes such as cell type specific transporters or channels, (2) transcellular transport by endocytosis and exocytosis (transcytosis) mechanisms, or (3) paracellular routes if the drug is small enough or when the TJ are open (see Figure 1.4). However, passage through the TJ is dependent upon the magnitude of the barrier (the permeability) as well as the molecular size and ionic charge of the molecule (reviewed in Hillery *et al.*, 2001). Currently a succession of absorption enhancers (e.g. N-trimethyl chitosan chloride) has been researched by the pharmaceutical industry, to enchance delivery through this pathway.

The gastrointestinal tract also contains various leukocyte cells that form the mucosal immune system.

1.5.3 Mucosal immune system

The mucosal immune system is one of the most dispersed, diverse and complicated systems in the body (reviewed by MacDonald, 2003; Kiyono and Fukuyama, 2004). As it is continuously presented with antigenic challenges from food and the native bacterial flora and pathogens it is highly specialised to rapidly respond to 'foreign' materials.

Scattered throughout the mucosal epithelia are T-cells, thought to have evolved to recognise commonly encountered inter-luminal antigens. In the underlying lamina propria there is a mixture of leukocytes including activated T-cells (thought to have responded to antigens in regional mesenteric lymph nodes and to have migrated to the intestine), B-cells, plasma, macrophage, dendritic, mast and eosinophil cells (reviewed in Abbas *et al.*, 2000). These collected cells form visibly distinct, dome-like lymphoid follicles termed Peyer's patches (Figure 1.8).

Peyer's patches (reviewed by Brayden *et al.*, 2005) were first described by Johann Peyer more than 300 years ago. They reside on the luminal surface in the intestine, and are an example of organised gut-associated lymphoid tissue (GALT). They do not bear afferant lymphatics, and they function to induce tolerance towards common antigens. Some of the epithelial cells that overlay Peyer's patches are specialised membranous (M)-cells that lack microvilli, are actively pinocytic, and transport lumenal antigens into the sub-epithelial tissues of the patches. These regions are rich in B-cells, B-cell germinal centres, and small numbers of $CD4^+$ T-cells in the interfollicular regions. Tissues containing Peyer's patches were used later in some of the transport studies conducted here (see Chapter 4 and Chapter 5).

1.6 Biological rationale for the choice of polymers selected for these studies

A range of synthetic and linear polymers of different molecular weight and architecture were used in these studies, and their structure and current uses are briefly discussed here.

1.6.1 Alginates

Alginates were selected for this project because they are abundant, biocompatible, polysaccharides that are widely used e.g. as pharmaceutical excipients and food additives (reviewed by Simsrod and Dragnet, 1996). Some alginates have been shown to induce cytokine production from immune cells *in vitro* (Espevik *et al.*, 1993; Jahr *et al.*, 1997; Flo *et al.*, 2000).

In their natural state, alginates can form insoluble complexes with calcium, magnesium, sodium and potassium salts. They are found in the cell walls and intracellular spaces of brown seaweed where they serve to provide the flexibility and strength needed for mechanical support during growth in the sea (reviewed by Simsrod and Dragnet, 1996). They also occur in some soil bacteria (Espevik *et al.*, 1993; Jahr *et al.*, 1997; Flo *et al.*, 2000). Alginates are composed of unbranched linear chains of β-D-mannuronate (M) and α-L-guluronate (G) acid monomers that link together in a 1→4 direction (Figure 1.9).

Alginates containing the high G-blocks possess the greatest ability to form gels, as the G monomers become cross-linked by means of calcium, or other multivalent cations (Figure 1.9), forming the so-called egg-box structure. These alginates have been exploited for stabilising and thickening agents in food, or as films and coatings

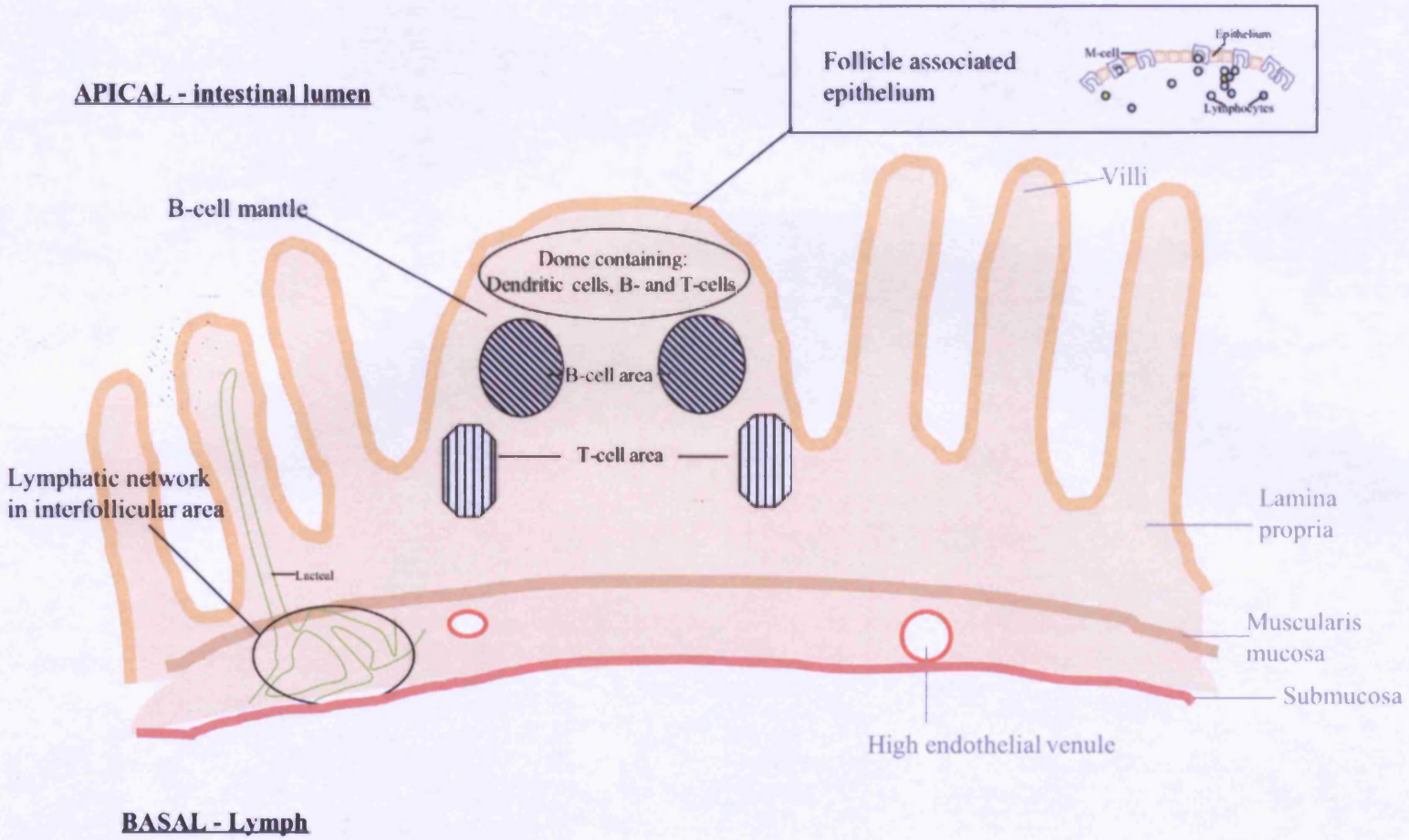

Figure 1.8 Schematic showing a Peyer's patch in the small intestine

Picture adopted from Lavelle et al. (1995)

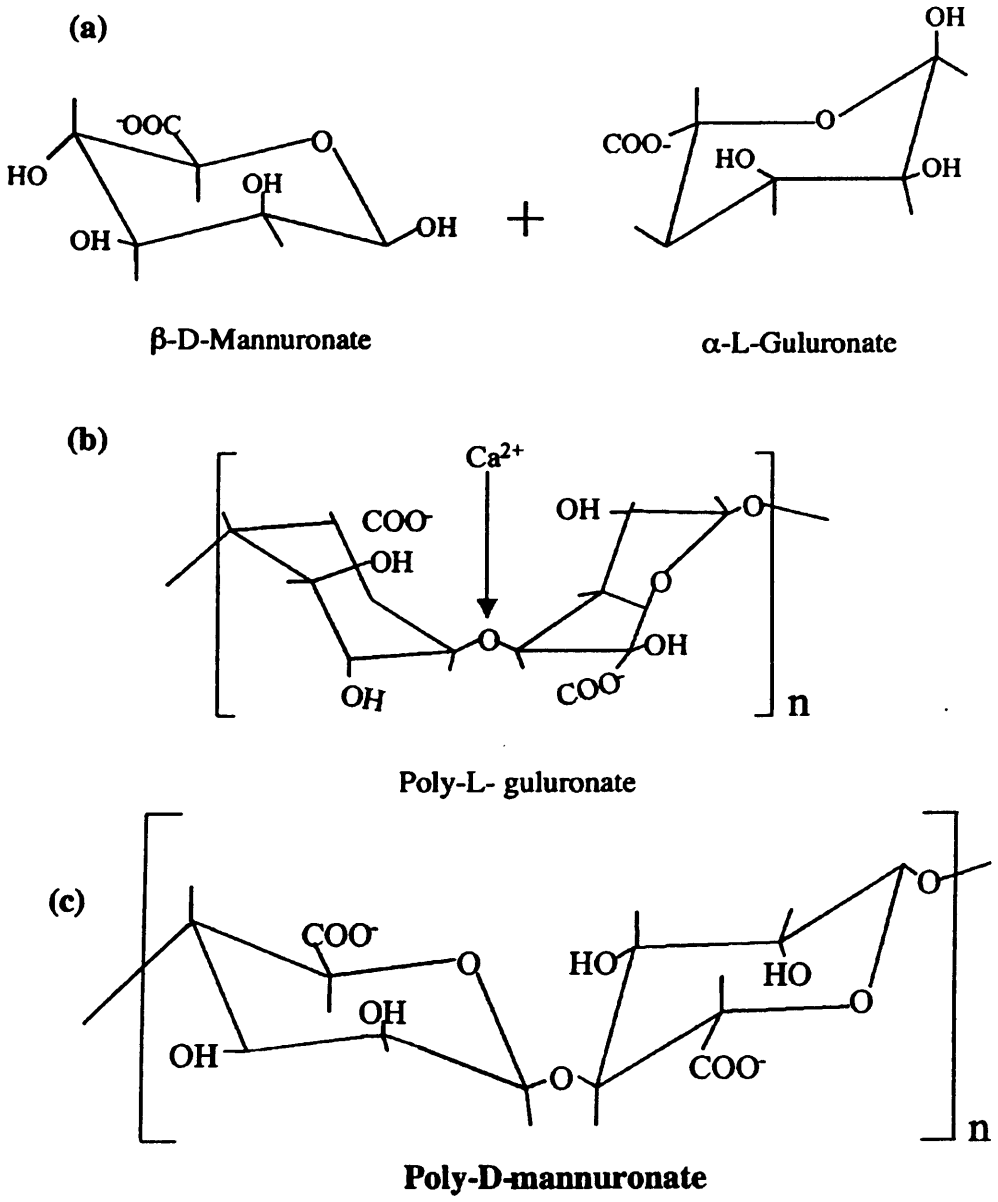

Figure 1.9 The chemical structure and conformation of alginates

for medicines. Alginate gels have also recently been used as microspheres, to encapsulate cells for transplantation (Lanza *et al.*, 1999). These structures act as a barrier between the transplanted tissues (e.g. chondrocytes, pancreatic cells and hepatocytes) and the immune system of the host (Loty *et al.*, 1998; Heald *et al.*, 1994; Haque *et al.*, 2005). Drugs can also be encapsulated within an alginate matrix or calcium alginate gels as a mechanism for sustained and controlled drug release. In addition, Duncan and colleagues (1995) developed alginate as water-soluble drug carriers e.g. for daunomycin (Al-Shamkhani and Duncan, 1995), and for the oral delivery of a human rhinovirus peptide (VP2) for oral immunisation (Morgan *et al.*, 1995). The group showed a reduction in the immunogenicity of the conjugated peptide, thought to be caused by the steric hindrance of the antigenic determinants from immune surveillance, and by the inhibition of the peptide epitopes from their matching immune receptors.

Conversely, alginates composed mainly of M monomers are inherently immunogenic and were used for these studies (Figure 1.9c). Otterlei and colleagues (1991) were the first to demonstrate that alginates stimulate human monocytes to produce TNF-α, IL-1 and IL-6. They found that only the M-blocks, not MG- or G-blocks of alginate were capable of producing high levels of all cytokines. Later, Otterlei *et al.* (1993) and Espevic *et al.* (1993) showed that binding of high M alginate to the CD14 receptor on monocyte cells, initiates TNF-α production. The CD14 receptor also binds lipopolysaccharides (LPS) (this is further discussed in Chapter 3), and uronic acid containing polysaccharides released from (and in the cell well as teichuronic acid) gram-negative bacteria (Jahr, 1997).

Optimal cytokine induction was induced by high M alginates MW ≥ 200,000 Da (Otterlei *et al.*, 1993). This implies that effects can only be obtained if the polymer presents a certain macromolecular conformation that results in a co-operative multiple-receptor aggregation (Berntzen *et al.*, 1998). To test this, Berntzen *et al.* (1998) covalently linked M-blocks to biodegradable bovine serum albumin (BSA) particles and found that the TNF-inducing potency of alginate was greatly enhanced in monocytes. The immunomodulatory effect of high M alginate has also been seen in murine peritoneal macrophages *in vivo*. Son *et al.* (2001), showed that macrophages isolated from high M alginate-treated mice, produce large amounts of the cytotoxic agents; nitric oxide, hydrogen peroxide and TNF-α. These

activated cells significantly inhibited the growth of tumour cells when compared to the effects seen for macrophages taken from control mice. In addition, Thomas *et al.*, (2000) have shown that alginates used in some wound dressings can activate macrophages leading to secretion TNF-α within the wound, and this aids wound healing.

1.6.2 Hyaluronic acid

HA is a unique, ubiquitous, linear, glucosaminoglycan (Figure 1.10). This polymer occurs as a hydrated gel in the extracellular matrix of higher organisms and streptococci, primarily as sodium hyaluronan. The polymer was chosen for these studies because of its documented immunological properties. Unlike other glucosaminoglycans, HA is synthesised at the inner face of the plasma membrane by hyaluronic acid synthases (HAS) 1, 2 and 3. It is not bound by protein, nor does it contain sulphuric groups. In animals, the highest concentrations of HA are found in connective tissue, hyaline cartilage, synovial fluid, the heart valve, fluids of the inner ear, and in the vitreous humor of the eye. The main source of HA is rooster combs, which contain the polymer at high concentration with respect to other tissue components. HA is also prepared from microorganisms, through a fermentation then isolation process.

The basic chemical structure of HA is repeated D-glucuronic acid and N-acetyl-D-glucosamine disaccharide units (linked together by β 1→3 and β 1→4 glycosidic linkages) (Figure 1.10). In solution, HA adopts a three-dimensional structure showing extensive intramolecular hydrogen bonding (Scott and Heatley, 1999). This restricts the conformational flexibility of the polymer chains, which gives hydrated HA its pseudoplastic and mucoadhesive properties, enabling it to function as a mechanical, transporting, or a water-retaining material.

Commercially, HA is used in a large number of applications including as components of cosmetics, and as treatment for rheumatology, orthopaedics and in ophthalmology. For example, the rooster comb HA, Healon® is used to protect exposed tissues during the insertion of an intraocular lens during eye surgery. Solutions of HA are also used as a vehicle for topical delivery of opthalmic drugs, and to produce synthetic tears. In osteoarthritis, HA is given to patients via intra-articular injections to reduce inflammation in the joints.

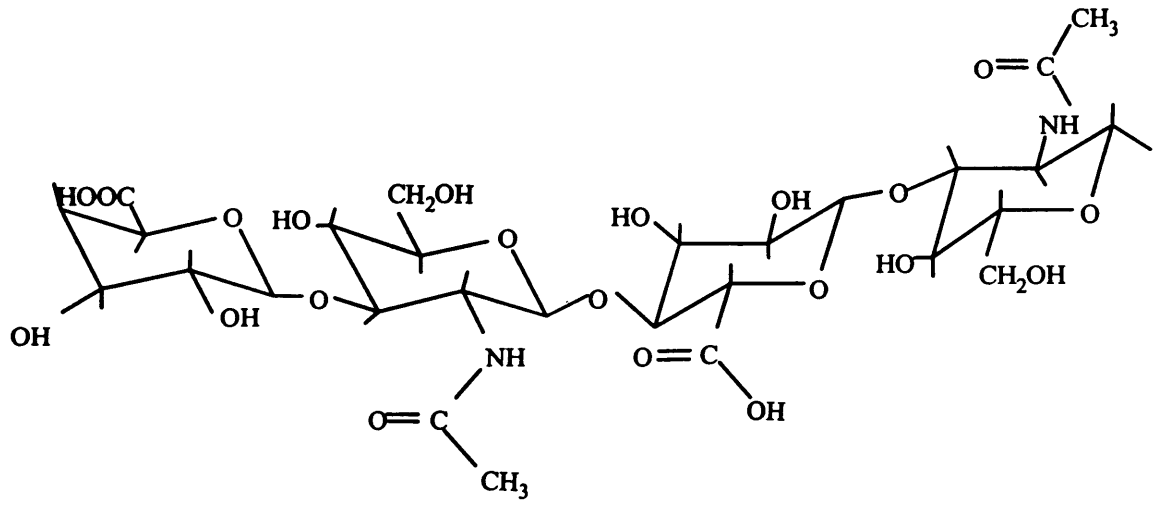

Figure 1.10 Hyaluronic acid

At the cellular level, protein-to-protein interactions with HA have been shown to play crucial roles in cell adhesion, cell motility, inflammation, wound healing, and cancer metastasis (Suzuki *et al.*, 2002; Kim *et al.*, 2004). More recently HA has been found to possess APC-stimulating activity (Mummert *et al.*, 2002) and the ability to induce cytokines (such as IL-12) from macrophage cells. Termeer *et al.* (2000) have recently shown that high molecular weight HA in the extracellular matrix is cleaved at sites of inflammation when it comes into contact with dendritic cells. In contrast, low molecular weight HA accumulates at sites of inflammation and can induce cytokine and/or chemokine production by alveolar and bone marrow derived macrophages (Hodge-Dufour *et al.*, 1997). These effects are highly specific for low molecular weight HA, as they are not induced by other glucosaminoglycans such as chondrotin sulfate, heparan sulfate or their fragmentation products (Termeer *et al.*, 2000).

Only small HA fragments of tetra- and hexasaccharide size, but not of intermediate size (80,000 – 200,000 Da) or high molecular weight (1000,000 – 6000,000 Da) induced immuno-phenotypic maturation of human monocyte-derived dendritic cells (Termeer *et al.*, 2000). This process is initiated by the Toll-like receptor 4 (TLR 4), a receptor complex associated with innate immunity and host defense against bacterial infection (Termeer *et al.*, 2002). Studies in mice have also shown HA to interact with CD44, the receptor for hyaluronic acid mediated motility (RHAMM) and intracellular adhesion molecule (ICAM) receptors. Binding of HA to CD44 induces murine B-cell activation, thus HA may play an important role in the regulation of autoimmune responses (Rafi *et al.*, 1997). The CD44 receptor is often up-regulated in cancerous cells, and has been shown to enhance the expression of c-Met, a proto-oncogene that encodes for a tyrosine kinase receptor, and thus tyrosine phosphorylation in human chondrosarcoma cells when stimulated by HA (Suzuki *et al.*, 2002).

1.6.3 Polyacrylic acid

PAcAs are synthetic, linear, mucoadhesive, homopolymers (Figure 1.11). They were chosen for these studies because besides their immune-stimulating activity, PAcA has also shown potential for enhancing drug delivery via the TJ pathway (discussed in Chapter 5, section 5.1). An overview of these polymers is given below.

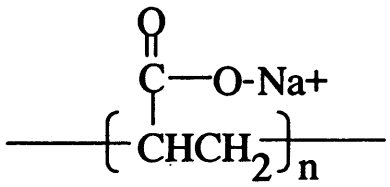

Figure 1.11 The chemical structure of the PAcA sodium salt

In the 1960's PAcAs were subject to intense interest as potential antiviral agents. De Somer and colleagues (1968a) were the first to demonstrate this phenomenon, initially using tissue culture, and later mice (De Somer *et al.*, 1968b). When investigating the mechanism of activity, De Somer and colleagues realised that the antiviral activity induced by PAcA was due to the induction of IFN (De Somer *et al.*, 1968b; De Clercq and De Somer 1969). The anionic nature of PAcAs appeared to be crucial for activity. Partially or completely neutralised PAcAs (containing < 85 % carboxyl groups) were inactive (De Somer *et al.*, 1968b). Another interesting observation is that the antiviral activity of PAcA persists in mice for at least 8 days after injection (De Clercq and Somer, 1969), suggesting the continuous presence of PAcA in the body. On another note, PAcA has also been found to be a mitogen for B-cells (Diamantstein *et al.*, 1976). Studies on the antiviral or immunomodulatory activity of PAcAs seem to have since ceased.

Today PAcAs are often cross-linked with an allyl ether pentaerythritol, allyl ether of sucrose, or allyl ether of propylene to be used as viscosity increasing, suspending, release modifying, tablet binding, or bioadhesive agents in pharmaceutical formulations. Recent studies with PAcAs have mainly focused on its use in oral drug delivery systems, particularly as a mucoadhesive (Smart *et al.*, 1984). Commercially available cross-linked PAcAs are marketed under the names Carbopol®, Carbomer® and Polycarbophil®, and have been used to aid gastrointestinal residence time and thus enhance drug uptake.

Microparticulate systems consisting of lightly cross-linked PAcA have also been found to widen the paracellular spaces between intestinal epithelial cells *in vitro*, by affecting their TJ (Kriwet and Kissel, 1996; this is discussed in more detail Chapter 5, section 5.1). This may be due to the chelation of extracellular calcium ions by the polymer, not its bioadhesive properties. Moving away from microparticles, PAcA has also recently been cross-linked with polyethyleneoxide and polypropylene, to form a new pH- and temperature-sensitive microgel that is suitable for drug delivery via the gut (Bromberg and Alakov 2003).

Once again, as with IFN induction, the density of carboxyl groups on the polymer chain also appears to be important for mucoadhesion. Park and Robinson (1987) have concluded that for mucoadhesion to occur, PAcA must have at least 80

% protonated carboxyl groups, and that adhesion occurs through hydrogen bonding. However, as these interactions are affected by ionic strength and pH, modified PAcAs have been created. For example, PAcA modified by the introduction of cysteine moieties has displayed excellent mucoadhesive properties (Nafee *et al.*, 2004). In addition, thiolated PAcA showed the ability to form covalent bonds with cysteine-rich subdomains of mucins (Gum *et al.*, 1992). It has been suggested that these polymers also enhance oral bioavailability by inhibiting the serine protease, trypsin (Anlar *et al.*, 1993).

1.6.4 Polyamidoamine dendrimers generation 3.5

Polyamidoamine (PAMAM) dendrimers are a family of well defined, highly branched, hydrophilic, globular macromolecules, that were first created by pioneering chemistry of Tomalia and colleagues during the 1980's (Tomalia, 1985). The production of these molecules (known commercially as Starburst® dendrimers) occurs via a procedure known as divergent synthesis, a process in which dendritic structures are grown by repetitive reaction steps starting from a multifunctional core (to give increasing 'generations'). The core of PAMAM dendrimers consists of ethylenediamine, and the number and charge of their dendritic end-groups (at neutral pH) differs depending on the generation of the molecule (Tomalia, 1995).

Half-generation PAMAM dendrimers e.g. generations 1.5 - 7.5, have anionic carboxyl terminal groups, whilst full generation PAMAM dendrimers e.g. generations 1 - 10, have amine terminal groups (www.sigmaaldrich.com/Area_of_interest/ Chemistry/Materials_Science/BiocompatibleBiodegradable/Polymers.html, accessed 13/12/02). Furthermore, the molecular size of each full generation PAMAM dendrimer increases by approximately 1 nm per generation (Tomalia *et al.*, 1993).

The unique chemistry of PAMAM dendrimers has enabled them to be applied to several disciplines within the pharmaceutical industry. The central core (dendritic box) regions of PAMAM dendrimers are relatively hollow compared to their densely-branched outer layers, and can thus be used to encapsulate (therapeutic or poorly soluble) molecules for drug (Kannan *et al.*, 2004) and gene (DeLong *et al.*, 1997; Bielinska *et al.*, 1997) delivery. Cationic PAMAM dendrimers have primarily been used for this purpose. Furthermore, the surface chemistry of PAMAM dendrimers, with their high number of end-groups, can be used to attach a variety of moieties for

targeting or bioadhesion. As a result, PAMAM dendrimers have also been used as platforms for the development of cancer therapeutics (Malik *et al.*, 1999).

More recently the use of PAMAM dendrimers as drug carriers for transepithelial and -endothelial transport has also been explored using a variety of epithelial and endothelial monolayer models (reviewed in Chapter 5, section 5.1). These dendrimers have shown the ability to cross epithelial barriers via both paracellular (El-Sayed *et al.*, 2003) and transcellular (Jevprasesphant *et al.*, 2003) pathways (see Figure 1.4, as discussed in Chapter 5, section 5.1).

The PAMAM generation 3.5 dendrimers (PAMAM 3.5) chosen for these studies have 64-carboxylate end groups (Figure 1.12), and are approximately 4.5 nm in size. They have been found to cross the rat intestine in an extremely rapid and efficient manner (Wiwatanapatapee *et al.*, 2000), making them of particular interest for the drug delivery objectives in this project (see section 1.12). Furthermore, the high number of anionic terminal end groups of these dendrimers may also enable them to induce cytokines.

1.7 Biological rationale for the cytokines chosen for this work

The majority of polymers selected for this project have been shown to be able to induce cytokine production from a range of cells including macrophage, mast, dendritic, NK, T- and B-cells (as summarised in Table 1.2). These cells are the main producers of cytokines, and are capable of making a wider spectrum of these proteins compared to all other cells. However, each nucleated cell has its own cytokines that it can synthesise. Furthermore, the particular cytokines made by a cell are dependant upon the type of stimulus, its nature, duration and intensity, as well as the presence of other factors (e.g. other cytokines, hormones, cell contact interaction etc).

Three cytokines were selected for these studies as each has been implicated in inducing TJ permeability or for its antitumour properties.

1.7.1 Interferon-gamma

IFN-γ is an interesting antiviral cytokine that plays an essential immunomodulatory role in virtually all cells. It is hugely upregulated in patients suffering from trauma, infections, cancer and autoimmune diseases (reviewed in Billau, 2000). The main sources of this lymphokine are $CD4^+$ and $CD8^+$ T-cells and

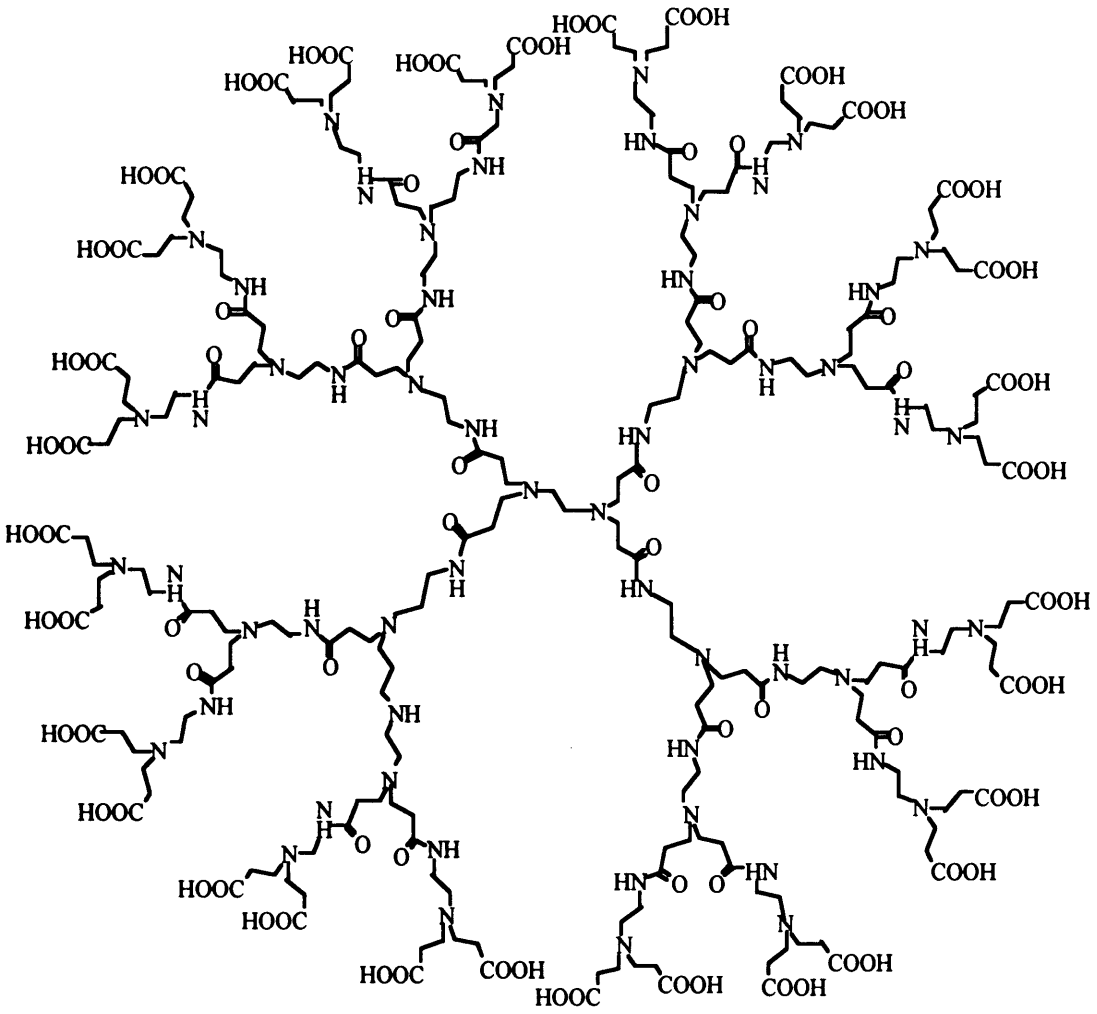

Figure 1.12 Molecular structure of the polyamidoamine generation 3.5 dendrimer

Table 1.2 Summary of the immunological properties of the polymers chosen for this work.

Polymer	Type	Charge	Immunomodulatory Activities	Reference
Alginic acid	Natural polysaccharide	Anionic	Binds CD14 receptors	(Jahr *et al.*, 1997); (Flo *et al.*, 2000)
			- IL-1, IL-6 & TNF-α from monocytes	(Otterlei *et al.*, 1991); (Jahr *et al.*, 1997)
			- TNF-α from macrophage	(Thomas *et al.*, 2000)
			Binds Toll-like receptor 2 & 4 in macrophages	(Flo *et al.*, 2002)
Hyaluronic acid	Natural polysaccharide	Anionic	Binds CD44 receptors	(Noble *et al.*, 1993)
			- TGF-β from eosinophils	(Ohkawara *et al.*, 2000)
			- IL-8 from lung epithelia	(Mascarenhas, 2004)
			- TNF-α from macrophage	(Boyce *et al.*, 1997)
			Induce B-cell activation	(Rafi, 1997)
			Involved in antigen presentation	(Mummert *et al.*, 2002)
			Activates dendritic cells via Toll-like receptor 4	(Termeer *et al.*, 2002)
PAcA	Synthetic, linear	Anionic	*- IFN-γ production from serum of mice*	(De Somer, 1968a); (De Somer, 1968b); (De Clercq, 1969); (Claes, 1970)
PAMAM 3.5	Synthetic, branched	Anionic	Rapid transcellular transport across rat gut[§]	(Wiwatanapatepee *et al.*, 2000); (El-Sayed *et al.*, 2003)
			Increase permeability of Caco-2 cells[§]	
PEI	Synthetic, branched	Cationic	Thought to stimulate the immune system	(Moroson, 1971)
			Induces IL-2, & TNF-α from Caco-2 cells	(Goricha, 2001); (Puckey, 2002)

[§] Cytokines may play a role in this process

NK cells, although production has also been observed in B-cells (reviewed in Abbas *et al.*, 2000). The biological function of IFN-γ *in vitro* and *in vivo* is cell-type specific, and differs in the presence of other cytokines. Generally, both TNF-α and IL-1 synergise with IFN-γ, whilst IL-4 antagonises its actions (reviewed in Billau, 2000).

An important role of IFN-γ is as a modulator of the cellular activities responsible for inflammation, as it induces macrophages to release reactive oxygen intermediates, hydrogen peroxide (Nathan, 1985) and TNF-α. Macrophages and monocytes are also induced to transcribe the genes encoding granulocyte-colony stimulating factor (G-CSF) and macrophage-colony stimulating factor (M-CSF). This series of events enhances the intracellular killing of parasites and tumour cells and is antagonised by IFN-α and -β (De Maeyer, 1998). Moreover, IFN-γ is a well-known activator for endothelial cells, T-cell proliferation, and the cytolytic induction of NK cells. Many cells including B-cells, T-cells, macrophages and tumour cells are induced by IFN-γ to express MHC class II antigens, thus IFN-γ is also responsible for regulating the antigen-specific immune response. However, it takes several hours for this to occur. IFN-γ also stimulates the expression of CD4 in T-helper cells and the expression of high-affinity receptors for IgG in myeloid cell lines, neutrophils, and monocytes (reviewed by Billiau and Vandenbroeck, 2000; reviewed by Tsanev and Ivanov, 2002).

Although immuno-modulation is undoubtedly the primary role of IFN-γ, it also exhibits a direct antiviral action by stimulating specific genes that are also involved in the antiviral activity of IFN-α and IFN-β (De Maeyer, 1998). Some of these genes contain the regulatory sequences; interferon-stimulated response elements (ISRE) and interferon response sequences (IRS), within their promoter regions that function as binding sites for a number of transcription factors.

1.7.2 Interleukin-2

This important lymphokine (mainly produced by $CD4^+$ T-cells) was chosen for this work not only because it is responsible for T-cell clonal expansion following antigen recognition (see Figure 1.3), but also because it plays a key role in regulating cellular immune responses by augmenting B-cells and macrophages to secrete

produce enough IL-2 to stimulate their own proliferation (see Figure 1.3).

The synthesis of IL-2 is tightly regulated at both transcripti translational levels. The promoter for IL-2 contains several specific bindin specific transcription factors (e.g. NF-AT and TCF-8) that regulate its prod variable repressor also modulates the post-transcriptional processing of IL- so that approximately 98 percent of the IL-2 mRNA remains unprocessed. I is recognised by the IL-2 receptor (IL-2R), which consists of three non-c associated α-, β- and γ-subunits. The α- and β-chains are involved in binding, whilst the β- and γ-chains function as signal transducers. B subunits are members of the type I cytokine receptor family (reviewed in *al.*, 2000). When IL-2 engages with its receptor a series of intracellu transduction pathways (JAK/STAT, phosphatidylinositol-3 kinase and Ras pathways) is initiated leading to a rapid intracellular rise of cyclin D2 and proteins. These proteins bind and activate different cyclin-dependant kin phosphorylate (i.e. activate) several proteins such as cyclin, that bring transition from the G1 to the S phase of the cell cycle. In addition, IL-2 als the cytosolic levels of p27, a protein inhibitor of the cyclin-kinase comp survival is promoted by IL-2-induced production of the anti-apoptotic protei

The potent immune stimulating activity of IL-2 has allowed it to b effective cancer therapy. Rosenberg and colleagues (1985) were the demonstrate the anti-tumour capability of IL-2 when they treated pati systemic metastasis. However the systemically high doses of IL-2 Rosenburg *et al.* (1985) showed severe toxic effects in approximately 20 % patients. In light of this, Otter and colleagues (1999) administered repeated IL-2 injections directly only at tumour sites to stimulate the activity of th infiltrating cells and avoid systemic toxic effects. Results from this st

promising in a range of cancers and experimental animals, but still showed some toxicity. Nonetheless, later experiments with a single high-dose of IL-2 at the tumour site gave no observable toxic effects (Otter, 1999). Therefore this cytokine would have great significance for the cancer therapy aspects of this work.

The consequences of a deregulated expression of IL-2 have been studied in transgenic mice expressing the human IL-2 gene. Mice expressing IL-2 in the thymus, spleen, bone marrow, lungs, muscle and skin, show pronounced growth retardation and die prematurely. They have few Purkinje cells in the cerebellum and show a focal infiltration of lymphocytes, leading to pneumonia. In addition, their spleens show a massive increase of lymphocytes. IL-2-deficient mice have also been analysed with respect to immune responses *in vivo*. Primary and secondary cytotoxic T-cell responses against the virus in these mice are normal, the T-helper cell responses are delayed but functional, and NK cell activities are markedly reduced but inducible. Collectively, these observations suggest that other factors may compensate for the IL-2 defects *in vivo*.

1.7.3 Tumour necrosis factor-alpha

TNF-α was originally identified as a factor present in animal serum after treatment with bacterial LPS that caused necrosis of tumours (reviewed in Abbas *et al.*, 2000). It is now known to kill transplanted and malignant tumours *in vivo*, and at picomolar concentrations in tumour cells *in vitro*. The anti-tumour effects of TNF-α are not based on tumour cytotoxic effects, but are actually largely due to the capacity of TNF-α to stimulate endothelial cells of newly formed blood vessels to produce clotting factors resulting in their occlusion and necrosis (Joost and Feldmann, 2001).

Therefore, the principle physiologic function of TNF-α (shown by recent transgenic mice studies) is to act as a key regulator of inflammation in host defence rather than a cytotoxic anti-tumour factor (reviewed in Tracey and Cerami, 1994). Depletion of TNF-α results in a failure to ward off infections, revealing its ability to stimulate the recruitment of neutrophils and monocytes to sites of infection and to activate these cells to eradicate microbes. TNF-α mediates these effects by evoking several effects on vascular endothelial cells and leukocytes. Firstly, TNF-α induces vascular endothelial cells to express leukocyte cell adhesion molecules, enabling them to bind circulating neutrophils, monocytes and lymphocytes respectively to

recruit them at sites of infection. Furthermore, TNF-α also stimulates endothelial cells and macrophages to secrete chemokines that induce leukocytes by chemotaxis. It also acts on mononuclear phagocytes to secrete IL-1.

The major cellular sources of TNF-α are activated mononuclear phagocytes, neutrophils, T- and NK-cells respectively (reviewed in Tracey and Cerami, 1994). Stimulated peripheral neutrophilic granulocytes, inactive cells, transformed cell lines, astrocytes, smooth muscle cells, and fibroblasts can secrete smaller amounts. In mononuclear phagocytes, TNF-α is synthesised as a non-glycosylated type II membrane protein and is expressed as a homotrimer. The amino terminus of membrane TNF-α is intracellular, whereas the carboxy terminus is large, extracellular and a ligand termed TNF-receptor 2 (TNF-R2). The secreted form of TNF-α is produced by the proteolytic cleavage of a 17,000 Da fragment of each subunit by metalloproteinase from the macrophage plasma membrane. Secreted TNF-α circulates in the body as a stable pyramidal-shaped homotrimer of 51,000 Da. Each side of the pyramid is formed by one subunit, and the base of this structure provides a large surface area for binding multiple receptors.

Two distinct TNF receptors of molecular sizes of 55,000 Da (TNF-R1) and 75,000 Da (TNF-R2) have been described on all somatic cells except mature erythrocytes. Both bind TNF-α with low affinity. When TNF-α engages with these receptors, TNF receptor-associated proteins (TRAFs) attach to their cytoplasmic domains, as the first step towards an intracellular signaling cascade that ultimately ends in the activation of the transcription factors; nuclear factor κB and activation protein-1 (AP-1). In addition, TNF-R1 induced signals have also been shown to trigger apoptosis in certain cell lines (reviewed in Abbas *et al.*, 2000).

1.8 Aims of this thesis

From a drug delivery perspective, it is interesting to tie together the observations that some biologically active polymers can modulate permeability, whilst others can stimulate the release of cytokines, as, at present there appear to be no studies on this area.

Before investigating whether alginate, HA, PAcAs or PAMAM generation 3.5 dendrimers could be used to enhance drug delivery across rat intestinal tissue, it was

first considered important to examine the cytotoxicity of these molecules *in vitro*. This information was then used to ascertain polymer concentrations that were non-toxic for further experiments. Each polymer was incubated with two model cancerous cell lines, at concentrations ranging from 1 – 0.001 mg/mL, and their effect on cell viability was measured using the MTT assay (Mossman, 1983). With this information, the effect of polymers on TNF-α, IFN-γ or IL-2 release from either B16F10 or RAW 246.7 cells was measured by ELISA assay (Chapter 3). Cytokine release from polymer-incubated DU937 cells (used as a positive control for TNF-α release) was also investigated.

To test the hypothesis that cytokines can permeabilise biological barriers, the effects of rTNF-α, rIFN-γ and rIL-2 on the transport of FITC-dextran across rat intestinal tissue with or without Peyer's patches was measured using the vertical diffusion system (Chapter 4).

The effects of polymers on FITC-dextran transport were also measured using the vertical diffusion system (Chapter 5), and to measure the effect of the polymers themselves on transport across rat intestinal tissue they were fluorescently labelled with Oregon green (OG). In parallel experiments the uptake of the OG-labelled polymers by Caco-2_{BBe} cells were also measured using flow cytometry (Chapter 6).

Details of the materials and general methods that were used for these studies are described in the following Chapter.

CHAPTER 2:

Materials and General Methods

2.1 Materials

All the materials and reagents used in these studies are given below, as are the suppliers. The general methods of the experiments used for this work are described in the following sections.

2.1.1 General chemicals

Methanol, ethanol and sodium chloride were from Fisher Scientific, UK. Phosphate buffered saline (PBS) tablets were from Oxoid, UK. Klericide 5® was obtained from Shield Medicare, UK. Sigmaclean® water bath treatment was from Sigma-Aldrich, UK. Pyruvate, nicotimanamide adenine dinucleotide (NADH), hydrochloric acid (HCl), and tris(hydroxymethyl)aminomethane (Tris) were from Sigma-Aldrich, UK. Limulus amoebocyte lysate (LAL), control standard endotoxin, and endotoxin-free LAL reagent water were purchased from Charles Rivers Laboratories, UK. 1-Ethyl-3-(-3dimethylaminopropyl)-carbodiimide (EDC), and N-hydroxysulfosuccinimide (sulfo-NHS) were from Fluka, Germany. Oregon green-cadaverine (OG_{cad}) was from Molecular Probes™, UK.

2.1.2 Polymers

PAcA in a sodium salt form ($sPAcA_{30}$; molecular weight (MW) = 30,000 Da; 40 % w/w in H_20), and PAcAs of MW = 100,000 Da ($PAcA_{100}$; 35 % w/w in H_20) and 450,000 Da ($PAcA_{450}$), PAMAM generation 3.5 dendrimers (MW = 12,931 Da; 10 % w/w in methanol), polyethylenimine (PEI; MW = 750,000 Da; 50 % w/v in H_20), dextran (MW = 68,800 Da), and fluorescienisothiocyanate-dextran (FITC-dextran) of MW = 4,000 Da, were obtained from Sigma-Aldrich, UK. Alginate (MW = 240,000 Da) and HA (MW = 50,000 - 8000,000 Da) were purchased from MP Biomedicals, USA. HA in a sodium salt form (sHA; MW = 3,000 - 58,000 Da), was obtained from Fluka, Germany. Pullulan standards (MW = 738, 5,900, 11,800, 22,800, 47,300 and 112,000 Da) for gel permeation chromatography (GPC) were from Polymer Laboratories, UK.

2.1.3 Animals and cell lines

Albino, male Sprauge Dawley (outbred) rats weighing from 200 - 250 g were obtained from Harlan, UK. B16F10 adherent, murine melanoma cells, and U937 non-adherent, human histocytic lymphoma (monocyte) cells, and Caco-2_{BBe} brush-

border expressing, colon caricnoma cells were from ATCC, UK. The RAW 246.7 semi-adherent, murine macrophage/monocyte, and ECV304 adherent, human bladder carcinoma, endothelial-like, epithelial cell lines were from ECACC, UK. The media used for all cells is given in Table 2.1.

2.1.4 Reagents for tissue and cell culture

Media (Table 2.1) and supplements for cell and tissue culture included Rose Park Memorial Institute (RPMI) 1640, minimal essential media (MEM), Dulbecco's minimal essential media (DMEM), Hank's balanced salt solution (HBSS) and foetal bovine serum (FBS) of both normal and low endotoxin grade were purchased from Invitrogen Life Technologies, UK, as was 0.05 % trypsin/0.53 mM sodium ethylenediaminetetraaceticacid (EDTA). Trypan blue solution, 0.4 % w/v, 3-(4,5-dimethylthiazol-2-yl)-2,5-diphenyl-2H-tetrazolium bromide (MTT), analytical grade, 98 % anhydrous, dimethyl sulphoxide (DMSO), and phorbol 12-myristate 13-acetate (PMA) were obtained from Sigma-Aldrich, UK. Medical grade carbogen (5 % CO_2, 95 % O_2), nitrogen gas, and liquid nitrogen were supplied by BOC, UK.

2.1.5 Cytokines and Quantikine® sandwich-ELISA kits

Lyophilised, recombinant rat IFN-γ (rIFN-γ) was from MP Biomedicals, USA, whilst lyophilised, recombinant rat TNF-α (rTNF-α) and IL-2 (rIL-2), with bovine serum albumin (BSA) as a carrier protein, were obtained from R&D Systems, UK. All sandwich-ELISA kits including murine TNF-α (mTNF-α), IL-2 (mIL-2) and IFN-γ (mIFN-γ) and human TNF-α (hTNF-α) and IL-2 (hIL-2), were also from R&D Systems, UK.

Each ELISA kit contained the following materials and reagents; wash buffer concentrate (25 x concentrated buffered surfactant solution), colour reagents A and B (stabilised hydrogen peroxide and stabilised chromogen (tetramethylbenzidine)), adhesive plate covers, 96-well polystyrene microplates (12 strips of 8 wells coated with immunoglobulins (Igs) against the cytokine of interest), conjugate (polyclonal Ig against cytokine of interest, conjugated to horseradish peroxidase (HRP)), standard (lyophilised recombinant cytokine in a buffered protein base), assay and calibrator diluents (buffered protein bases), and an acid stop solution.

Table 2.1 Tissue culture media and passage numbers of each cell line used.

Cell line	**Culture media (with 10 % v/v FBS)**	**Cell passage numbers used**
ECV304	DMEM	158 - 168
B16F10	RPMI with 25 mM HEPES, L-glutamine and phenol red	9 – 29
U937 and DU937	RPMI with L-glutamine and phenol red	1 – 21
RAW 246.7	DMEM with 1000 mg/L glucose, Glutimax™, pyruvate and phenol red	9 – 29
Caco-2_{BBE}	DMEM with 4000 mg/L glucose, Glutimax™, pyruvate and phenol red HBSS (for flow cytometry only)	60 – 80
Rat intestinal epithelium	MEM with Earle's salts, without glutamine or phenol red	-

2.2 Equipment

2.2.1 General equipment

Disposable, black, flat-bottom 96-well plates, and transparent, sterile 96- and 24-well plates for tissue culture, were from Corning Incorporated, UK. Vented-cap tissue culture flasks of 25 cm^2, 75 cm^2, and 150 cm^2 volumes, and cell scrapers were obtained from Fisher Scientific, UK. Single and multichannel, variable volume, manual pipettes, and a caprex L2G Charles Austen aspirator, for the removal of cell supernatants, was from Jencons, UK. The sterile quills to attach to the aspirator were from Fisher Scientific, UK. Sterile pots and containers including 7 cm^3 bijous, 25 cm^3 universal containers, 60 cm^3 containers, disposable plastic pipette tips, sterile plastic syringes and stripettes (for volumes of 5 mL, 10 mL and 25 mL) were from Elkay, UK. The automatic pipetter for measuring these volumes was from Fisher Scientific, UK. Sterile needles (23 G) were from WLS, UK. Filters with 0.2 μM pores were from Sartorius Ltd, UK. A Class II Microflow Biological safety cabinate for tissue culture work was from Servicecare, UK. The 37 °C tissue culture incubator (supplemented with 95 % O_2, 5 % CO_2 gas), was supplied by Wolf Laboratories, UK.

A DM IL Leica light microscope to view cells between and during experiments was from Leica, Germany. Photographs of individual cell lines were taken with a Leica DM IRB microscope and camera, using Improvision® Openlab™ software. A Varifuge 3.0 RS centrifuge was obtained from Heraeus Instruments, Germany, and the Toledo 320 pH meter from Mettler Toledo, Switzerland. The sonicator was supplied from Decon®, UK. The lyophiliser was from FTS Systems, Holland. Protein de-salting (PD)-10 columns were from Amersham Biosciences, UK. All endotoxin-free disposable pipette tips, 96-well plates and dilution tubes, were from Charles Rivers Laboratories, UK. The vertical diffusion chamber was obtained from Precision Instruments Design, USA. Thin layer chromatography (TLC) plates (0.2 mm silica 60 with fluorescent indicator UV_{254}) were from Macherey-Nagel, Germany. Dialysis membrane was from Spectrum® Laboratories Inc, USA. Glass microscope slides (76 x 26 mm) and coverslips (22 x 40 mm) were from Menzel-Glaser®, Germany.

2.2.2 Analytical equipment

Ultraviolet (UV) absorbance was measured using a sunrise UV-absorbance plate reader from Tecan, Australia, and a Cary 1G UV-visible spectrophotometer from Varian, Australia. A hand-held UV lamp was from UVP, UK. Fluorescence

was measured using a Fluorostar Optimar plate reader from BMG Labtechnologies, Germany. Single detection GPC was performed using a Gilson 133 refractive index (RI) detector from Gilson Inc., USA, a Jasco PU-980 intelligent high-performance liquid chromatography pump from Jacso UK Ltd, UK, and two GPC columns (TSK-gel G3000PW$_{XI}$ and TSK-gel G4000PW$_{XL}$), were from Supelco, UK. Polymer Laboratories, UK, provided Caliber software for GPC analysis. A kinetic, heated plate reader for Limulus amoebocyte lysate (LAL) assays was purchased from Charles Rivers Laboratories, UK.

2.3 General methods

All methods specified below describe the common procedures used in this thesis. In some cases, a more detailed description of these methods, and more specific technical methods are given in each experimental chapter.

2.3.1 Cell culture

All cell lines utilised for this thesis were kept under aseptic conditions, without the addition of penicillin or strepomycin, and were mycoplasma-free. The manipulation of all cell lines was carried out in a Class II laminar flow hood, pre-sterilised by Klericide®, and 70 % v/v ethanol (in ddH_2O) spray. Only sterile (autoclaved) PBS and double-distilled water (ddH_2O), or tissue culture medium containing 10 % v/v FBS were used. Any disposable tissue culture equipment that came into contact with the hood was first sprayed with 70 % v/v ethanol in ddH_2O. In addition, all solutions that were added to cells were pre-warmed to 37 °C in the water bath (containing 5 L ddH_2O and 1 mL Sigmaclean® water bath treatment). It is also important to note that all polymer solutions that were added to the cells were filter-sterilised first.

Thawing of cryopreserved cells

Cryogenic vials of frozen cells were kept at –196 °C in liquid nitrogen until required. Upon use, the frozen ampoules were removed from the liquid nitrogen and were briefly defrosted in the water bath. Tepid cell suspensions were added to a universal container with 20 mL of media, and were pelleted by centrifugation for 5 min at 1000 g. Supernatants were aspirated from the pelleted cells and were replaced with 5 mL of fresh media. A syringe and needle was then used to gently break the pellets and re-suspend cells before they were placed into 25 cm^2 flasks. Cells were

then grown for 48 h in the incubator before being viewed under the light microscope to check their growth. Their culture medium was then changed.

Routine maintenance of cells

Cells were kept for 20 passages and were routinely viewed under a light microscope to check their growth. Media in the flasks was changed twice weekly to avoid depletion of essential nutrients. Only flasks that were > 70 % confluent were sub-cultured at a 1:10 ratio, into 75 cm^2 flasks. For adherent cell lines, confluent flasks were aspirated of medium, washed once with PBS, and briefly incubated with 1 mL trypsin-EDTA at 37 °C (to cause cell detachment). Trypsin-EDTA was then diluted with 10 mL of tissue culture media and cell suspensions were centrifuged for 5 min (1000 g) at room temperature. Semi-adherent cell lines were removed with a cell scraper, whilst non-adherent cells were centrifuged in their medium. A 1 mL aliquot of cells re-suspended in fresh media was added to 9 mL of new media inside new 75 cm^2 flasks.

Cell counting and assessment of viability using trypan blue

Aliquots (100 μL) of suspended cells were mixed at a 1:1 v/v ratio with trypan blue solution (containing 50 % v/v PBS) in an eppendorf tube. Trypan blue is a blue dye that only penetrates the membranes of dead cells and was thus used to approximate cell viability. A 20 μL volume of the trypan blue-cell mixture was added to a Heamocytometer slide, with silver-stained Neubauer ruling, roofed with a glass cover slip (adhered by capillary force). The light microscope was used to count the number of cells in each of the 4-squared Neubaur grids (each divided into 16 sections) surrounding the central square with 25 sections. Non-viable cells were stained blue and were not counted. The average number of cells per grid was found by dividing the total number of cells counted by 4. This number was then multiplied by 2 to account for trypan blue dilution. This gave the number of cells per mL of cell suspension, and was used to calculate the dilution factors for each experiment.

Freezing cells for cryopreservation

Batches of cells were routinely frozen to maintain stocks. Cells were grown to confluency in 150 cm^2 flasks, removed, centrifuged into a pellet, re-suspended, counted (as described above), and diluted to give 1 x 10^6 cells/mL suspension in

sterile-filtered FBS containing 10 % v/v DMSO. One-mL aliquots of this suspension were placed into 1 mL cryogenic vials, wrapped in damp tissue paper and placed at – 20 °C for 1 h, – 80 °C overnight, and at – 196 °C in liquid nitrogen the following morning.

2.3.2 Measurement of cell growth curves using the MTT assay

Before looking at the cytotoxicity of our polymers, growth curves for each cell line (B16F10, ECV304, RAW 246.7, Caco-2_{BBe} and U937) were determined using the colourimetric MTT assay (Figure 2.1). This ensured all experiments were carried out during the exponential phase of cell growth (Figures 2.2a, b, c, d and e respectively).

The MTT assay was initially introduced by Mosmann (1983), and was later developed by Sgouras and Duncan (1990), for screening polymer biocompatibility. This assay is based upon the fact that MTT is a soluble, yellow hydrogen acceptor that can only be reduced by the products (NADH and NADPH) of the mitochondrial enzyme succinate-dehydrogenase (Slater *et al.*, 1963) in respiring cells. Metabolised MTT forms dark-blue formazan crystals that are readily dissolved in DMSO and can be read spectrophotomically (see below), where the optical density is proportional to the quantity of viable tissue.

For this assay, cells were first seeded into sterile, flat-bottomed, 96-well plates (100 μL/well using a multi-channel pipette), by removing them from their flasks, centrifuging (1000 g), re-suspending, counting and diluting them in media to 1 x 10^4 cells/mL. The wells around the perimeter of the plates were always laced with 100 μL/well of PBS (to prevent surrounding wells from dehydration). Seeded plates were incubated for 24 h before the addition of MTT[†].

Each day 20 μL of MTT solution/well was added to a column of wells in the 96-well plates and the plates were returned to the incubator for 5 h. Following this media was carefully aspirated from the wells and was replaced with DMSO (100 μL/well) to solubilise blue formazan crystals. Plates were then incubated for a further 30 min, until the crystals had dissolved. The optical density of the plates was then read in a UV plate reader set at 550 nm. The formazan-DMSO mixture was then removed from the wells (under local exhaust), and replaced with PBS (100 μL/well).

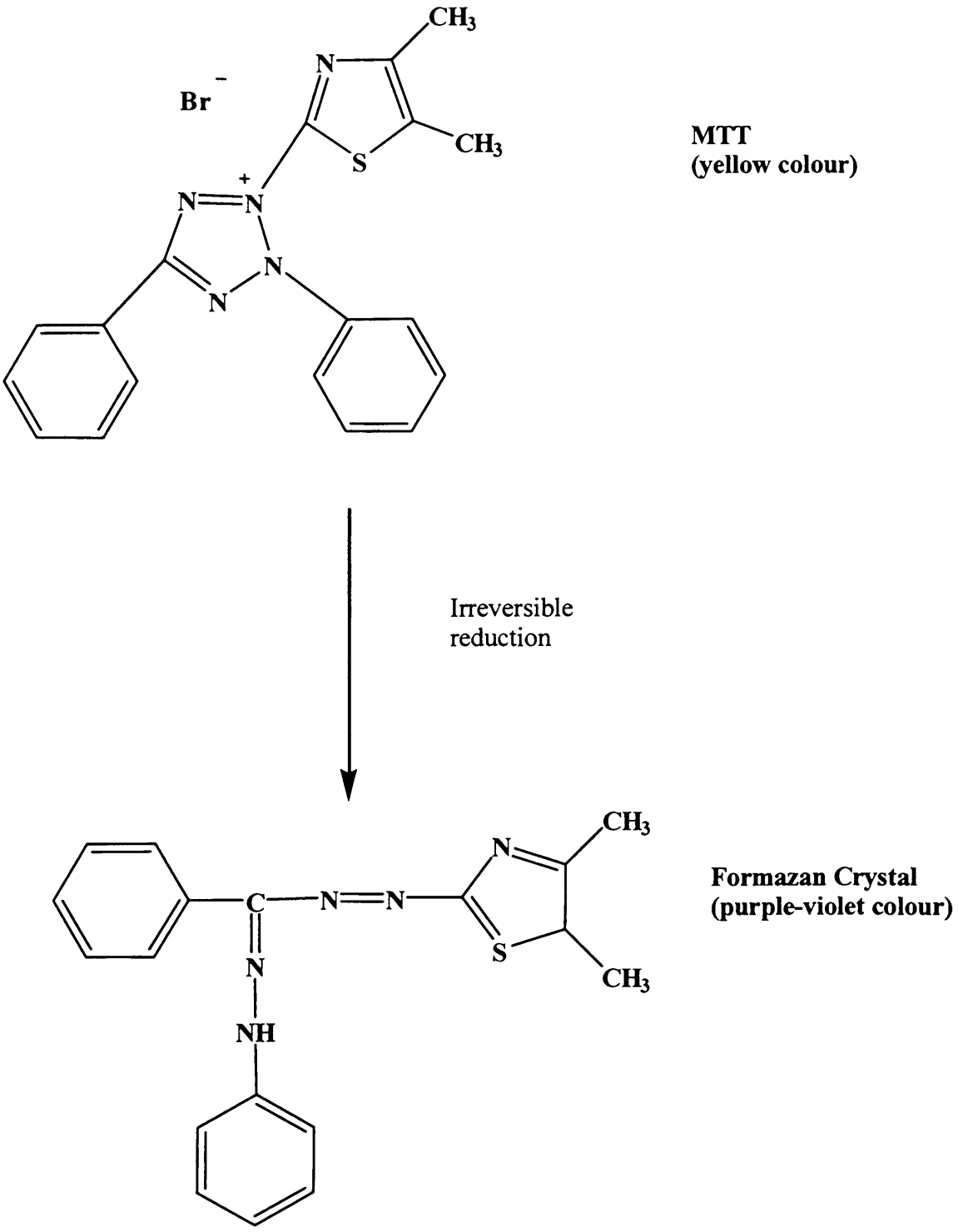

Figure 2.1 Chemical structure of MTT before and after reduction by respiring cells

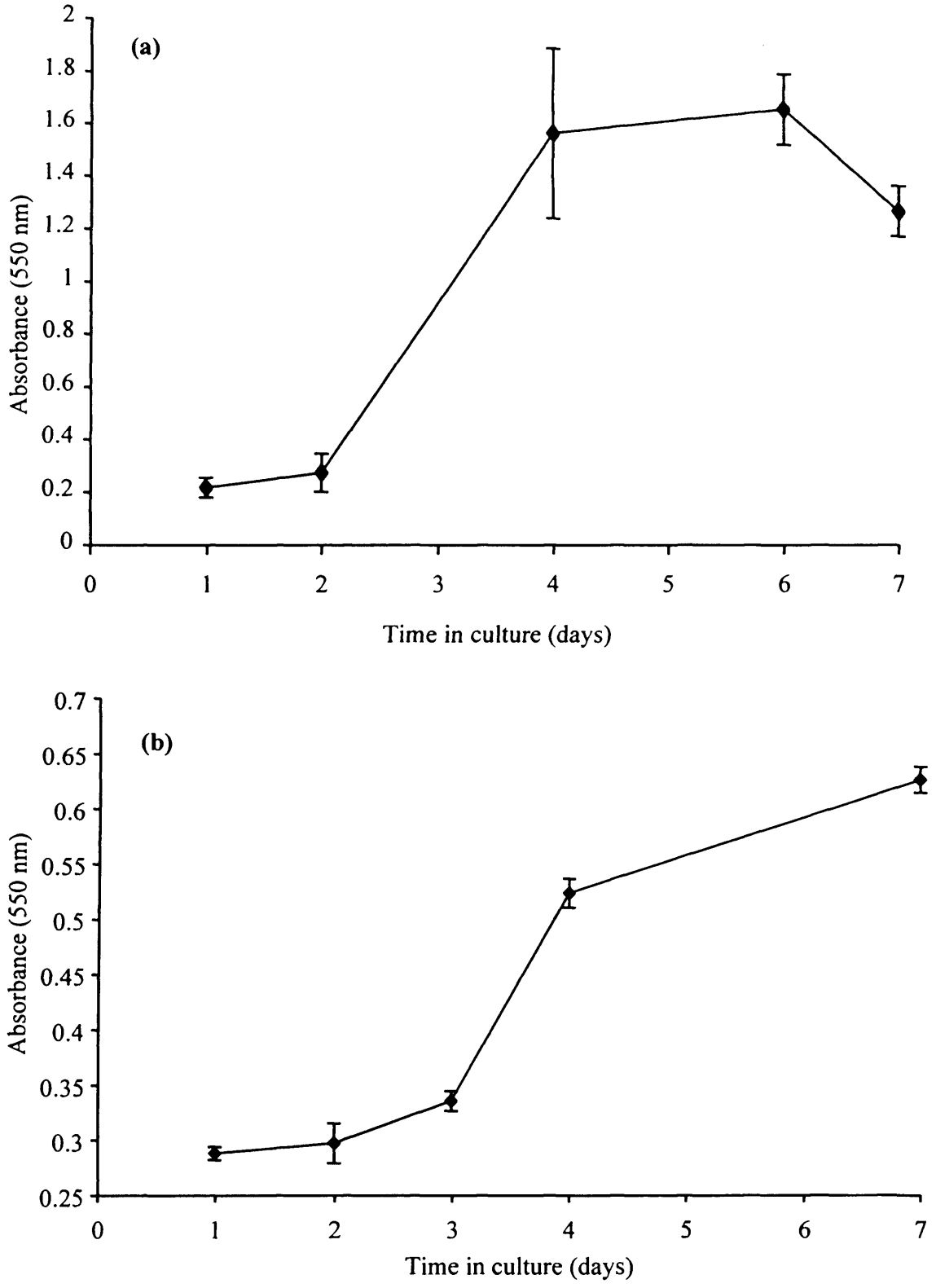

Figure 2.2 (a & b) Cell growth curves. Panel (a) B16F10 cells, panel (b) ECV304 cells. Cells were seeded at 1 x 10^3 cells/well in 96-well plates. Data represent mean ± SEM (n = 18).

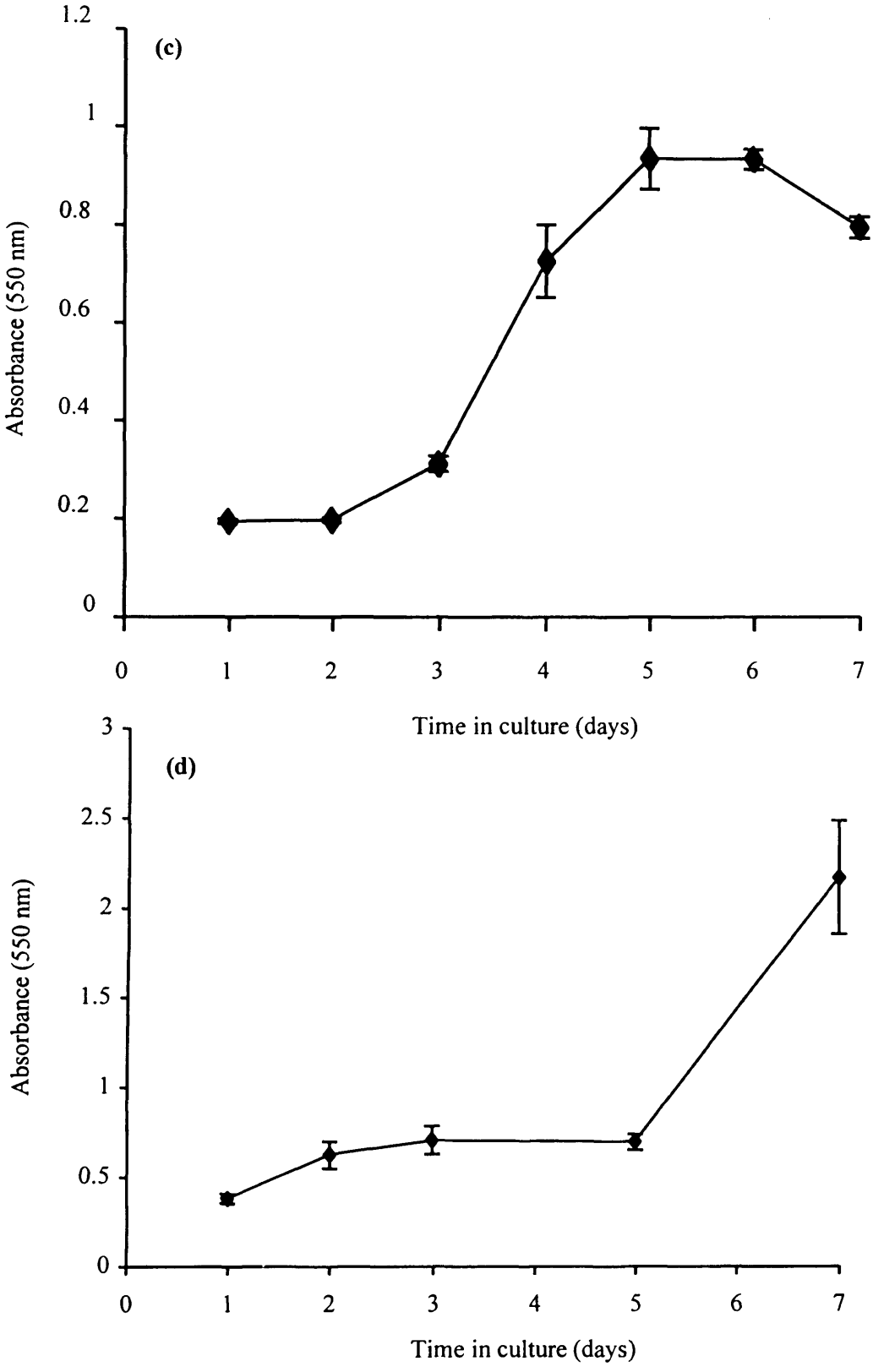

Figure 2.2 (c & d) Panel (c) RAW 246.7 cells, panel (d) Caco-2_{BBe} cells. Cells were seeded at 1 x 10^3 cells/well in 96-well plates. Data represent mean ± SEM, n = 18.

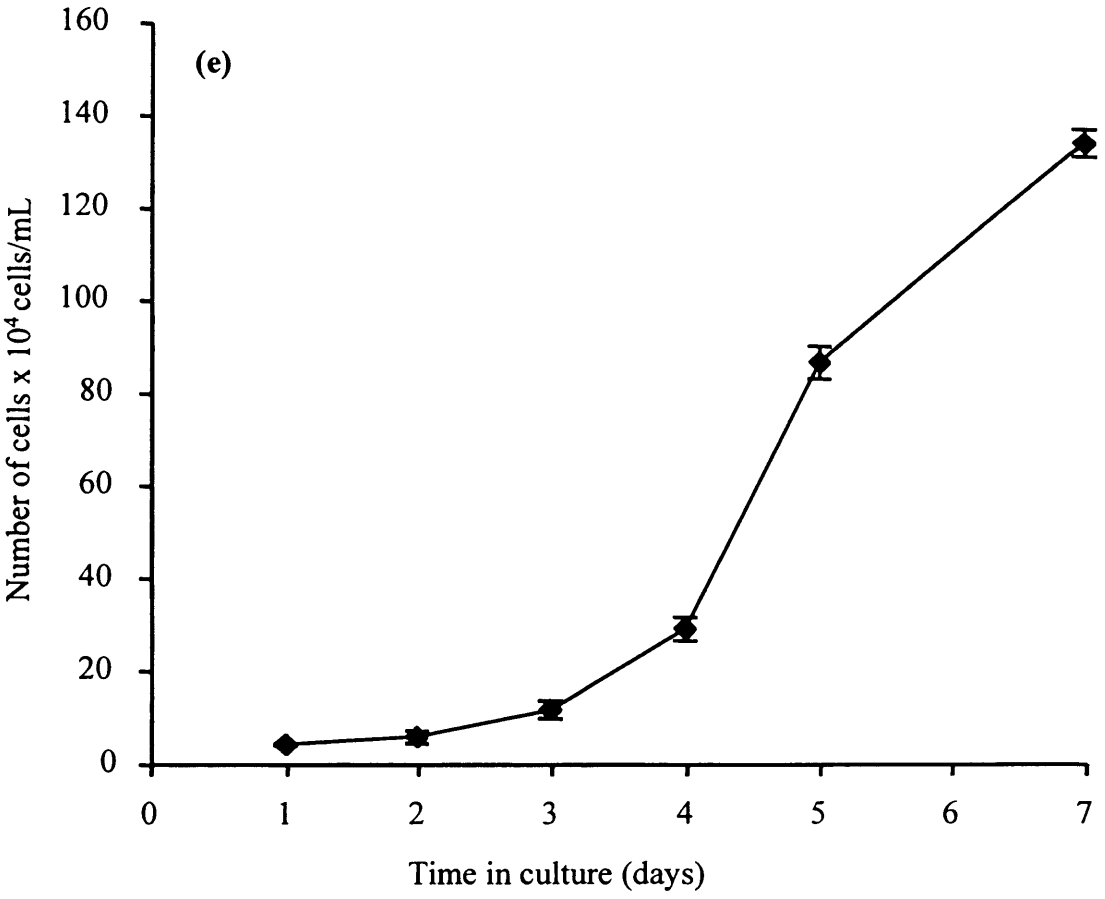

Figure 2.2 (e) U937 cells. Cells (1 x 10^4 cells/mL in 6-well plates) were counted on a daily basis. Data represent mean ± SEM, n = 3.

Plates were returned to the incubator, and this process was continued for 7 days.

U937 cell growth curves were measured by counting cells (seeded into 6-well plates at 1 x 10^4 cells/mL per well) on a daily bases to give the number of cells per mL. Trypan blue was used to discount dead cells from the suspension.

†MTT solutions were prepared by dissolving 5 mg/mL of the compound in autoclaved PBS. As MTT is light sensitive it was always protected from light. Dissolved MTT solutions were squeezed through a syringe attached to a 0.2 μM filter, placed into sterile, foil-wrapped containers and were stored at 4 °C.

2.3.4 Measuring polymer cytotoxicity using the MTT assay

The MTT assay was also used to measure polymer cytotoxicity. Polymers were always added to cells during their logarithmic growth phase, as the metabolism of MTT is slower when cells reach confluence (Sgouras and Duncan, 1990). Sterile, flat-bottomed, 96-well plates were seeded as described above. Twenty-four hours post-seeding, polymers dissolved in media (2 mg/mL) were diluted with media to give concentrations ranging from 1.25 to 1000 μg/mL (Table 2.2). Polymer-laced plates were then incubated for 1 - 67 h (see Chapter 3, section 3.2.2) before MTT was added (20 μL/well). Plates were then returned to the incubator for a further 5 h, before supernatants were removed, DMSO was added, and the UV-absorbance of the plates was read (as described above).

Data from these experiments, were analysed using Microsoft Excel®, and were expressed as a percentage of the viability seen in the control (untreated) cells. The concentration-response curves generated from this data were then fit to the logarithmic function derived from the Hill equation (below) using Biograph v1.2c for Microsoft Windows 1995:

$$y = (R_{min} + (R_{max} - R_{min})/(1 + (x/IC_{50})^P)$$

Where R_{max} was fixed at 100, and R_{min} was fixed at 0 (Kean *et al.*, 2005). The IC_{50} value is the polymer concentration at which cell growth was inhibited by 50 %.

Table 2.2 Dilutions made to establish polymer cytotoxicity.

Vol. of media added to plate (μL)	**Vol. of polymer solution (2 mg/mL) added to plate (μL)**	**Polymer conc. in plate (μg/mL)**
0	100	1000.0
20	80	800.0
40	60	600.0
80	20	200.0
90	10	100.0
0	*100	25.0
50	50	12.5
90	10	2.5
95	5	1.25
100	0	0

* Denotes from when dilutions were made using 0.05 mg/mL polymer solutions

2.3.5 Measuring cytokine release with Quantikine® sandwich-ELISA kits

Sandwich-ELISA assays allow the quantitative detection of specific cytokines that are secreted into tissue culture medium. Details of individual ELISA experiments are given in Chapter 3 (section 3.2.3).

To collect samples for ELISA assays, cells were seeded into tissue culture plates and were left for 24 h, before the addition of polymers. Polymers were incubated with cells for 1 – 24 h, before the medium was collected, centrifuged and frozen. Frozen samples were thawed and were assayed according to directions in the R&D Systems kit-manuals (Tables 2.3 and 2.4).

A schematic showing how the ELISA assays were conducted is given in Figure 2.3. In brief, before conducting ELISA work, all reagents were brought to room temperature (kits were kept at 4 °C), and the cytokine standard was reconstituted. Assay diluent was added to each well, and calibrator diluent was used to make a dilution series (calibration curve) with the cytokine standard. Dilutions or samples were then added to the microplate in duplicate. The plate was then sealed and left to allow cytokines to anneal, before it was washed using kit wash buffer. Next, immunoglobulin (Ig)-HRP conjugate was added, the plate was sealed, and was then left to allow the Ig-HRP conjugates to anneal to cytokines bound (to Ig) in the plate. After several washing steps, substrate solutions were added and converted into a blue-coloured liquid by horseradish peroxidase. At 30 min the reaction was stopped with acid, and the optical density of the plate was read in the UV plate reader at 540 and 450 nm. All data obtained were transformed using Microsoft Excel®.

To correct for optical imperfections in the plate, plate readings at 540 nm were subtracted from readings made at 450 nm. Next each duplicate reading was averaged. The zero standard optical density was then subtracted from these values. Plotting the log optical density against log cytokine concentration created a standard curve with the equation;

$$y = ax^b$$

Where a and b are constants, and b is the slope of the curve.

Standard curves were generated for each set of samples assayed (Figures 2.4a, b for human kits, and Figures 2.5a, b and c for murine kits), and the following

Table 2.3 Protocol for R&D Systems human ELISA kits.

Assay	Reagents	Assay procedure	Sample
hTNF-α	TNF-α standard:	Reconstitute with 1 mL ddH_2O = 10,000 pg/mL, agitate for 15 min before use.	200 µL/well
	Calibrator diluent:	900µL to 1st of 7 eppendorf tubes (labelled 1000, 500, 250, 125, 62, 31, 15 pg/mL), 500µL to remaining tubes. Add 100µL TNF-α into 1st tube, mix, transfer 500µL into next tube, mix and continue dilution.	
	Assay diluent:	50 µL/well	
	Conjugate, substrate:	200 µL/well	
	Stop solution:	50 µL/well	
hIL-2	IL-2 standard:	Reconstitute with 5 mL calibrator diluent = 2000 pg/mL, agitate for 15 min before use.	100 µL/well
	Calibrator diluent:	500µL/tube to 6 ependorf tubes (labelled 1000, 500, 250, 125, 62, and 31 pg/mL). Add 500µL IL-2 to 1st tube, mix, transfer 500µL into the next tube, mix and continue dilution.	
	Assay diluent:	100 µL/well	
	Conjugate, substrate:	200 µL/well	
	Stop solution:	50µL/well	

Table 2.4 Protocol for R&D Systems murine ELISA kits.

Assay	Reagents	Assay procedure	Sample
mTNF-α	TNF-α standard:	Reconstitute with 2 mL calibrator diluent = 1500 pg/mL, agitate for 5 min before use.	100 µL/ well
	Calibrator diluent:	200 µL/tube to 6 eppendorf tubes labelled 750, 375, 187, 93, 46 and 23 pg/mL. Add 200µL TNF-α in to 1st tube, mix and continue dilution.	
	Assay diluent:	50 µL/well	
	Conjugate, substrate:	100 µL/well	
	Stop solution:	50µL/well	
mIFN-γ	IFN-γ standard:	Reconstitute with 2 mL calibrator diluent = 3000 pg/ml agitate for 5 min before use.	50 µL/ well
	Calibrator diluent:	200µL/tube to 7 eppendorf tubes labelled 600, 300, 150, 75, 37, 18, and 9 pg/ml. Add 100µL IFN-γ in to 1st tube, mix and continue dilution.	
	Assay diluent:	50 µL/well	
	Conjugate, substrate:	100 µL/well	
	Stop solution:	100µL/well	
mIL-2	IL-2 standard	Reconstitute with 2 mL calibrator diluent = 1000 pg/ml agitate for 5 min before use.	50 µL/ well
	Calibrator diluent:	200µL/tube to 6 eppendorf tubes labelled 500, 250, 125, 62, 31 and 15 pg/ml. Add 200µL IL-2 in to 1st tube, mix and continue dilution.	
	Assay diluent:	50 µL/well	
	Conjugate, substrate:	100 µL/well	
	Stop solution:	100µL/well	

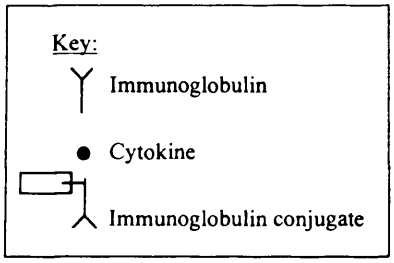

1. Prepare all reagents as directed

↓

2. Add assay diluent to each well

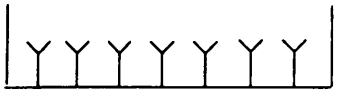

Anti cytokine Ig bound to the surface of 96-well microplate

3. Add dilution series, assay diluent (-ve control), or sample (thawed supernatant) to each well and incubate

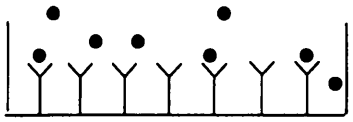

Plate sealed with plastic cover, and left at room temp.
Cytokine binds to Ig in plate

4. Aspirate and wash

↓

5. Add conjugate to each well and incubate

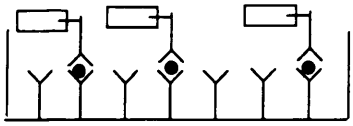

Plate sealed with plastic cover, and left at room temp.
Anti-cytokine Ig conjugate binds to cytokines bound to plate

6. Aspirate and wash

↓

7. Add substrate solution to each well, incubate for 20 min and protect from light

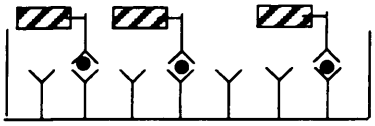

HRP converts substrates to blue colour
Stop solution turns blue colour yellow

↓

8. Add stop solution to each well, read at 450 nm and 540 nm (within 30 min).

Figure 2.3 Schematic showing the protocol for ELISA assays

equation was used in Microsoft Excel®, to quantify the amounts of cytokine in each sample.

$$= (O.D./a) \wedge (1/b)$$

Where O.D. is the optical density of the corrected sample, a is a constant from the calibration curve, ^ is to the power of, and b is the slope of the curve.

2.3.6 Use of the vertical diffusion system to study transport across rat intestinal tissue

The vertical diffusion system (Figure 2.6) was used to measure the transport of FITC-dextran across adult rat small intestinal tissue. Experiments were set up to measure transport in an apical to basal, or basal to apical direction (see Figure 2.6a). Intestinal tissue with or without Peyer's patches was used. In some experiments cytokines (see Chapter 4) or polymers (see Chapter 5) were added into the system and their effect on FITC-dextran transport was measured. The transport of the polymers themselves was also measured using this system after they had been fluorescently labelled (see Chapter 6). A general outline of this method is given below, and the specific details of this work are given in each appropriate experimental chapter.

For each experiment, Sprauge Dawley rats were fasted overnight prior to sacrifice by cervical dislocation. Fasted animals were allowed free access to water. Post-sacrifice, the small intestine was quickly excised by cutting along the mesentery that supports it. The excised, extended intestine was then flushed through with a 50 mL syringe of 85 % w/v NaCl in ddH_2O. The first 15 cm of the intestine, (corresponding to the duodenum and first half of the jejunum) was always discarded (see Figure 1.6), leaving the distal jejunum and ileum, from which 1 cm segments (with or without Peyer's patches) were cut and kept in MEM at 4 °C on ice. The tissue preparation method is shown in Figure 2.7.

Tissue was placed on an up-turned plastic weighing boat held on a tray of ice. It was cut along the mesenteric border, was pinned as a flat sheet to a plastic support, and the muscle layers and vasculature were removed with a scalpel. The remaining mucosal layer was carefully laid over the hole of one half of the diffusion

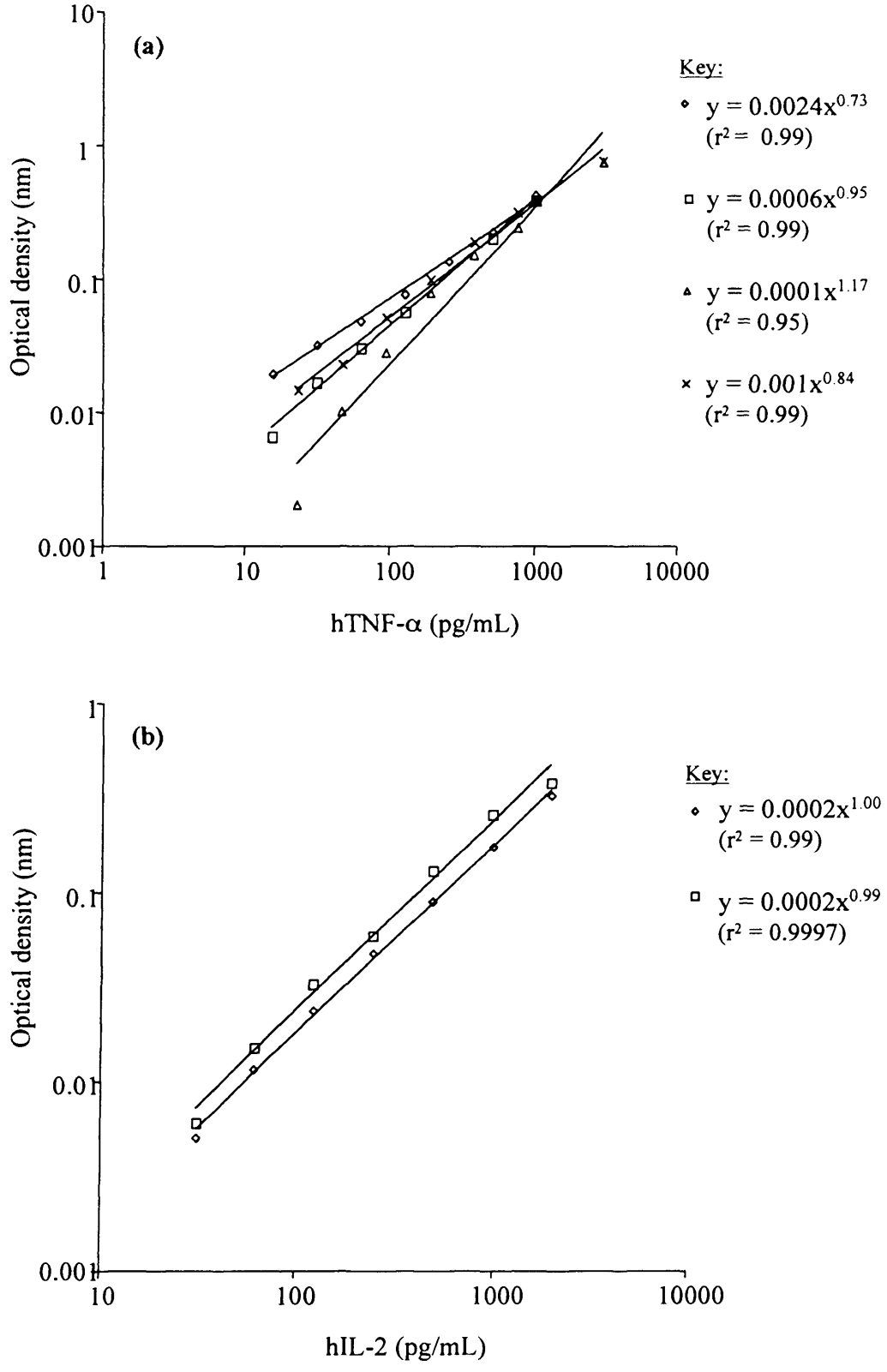

Figure 2.4 (a & b) Calibration curves observed for human TNF-α and IL-2. Panel (a) hTNF-α and panel (b) hIL-2. In each curve, the data points represent a mean of duplicate samples and the calibration curves observed in more than one experiment.

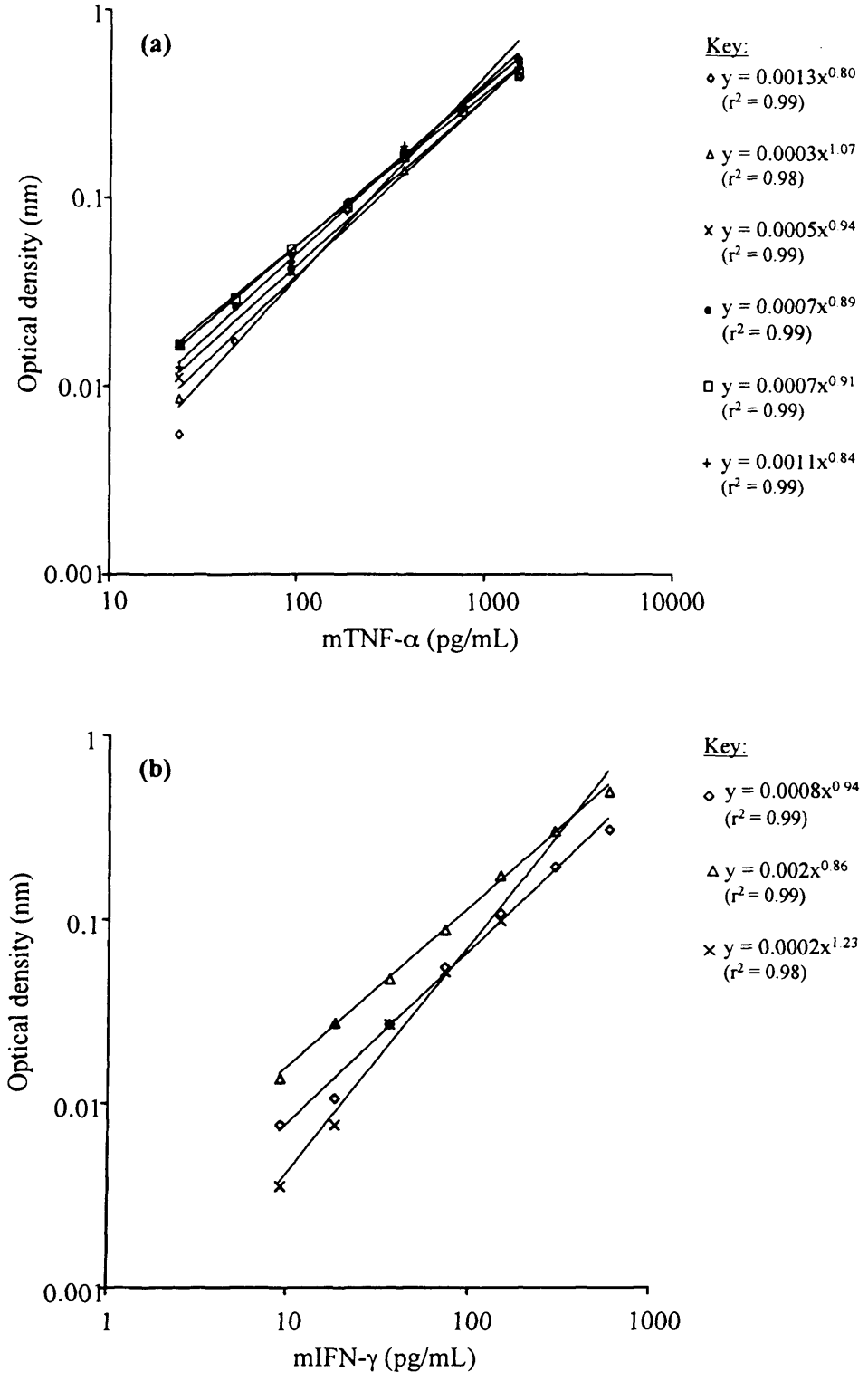

Figure 2.5 (a & b) Calibration curves observed for murine TNF-α and IFN-γ. Panel (a) mTNF-α and panel (b) mIFN-γ. In each curve, the data points represent a mean of duplicate samples and the calibration curves observed in more than one experiment.

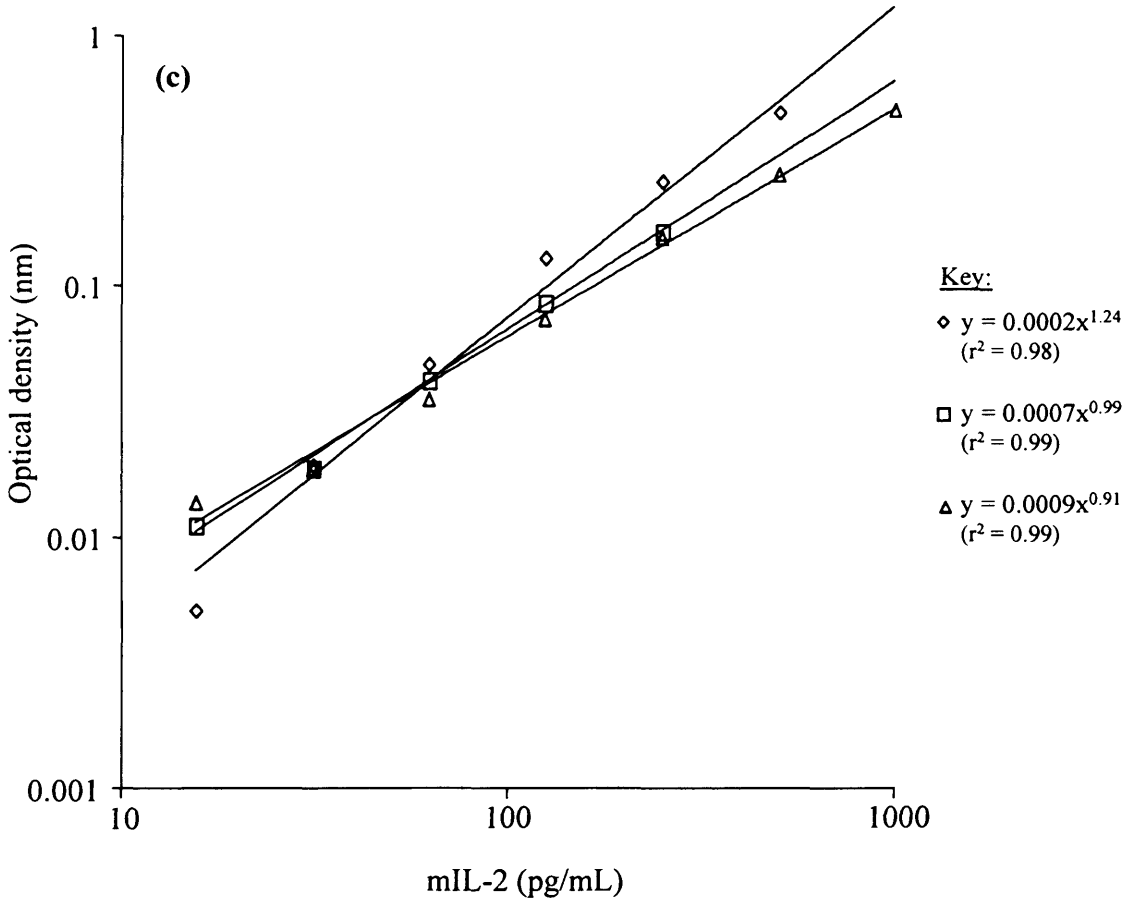

Figure 2.5 (c) mIL-2. In each curve, the data points represent a mean of duplicate samples and the calibration curves observed in more than one experiment.

(a)

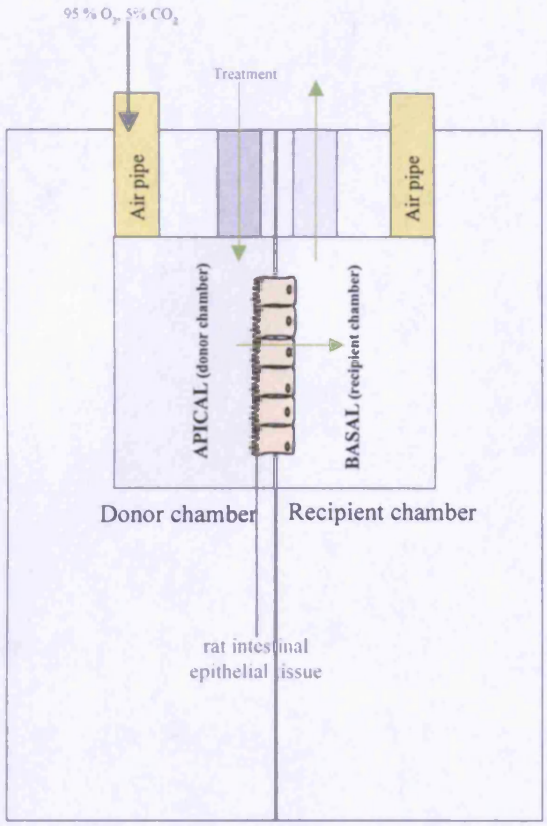

(b)

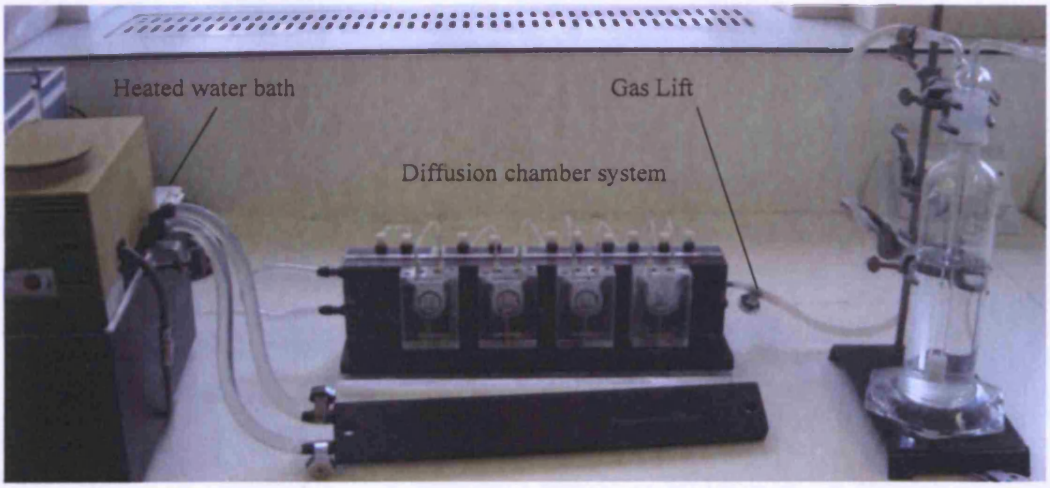

Figure 2.6 (a & b) Schematic diagram of a vertical diffusion cell (panel a), and a photograph showing the vertical diffusion system (panel b)

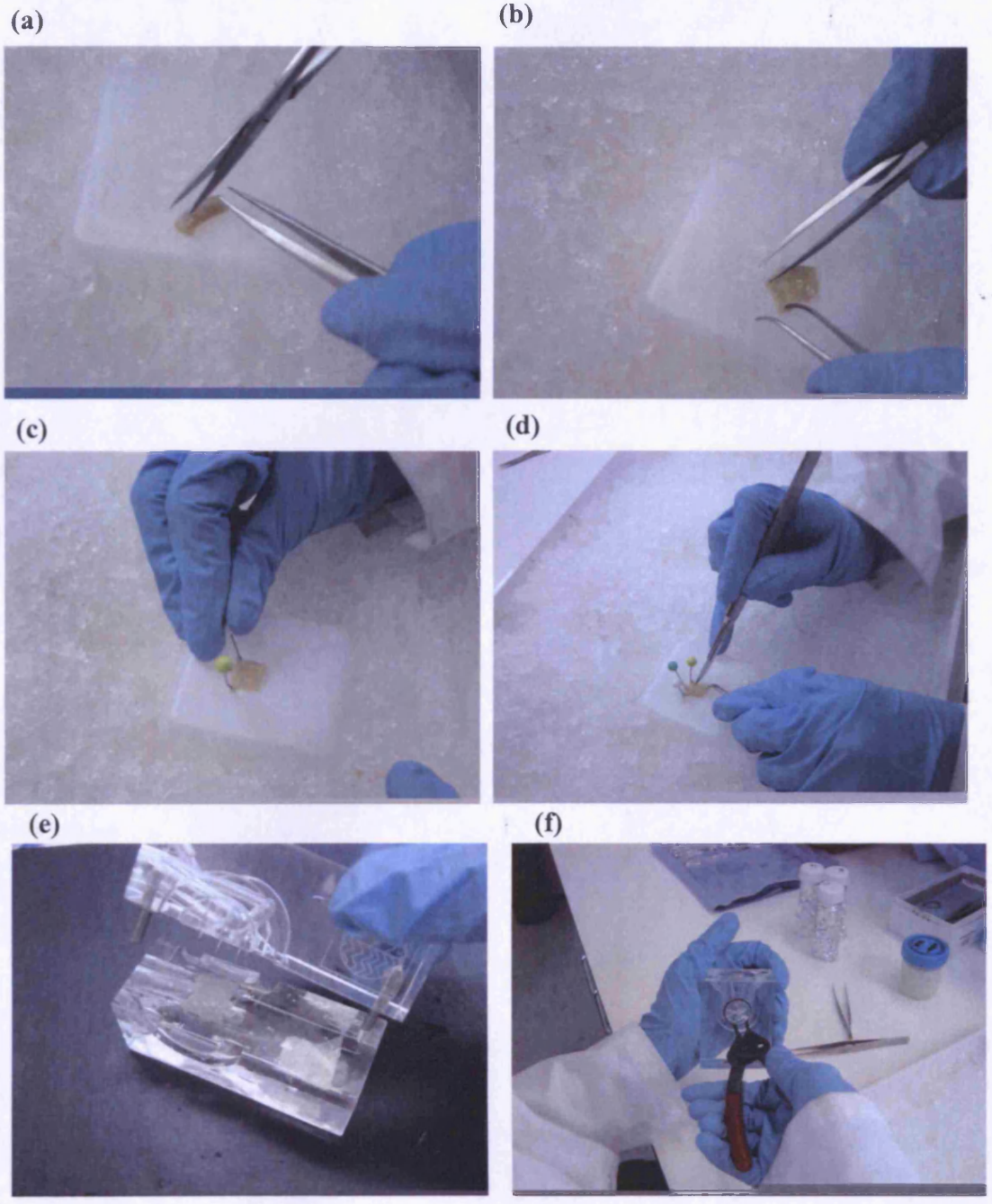

Figure 2.7 Preparation of tissue for the vertical diffusion system

See text (section 2.3.6) for details

chamber and both chambers were tightly clamped together. Warmed MEM (37 °C in a water bath) was carefully placed in each half of the chamber simultaneously to avoid the effects of hydrostatic pressure. Two air-pipes were then attached to each side of the chamber to allow mixing and oxygenation to occur, and the system was kept at 37 °C via a heated block connected to a water bath.

After a few minutes the medium was removed (to clear any debris not flushed from the lumen), and was carefully replaced with 1.5 mL of fresh medium/chamber. Immediately any treatment containing fluorescent probes (see Chapters 4, 5 and 6 for details) was applied to the donor chambers (on either mucosal or serosal sides of the tissue). Transport across the tissue was measured at 10 min intervals (from t = 0 – 60 min) by the collection of 25 μL samples from the recipient chamber. Fresh media (25 μL) was quickly added to the chamber after each sample had been taken. At the end of each experiment, all acrylic diffusion cells were soaked in ethanol (70 % v/v in ddH_2O), and were then sonicated and rinsed with ddH_2O.

In most cases FITC-dextran was used as a fluorescent paracellular marker for this work (see Chapters 4 and 5). Samples containing this compound were collected into black 96-well plates, and were protected from light using silver foil. Plates were read in a fluorescent plate reader set at an excitation value of 485 nm, and an emission value of 520 nm. The gain on the plate reader was always kept at 1000. All fluorescence data were then manipulated using Microsoft Excel®.

To account for dilutions made by collecting 25 μL samples, the following equation was formulated:

$$F - (0.025/ 1.5 * Ls)$$

Where, F equals the fluorescence value of the cell of interest, 0.025 equals the volume removed in mL, 1.5 equals the total volume in the chamber in mL, * denotes the multiplication symbol, and Ls equals the fluorescence of the sample(s) previously taken.

Permeability coefficients (Papp) for transported molecules were calculated as:

$$Papp = (dQ/dt)/ (Co*A)$$

Where, Papp equals the apparent permeability coefficient (cm/s), dQ/dt is the amount of drug transported, A is the diffusion area of the mucosa (cm^2), and Co is the initial concentration of the test compound in the donor compartment (μM) (Lacombe *et al,* 2004).

2.3.7 Measurement of tissue viability using the lactate dehydrogenase assay

Lactate dehydrogenase (LDH) is a soluble, cytosolic, glycolytic enzyme found in most body tissues. It functions to catalyse the conversion of pyruvate (a respiratory product continually produced in tissues) into lactate, and is therefore important for energy production in cells. It is because LDH is such an abundant, cytosolic enzyme, that the presence of free LDH in the tissue culture media of cells is often measured to assess tissue (particularly membrane/plasma) damage. In these studies, LDH release from excised rat intestinal tissue (used in the vertical diffusion chamber) was measured, to gauge any cellular damage when cytokines were added.

First two stock solutions were prepared. A Tris/NaCl buffer was made using 81.3 mM Tris, and 203.3 mM NaCl dissolved in ddH_2O to a total volume of 500 mL. The pH of the solution was adjusted to 7.2 using 5 M HCl. This solution was then split into two flasks, to which either 0.244 mM of NADH, or 9.70 mM pyruvate was added.

Using 2 mL plastic cuvettes, 1.5 mL of the Tris/NaCl/NADH solution was mixed with 50 μL incubation medium, and the cuvettes were then heated in the UV spectrophtometer to 30 °C for 5 min. The absorbance of the spectrophotometer was set to 339 nm using an enzyme kinetic programme. Once the programme had been set up, 300 μL of Tris/NaCl/pyruvate was quickly added and the absorbance was quickly, and continuously monitored for 2 minutes. LDH activity was measured as the amount of pyruvate consumed due to oxidation of NADH, as shown below:

$$\text{Pyruvate} + \text{NADH} + H^+ \overset{\text{LDH}}{\Leftrightarrow} \text{L (+) - lactate} + NAD^+$$

The amount of LDH activity within the samples (expressed as enzyme units mU/mL) was calculated using the following formula;

$$\text{LDH activity} = [(d * \text{absorption}/ dt) * 1000 * V_{assay}]/ (EC * d * V_{sample}),$$

Where (d * absorption/ dt) equals the reduction rate of pyruvates absorption, V_{assay} equals the volume of the assay, EC denotes the extinction coefficient for NADH at 339 nm (6317l/ mol/cm), d is the pathway length of the laser, and V_{sample} is the volume of the sample.

2.3.8 Gel permeation chromatography

Also known as size exclusion chromatography (SEC) and gel filtration chromatography, GPC is used to separate and characterise polymers according to their size. GPC can also be used to determine the polydispersity index (PDI) of polymers that have a wide distribution of molecular weights. This is the ratio between MW and Mn averages of polymers, where;

MW = the weight average molecular weight
Mn = the number average molecular weight

Theory:

During GPC the mobile phase moves through the stationary phase and it is temporarily retained. The retention is controlled by the stationary phase which is made of finely divided porous beads, whose size is chosen specifically for the polymer MW ranges of interest. Polymer molecules dissolved in solvent are separated on the basis of their hydrodynamic volume. The smaller molecules pass through the pores and thus have a longer path and transit time than larger polymer molecules that continue following the solvent flow. Therefore, larger molecules elute earlier in the chromatogram. Polymer motion in and out of the pores is statistical, and is governed by Brownian motion. Usually a refractive index detector is used to monitor polymer samples as they are eluted from the column.

The solvent used in these studies was PBS pH 7.4 that was first filtered then sonicated to remove any air bubbles. Polymers for analysis were dissolved in this PBS at a concentration of 5 mg/mL and were sterile-filtered. One mL of each polymer solution was carefully drawn up into a glass syringe, and 60 μL of this solution was injected into the column to avoid any air bubbles. The flow rate was kept at 1 mL/min, and the refractive index detector was calibrated to monitor samples as they eluted over 30 minutes. Pullulan polysaccharide standards of known

molecular weight (738 - 112,000 Da) were used as molecular weight standards (Figure 2.8).

2.3.9 Determination of LPS contamination of polymer solutions

The Limulus amebocyte lysate (LAL) test was used to measure LPS. This assay was developed following the discovery that a clotting reaction occurs when the amoebocyte blood cells of the horse-shoe crab, *Limulus polyphemus*, come into contact with LPS. This process was later found to be mediated by enzymes located in the amoebocyte granules i.e. LAL.

The particular LAL assay used in this thesis is kinetic. Serial dilutions of control standard endotoxin reconstituted with endotoxin-free LAL reagent water (following the lot specific certificate of analysis) was used to produce an endotoxin standard curve in endotoxin-free, sterile tubes. Polymers dissolved in LAL water at 1 mg/mL were sterile filtered and assayed alone, or when spiked with 5 endotoxin units (EU)/mL of CSE. LAL water alone was used as a negative control. A template of the plate was set on the kinetic plate reader, and 100 μL of the negative controls, standards and samples were added, followed quickly by 100 μL of lysate that had just been reconstituted with LAL reagent water (amount at which was specified on the vial). The pipette tips for this work were all endotoxin-free. The plate without its lid was read in the plate reader over an hour.

2.4 Statistics

All data are expressed as an average ± S.E.M. When comparing a single sample against a control, two-tailed Students t-tests were used. The differences between multiple groups of data and the control were compared by one-way or two-way analysis of variance (ANOVA), depending on the experimental design. The p value for these studies was always set as 0.05.

If a significant difference between the control and groups of data was seen with ANOVA ($p < 0.05$), a post-hoc test was performed. Bonferroni post-hoc tests were used for most occasions.

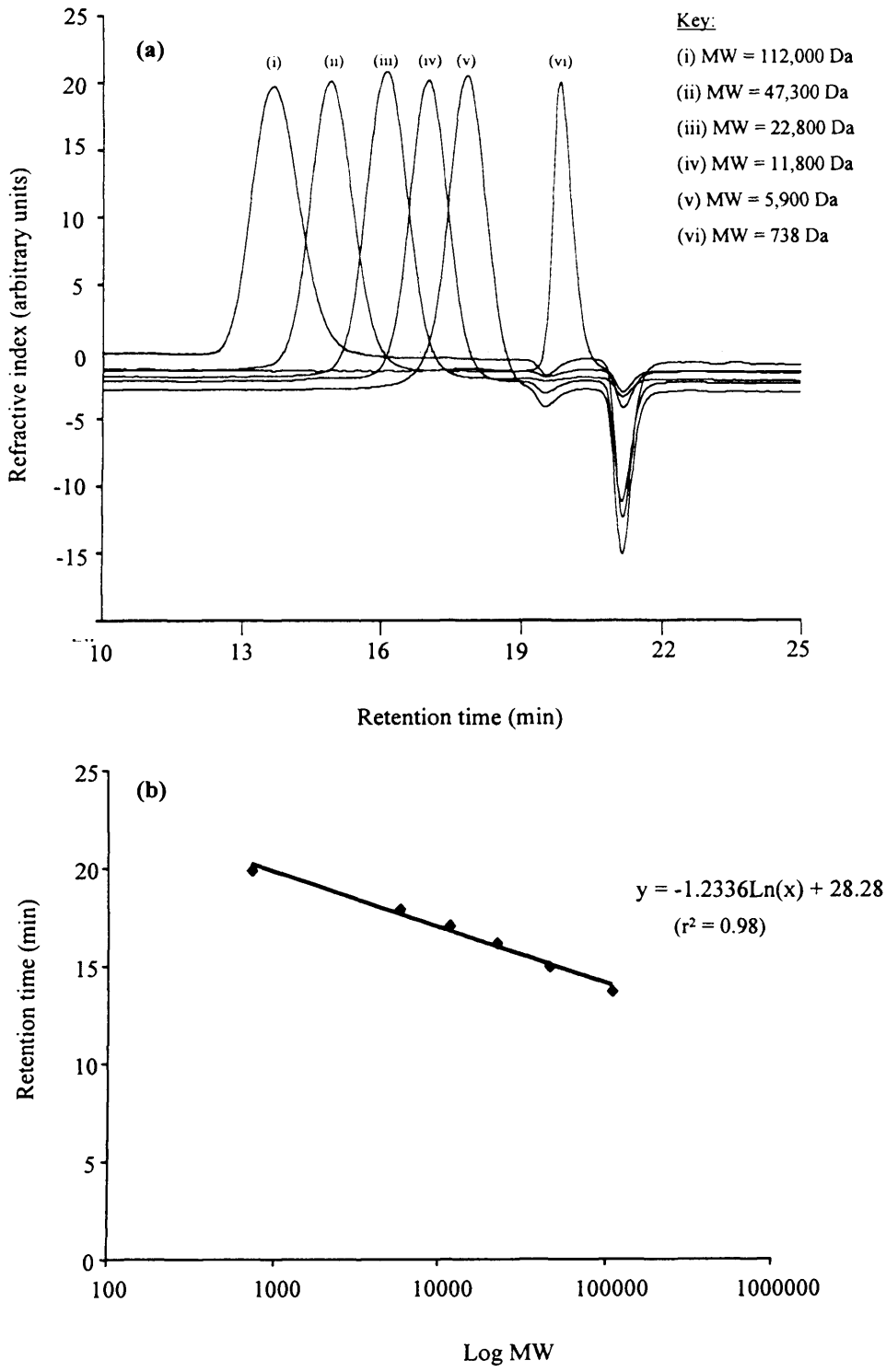

Figure 2.8 (a & b) GPC chromatogram for pullulan polysaccharide standards (panel a), calibration curve (panel b).

CHAPTER 3:

Investigating Polymer Cytotoxicity and Ability to Induce Cytokine Release from B16F10, RAW 246.7 and DU937 Cells

3.1 INTRODUCTION

Before using the polymers in biological assays it was first necessary to establish their cytotoxicity, as this would enable non-toxic polymer concentrations to be identified for further experiments. Therefore during the first part of this study, the cytotoxicity of alginate, HA, PAcAs, and PAMAM 3.5 dendrimers, towards B16F10 (murine melanoma) and ECV304 (human bladder carcinoma) cell lines was defined. Subsequent experiments then investigated whether these polymers would induce cytokine (TNF-α, IFN-γ and IL-2) release from B16F10 or RAW 246.7 and DU937 cells. The polymers and cytokines selected for these studies were chosen for the reasons explained earlier (Chapter 1, sections 1.6 and 1.7 respectively). The rationale for the cell lines and assays used for these studies are given below.

Rationale for the choice of cell lines used

Four cell lines were selected for these studies and the growth curves for each are shown in Chapter 2 (Figure 2.2). B16F10 murine melanoma and ECV304 human bladder carcinoma cells have commonly been used to study the biological activity of polymers (Wan *et al.*, 2004) and polymer-anticancer drug conjugates (O'Hare *et al.*, 1993) as well as polymeric non-viral vectors for gene delivery (Richardson *et al.*, 1999; Fischer *et al.*, 1999; Lavignac *et al.*, 2004; Wan *et al.*, 2004; Andersson *et al.*, 2005). ECV304 cells are endothelial-'like' and have been widely used as an endothelial model (Hughes, 1996). Both cell lines were used for initial cytotoxicity screening because (i) it was thought that B16F10 cells might be later used as an *in vitro* tumour model, and (ii) it was thought that ECV304 cells might be used as an endothelial monolayer model for permeability experiments (see section 1.9). In-fact they were not used for such experiments. Nevertheless both cell lines provide useful data on polymer toxicity that can be compared to literature values (Andersson *et al.*, 2005; Vicent *et al.*, 2004; Veronese *et al.*, 2005; Tomlinson *et al.*, 2003; Fischer *et al.*, 2003). The RAW 246.7 and DU937 macrophage-like cell lines were chosen to provide a positive control for measurement of TNF-α release (Heming *et al.*, 2001; Boyce *et al.*, 1997).

Polymer cytotoxicity

Before assessing polymer cytotoxicity it was necessary to choose an appropriate assay. Non-radioactive methods routinely used to assess cytotoxicity

include; cell counting assays such as the Coulter Counter® (Pruden and Winstea 1964; Sgouras and Duncan 1990), assays that involve measurement of increases in membrane permeability, such as trypan blue exclusion (Cowan *et al.*, 1984), measurement of metabolic activity using dyes such as MTT (Mossman, 1983) or XTT (sodium 3,3'-[1[(phenylamino)carbonyl]-3,4-tetrazolim]-*bis*-(4-methoxy-6-nitro) benzene sulfonic acid hydrate), tetrazolium salt (Roehm *et al.*, 1991), or the measurement of LDH release (Korovkin *et al.*, 1963).

For these studies the MTT assay (described in Chapter 2, section 2.3.2) was preferred, as it is a rapid, quantitative screening method that can be easily adapted to measure a wide range of polymer concentrations using 96-well plates (Sgouras and Duncan 1990; Kean *et al.*, 2005; Peng *et al.*, 2005). The small well volume of the plates means that minimal amounts of polymer are needed. Polymer cytotoxicty was initially assessed using a 72 h incubation time in accordance with Sgouras and Duncan (1990). However, as the cytokine release studies were conducted using an incubation time of 1 or 24 h, it was also considered important to define polymer cytotoxicity over these incubation periods. High molecular weight PEI (MW = 750,000 Da) and dextran (MW = 68,800 Da) were used as positive and negative reference polymers for these studies, in accordance with the literature (Kean *et al.*, 2005; Fischer *et al.*, 2003).

High molecular weight PEI (Figure 3.1a) is a highly branched, synthetic, polycation that has a higher charge density than most linear polycations of the same size (Fischer *et al.*, 2003). The cytotoxicity of this polymer is molecular weight-dependent (Fischer *et al.*, 2003; Kunath *et al.*, 2003), and as such, only low molecular weight PEI (MW = 25,000 Da) is being studied as a gene delivery vector (Wagner, 2006). The flexible structure of PEI allows it to electrostatically interact with DNA, or in the case of cytotoxicity, with cell membranes (via the negatively charged phospholipid head groups). This induces curvature, which destroys membrane integrity (Fischer *et al.*, 2003; Moghimi *et al.*, 2005).

Dextran (Figure 3.1b) on the other hand is a highly water-soluble polysaccharide (β, 1-6 polyglucose produced by bacteria) that has a 50-year clinical history as a plasma expander (reviewed in Thoren, 1980). The chemical inertness and high number of hydroxyl groups of this polymer has also allowed it to be

(a)

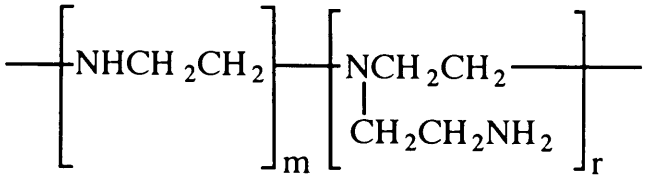

(b)

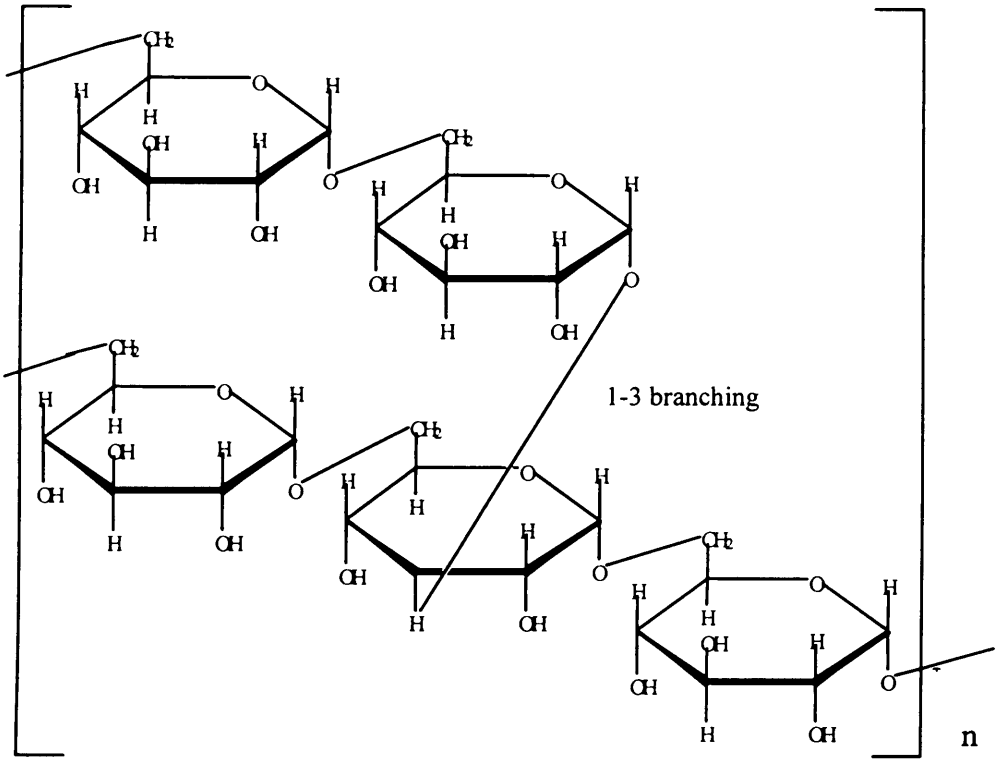

Figure 3.1 (a & b) Chemical structures of (a) PEI and (b) dextran.

Note PEI essentially has no monomer. It is a branched chain polymer with 1:2:1 primary:secondary:teriary amines with a branching site every 3 - 3.5 nitrogen atoms

conjugated to a variety of pharmaceutical agents. Hence it has recently been investigated as a polymer-protein conjugate (to increase stability and decrease the immunogenicity of proteins), and as a polymeric drug carrier (reviewed in Mehvar, 2000).

Cytokine release

The ability of polymers to induce TNF-α, and IL-2 release from DU937 (human macrophage-like) cells, TNF-α, IFN-γ and IL-2 release from B16F10 cells, and TNF-α, IFN-γ and IL-2 from RAW 246.7 (murine macrophage/monocyte) cells was studied. For many years ELISA and bioassays have been most commonly used as methods to measure cytokine release (Whicher and Ingham, 1990). ELISA is more convenient and more sensitive than most bioassays (Whiteside, 2002) so it was used throughout the studies described here. Before using ELISA assays it was necessary to establish; (i) the reproducibility of the standard curve for each cytokine (ii) the recovery of cytokine from tissue culture medium and (iii) the effect of the presence of polymers on cytokine recovery from the tissue culture medium. In addition, to investigate whether PEI would interfere with ELISA kits, calibration curves were made with and without this polymer. As mentioned above, to establish a positive control cytokine-release experiments were conducted using DU937 cells, cultured with sodium hyaluronate (sHA) as this polymer had been shown previously to induce TNF-α (using L929 cells as a bioassay) when incubated with these cells for 24 h (Boyce *et al.*, 1997). The profile of TNF-α release induced by LPS and HA was also measured over time.

The ability of HA, alginate, PAcA sodium salt (MW = 30,000 Da; $sPAcA_{30}$) and PAMAM 3.5 to induce release of TNF-α from DU937 cells was examined after 24 h and DU937 cells incubated with alginate and PAMAM 3.5 were also assayed for the release of IL-2 after 24 h. A time point of 1 h was chosen to assess polymer-mediated TNF-α, IFN-γ and IL-2 release from RAW 246.7 and B16F10 cells, PEI was used as a positive control in these assays, as it has been shown to induce TNF-α and IL-2 release from B16F10 cells after a 1 h incubation time (Puckey, 2002).

As the polymers used for this work were not of pharmaceutical grade, it was considered possible that they could contain LPS. In humans, the tolerance levels of LPS (defined by the Food and Drug Association (FDA)) depend on the route of

administration. For instance, the endotoxin tolerance for parentally delivered drugs and liquids is 5 EU/mL. Drugs and liquids in the circulation can have up to 0.5 EU/mL, whilst for devices that contact the cerebralspinal fluid, the limit is much lower 0.06 EU/mL. The way in which LPS induces cytokine release from macrophage cells has also been well characterised (Figure 3.2).

Circulating LPS binds LPS-binding protein (LBP) and is delivered to the CD14 receptor either in the circulation, or on the macrophage surface. When this occurs, LBP is released, and the CD14 receptor triggers the Toll-like receptor to phosphorylate and activate several cytoplasmic MAP kinases. This activates several transcription factors, mainly AP-1 and NF-κB, and corresponding genes, that encode cytokines (such as TNF-α, IL-1, IL-6 and IL-8), and enzymes of the respiratory burst.

As LPS contamination might cause spurious results in ELISA assays, it was important to try to determine the concentration of LPS in all polymer stocks. This was investigated using the LAL assay (Jorgensen and Lee, 1978). However, it later proved difficult (and potentially unnecessary) to determine the LPS content.

The specific aims of these studies were to:

(i) Set up MTT assays to measure the cytotoxicity of alginate, HA, PAcAs and PAMAM generation 3.5 dendrimers in different cell lines.
(ii) Establish ELISA assays to determine whether the polymers can induce TNF-α, IFN-γ and IL-2 release from cells.
(iii) Devise a method in which LPS levels in polymers can be determined.

3.2 METHODS

The general methods used for this work have already been described in Chapter 2 (sections 2.3.4, 2.3.5, and 2.3.9). Unless otherwise stated all experiments were carried out in triplicate, and all polymer and LPS solutions were prepared in serum-supplemented media, and were sterilised by filtration (through 0.2 μm Sartorious filters) before use.

The method used to grow U937 cells is described in Chapter 2 (section 2.3.1). However, to mature this cell line into an adherent macrophage phenotype, cells were counted and diluted with media to give a 2 x 10^5 cells/mL suspension in 30 mL of media containing 2.5 x 10^{-7} M PMA. After gently mixing the suspension with a

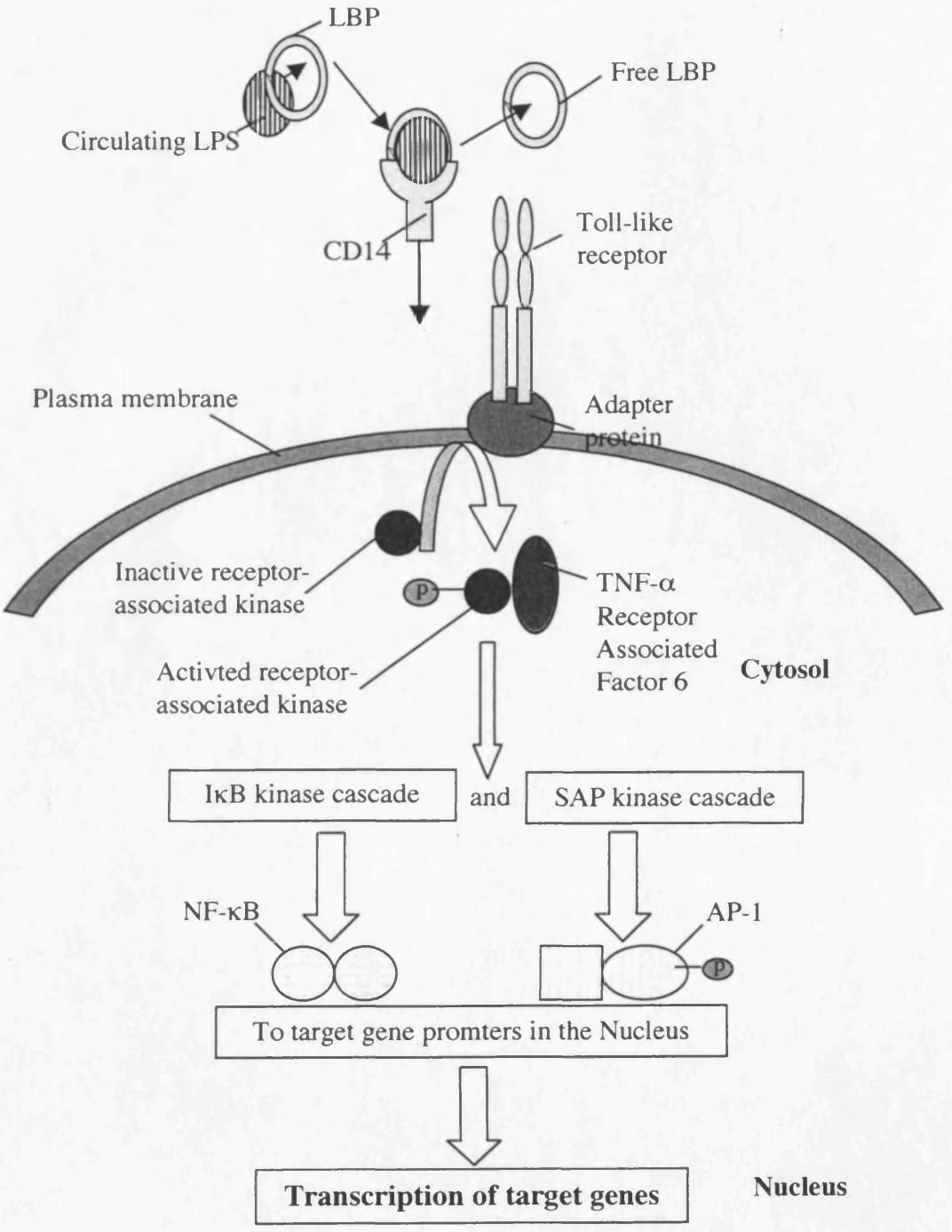

Figure 3.2 Effects of LPS on macrophage cells

manual pipette, 1 mL of the suspension was added/well to 24 well plates. Seeded plates were then incubated for 48 h to allow cell attachment and maturation to occur.

3.2.1 Setting up MTT assays

Firstly it was important to establish whether polymers being used would affect the pH of the tissue culture medium, as a change in pH could itself affect cell viability (Mackenzie *et al.*, 1961). To conduct the MTT assays, polymers (1.25 μg/mL to 1 mg/mL) were added to cells (seeded at 1 x 10^3 cells/well in 96-well plates) and were then incubated for 1, 24 or 72 h (in total). The experimental procedure is described in detail below, and in all cases the data are expressed as mean ± SEM.

72 h MTT assay: B16F10 and ECV304 cells were incubated with polymers for 67 h, at which MTT (5 mg/mL in PBS) was added (20 μL/well). After adding MTT, the plates were further incubated for 5 h. The tissue culture medium was then carefully removed before addition of spectrophotometric grade DMSO to dissolve the MTT crystals (100 μL/well). Plates were then incubated at 37 °C for 30 min before being read in the plate reader (550 nm).

24 h MTT assay: DU937 cells were incubated with PEI or sHA for 19 h, before the addition of MTT. After adding MTT, plates were incubated for a further 5 h before they were processed as described above.

1 h MTT assay: B16F10 cells were incubated with polymers for 1 h before the cell culture medium containing polymer was removed using a multichannel pipette. The cells were then washed twice with warm media, and fresh media (without polymer) was then added to plates (100 μL/well). The cells were further incubated for 66 h, and at 67 h MTT was added. After a further 5 h incubation (i.e. 72 h) the plates were processed as described above.

3.2.2 Use of ELISA assays to monitor cytokine release

The general procedures used for ELISA kits are given in section 2.3.5. First, to investigate the possibility that the polymers (alginate, HA, sHA, PEI, PAMAM 3.5, and PAcAs) might interfere with ELISA assays, polymer solutions (1 mg/mL) were

prepared in tissue culture medium plus serum, and were spiked with mTNF-α (93.75 pg/mL). Each polymer solution was then assayed for mTNF-α recovery using the calibration curve. Next, to investigate whether the polymers stimulated cytokine release from cells, each cell line was incubated with polymers for times between 10 min – 5 h as detailed below.

Investigating cytokine release from DU937 cells

Twenty-four well plates seeded with DU937 cells (2 x 10^5 cells/mL) were viewed under the light microscope after 48 h (to check whether the cells had adhered and expanded). They were then washed twice with media to remove PMA (see pages 17 and 77) and any dead cells. The polymer solutions (HA, sHA, alginate, $sPAcA_{30}$ and PAMAM 3.5 at 0.1, 1, 10 and 100 μg/mL), and LPS (50 μg/mL) were then added to the plates (1 mL/well) and they were returned to the incubator. Medium was carefully collected from wells using a 1 mL pipette at 0 - 5 or 24 h (in duplicate).

At each time point the medium samples were quickly transferred into labelled 25 mL universal containers, and were then centrifuged at 1500 g (for 3 min) to pellet any dead cells. The supernatant was then gently (but quickly) removed from each container using a manual pipette, and was placed into a labelled bijous bottle and stored at – 20 °C until assayed (as described in Chapter 2, section 2.3.5).

Investigating cytokine release from B16F10 and RAW 246.7 cells

B16F10 and RAW 246.7 cells were seeded into 96-well plates (1 x 10^3 cells/mL) and were left for 24 h to adhere. In this case, polymer solutions (2 mg/mL in medium) were added to each well to give a final content of 1 mg/mL. In most experiments the plates were then returned to the incubator for 1 h. Following this h incubation period, the medium was collected from each well and quickly transferred into 1.5 mL eppendorf tubes, which were immediately frozen in liquid nitrogen, and then stored at – 80 °C until assayed. Before these samples were assayed by ELISA, eppendorf tubes were spun at 235 rpm (1500 g) in a bench-top centrifuge for 3 min, to pellet any cells.

In one experiment, the effect of HA (100 μg/mL) or LPS (50 μg/mL) on the time-dependent (10 min – 24 h) release of cytokines from RAW 246.7 or B16F10 cells was studied. In this case cells were seeded into 24-well plates (2 x 10^5 cells/mL/well), and were left for 24 h before HA or LPS was added. At each time-

point the medium was collected and processed as described above for DU937 cells.

The method used for the LAL assay is described in Chapter 2 (section 2.3.7).

3.3 RESULTS

When dissolved in RPMI and DMEM media (Table 3.1) the polysaccharides (alginate, HA, dextran) and lower molecular weight PAcA ($sPAcA_{30}$) produced little change in pH giving values around pH 7.0. Conversely, the higher molecular weight PAcAs ($PAcA_{100}$ and $PAcA_{450}$ Da) caused a decrease in pH, whilst PAMAM 3.5 and PEI caused an increase in pH. For example, for PEI the pH increased to pH 8.68 in DMEM media, and pH 9.03 in RPMI media.

3.3.1 Evaluation of polymer cytotoxicity by MTT assay

Of the synthetic polymers tested, PEI displayed the highest cytotoxicity, and this increased with increasing polymer concentrations in DU937 (Figure 3.3), B16F10 (Figure 3.4a), ECV304 cells (Figure 3.4b), and to increasing incubation times in B16F10 cells.

The polysaccharides (alginate, HA and dextran) had IC_{50} values of greater than 1 mg/mL, regardless of the incubation time (figure 3.5a and 3.5b). Although HA caused a concentration-dependent cytotoxicity (from 0.12 mg/mL - 1 mg/mL) in ECV304 cells after a 72 h incubation, it displayed an IC_{50} value of > 1 mg/mL (Figure 3.5b).

$sPAcA_{30}$ showed some toxicity in B16F10 cells from 0.1 mg/mL concentrations at 72 h, though the IC_{50} value of this polymer was still greater than 1 mg/mL (Figure 3.6a). In ECV304 cells, it was less cytotoxic (Figure 3.6b). $PAcA_{100}$ and $PAcA_{450}$ also displayed concentration-dependant cytotoxicity in B16F10 cells (Figure 3.6a) and ECV304 cells (Figure 3.6b), and when the incubation time was decreased from 72 h to 1 h, cytotoxicity was reduced in B16F10 cells. PAMAM 3.5 had an IC_{50} value > 1 mg/mL in B16F10 cells after a 1 h and 72 h incubation (Figure 3.7a) and in ECV304 cells at 72 h (Figures 3.7b). All polymer IC_{50} values are shown in Table 3.2. With hindsight, it would have been a good idea to match the control cells for these experiments with the polymers being studied. Unfortunately however, this was not done at the time. Nevertheless, no correlation between the pH of the polymer solutions added to the cells and polymer cytotoxicity was found, though caution has to be taken when making this assumption. It is difficult to truly estimate the extent of polymer cytotoxicty without this important control.

Table 3.1 Effect of polymers on the pH of medium (containing 10% FBS).

Polymer*	**pH in RPMI**	**pH in DMEM**
Medium only	7.49	7.56
PEI	9.03	8.68
Dextran	7.85	7.62
Alginate	7.13	7.20
HA	7.92	7.85
PAMAM 3.5	8.18	8.06
$sPAcA_{30}$	7.78	7.63
$PAcA_{100}$	6.63	6.71
$PAcA_{450}$	6.54	6.70

* 1 mg/mL in media

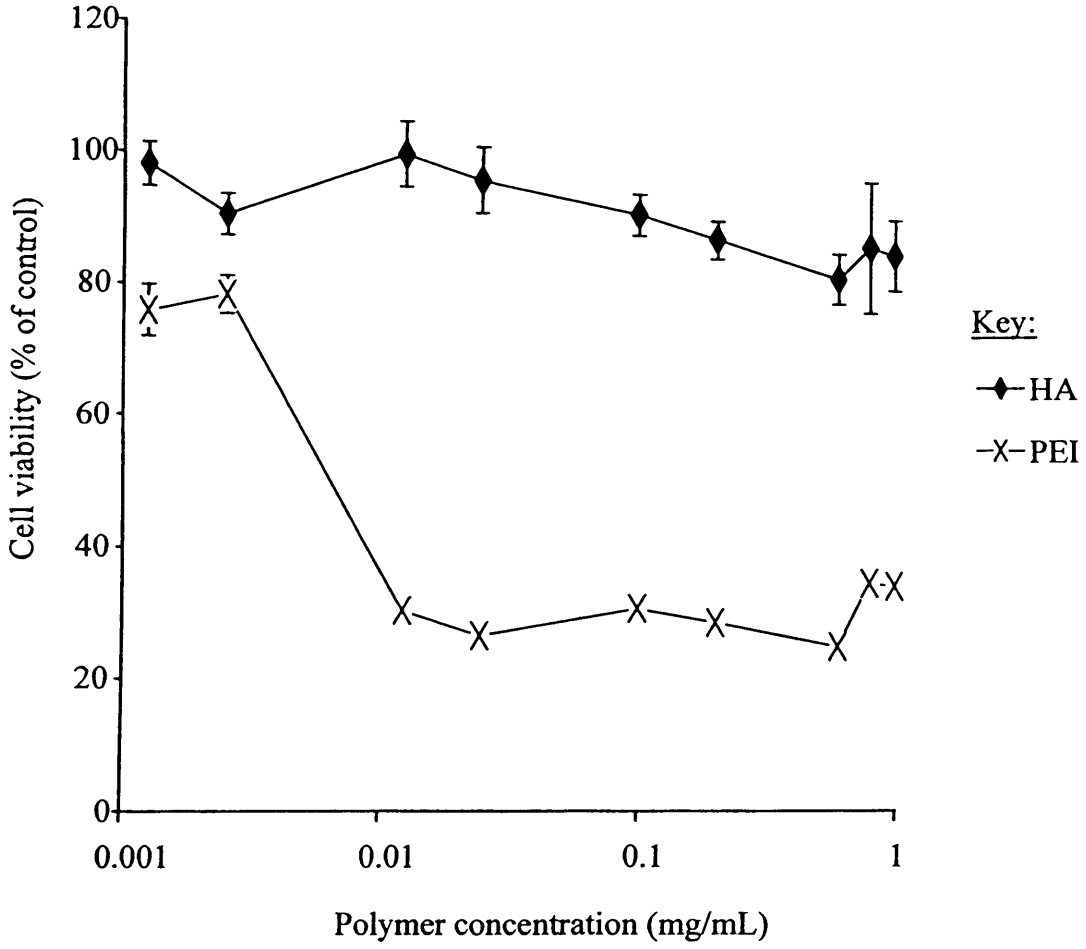

Figure 3.3 Effect of sHA on the viability of DU937 cells (24 h incubation). The cytotoxic reference control, PEI, is also shown. The data shown are mean ± SEM (n = 18).

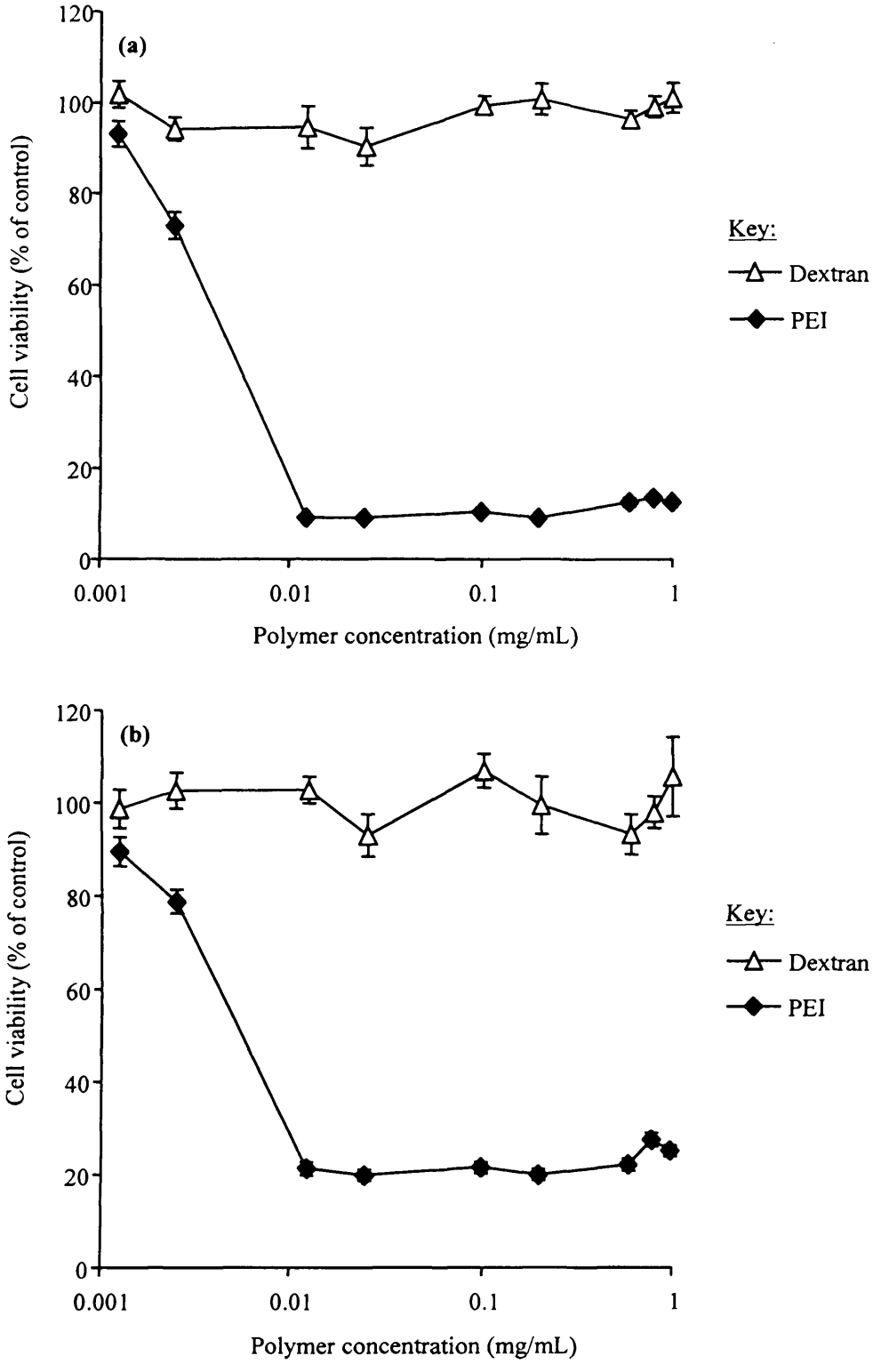

Figure 3.4 (a & b) Effect of PEI and dextran on cell viability (72 h incubation). Panel (a) B16F10 cells and panel (b) ECV304 cells. The data shown are mean ± SEM (n = 18).

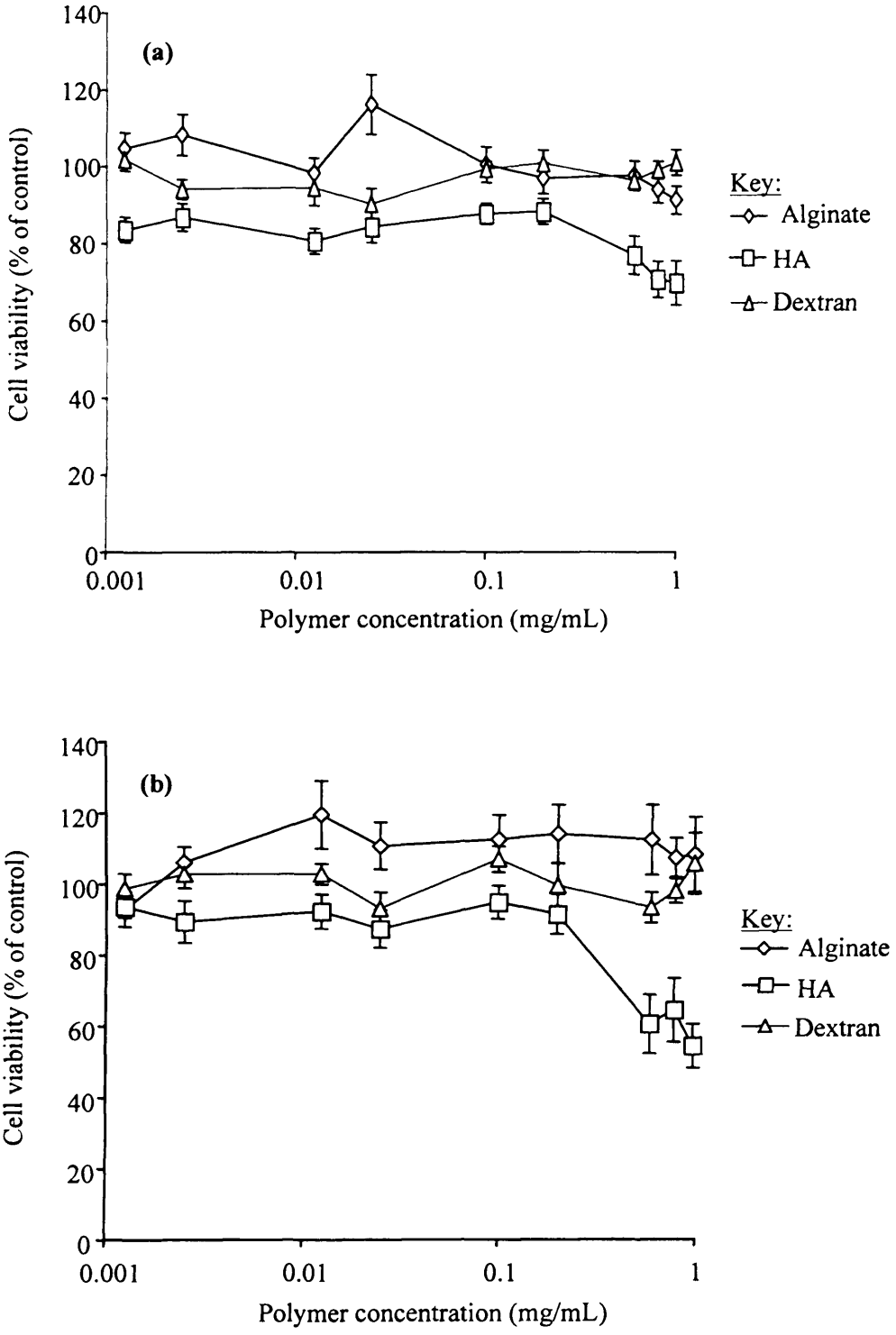

Figure 3.5 (a & b) Effect of polysaccharides on cell viability (72 h incubation). Panel (a) B16F10 cells and panel (b) ECV304 cells. The data shown are mean ± SEM (n = 18).

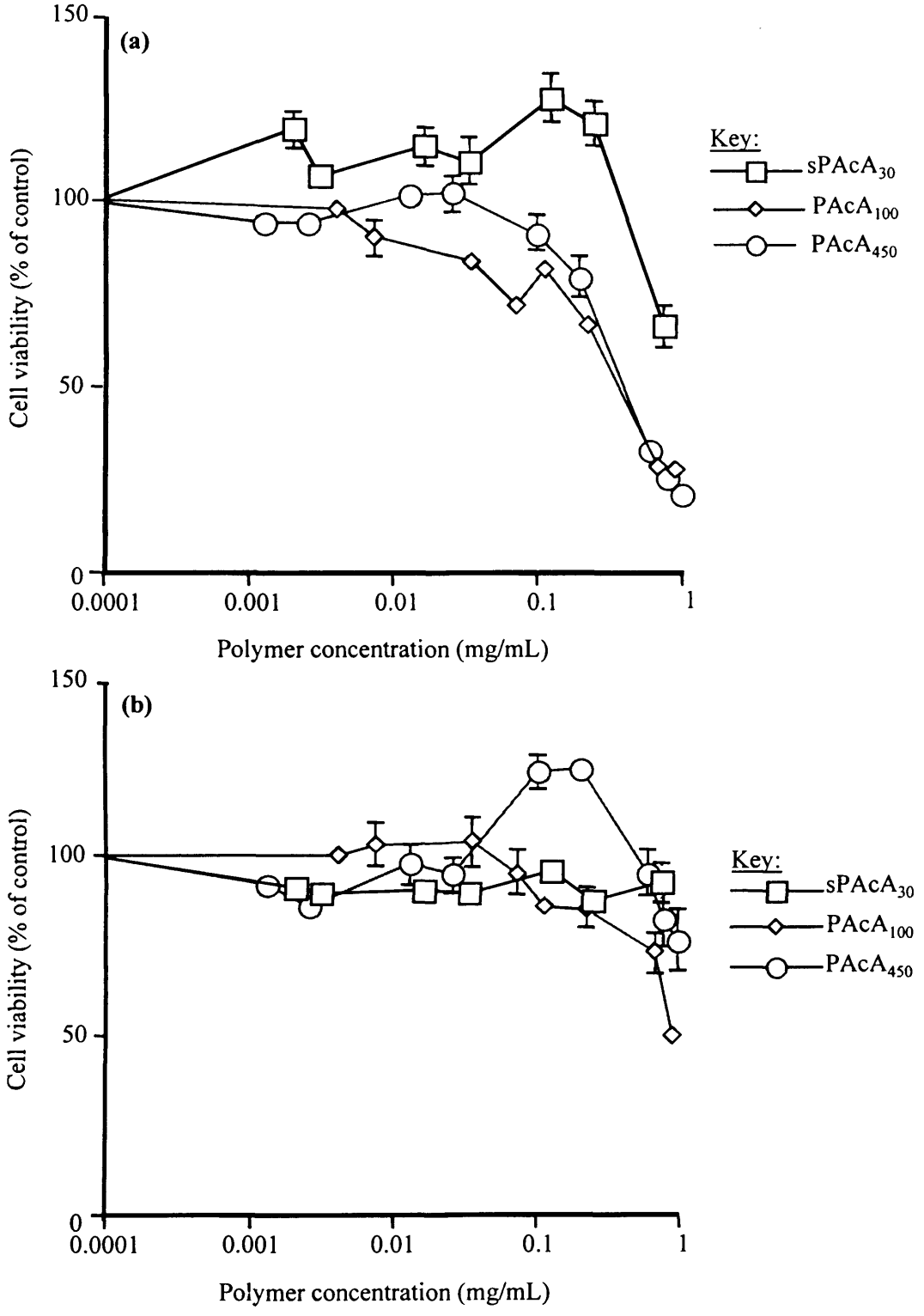

Figure 3.6 (a & b) Effect of PAcAs on cell viability (72 h incubation). Panel (a) B16F10 cells and panel (b) ECV304 cells. The data shown are mean ± SEM (n = 18).

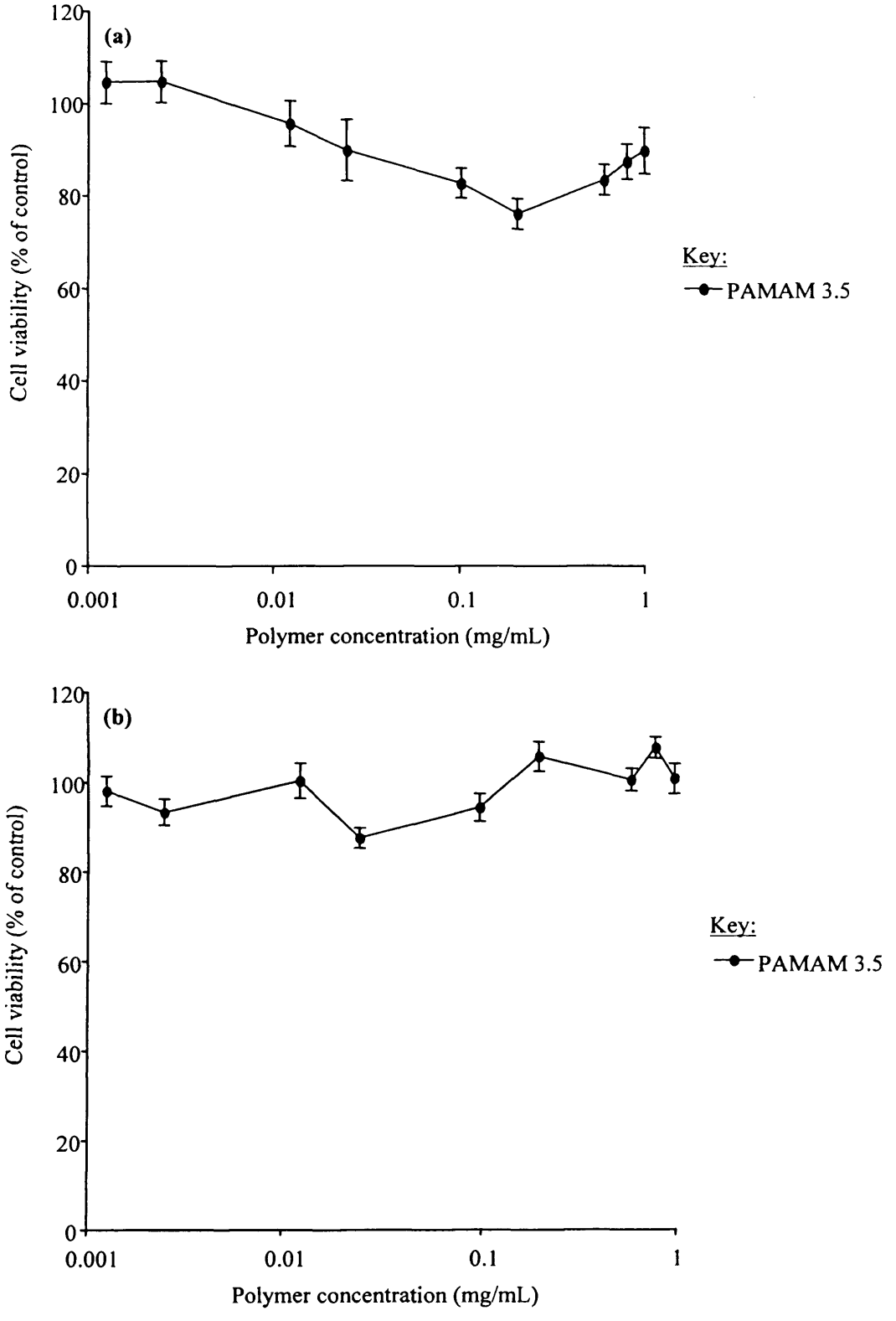

Figure 3.7 (a & b) Effect of PAMAM 3.5 on cell viability (72 h incubation). Panel (a) B16F10 cells and panel (b) ECV304 cells. The data shown are mean ± SEM (n = 18).

Table 3.2 Summary of the IC_{50}[†] values observed.

Polymer	Polymer MW (Daltons)	B16F10 IC_{50} ± SEM (mg/mL) [††]		ECV304 IC_{50} ± SEM (mg/mL) [††]	DU937 IC_{50} ± SEM (mg/mL) [††]
		1 h	72 h	72 h	24 h
Alginate	240,000	> 1	> 1	> 1	ND
Dextran	68,000	> 1	> 1	> 1	ND
HA	50 - 800,000	> 1	> 1	> 1	ND
sHA	3 - 58,000	ND	ND	ND	> 1
$sPAcA_{30}$	30,000	> 1	> 1	> 1	ND
$PAcA_{100}$	100,000	> 1	0.333 ± 0.04	0.958 ± 0.09	ND
$PAcA_{450}$	450,000	> 1	0.418 ± 0.02	> 1	ND
PAMAM 3.5	12,931	> 1	> 1	> 1	ND
PEI	75,000	0.039 ± 0.00	0.004 ± 0.00	0.005 ± 4 x 0.00	0.008 ± 0.00

[†] Inhibitory concentrations at which 50% cell death occurs

[††] Data show the mean (n = 18)

ND = not determined

3.3.2 Establishing ELISA assays

When examining the recovery of cytokine from tissue culture medium in the presence and absence of polymers, medium alone gave a recovery of mTNF-α (97.4%) that was close to the spiked level of cytokine (93.4 pg/mL). In the presence of polymers recovery was apparently higher in almost all cases. Recovery of mTNF-α from media containing PEI (82.4 %) was closest to the value recovered from the media (Figure 3.8). When calibration curves were made with and without PEI, the PEI appeared to reduce the levels of cytokine assayed (Figure 3.9).

3.3.3 Cytokine release from DU937 cells

TNF-α and IL-2 release at 24 h: LPS induced the highest amounts of hTNF-α from DU937 cells (see Figures 3.10, 3.11 3.12 and 3.13), but no hIL-2 (data not shown). A concentration-dependent increase in hTNF-α release was seen with increasing concentrations of sHA and HA, and 100 μg/mL of both polymers induced the highest TNF-α levels (Figures 3.10a and b and respectively). No hTNF-α or hIL-2 release was found when alginate (Figure 3.11), $sPAcA_{30}$ (Figure 3.12) or PAMAM generation 3.5 dendrimers (Figure 3.13), were introduced to the culture. In addition, no hIL-2 release was found when HA was added (data not shown).

Time-dependent TNF-α release: hTNF-α release was detectable at the earliest incubation time of 10 min, and increased quickly with time (Figure 3.10c). Highest levels of hTNF-α for both HA (175 ± 20 pg/mL) and LPS (1301 ± 127 pg/mL) were found at the final incubation time of 5 h. These values are lower than those found after a 24 h incubation (Figure 3.10a).

3.3.4 Cytokine release from B16F10 and RAW 246.7 cells

TNF-α, IFN-γ and IL-2 at 1 h: PEI induced the highest levels of mTNF-α (Figure 3.14a and b), mIFN-γ (Figure 3.15a and b) and mIL-2 (Figure 3.16a and b) in both B16F10 and ECV304 cells respectively. No other polymers induced cytokines.

Time-dependent TNF-α release: No mTNF-α release was detectable when B16F10 cells were incubated with HA or LPS at times up to 24 h (data not shown). In RAW 246.7 cells however, mTNF-α release from HA and LPS-incubated cells was detectable from 10 min (Figure 3.17). mTNF-α levels peaked at 12 h, before slightly decreasing at 24 h. LPS induced more mTNF-α release compared to HA.

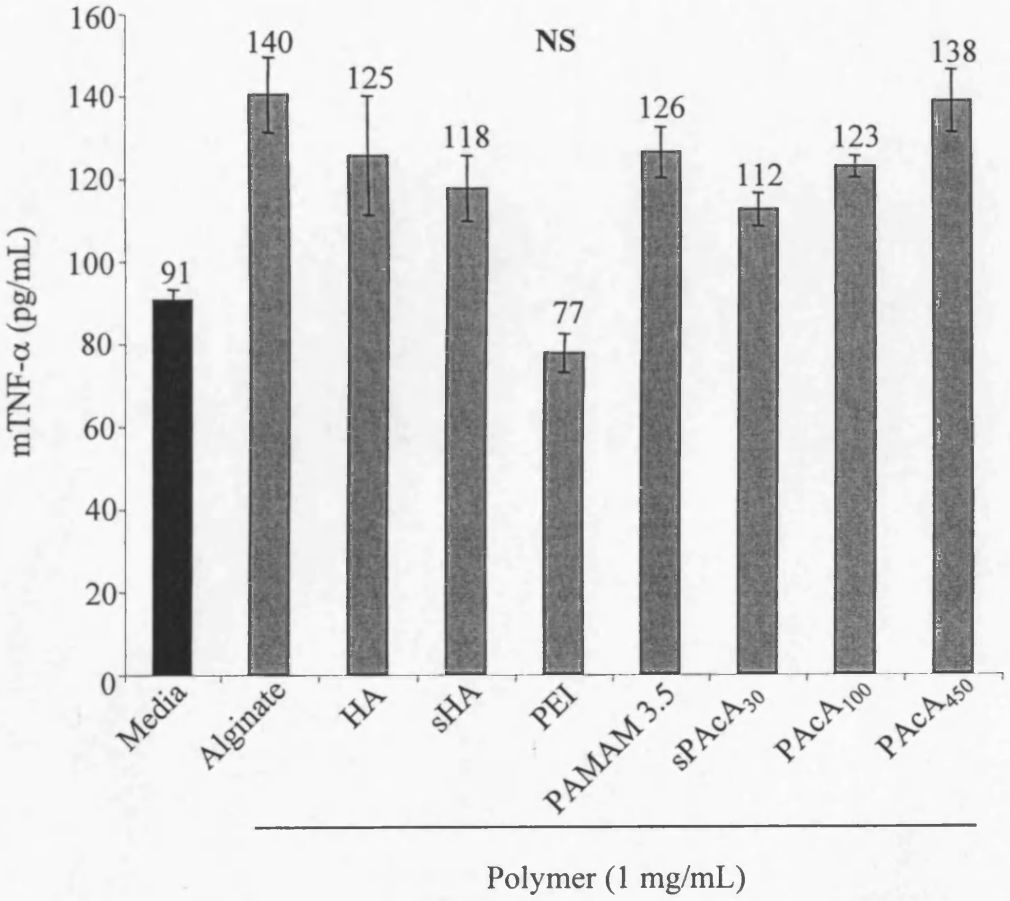

Figure 3.8 Effect of the addition of polymers (1 mg/mL) on the recovery of mTNF-α from tissue culture medium. The data shown are mean ± SEM (n = 3), and were non-significant (NS) according to analysis by one-way ANOVA.

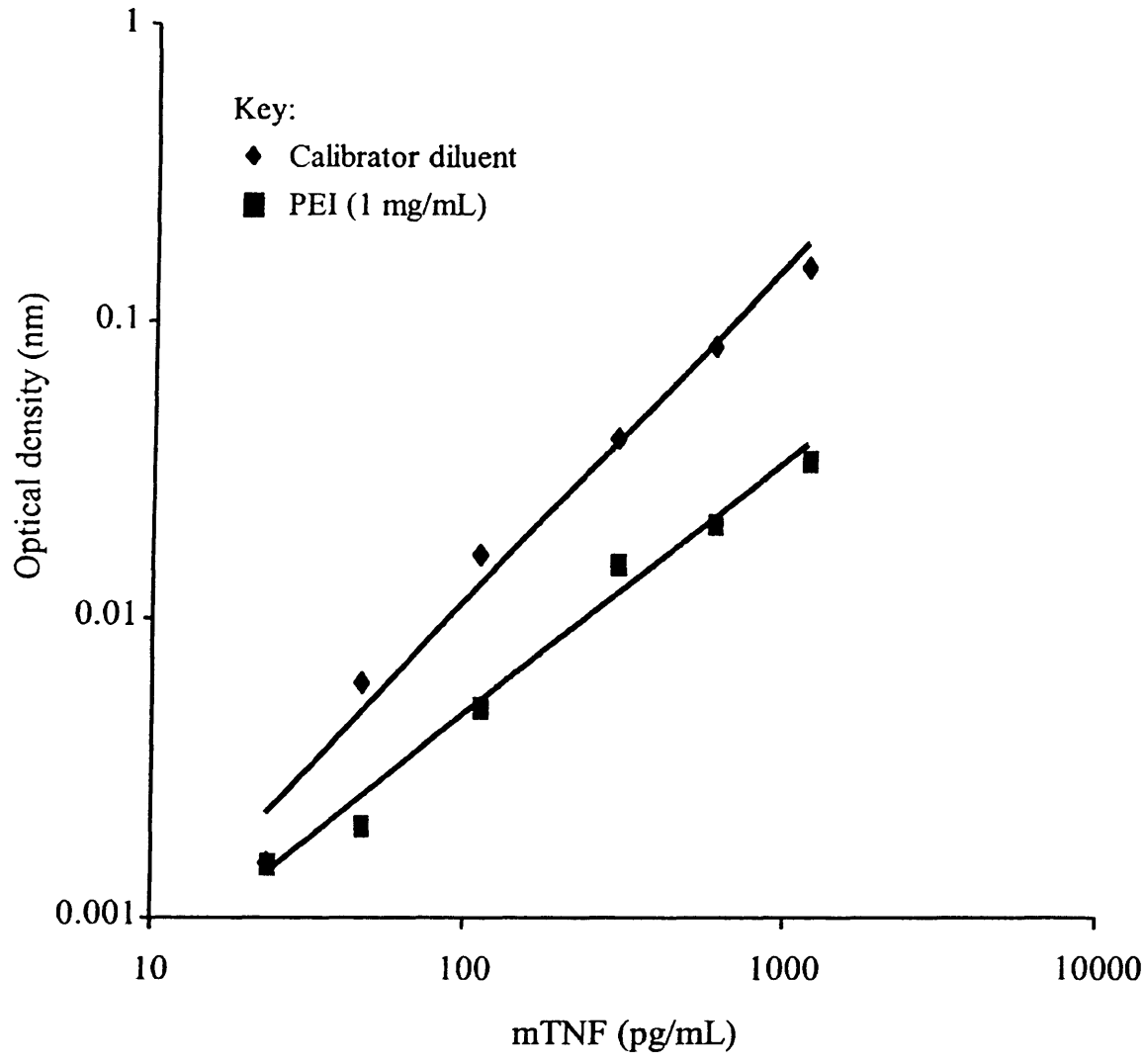

Figure 3.9 Effect of the addition of PEI to the calibration curve observed for mTNF-α. Data were assayed in duplicate (n = 2).

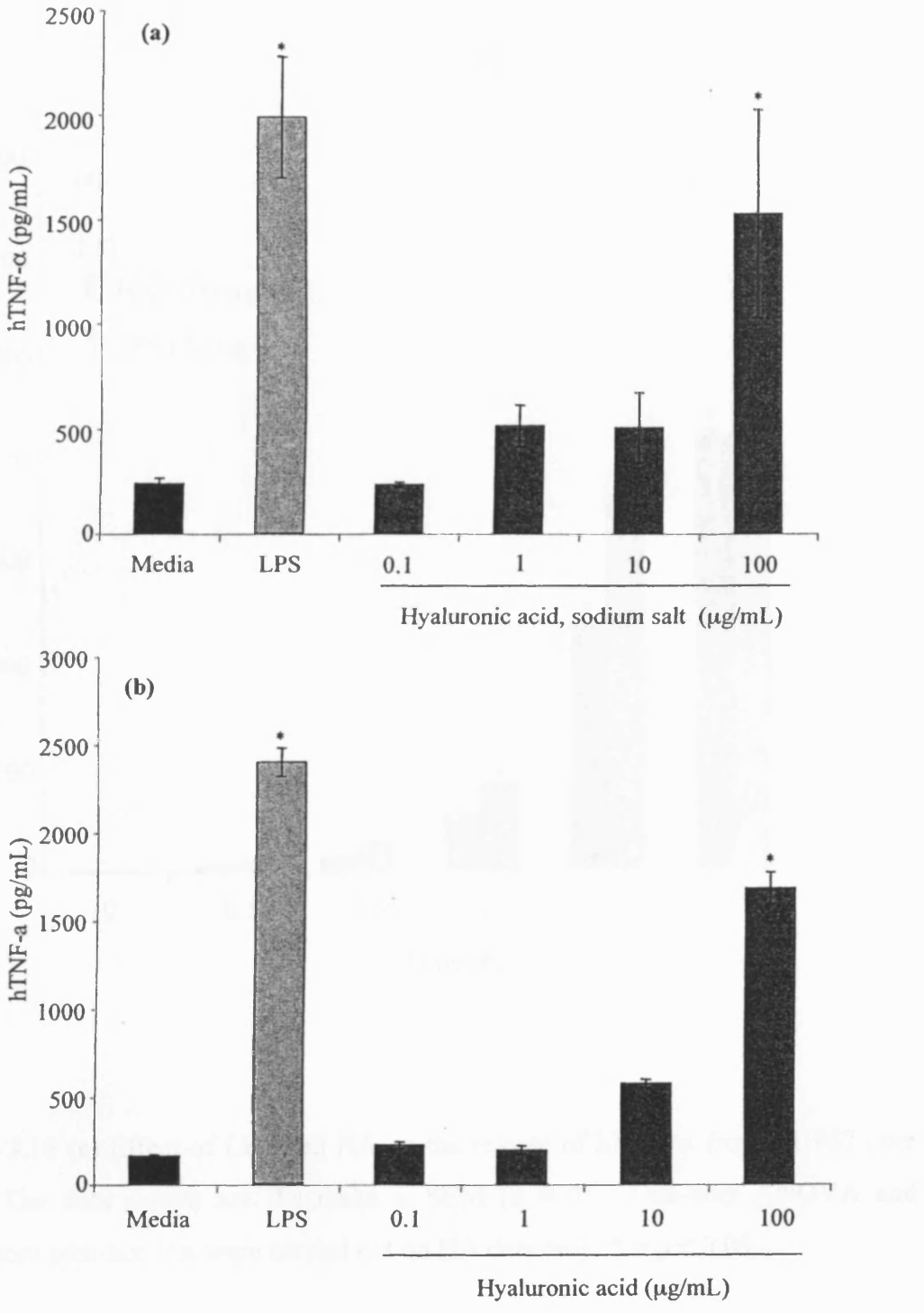

Figure 3.10 (a & b) Effect of concentration and time of exposure on the ability of HAs to induce hTNF-α release from DU937 cells (24 h incubation). RPMI media and LPS were used as positive and negative controls respectively. The data shown are mean ± SEM (n = 3), and were analysed by one-way ANOVA and Bonferroni post-hoc tests. * = $p < 0.05$

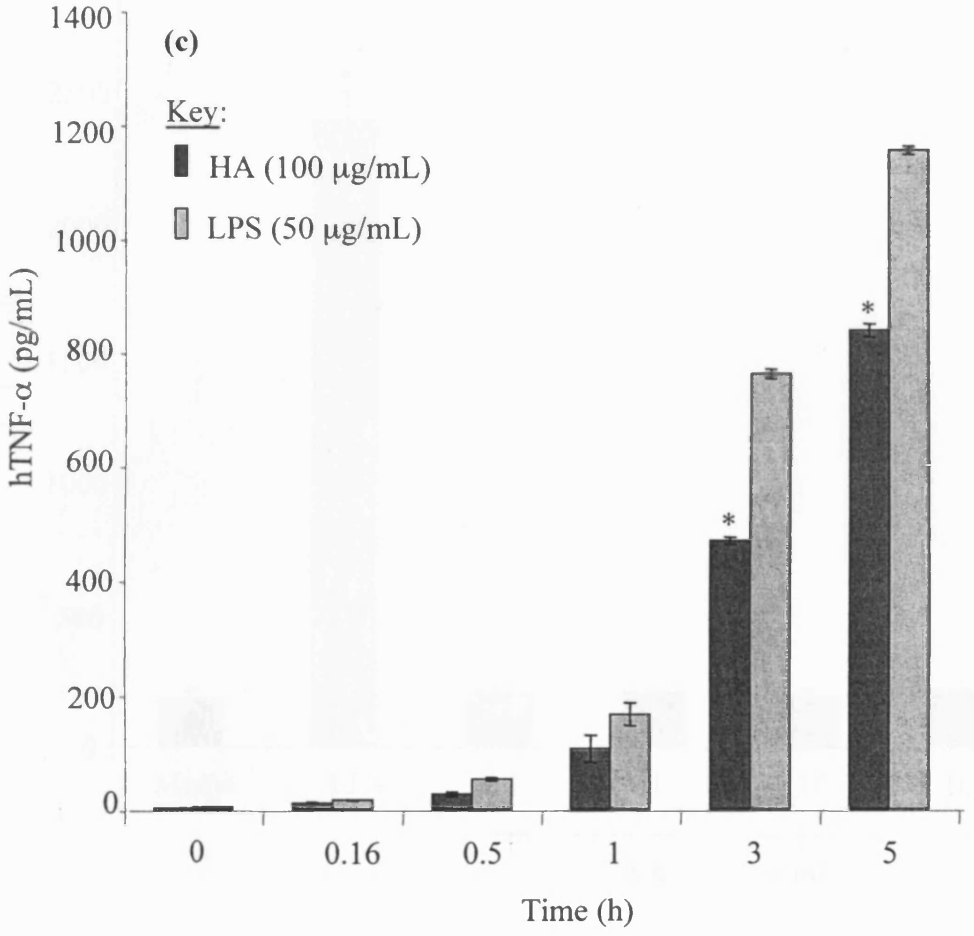

Figure 3.10 (c) Effect of LPS and HA on the release of hTNF-α from DU937 over time. The data shown are the mean ± SEM (n = 3). One-way ANOVA and Bonferroni post-hoc test were carried out on HA data only, * = $p < 0.05$.

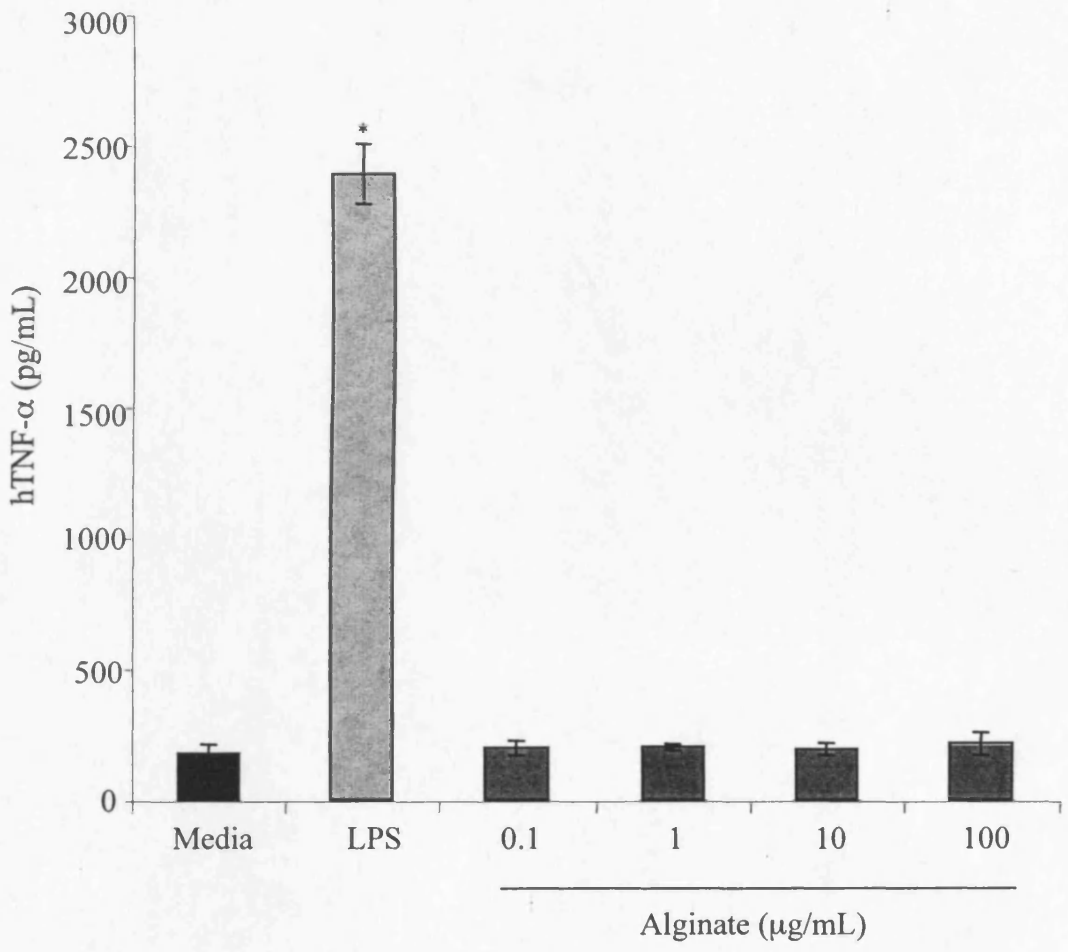

Figure 3.11 Effect of LPS and alginate on release of hTNF-α from DU937 cells (24 h incubation). RPMI media and LPS were used as positive and negative controls respectively. The data shown are mean ± SEM (n = 3), and were analysed by one-way ANOVA and Bonferroni post-hoc test, * = $p < 0.05$.

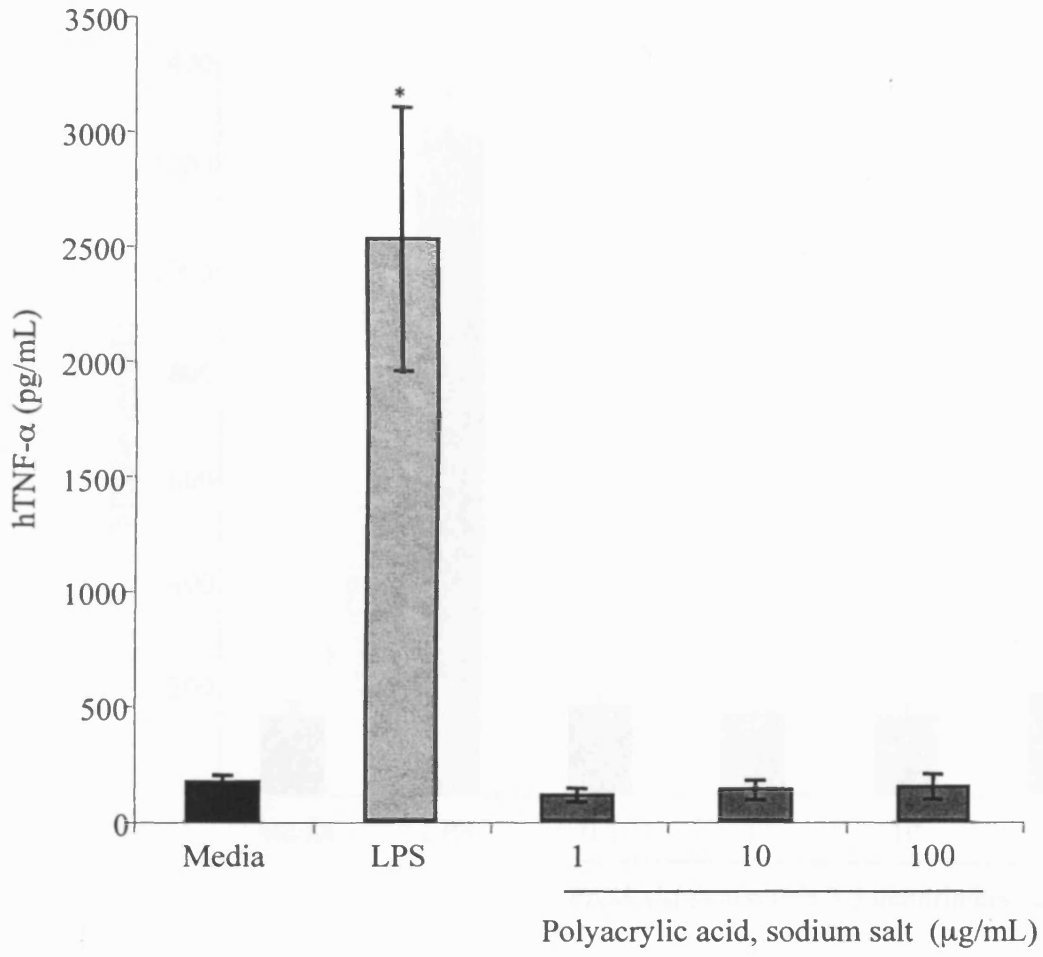

Figure 3.12 Effect of LPS and $sPAcA_{30}$ on release of hTNF-α from DU937 cells (24 h incubation). RPMI media and LPS were used as positive and negative controls respectively. The data shown are mean ± SEM (n = 3), and were analysed by one-way ANOVA and Bonferroni post-hoc test, * = $p < 0.05$.

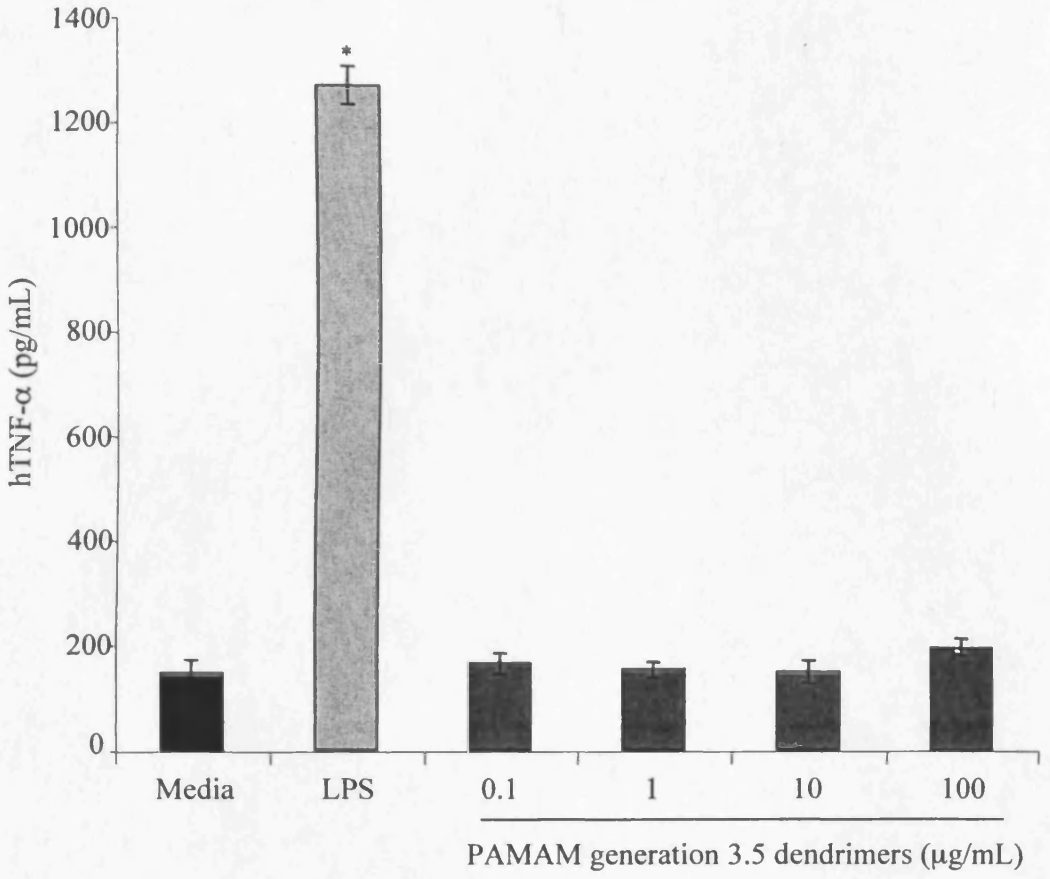

Figure 3.13 Effect of LPS and PAMAM 3.5 on the release of hTNF-α from DU937 cells (24 h incubation). RPMI media and LPS were used as positive and negative controls respectively. The data shown are mean ± SEM (n = 3), and were analysed by one-way ANOVA and Bonferroni post-hoc test, * = $p < 0.05$.

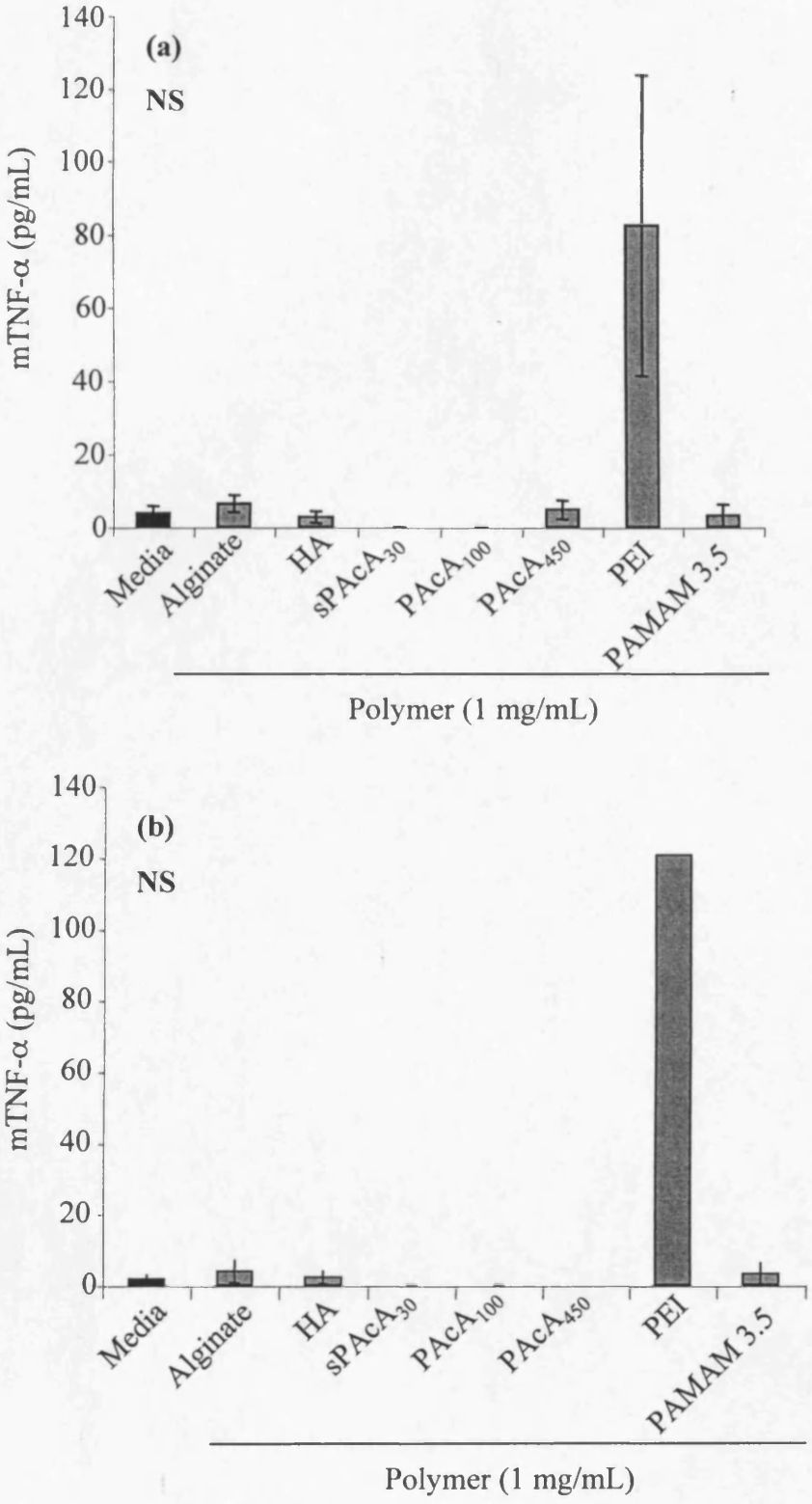

Figure 3.14 (a & b) Effect of polymers on mTNF-α release at 1 h from B16F10 cells (a) and RAW 246.7 cells (b). Data shown are mean ± SEM (n = 3), and NS according analysis by to one-way ANOVA.

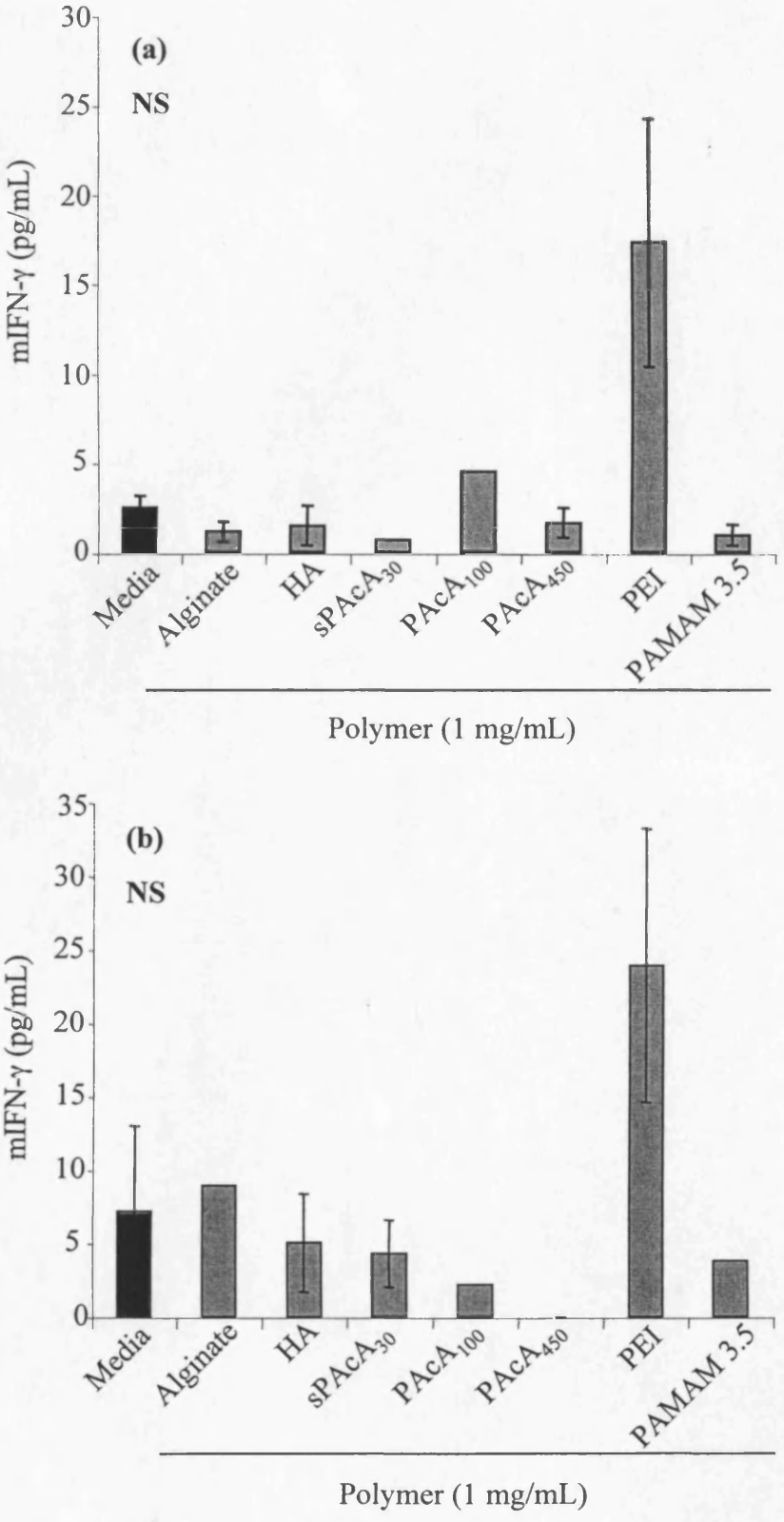

Figure 3.15 (a & b) Effect of polymers on release of mIFN-γ at 1 h from B16F10 cells (a) and RAW 246.7 cells (b). Medium alone is shown as a control. Data shown are mean ± SEM (n = 3), and NS according analysis by to one-way ANOVA.

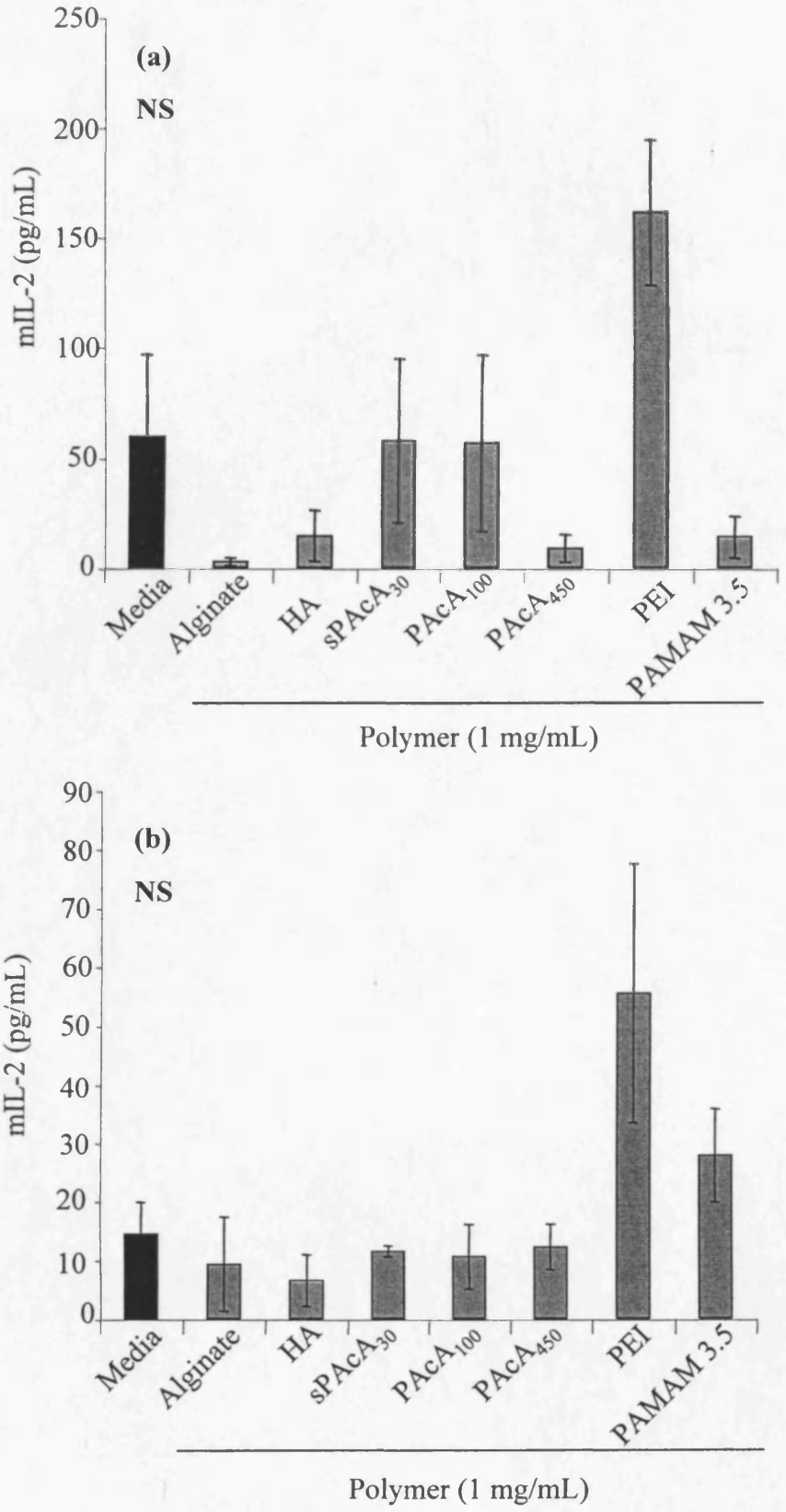

Figure 3.16 (a & b) Effect of polymers on release of mIL-2 at 1 h from B16F10 cells (a) and RAW 246.7 cells (b). Medium alone is shown as a control. Data shown are mean ± SEM (n = 3), and NS according analysis by to one-way ANOVA.

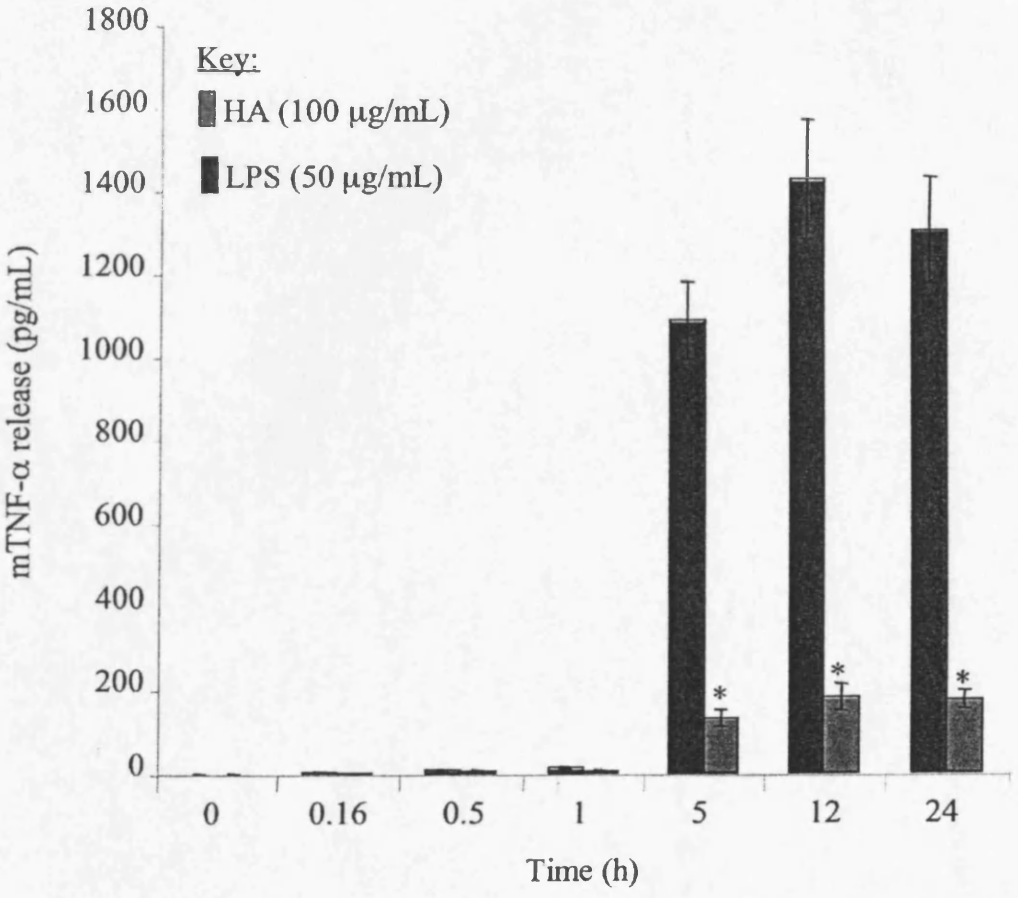

Figure 3.17 Effect of LPS and HA on the release of mTNF-α from RAW 246.7 cells over time. The data shown are the mean ± SEM (n = 3). One-way ANOVA and Bonferroni post-hoc test were carried out on HA data only, * = $p < 0.05$.

3.4 DISCUSSION

The purpose of these studies was to evaluate the cytotoxicity of the chosen polymers using the MTT assay in B16F10, ECV304 and DU937 cell lines, and thus to enable the subsequent use of non-toxic polymer concentrations. ELISA assays were then set up and used to determine the ability of the polymers to induce the release of the cytokines hTNF-α and hIL-2 from DU937 cells, and mTNF-α, mIL-2 and mIFN-γ from B16F10, and RAW 246.7 cells.

Before conducting cytotoxicity experiments, it was important to have documented the growth rate of each cell line, as polymers should only be added to the cells during their logarithmic growth phase. The metabolism of MTT is slower when cells reach confluence (Finlay *et al.*, 1986), thus cells should be used pre-confluence to ensure reproducibility. Moreover, the pH of the tissue culture media containing dissolved polymers was also measured (see Table 3.1), as cell growth is known to decline suddenly on the alkaline side, and more steadily on the acid side of the pH range 7.38 - 7.87 (Mackenzie *et al.*, 1961). Optimum cell growth occurs at pH 7.4. It was therefore important to measure the pH of the polymer solutions used for these studies. Unfortunately however, during cytotoxicity experiments the pH of the control cells were not matched with those incubated with the polymer solutions. This was important, as it would have allowed the cytotoxicity of only the polymers to be assessed, and the effect of pH to be discounted from the MTT assay results.

As expected the high charge density of PEI caused an increase in the pH of the culture medium (pH 8 - 9) (Table 3.1). PAMAM generation 3.5 dendrimers also increased the pH of the culture media (pH 8), despite their 64 anionic (-COOH) terminal end groups. This increase in pH is likely to be due to the exposure of the NH_2 groups within the dendrimer's inner structure (Chen *et al.*, 2000; Rietveld *et al.*, 2001). The polysaccharides dextran, alginate and HA had little effect on the pH of the culture media. $PAcA_{100}$ and $PAcA_{450}$ were the most acidic polymers, and reduced the pH of the media (pH 6). $sPAcA_{30}$ was less acidic in media, as the Na^+ groups on this polymer would neutralise some of its negative charges.

Polymer cytotoxicity

Since the MTT assay was first used to look at the cytotoxicity of polymers in the early 1990's (Sgouras and Duncan, 1990), several general trends with regard to

polymer cytotoxicity have been identified. It is now widely accepted that polymer cytotoxicity increases with polymer molecular weight (Malik *et al.*, 2000; El-Sayed *et al.*, 2003b; Fischer *et al.*, 2003) and that polycations are more destructive to cell membranes than polymers that display negative charges (El-Sayed *et al.*, 2003b; Fischer *et al.*, 2003; Chen *et al.*, 2004). It is for these reasons that the highly branched, high molecular weight, cationic polymer, PEI, was used as a positive control for cytotoxicity experiments.

As expected PEI was more cytotoxic towards B16F10 and ECV304 cells, than the acidic polymers: PAcAs, alginate and HA, or the negative reference control polymer dextran (Table 3.2). It was also more cytotoxic than sHA in DU937 cells (Table 3.2), and thus provided a good positive control. Dextran also provided a good negative control polymer for cytotoxicity studies, as in accordance with literature, both B16F10 and ECV304 cells remained 100 % viable when incubated with it (up to 1 mg/mL) over 72 h (Figure 3.4a and b respectively). A summary of IC_{50} values reported for the polymers used in this study is given in Table 3.3, however, caution should to be taken when comparing experiments conducted in different laboratories. The phenotype and characteristics of cells (i.e. if a suspension or an adherent line), as well as the incubation times with polymers are both important, as these factors affect the IC_{50} values observed (Sgouras and Duncan, 1990; Fischer *et al.*, 2003).

$PAcA_{100}$, $PAcA_{450}$ and PEI for example showed time-dependent cytotoxicity toward B16F10 cells. They were less cytotoxic at 24 h than at 72 h (Table 3.2). In addition, the B16F10 cells were more sensitive to polymer-induced cell damage than ECV304 cells (Table 3.2), and this effect is likely to be due to a difference in cell metabolism. B16F10 cells have a faster growth rate (doubling time = 1 day) than ECV304 cells (doubling time = 4 days), though it could also be due to a difference in extracellular cell-membrane composition. Furthermore, the culture conditions of the cells used can also affect results obtained in cytotoxicity experiments. For example, unlike Sgouras and Duncan (1990) who investigated polymer cytotoxicity in heptacellular carcinoma and lymphoblastic leukemia cells, the polymers used in this study were always dissolved in media containing 10 % FBS. This was because B16F10 cells have shown arrested growth at low serum concentrations (Rodriguez-Ayerbe and Smith-Zubiaga, 2000).

Table 3.3 Summary of IC_{50} values from literature.

Polymer	Cell line	Polymer MW (Daltons)	Assay method	Total polymer incubation (h)	IC_{50} value (μg/mL)	Reference
PEI	L929	750,000	MTT	1	31.0	(Fischer *et al.*, 2003)
				24	9.0	
	Eyrthrocytes	25,000	RBCL†	-	Complete lysis ≥ 1000	(Fischer *et al.*, 2003)
	B16F10		MTT	72		(Malik *et al.*, 2000)
	COS-7		MTT	24	< 20	(Kean *et al.*, 2005)
PAMAM 3.5	Caco2	12,931	MTT	3	> 1000	(Jevprasesphant *et al.*, 2003)
	B16F10		MTT	72	> 2000	(Malik *et al.*, 2000)
Dextran	CCRF*	40,200	MTT	72	98.0 ± 11.9	(Sgouras and Duncan 1990)
	B16F10	70,000	MTT	72	> 2000	(Malik *et al.*, 2000)

* cells grown in the absence of serum proteins.

† Red blood cell lysis

Cytotoxicity of the polymer library

Alginate and HA had IC_{50} values of greater than 1 mg/mL in ECV304, B16F10 (72 h incubation), and DU937 cells (24 h incubation) (Table 3.2). This was expected, as both polymers are routinely used in a variety of applications (see Chapter 1, sections 1.6.1 and 1.6.2 respectively), and have been adopted by the European Pharmacopoeia.

PAcAs (introduced in Chapter 1, section 1.6.3) are also regarded as non-toxic and non-irritant polymers, and are included in the FDA inactive ingredients guide. They are commonly used in non-parental medicines. The lethal dose 50 values (LD_{50}; chemical dose that is lethal to 50 % of a test population) for the PAcAs used for these studies according to the supplier (www.sigmaaldrich.com) are: 2000 mg/kg for $PAcA_{100}$, 2500 mg/kg for $PAcA_{450}$, and > 40,000 mg/kg for $sPAcA_{30}$ when orally administered to rats. The rank order for PAcA cytotoxicity in both B16F10 and ECV304 cells at 72 h also showed this trend, where $PAcA_{100} > PAcA_{450} > sPAcA_{30}$ (Figure 3.6, Table 3.2). The IC_{50} value of $sPAcA_{30}$ was greater than 1 mg/mL.

Due to increasing interest in the possibility of using PAMAM dendrimers for drug and gene delivery, the cytotoxicity of these molecules has been widely investigated. The toxicity of these molecules is dependent upon their generation, and terminal end groups. Lower generation PAMAM dendrimers are sometimes cytotoxic due to their open molecular structure (as their core is more accessible to cells (Malik *et al.*, 2000)), whilst full generation, cationic, PAMAM dendrimers (displaying $-NH_2$ termini) show generation-dependent cytotoxicity (Malik *et al.*, 2000; El-Sayed *et al.*, 2003b). Quaternised (-OH) and half (-COOH) generation PAMAM dendrimers have a lower level of cytotoxicity thought to be due to the shielding of their internal cationic charges (Lee *et al.*, 2005).

In accordance with the literature (Table 3.3), in these studies PAMAM generation 3.5 dendrimers did not have an effect on B16F10 or ECV304 cell viability at concentrations up to 1 mg/mL over 72 h.

Cytokine release caused by the polymer library

Before conducting ELISA experiments, it was important to determine whether the polymers would interfere with the assays. Addition of cytokine standard (mTNF-α) to tissue culture media did not affect recovery (Figure 3.8). This was expected as

the supplier information states that the kits can be used for this purpose (www.rndsystems.com). PEI appeared to interact with the assay, as the mTNF-α standard calibration curve spiked with this polymer gave a lower recovery (Figure 3.9). This is likely to be due to the electrostatic interaction of PEI with the cytokine or the Ig bound in the ELISA plates.

One draw back of using ELISA kits to assay for cytokines is that samples have to be measured in duplicate, and they are costly (approximately £250 - £500 depending on the kit). This limits the number of experiments that can be conducted. As a result, the calibration curves spiked with PEI were only conducted once.

Using a well-known cell line and standard it was important to verify that the assays used were working. DU937 macrophage-like cells and LPS provided good positive controls for hTNF-α ELISA assays. In accordance with Boyce and colleagues (1997) (who used L929 cells as a bioassay), sHA stimulated the release of hTNF-α from these cells in a concentration-dependent (0.1 – 100 μg/mL) manner, after 24 h incubation (Figure 3.10a). Likewise, HA also had the same effect (Figure 3.10b), suggesting that the salt form of HA is not important for hTNF-α release. The release of hTNF-α from DU937 cells also increased with incubation time from 0 - 5 h (Figure 3.10c).

The ability of (s)HA to induce hTNF-α release from DU937 macrophage cells (Boyce *et al.*, 1997), is probably due to a receptor mediated reaction. HA has been shown to interact with several cell surface receptors including CD44, ICAM, and RHAMM, and to activate cells accordingly (as reviewed in Chapter 1, section 1.6.2). Similarly, the positive response of DU937 cells to LPS was also expected (see section 5.1), as macrophage cells express CD14, and thus react to picogram (pg) quantities of this molecule (Ulevitch, 1993; Wright *et al.*, 1990).

However, when DU937 cells were incubated with alginate (Figure 3.11), $sPAcA_{30}$ (Figure 3.12) and PAMAM 3.5 (Figure 3.13) for 24 h, no hTNF-α release was seen. In the case of alginate, this result was surprising. As mentioned in Chapter 1 (section 1.6.1), many reports have shown that high M alginates induce TNF-α from macrophage (Thomas *et al.*, 2000; Son *et al.*, 2001) and monocyte (Otterlei *et al.*, 1991; Otterlei *et al.*, 1993; Espevik *et al.*, 1993; Jahr *et al.*, 1997; Berntzen *et al.*, 1998; Jahr *et al.*, 1997) cells via interaction with CD14, and this response is not due

to LPS contamination. Though attempts were made in this study to measure the LPS content of polymer stocks, the polymers appeared to interfere with the assay. However, as no cytokine release was seen from polymer-incubated cells, the assay was considered unnecessary.

Possible reasons for the negative response of alginate in ELISA assays

Alginates have been found to bind not only to CD14, but also to bind LBP and the bactericidal/permeability-increasing protein (Jahr *et al.*, 1997). It induces TNF-α release in a similar way to LPS.

As membrane-bound CD14 lacks a cytoplasmic tail, it is thought to aggregate LPS or alginate at the cell surface, to interact with TLRs (possibly TLR 4 or TLR 2) for signal transduction (Flo *et al.*, 2000). Both receptors are present on PMA-differentiated U937 cells (Greene *et al.*, 2004), thus it is not clear why no hTNF-α release was seen from this cell line. It was considered that the sterile-filtration (through 0.2 μM pore filters) of alginate-containing tissue culture media could have reduced the quantity of alginate added to the cells, if the polymer had stuck to the filter, yet in the literature, alginates of up to 550,000 Da have also been sterilised via this method (Otterlei *et al.*, 1991; Otterlei *et al.*, 1993).

As polymer-incubation time is also important for cytokine production (Figure 3.10c), it was also considered that simply investigating hTNF-α release after 24 h might not have been useful. In the literature reports have demonstrated hTNF-α release from alginate-incubated monocytes after 6 - 24 h incubations (Otterlei *et al.*, 1991; Otterlei *et al.*, 1993; Espevik *et al.*, 1993; Jahr *et al.*, 1997; Berntzen *et al.*, 1998; Flo *et al.*, 2000). As previously mentioned, the M-content of the alginate is important, and although a high M alginate was selected for this work, the exact M content is not known. Alginates in the literature were mainly from bacteria, and were 85-99 % M. It would be interesting to determine the M content of the alginate used for these studies, perhaps by using ^{1}H nuclear magnetic resonance spectroscopy.

In comparison to DU937 cells, a different TNF-α release profile was seen in RAW 246.7 cells incubated with HA and LPS, where release of the cytokine remained low until 5 h (Figure 3.14). As with cytotoxicity, this is likely to be due to a difference in cell metabolism and cell surface composition. What's more, a recent report in the literature has shown that CD44, TLR 4 and RHAMM receptors are

Table 3.4 Phenotype, origin, common experimental applications, and cytokines produced by the cell lines chosen for this work.

Cell line	Species and Phenotype	Cell origin	Cytokines secreted	Experimental applications	References
B16F10	Murine, dendritic pigmented macrophages	From B16 murine melanoma cells after isolation of metastases and serial passages in culture.	IL-2 IL-18	Tumour model in mice. Their pigment allows them to be visualised when metastasised	(Garcia de Galeano *et al.*, 1996)
ECV304	Human, endothelial-like cells	Spontaneously transformed human umbilical vein cell line, taken from a newborn Japanese female.	VEGF TGF-β1	Endothelial model for angiogenesis, cell migration, glucose transport, and blood-brain barrier studies	(Huges *et al.*, 1996
RAW 246.7	Murine, monocyte and macrophage-like cells	Established from tumour ascites of a male mouse, induced by an i.p. injection of Abselon Leukaemia Virus.	IL-1ra TNF-α IL-6 VEGF	Widely used as a model marcophage cell line	(Heming, 1996)
DU937	Human, macrophage-like cells	DU937 cells are a mature from of promonocytic, U937 cells that were established from a human diffuse histiocytic lymphoma patient.	IL-1 ra TNF-α TGF-β M-CSF	Served as a model for monocyte-macrophage differentiation.	(Boyce *et al.*, 1997)

responsible for mTNF-α release from HA-incubated cells in this cell line (Wang *et al.*, 2006). No cytokine release was seen in B16F10 cells when incubated with the above over 24 h. There appear to be no reports in the literature that have detected the release of mTNF-α from this cell line (Table 3.4), and they do not express TLR 2 or TLR 4 (Manjili *et al.*, 2006), but do express high levels of CD44 (Zawadzki *et al.*, 1998).

Only PEI induced mTNF-α, mIFN-γ and mIL-2 release from B16F10 and RAW 246.7 cells at 1 h. This data is in accordance with Puckey 2002, who reported high levels of mTNF-α release from B16F10 cells incubated with this polymer (3 mg/mL). As B16F10 cells were unresponsive to LPS, PEI was used as a positive control for ELISA experiments with these and the RAW 246.7 cells.

The exact mechanism of cytokine release caused by PEI is not known, though it can be speculated that disruption of the cell membrane and release of cytosolic proteins into the culture media from cells killed by this polymer, may have interfered with the ELISA assay. Additionally, PEI could have caused membrane proteins to gather into two-dimensional clusters (Godbey *et al.*, 1999), and the gaps between the aggregated proteins could then play the part of pores allowing potassium ions to rush out from the cell, and Ca^{2+} to rush in along a concentration gradient (reviewed by Kabanov, 2004). To compensate for this difference, the cell would then increase its consumption of ATP, resulting in the activation of molecular pumps that would give start-up signals to other intracellular systems that could lead to cytokine release. PEI has already been shown to enhance the immune system towards transplanted tumour cells in test animals (Moroson, 1971), and to activate macrophage cells *in vitro* (Bogwald *et al.*, 1984).

CHAPTER 4:

Effect of TNF-α, IFN-γ and IL-2 on FITC-dextran Transport Across Rat Intestinal Tissue

4.1 INTRODUCTION

Although most of the polymers studied in the previous chapter did not show cytokine release from the cell lines used, it was decided to move forward and examine the ability of cytokines (rTNF-α, rIFN-γ or rIL-2) to stimulate the transport of FITC-dextran across rat intestinal tissue. This physiological tissue was used as a model epithelial barrier as it was thought to provide the best opportunity to explore the effects of rTNF-α, rIFN-γ or rIL-2 on a 'mixed cell population', and thus to provide maximum opportunity to stimulate transport.

Progression to these studies was important as a growing number of papers were suggesting that the polymeric excipients such as PAcA (Kast and Bernkop-Schnürch, 2002), chitosan (Borchard *et al.*, 1996; Kotze *et al.*, 1997; Kotze *et al.*, 1999; Thanou *et al.*, 2000) and PAMAM dendrimers (El-Sayed *et al.*, 2003; El-Sayed *et al.*, 2003; as well as cytokines (most notably TNF-α and IFN-γ), could increase cellular permeability. However it is also known that both cytokines are also involved in hyper-permeable inflammatory bowel diseases (IBD).

Elevated levels of TNF-α are associated with the pathogenesis of Crohn's disease (CD) (reviewed in VanDeventer, 1997; Yamamoto *et al.*, 2004) and ulcerative colitis (UC) (Murch *et al.*, 1993; Masuda *et al.*, 1995; Scarpa *et al.*, 2004). TNF-α is thought to play a key role in these diseases by damaging the integrity of epithelial (Chakravortty and Kumar, 1999; Schmitz *et al.*, 1999; Gitter *et al.*, 2000a; Gitter *et al.*, 2000b; Bruewer *et al.*, 2005; Poritz *et al.*, 2004) and endothelial membranes and increasing inflammatory cell recruitment (reviewed in VanDeventer, 1997). High concentrations of this cytokine have been identified in the inflamed mucosa, serum and stools (Breagger, 1992) of these patients, and inhibitors for TNF-α (see Chapter 1, section 1.3.1) are known to alleviate their symptoms.

IFN-γ is also known to be involved in the pathogenesis of Crohn's disease, and has been identified in the inflamed intestine of these patients, where it is produced by large numbers of active lymphocytes (Fais *et al.*, 1991; Agnholt *et al.*, 2001; Olaussen *et al.*, 2002).

To study the effect of cytokines on transport across the rat intestine, FITC-dextran (Figure 4.1) was chosen as a marker for paracelluar integrity and the vertical diffusion system was used as a model. The rationale for this selection is discussed in the following sections.

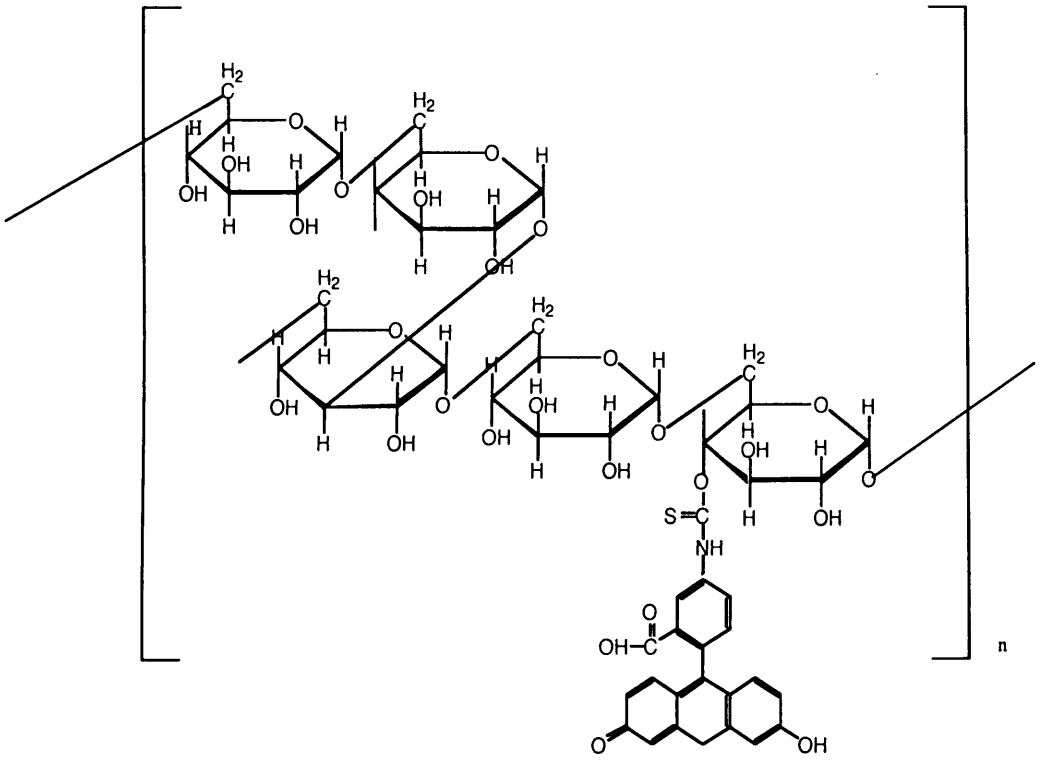

Figure 4.1 Chemical structure of FITC-dextran

Rationale for the choice of paracellular marker

FITC-dextran (MW = 4,000 Da; a hydrophilic, fluorescently labelled dextran polymer; see Figure 4.1) was chosen as a model paracellular probe for these studies, as it has been widely used by others to study TJ integrity in Caco-2 cells (Sakai *et al.*, 1997; Lindmark *et al.*, 1997), porcine and human buccal mucosa (Hoogstraate *et al.*, 1994; Junginger *et al.*, 1999 and Van der Bijl *et al.*, 1998 respectively) and the rat intestine (Horie *et al.*, 2001; Nakamura *et al.*, 2003). Like most hydrophilic drugs e.g. bisphosphonates (reviewed by Lin, 1996), and macromolecular therapeutics including proteins (e.g. monoclonal antibodies) peptides (e.g. insulin), and many polymers, FITC-dextran is normally excluded from the paracellular pathway (see Figure 1.4) due to the restriction of TJ.

Rationale for the choice of transport model used

A number of *in vitro* models have been developed to study the intestinal permeability of drugs and polymers (reviewed in Barthe *et al.*, 1999). The simplest involve the use of epithelial cell monolayers, namely human colon carcinoma cells such as T84 (Madara *et al.*, 1987) and HT29 (Zweibaum *et al.*, 1985), or Caco-2 human primary colon carcinoma cells (Fogh *et al.*, 1977; Hidalgo *et al.*, 1989; Hilgers *et al.*, 1990). The cells are grown on filters until they reach a confluent monolayer (often monitored by reading the TEER) and they are then used to measure intestinal permeability. Of them, Caco-2 cell monolayers are the most commonly used model, and have been widely adopted by the pharmaceutical industry, for screening the potential oral bioavailability of new drugs. Caco-2 monolayers have advantages over other intestinal cell lines, as they differentiate (spontaneously) into polarised cells that possess the greatest number of adult entrocyte features, including a brush-border (Pinto *et al.*, 1982) with ectoenzymes (Zweibaum *et al.*, 1983; Zweibaum *et al.*, 1984; Hauri *et al.*, 1985). However, they require culture for up-to 20 days in order to develop an intact monolayer (Pinto *et al.*, 1983), and as a consequence are usually grown in media containing antibiotics. Moreover, mature Caco-2 cells are devoid of a mucus layer (Wikman-Larhed *et al.*, 1995; Hilgendork *et al.*, 2000), as expressed by goblet cells *in vivo*, over-express P-gp (Hosoya *et al.*, 1996; Goto *et al.*, 2003; Anderle *et al.*, 2003), and possess tighter TJ compared to other epithelial models. This is thought be due to them having smaller paracellular pores (Artursson *et al.*, 1993; Collett *et al.*, 1997).

Consequently, more physiological models that use segments or explants of intestinal tissue are sometimes preferred. These methods offer some benefit over monolayer models as they are more physiological, and they possess mucus. They can also be used to investigate permeability differences across different regions of the GI tract, and can be selected to contain Peyer's patch regions.

The closest example to the intestine *in vivo,* is the single pass perfusion model (reviewed by Roig and Vinardell, 1991; reviewed by Barthe *et al.,* 1999), which uses segments of the intestine from anesthetised animals that are cannulated, flushed, and perfused with a drug-containing solution. In this case the blood supply and clearance capabilities of the animal remain intact, and the amount of drug absorbed from the perfusate can be calculated from blood samples taken from the mesenteric vein. However, no information about drug permeation at the cellular level is gained with this method, and some evidence has shown that the anaesthesia and surgical manipulation of the animals can have pronounced effects on absorption (Uhing and Kimura, 1995). Moreover, the flow rate of the perfused intestine is often higher than that *in vivo*, resulting in increased luminal hydrostatic pressure that may also affect permeability (Chiou, 1994).

In contrast, the everted gut sac method first described by Wilson and Wisemann in 1954, and developed as a screening tool by Barthe and colleges (1998), is a relatively quick and simple model that can be used to gain an insight into the mechanism of drug absorption. Excised intestine from fasted rats, is flushed with saline, placed into oxygenated (TC 199) medium, and everted over a glass rod (3 mm in diameter). The resultant intestinal tube is filled with fresh oxygenated medium, and divided into (2-4 cm) sacs using silk suture. Each sac is then incubated with test compounds for up to 2 h, with shaking to ensure mixing (that would occur naturally as a result of peristalsis), and at the end of each experiment test compounds are analysed in the sac tissue and the serosal fluid (Diamanti, 2004). Compounds that are metabolised by cell surface enzymes in the intestine are detectable in the medium following incubation, whilst drugs that are absorbed by cells may be susceptible to first-pass metabolism. These drugs may be transported into the serosal space, or confined to the cell interior. If compounds are transported via the paracellular route, they will only be found in the serosal space. This form of transport would also be

concentration-dependent. Finally, to normalise each sac to per unit protein, each sac is also dissolved in acid (NaOH), so that tissue protein content can be measured.

The only disadvantage of using this model are that the serosal compartment of each sac is a closed system, which could misrepresent the absorption kinetics of drugs during long incubations, or if a drug is very rapidly absorbed (reviewed in Barthe *et al.,* 1999).

The Ussing chamber is an electrophysiological technique that has proved a popular alternative for studying transport. This method was originally developed by Ussing, who used it to prove the active transport pathway, when he measured Na^+ transport across frog skin (Ussing and Zehran, 1951). To-date, virtually all types of epithelial tissue has been studied using this model. The Ussing chamber essentially consists of two functional halves: one is the chamber itself, whilst the other is the electric circuitry. To measure transport across the intestine using this method, small sections of tissue are clamped between two chambers (containing medium), so that the transport of detectable compounds between the chambers can only occur across the tissue. Electrodes positioned in each chamber accompany measurement of transport, by measuring the electrical potential, which indicates the rate of ion flow across the tissue.

The vertical diffusion system (Grass and Sweetana, 1988) as used for these studies is a relatively quick and simple adaptation of the Ussing chamber model. It contains six transparent acrylic chambers (though only four were used for these studies) that are kept at 37 °C via a heated block, and are supplied with gas (95 % O_2, 5 % CO_2) to circulate the buffer, and to keep the tissue viable (see Figure 2.8). The benefits of using this model are that (i) several experiments can be carried out simultaneously using all the chambers, (ii) using physiological tissues provides a mixed cell population (unlike many of the traditional monolayer models), in which Peyer's patches can be included, and (iii) transport can be measured in both an apical to basal (Ap→Bas) direction, corresponding to transport from the intestinal lumen to the blood/lymph, or a basal to apical (Bas→Ap) direction, corresponding to transport from the blood/lymph to the intestinal lumen (see Figure 2.6a). As cytokine receptors are known to be largely present on the basal side of intestinal epithelial cells (Adams *et al.,* 1993), transport was measured in both directions.

Finally, to reflect the permeation of FITC-dextran across only the intestinal mucosa, the rat tissues used for these studies were stripped of muscle layers by blunt dissection (Dickens and Weil-Malherbe, 1941). Therefore, the main disadvantage of this method is that the stripping of the muscle and serosal layers can compromise the integrity of the mucosal layer. The toxicity of test compounds during this work can also be easily assessed, by measuring LDH release (see Chapter 2, section 2.2.7).

The specific aims of the experiments conducted here were to:

(i) Set up a model that could be used to measure FITC-dextran transport.
(ii) Establish tissue viability using the LDH assay.
(iii) Study the effects of rTNF-α, rIFN-γ or rIL-2 on transport across tissue with or without visible Peyer's patches.

However, before work could begin, it was important to carefully consider which concentration of cytokines would be used for the experiments. It was initially decided to use physiological concentrations (pg/mL) of cytokines, though in the literature, studies using epithelial cell line models have used higher (ng/mL) levels of TNF-α and/or IFN-γ to decrease TJ integrity (Madara and Stafford, 1989; Rodriguez *et al.*, 1995; Mahraoui *et al.*, 1997; Marano *et al.*, 1998; Fish *et al.*, 1999; Schmitz *et al.*, 1999; Gitter *et al.*, 2000a; Bruewer *et al.*, 2003; Ma *et al.*, 2004; Poritz *et al.*, 2004; Kawaguche *et al.*, 2005; Utech *et al.*, 2005; Wang *et al.*, 2005). To enable comparisons with this data, the later experiments used similar levels of these cytokines. In some experiments, the synergistic effects of rTNF-α and rIFN-γ on FITC-dextran transport across the intestinal tissue were also measured.

4.2 METHODS

The general methods (i.e. the vertical diffusion chamber, LDH assay and GPC) applied to this study have previously been described in Chapter 2 (sections 2.3.6, 2.3.7 and 2.3.8 respectively). Throughout FITC-dextran was dissolved in MEM (with Earles salts, without L-glutamine or phenol red; see Table 2.1), at a concentration of 0.1 mg/mL. To prevent photo bleaching, all FITC-dextran solutions were protected from light, and the fluorescence of this polymer was read using the fluorescence plate reader (see Chapter 2, section 2.3.6).

4.2.1 Characterisation of FITC-dextran

As different batches of FITC-dextran were used for these studies, it was considered important to define the molecular weight characteristics and fluorescence of the batches used, and also to investigate the effect of storage on molecular weight.

The molecular weight and polydispersity of FITC-dextran was measured using GPC (for general method see Chapter 2, section 2.3.8). PBS at pH 7.4 was used as a solvent for this work, and was filter-sterilised, and sonicated to remove contaminants and air bubbles respectively. FITC-dextran (5 mg/mL) in PBS was sterilised by filtration (through 0.2 μm filters). To conduct GPC, 80 μL of FITC-dextran solution was carefully drawn up into a glass syringe (to avoid air bubbles), and 60 μL of this was injected onto the first column. A TSK G3000PW$_{XL}$ - TSK G4000PW$_{XL}$ column set run in series was used (as described in section 2.3.8). In brief, the flow rate through the column was 1 mL/min, and a refractive index detector was used to monitor samples as they eluted over 30 min. A calibration curve was made using six pullulan polysaccharide standards (5 mg/mL in PBS) of known molecular weights (738 – 112,000 Da) and this was used to determine the molecular weight of each sample (see Chapter 2, Figure 2.8).

Using this system, the molecular weight characteristics of two different batches of FITC-dextran were compared, as was the effect of FITC-dextran (5 mg/mL in PBS) storage at room temperature, - 20 °C and 4 °C, for 24 h.

To determine the fluorescence yield of different batches of FITC-dextran, and also the effect of storage on fluorescence output, solutions were made up in MEM (1-0.03 mg/mL), by serially diluting a 1 mg/mL FITC-dextran stock solution in MEM (at a 1:2 ratio) into eppendorf tubes containing 500 μL of MEM only. The fluorescence of these solutions (200 μL/well in a black 96-well plate) was read in the fluorescence plate reader. To measure the effect of freezing (- 20 °C) on the fluorescence output of FITC-dextran, serial dilutions of the polymer in MEM were made (1 - 0.03 mg/mL as above), and were immediately read in the fluorescence plate reader (as above). Remaining dilutions were frozen (- 20 °C) for 24 h, and the fluorescence output of these samples were also read the using the fluorescence plate reader, once they had thawed. Each of these experiments was carried out on three separate occasions, and the data were expressed as an average ± standard deviation (S.D).

4.2.2 Evaluation of FITC-dextran transport in the presence of cytokines using the vertical diffusion system

The intestinal epithelial tissue used for this work, was prepared by stripping the muscle layers (as shown in Chapter 2, section 2.3.6). To look for any tissue damage caused during preparation, stripped and un-stripped tissues were viewed under the light microscope (Leicia, Germany). Tissues were placed on a glass microscope slide (76 x 26 mm) and were covered with a glass cover slip (22 x 40 mm). Each slide was immediately viewed under the x 40 and x 63 oil emersion objectives, and photographs of the tissue were taken using the Leica camera. These photographs were processed using Improvision® Openlab™ software.

In addition, in some experiments tissue viability was also assessed by measuring LDH release as described in section 4.2.4.

The effect of cytokines on FITC-dextran transport from both the Ap→Bas or Bas→Ap directions were studied, and comparisons were made using tissue with or without visible Peyer's patches. Cytokines were always reconstituted with autoclaved PBS (1 mL) containing 0.1 % BSA, that had been sterilised by filtration (through 0.2 μm Sartorious filters). The stock concentrations of each cytokine were 10 μg/mL for rTNF-α and rIL-2, and 100 μg/mL for rIFN-γ, and each reconstituted cytokine was serially diluted with PBS and 0.1 % BSA, into autoclaved, labelled eppendorf tubes. Aliquoted tubes (1000 ng/mL) were then bagged and stored at - 70 °C until use. All aliquoted cytokines were used within 6 months of reconstitution, as the activity of these proteins is known to decrease after this time (R&D systems product data sheets: www.rndsystems.com).

Before each transport experiment, thawed cytokine solutions were serially diluted with MEM containing FITC-dextran (1 mg/mL) to reach the cytokine concentration required. An aliquot (150 μL) of each stock solution was then added to the vertical diffusion chamber on either the mucosal or serosal sides of the tissue, thereby adjusting the total volume of this compartment to 1.5 mL (i.e. 1.35 mL of MEM plus 150 μL of cytokine and FITC-dextran). The recipient chamber also contained 1.5 mL of MEM only. Samples (25 μL) were collected from the recipient chamber at 10 min intervals (at t = 0 - 60 min), and were placed into black 96-well

plates (covered in foil). All samples were stored at room temperature until they were read in the fluorescence plate reader as described in Chapter 2 (section 2.3.6).

There were many ways in which the data from these experiments could be expressed. For example, the effect of cytokines on FITC-dextran transport could be expressed as a % of the control (FITC-dextran only). Alternatively, the flux rate and the apparent permeation coefficients (Papp values), of each sample transported across the tissue could also be calculated as previously described (Chapter 2, section 2.3.6). This would enable comparisons in the permeability of FITC-dextran across the rat intestinal tissue to be made with the literature.

4.2.3 FITC-dextran stability during incubation in the vertical diffusion system

The stability of FITC-dextran during transport experiments was measured using a Sephadex™ G-25, PD-10 column. This commercially available disposable chromatography column, separates samples of 1000 - 5000 Da in molecular weight, by gravity flow. For these experiments, samples of FITC-dextran in MEM (0.5 mL) were collected from the vertical diffusion system before and at the end of the 60 min incubation period, and were stored frozen (- 20 °C) until assay. The columns were equilibrated with 10 mL of PBS before use. Samples (0.5 mL) were added to the column when thawed, and were eluted with PBS (80 x 0.5 mL). The fractions (0.5 mL) were collected into eppendorf tubes, and 200 μL of each was then transferred into a black 96-well plate, to be read in the fluorescent plate reader. Free FITC (5 μg/mL in MEM) was used as a control for this experiment. The data were plotted as eluted fraction number against fluorescence.

4.2.4 Use of the LDH assay to measure tissue viability

The LDH assay was carried out as described in Chapter 2, section 2.3.7. In brief, samples of medium (50 μL) were collected from each diffusion cell at t = 0 and at t = 60 min. Each sample was always taken from the recipient chamber, to minimise any possible interference with the assay that may be caused by FITC-dextran, and/or added cytokines. These samples were then immediately frozen at – 20 °C until they were assayed. The data from these experiments are expressed as enzyme activity in units (U)/mL.

4.3 RESULTS

4.3.1. Properties of FITC-dextran batches and their stability

GPC analysis of two different batches of FITC-dextran, showed no difference between the molecular weight of each sample (Figure 4.2a). Furthermore, the molecular weight of FITC-dextran was not affected by storage in MEM at room temperature, – 20 °C, or at 4 °C for 24 h (Figure 4.2b). Serial dilutions of different FITC-dextran batches in MEM (1 - 0.03 mg/mL) showed no differences in fluorescent output (Figure 4.3a). A linear relationship between fluorescence and concentration was seen for the FITC-dextran concentration range (0.1 mg/mL) used for transport work (Figure 4.3b). Freezing (- 20 °C) FITC-dextran for 24 h also had no effect on its fluorescence (Figure 4.4).

N.B. It should be noted that FITC fluorescence output is strongly dependent on pH (see Chapter 5).

4.3.2. Establishment of the vertical diffusion system

Although stripping the intestinal tissue of muscle layers (by scalpel) is quite harsh, no visible holes in Peyer's patch or non-Peyer's patch tissues, could be seen after tissue preparation, when viewed under a light microscope at x 40 magnification (Figure 4.5). During transport experiments the levels of LDH released into the culture media, over the 1 h incubation, increased by 72 % (a 4.5-fold increase) from t = 0 min, even in the absence of FITC-dextran (Figure 4.6a). When FITC-dextran (0.1 mg/mL) was introduced into the system, the LDH levels released into the culture media increased by 85 % (a 6.8-fold increase) from t = 0 min (Figure 4.6b). Therefore it was possible to progress onto the transport studies.

4.3.3 Transport of FITC-dextran across rat intestinal tissue in the vertical diffusion system

Ap→Bas and Bas→Ap FITC-dextran transport across non-Peyer's patch tissue

The transport of FITC-dextran across non-Peyer's patch tissue increased linearly with time in both the Ap→Bas and Bas→Ap directions (Figure 4.7a). Ap→Bas FITC-dextran transport was greater than Bas→Ap transport, and highest amounts of transported FITC-dextran were seen at t = 60 min. The apparent permeability coefficient for Ap→Bas FITC-dextran transport was 2.69 x 10^{-6} cm/s. In the Bas→Ap direction the apparent permeability coefficient was 1.85 x 10^{-6} cm/s.

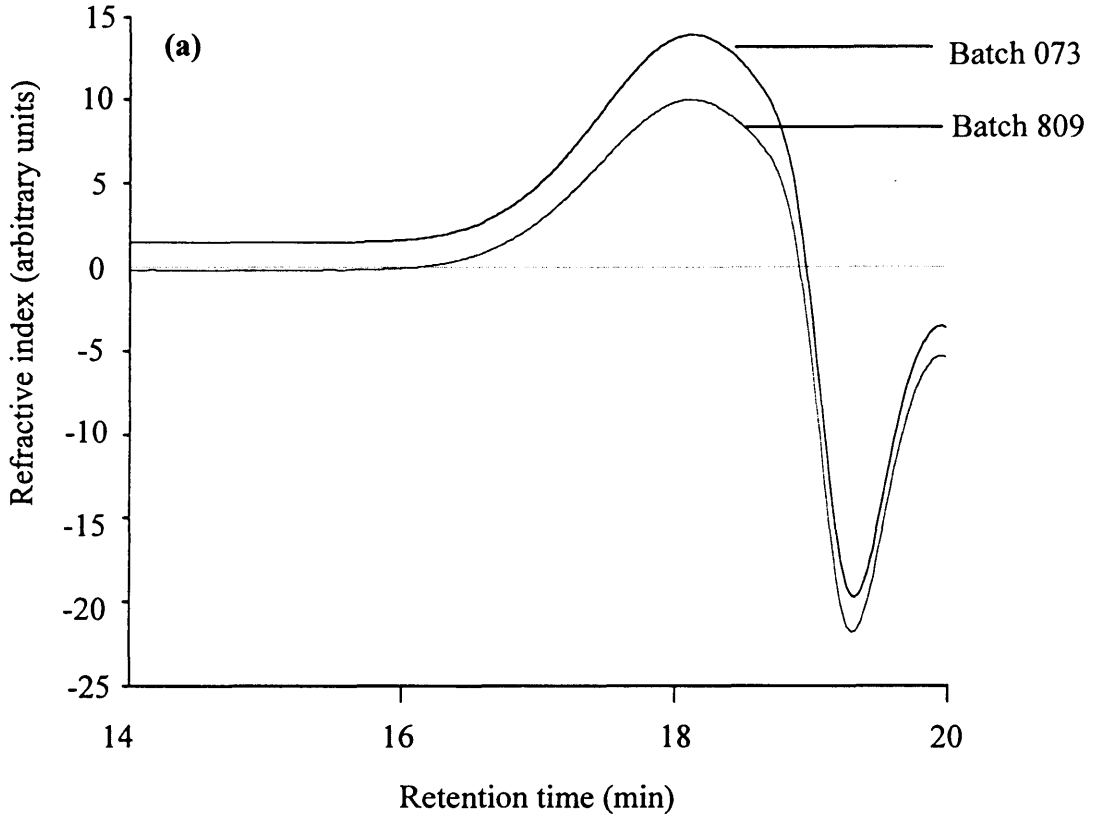

FITC-dextran batch number	Mn (g/mole)	MW (g/mole)	Polydispersity MW/Mn
073	4078	4892	1.2
809	4027	4848	1.2

Figure 4.2 (a) Molecular weight and polydispersity of different FITC-dextran batches (5 mg/mL in PBS).

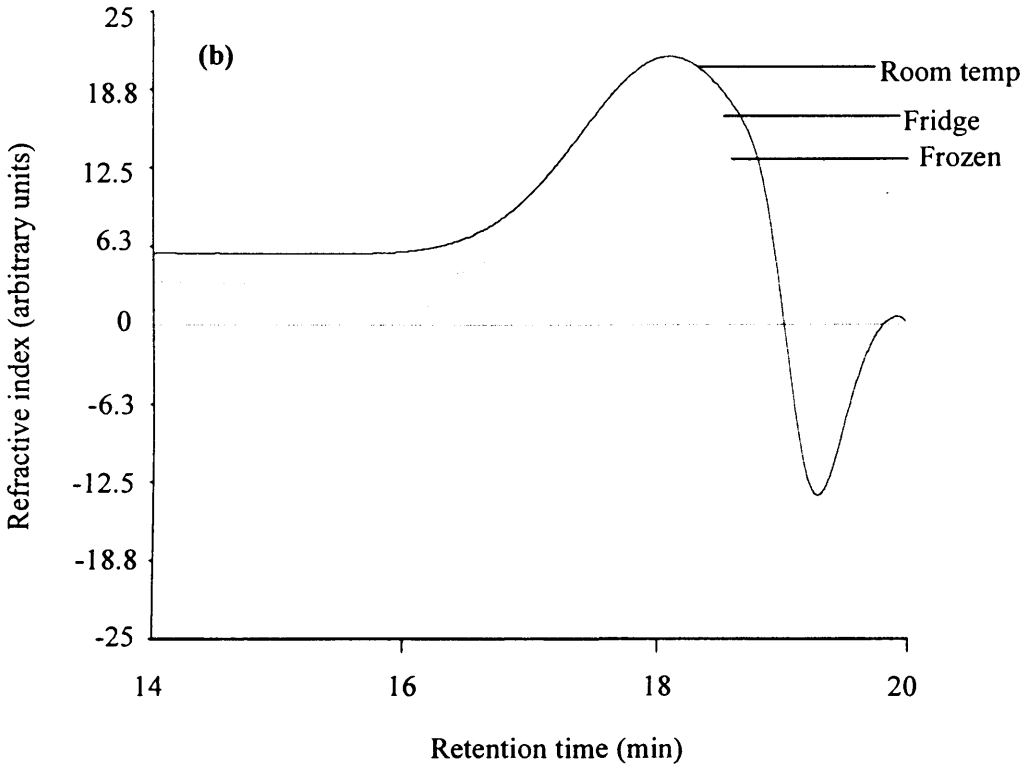

FITC-dextran (batch 073)	Mn (g/mole)	MW (g/mole)	Polydispersity MW/Mn
Room temp (20 °C)	4133	5060	1.2
Fridge (4°C)	4081	4978	1.2
Freezer (-20°C)	4105	5012	1.2

Figure 4.2 (b) Molecular weight and polydispersity of FITC-dextran (5 mg/mL in PBS) after storage at different temperatures for 24 h.

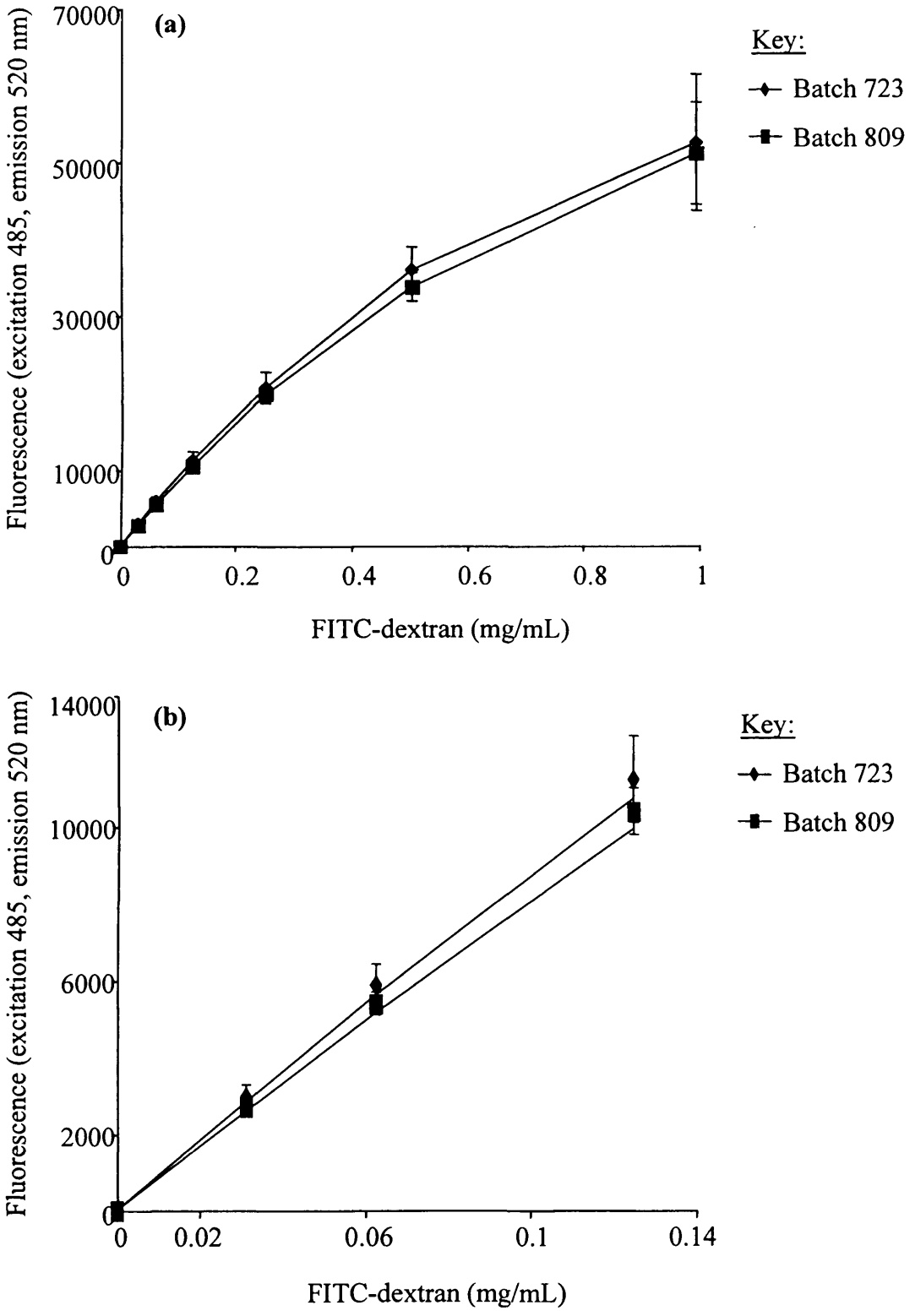

Figure 4.3 (a & b) Fluorescence output of different FITC-dextran batches diluted in MEM. Panel (a) dilutions in MEM 0.03 mg/mL - 1 mg/mL, panel (b) 0.03 mg/mL - 0.125 mg/mL, showing a linear relationship between fluorescence and concentration. The data shown are mean ± SD (n = 3).

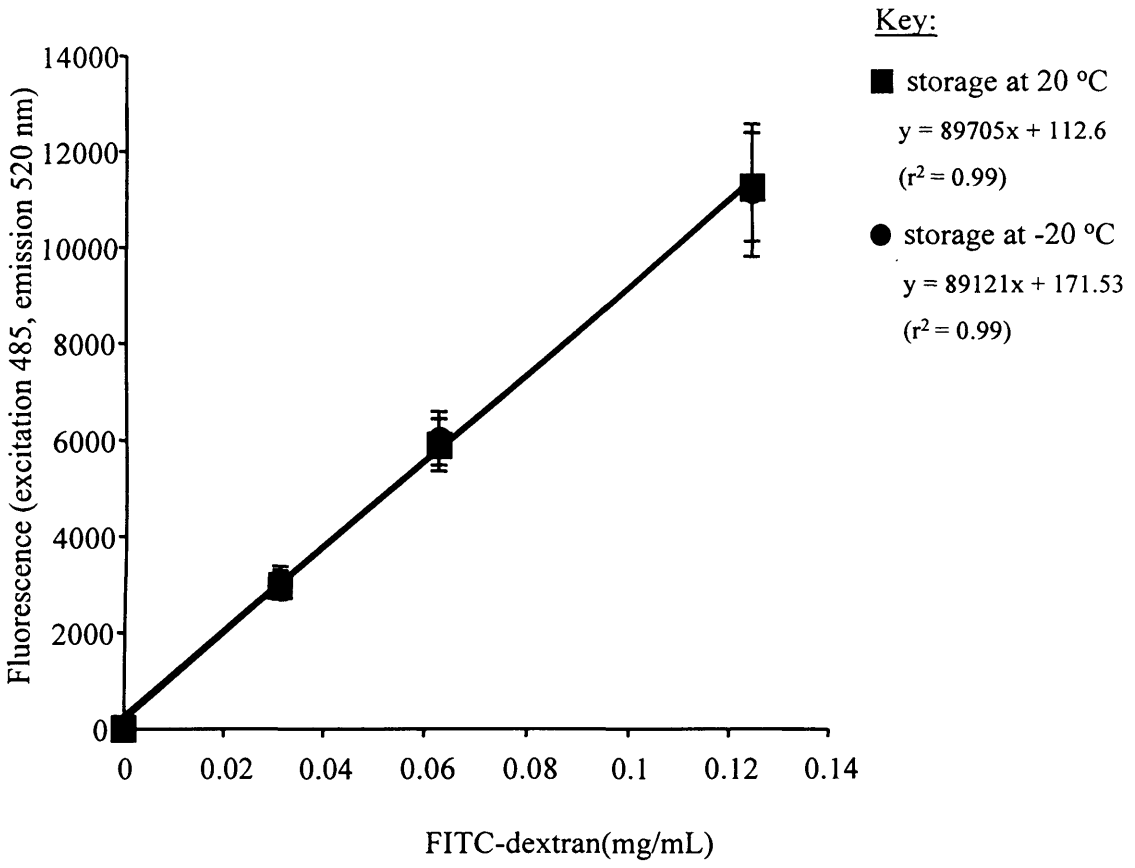

Figure 4.4 Fluorescence output of FITC-dextran (batch 073) after storage in MEM at different temperature for 24 h. The data shown are mean ± SD (n = 3).

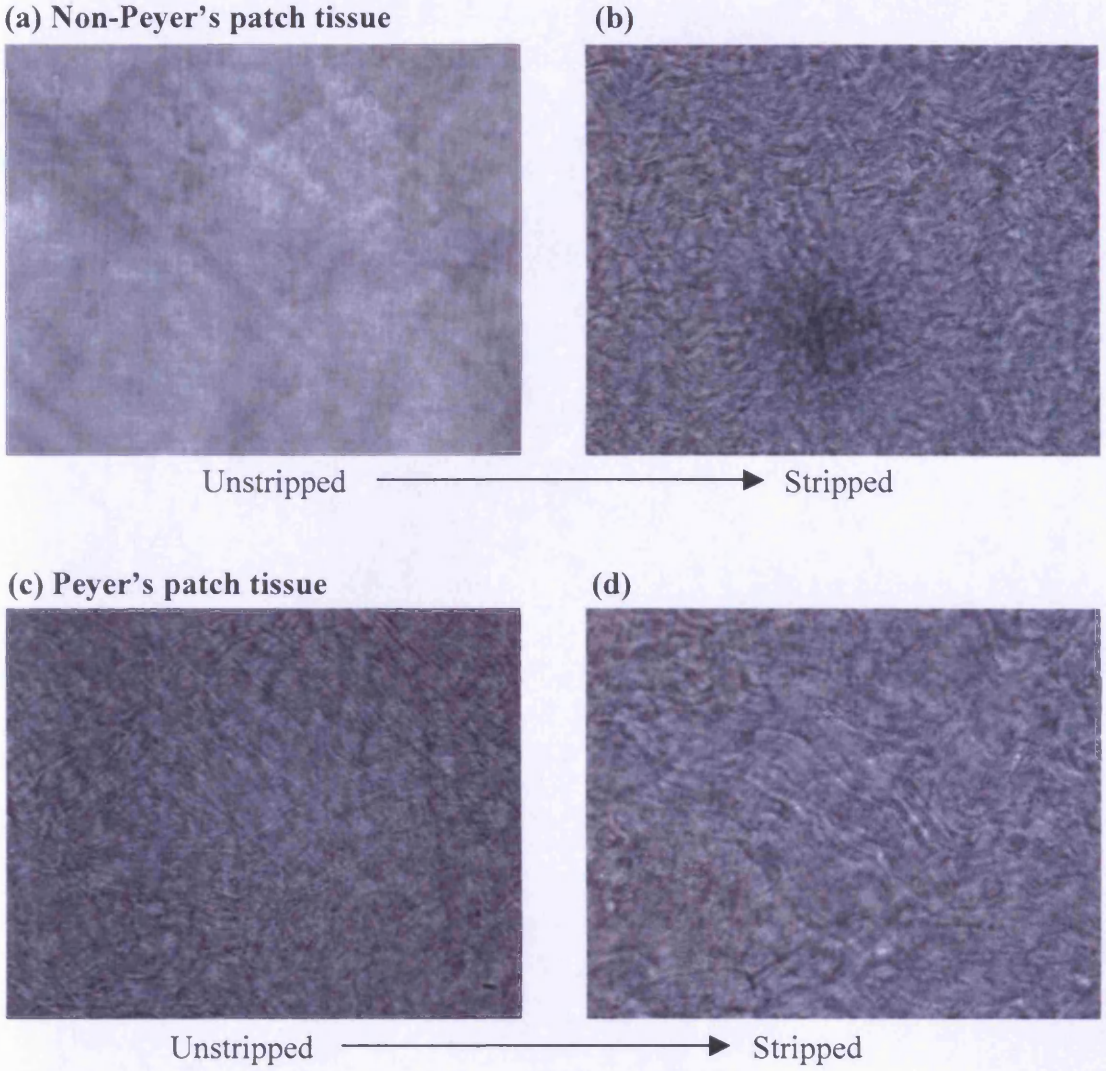

Figure 4.5 Photographs of rat intestinal tissue at x 40 magnification. Panel (a) unstripped non-Peyer's patch tissue, panel (b) stripped non-Peyer's patch tissue, panel (c) unstripped Peyer's patch tissue, and panel (d) stripped Peyer's patch tissue.

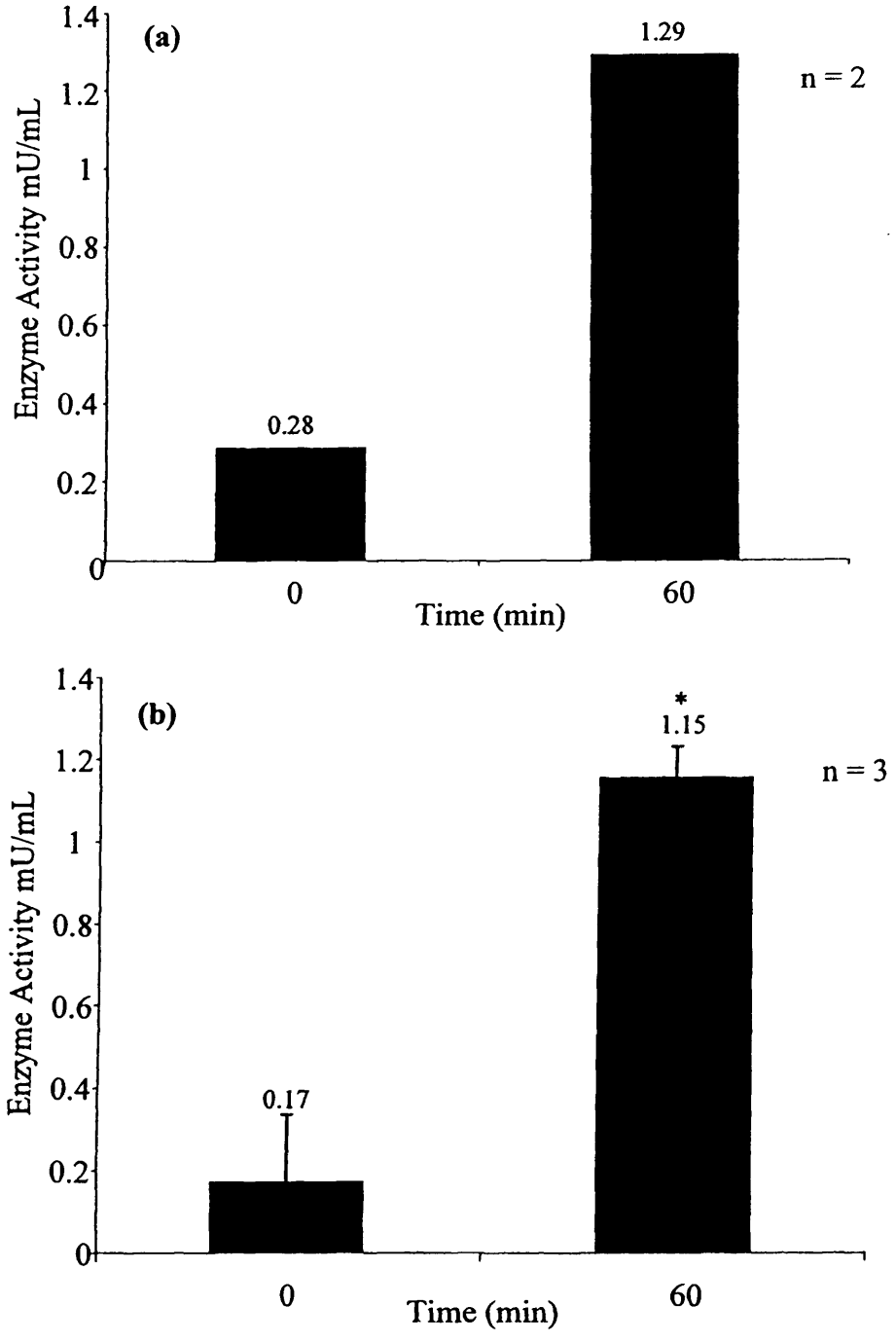

Figure 4.6 (a & b) LDH release from rat intestinal tissue during 60 min incubation in the vertical diffusion system. Panel (a) MEM only, panel (b) MEM and FITC-dextran (0.1 mg/mL). Data were analysed by paired t-test, * = $p > 0.05$.

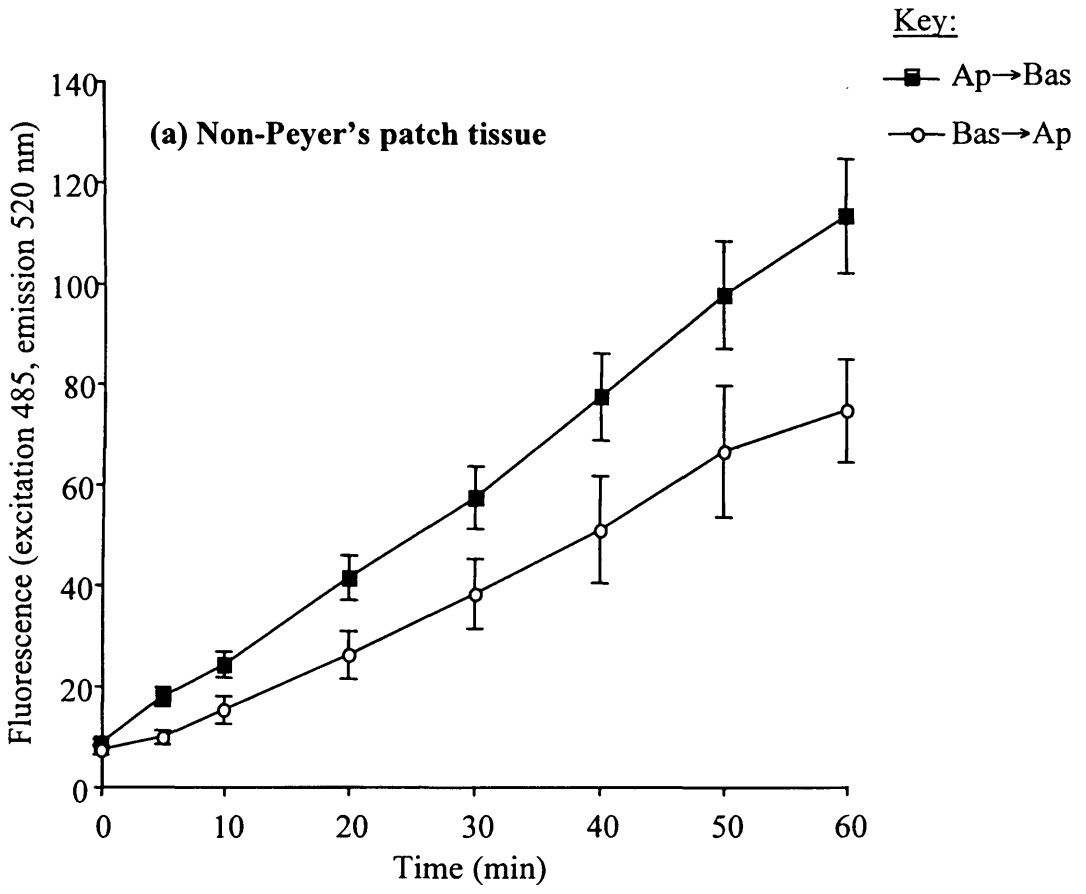

Figure 4.7 (a) Ap→Bas and Bas→Ap transport of FITC-dextran across non-Peyer's patch tissue. The data shown are mean ± SEM (n > 15). The Papp values for Ap→Bas transport = 2.69 x 10^{-6} cm/sec; Bas→Ap transport = 1.85 x 10^{-6}.

Whilst setting up this assay it became apparent that there was considerable daily variation in the rate of FITC-dextran transport across the tissue in both Ap→Bas (Figure 4.7b) and Bas→Ap (Figure 4.7c) directions. Although sometimes this could be attributable to equipment malfunction (e.g. difficulties in controlling adequate oxygenation into all chambers, or sample leakage across the tissue), on other occasions it could not. The rates of transport did get more consistent with practice at tissue preparation, but there was still considerable variability. Nevertheless a large number of replicate experiments were always needed to reduce the size of the error bars (the standard error of the mean (SEM)). Note for Ap→Bas transport, n was 40 (Figure 4.7b), and for Bas→Ap transport n was 20 (Figure 4.7c).

Ap→Bas and Bas→Ap FITC-dextran transport across Peyer's patch tissue

The transport of FITC-dextran across Peyer's patch tissue was lower than that seen for tissue without Peyer's patches. Transport increased in a time-dependent manner over the 1 h incubation period and was linear with time. A 5 min lag phase in FITC-dextran transport was seen in both Ap→Bas and Bas→Ap directions across this tissue (Figure 4.8). Once again, Ap→Bas (Papp = 1.24 x 10^{-6} cm/s) FITC-dextran transport was greater than Bas→Ap (Papp = 0.78 x 10^{-6} cm/s). Highest amounts of FITC-dextran transport were seen at t = 60 min.

4.3.4 Stability of FITC-dextran during incubation

FITC-dextran eluted first, in fractions 3 - 79, during PD-10 column chromatography, whilst free FITC eluted later in fractions 8 - 123 (Figure 4.9). Free FITC seemed to adsorb to the column, and when the column was viewed under a UV-lamp, there were traces of fluorescence until 125 (0.5 mL PBS) fractions had been collected (Figure 4.9). When samples taken from either the donor or recipient chambers after the 60 min incubation were analysed by PD-10 chromatography, there was no increase in free FITC compared to the FITC-dextran standard (Figure 4.9).

Furthermore, only a small amount of FITC-dextran was transported across the tissue into the recipient chamber at t = 60 min (Figure 4.9). The fluorescence units detected in the fractions from these samples was very low compared to the donor chamber samples. These studies showed FITC-dextran was not degraded during the transport studies.

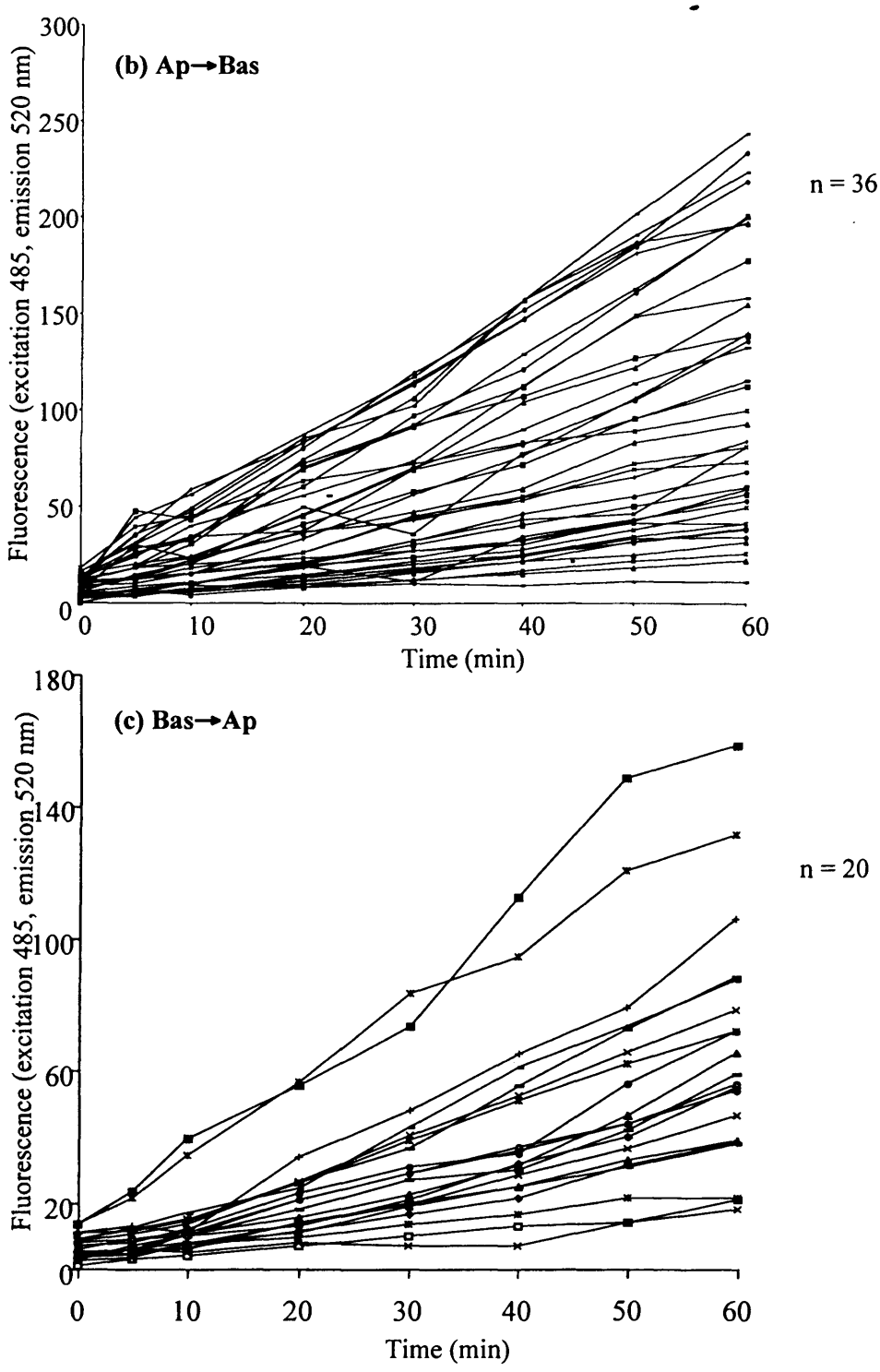

Figure 4.7 (b & c) Ap→Bas (panel b) and Bas→Ap (panel c) transport of FITC-dextran across non-Peyer's patch tissue. The data shown were collected in individual experiments. Although these data were variable, only experiments in which the fluorescence at t = 0 min was below a value of 15 were used.

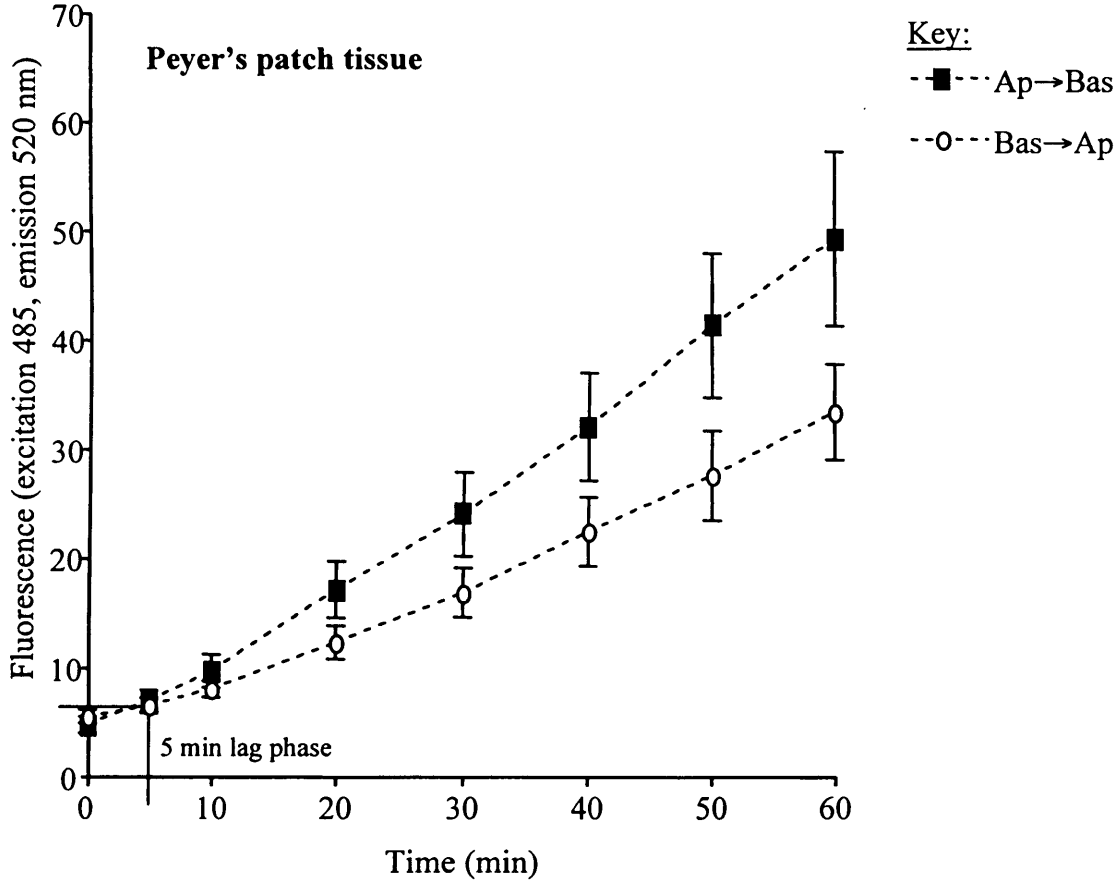

Figure 4.8 Apical→Bas and Bas→Ap transport of FITC-dextran across tissue with Peyer's patches. The data shown are mean ± SEM (n > 5). The Papp values for Ap→Bas transport = 1.24 x 10^{-6} cm/sec; Bas→Ap transport = 0.78 x 10^{-6}.

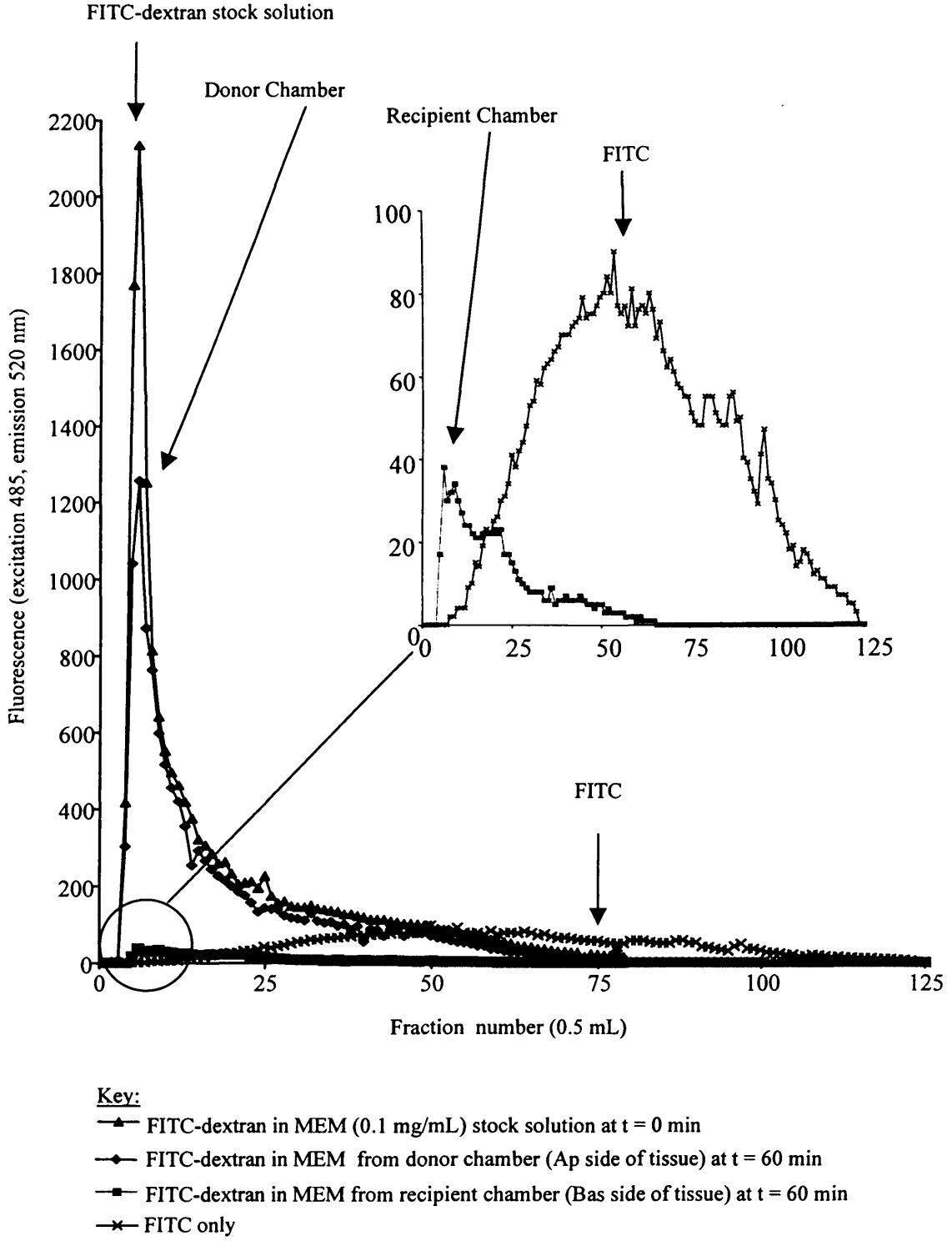

Figure 4.9 Elution profile of FITC-dextran fractions from a PD-10 column.

4.3.5 Effect of cytokines on FITC-dextran transport across rat intestinal tissue with or without Peyer's patches

Physiological concentrations of rTNF-α (pg/mL)

As above, in tissue without Peyer's patches the Ap→Bas transport of FITC-dextran was linear with time (Figure 4.10a). No increase in Ap→Bas FITC-dextran transport occurred in the presence of rTNF-α over the concentration range 30 - 100 pg/mL. Similarly, Bas→Ap transport of FITC-dextran was linear over time in both the presence and absence of rTNF-α. Again, rTNF-α caused no increase in transport at all concentrations tested (Figure 4.10b).

As mentioned above, (section 4.3.2) when using Peyer's patch tissue the transport of FITC-dextran was slower (in both directions) than seen in non-Peyer's patch tissue. However, again in these studies, there was no significant change in Ap→Bas or Bas→Ap transport when rTNF-α was added (Figure 4.10c and d).

Physiological concentrations of rIFN-γ (pg/mL)

In non-Peyer's patch tissues, the Ap→Bas transport of FITC-dextran was linear up to 50 min, then plateaued at 60 min (Figure 4.11a). The reason for the differences in the controls was not clear, but the inherent variability of these experiments is mentioned above. Again, Bas→Ap transport was linear over the 60 min incubation. Once more, the transport of FITC-dextran in the Bas→Ap direction was lower than seen for Ap→Bas transport. No increases in either Ap→Bas (Figure 4.11a) or Bas→Ap (Figure 4.11b) FITC-dextran transport were seen when rIFN-γ (10 - 60 pg/mL) was added to the donor chamber.

When tissue containing Peyer's patches was used in these experiments, the Bas→Ap (Figure 4.11d) transport of FITC-dextran was greater than Ap→Bas (Figure 4.11c). Nevertheless, once again, no significant changes were observed in FITC-dextran transport in the Ap→Bas (Figure 4.11c) or the Bas→Ap (Figure 4.10d) directions when rIFN-γ (10 - 60 pg/mL) was added.

Effect of rTNF-α and rIFN-γ on LDH release

For experiments in which rTNF-α was used, the control tissue incubated with this cytokine showed an LDH increase in the recipient compartment that increased by 43 % over the 60 min (Figure 4.12a). This compared to a control value 76 % LDH

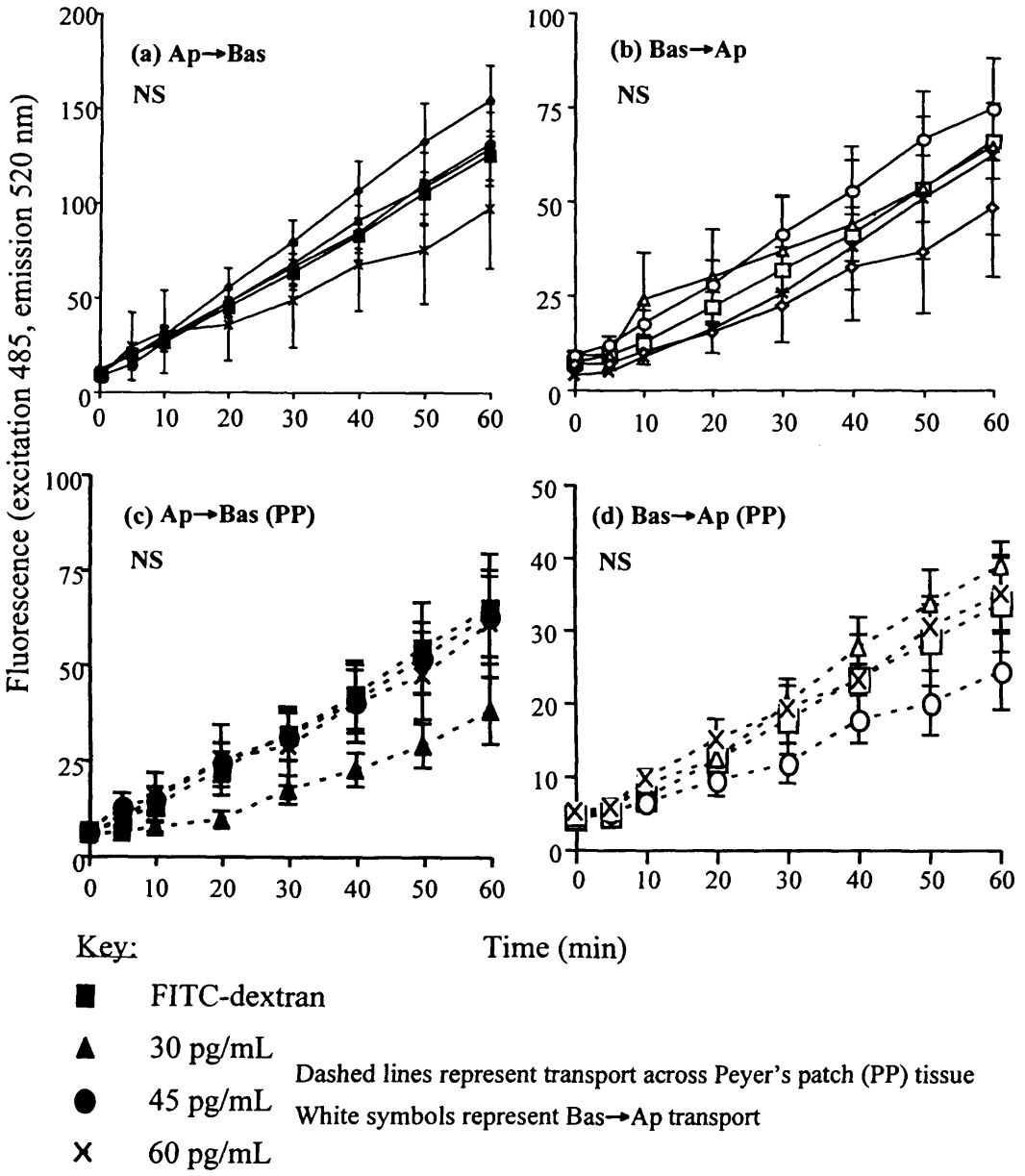

Figure 4.10 (a, b, c & d) Effect of rTNF-α on the transport of FITC-dextran across rat intestinal tissue. The data shown are mean ± SEM (n > 6), and NS at t = 60 min according to one-way ANOVA.

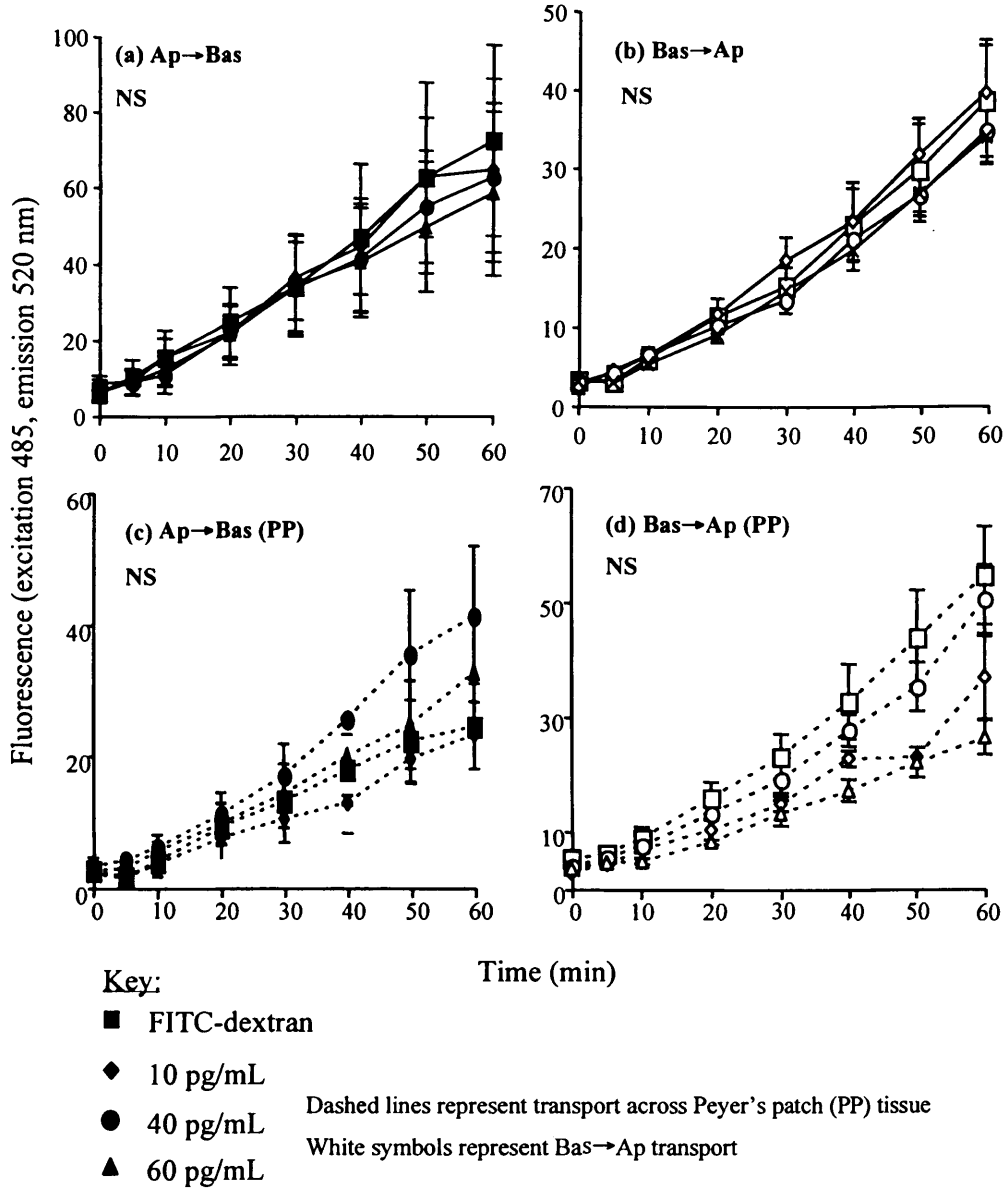

Figure 4.11 (a, b, c & d) Effect of rIFN-γ on the transport of FITC-dextran across rat intestinal tissue. The data shown are mean ± SEM (n > 6), and NS at t = 60 min according to one-way ANOVA.

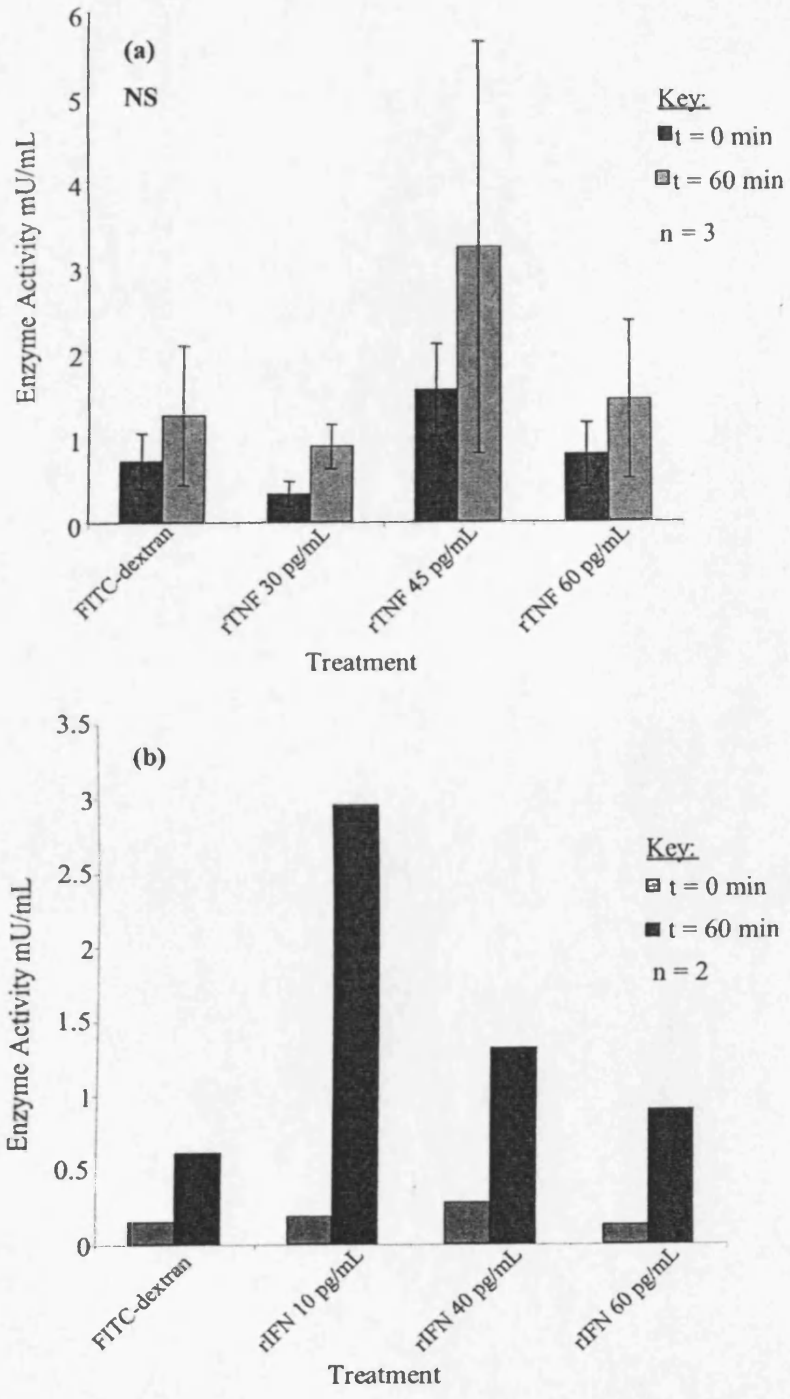

Figure 4.12(a & b) LDH release from rat intestinal tissue. The data are NS according to one-way ANOVA.

release in the rIFN-γ experiments (Figure 4.12b).

Throughout all experiments in which rTNF-α or rIFN-γ was added, there was no correlation between the concentration of cytokine and LDH release, and the results obtained were often quite variable (Figure 4.12). The levels of LDH (expressed as enzyme activity mU/mL) released into the culture media from tissues incubated with rTNF-α (Figure 4.12a) and rIFN-γ (Figure 4.12b), did not change significantly from the control (FITC-dextran only). It can therefore be concluded that the cytokines had no detrimental effect on tissue viability over 60 min.

Physiological concentrations of IL-2 (pg/mL)

As above in tissue without Peyer's patches no increases in FITC-dextran transport were seen when rIL-2 was added to the apical (Figure 4.13a) or basal (Figure 4.13b) compartments with FITC-dextran.

Similarly, no significant changes in transport were observed with tissues containing Peyer's patches where Ap→Bas (Figure 4.13c) and Bas→Ap (Figure 4.13d) transport of FITC-dextran was unaltered by rIL-2 at all concentrations used (30 - 60 pg/mL).

4.3.6 Effect of high concentrations (ng/mL) of rTNF-α and rIFN-γ on FITC-dextran transport

As before in all control experiments, the transport of FITC-dextran with and without the addition of cytokines was greater in tissue without Peyer's patches (Figures 4.14a and b; 4.15a and b; 4.16a and b). As before, Bas→Ap FITC-dextran transport occurred at a lower rate than rate in the Ap→Bas direction.

The higher concentration of rTNF-α (10 ng/mL) did not affect either the Ap→Bas (Figure 4.14a) or Bas→Ap (Figure 4.14b) transport of FITC-dextran in both Peyer's patch and non-Peyer's patch tissue respectively. However, addition of a higher concentration of rIFN-γ (10 ng/mL) to non-Peyer's patch tissue appeared to enhance the transport of FITC-dextran in both the Ap→Bas (Figure 4.15a) and Bas→Ap (Figure 4.15b) directions, though this was not significant. This was in contrast to the results seen in tissue containing Peyer's patches where no effect on the Ap→Bas (Figure 4.15a) or Bas→Ap (Figure 4.15b) transport was found.

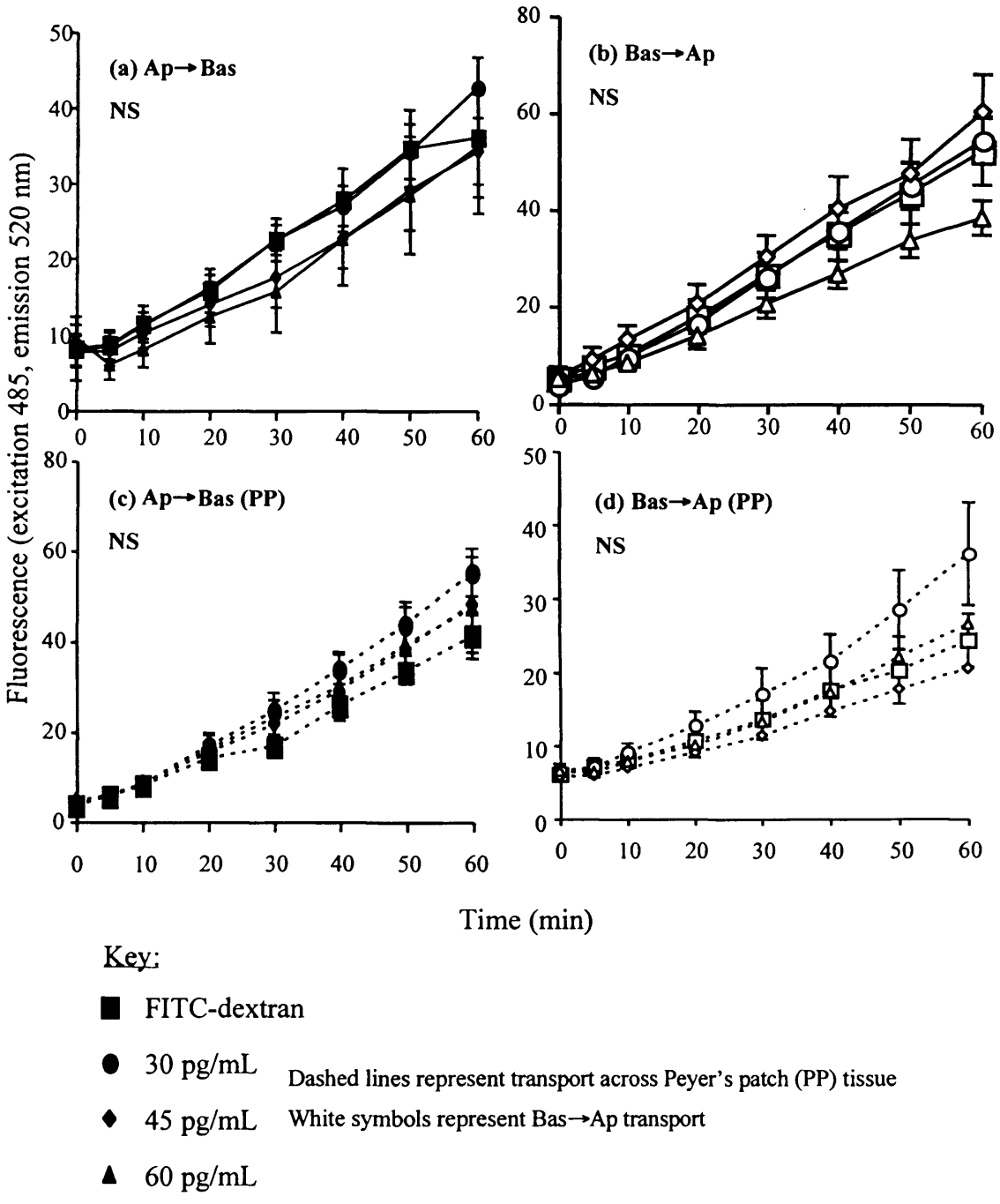

Figure 4.13 (a, b, c & d) Effect of rIL-2 on the transport of FITC-dextran across rat intestinal tissue. The data shown are mean ± SEM (n > 6), and NS at t = 60 min according to one-way ANOVA.

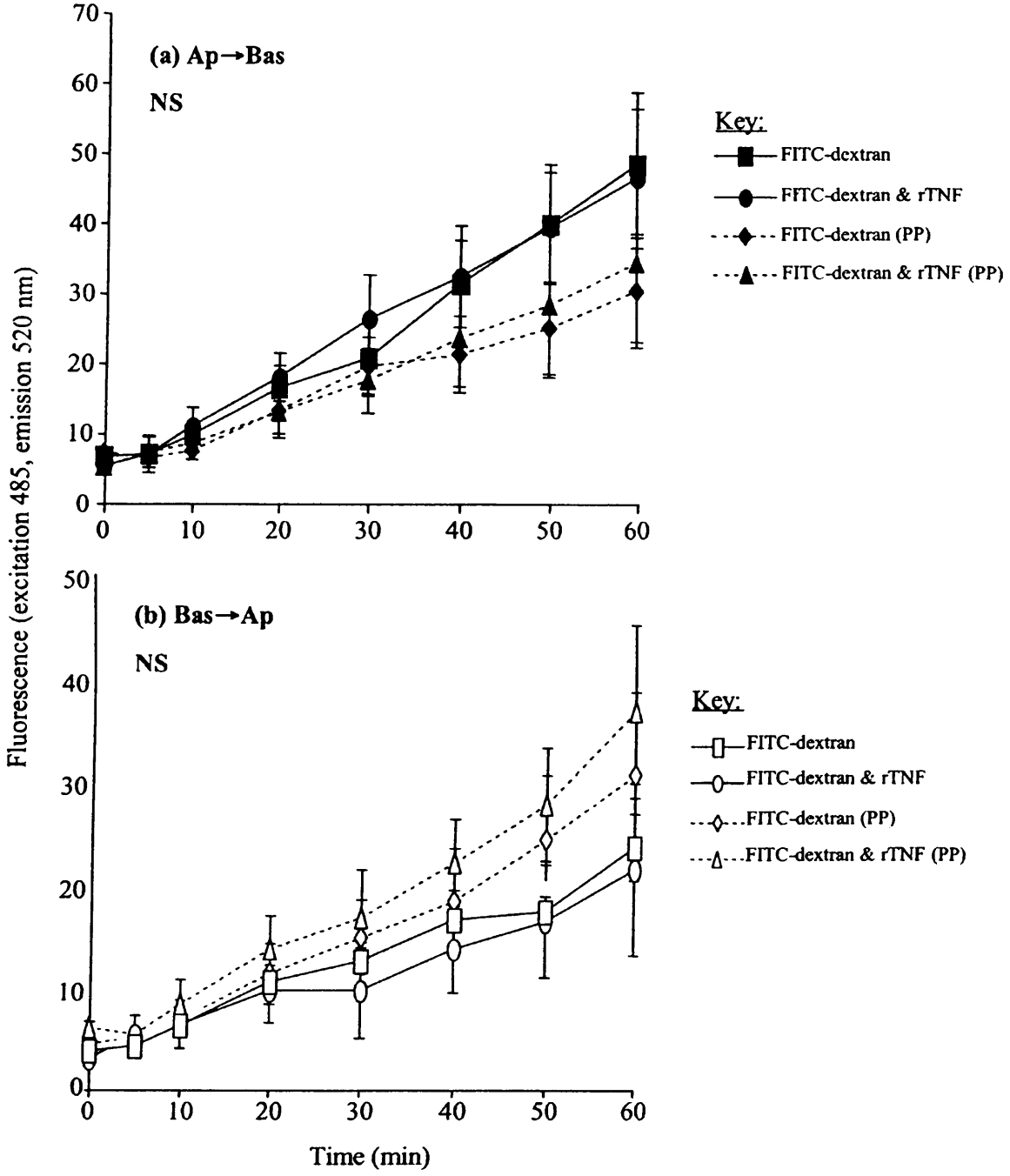

Figure 4.14 (a & b) Effect of rTNF-α (10 ng/mL) on the transport of FITC-dextran across rat intestinal tissue. Panel (a) Ap→Bas, panel (b) Bas→Ap. The data shown are mean ± SEM (n> 6), and NS at t = 60 min according to one-way ANOVA.

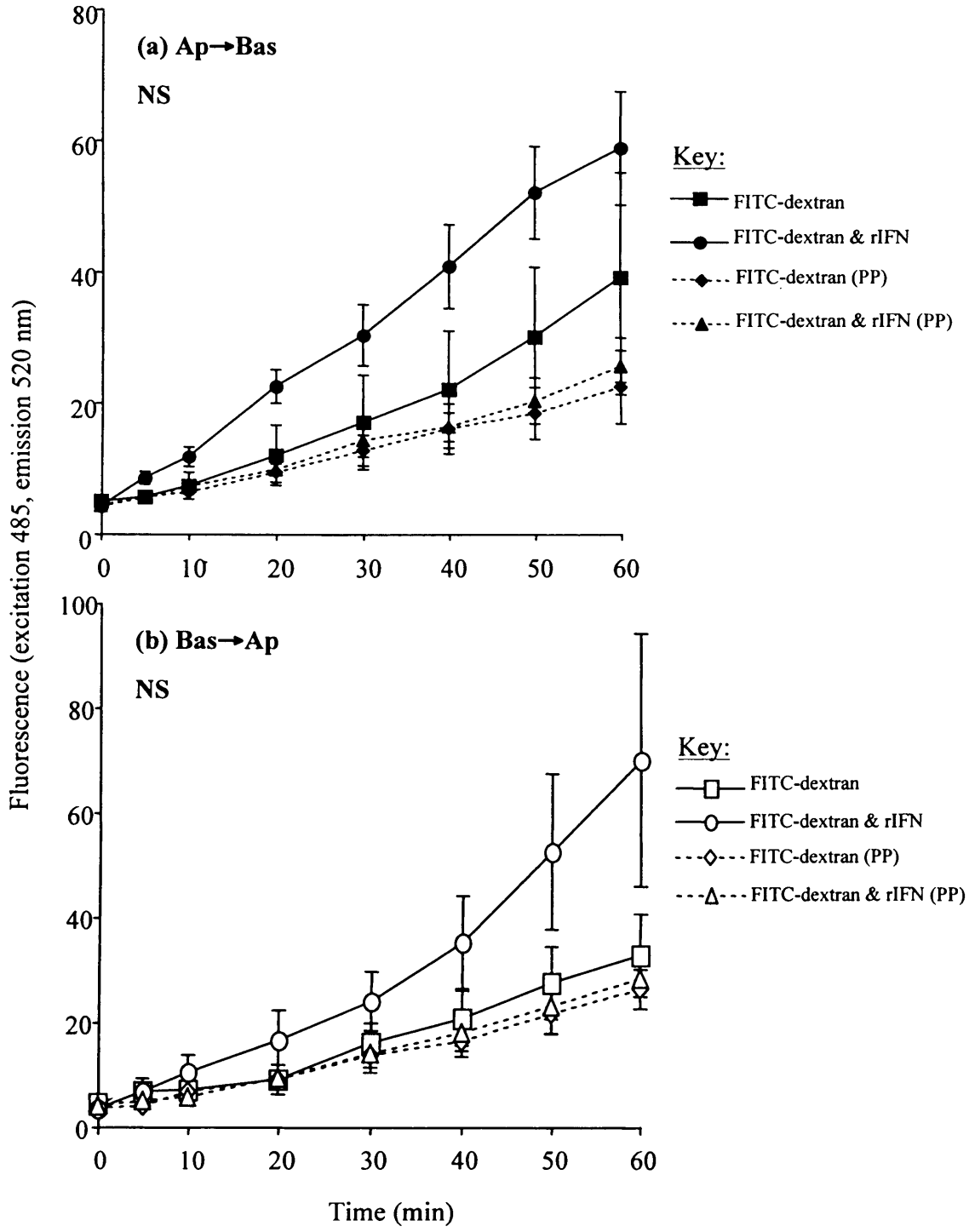

Figure 4.15 (a & b) Effect of rIFN-γ (10 ng/mL) on the transport of FITC-dextran across rat intestinal tissue. Panel (a) Ap→Bas, panel (b) Bas→Ap. The data shown are mean ± SEM (n> 6), and NS at t = 60 min according to one-way ANOVA.

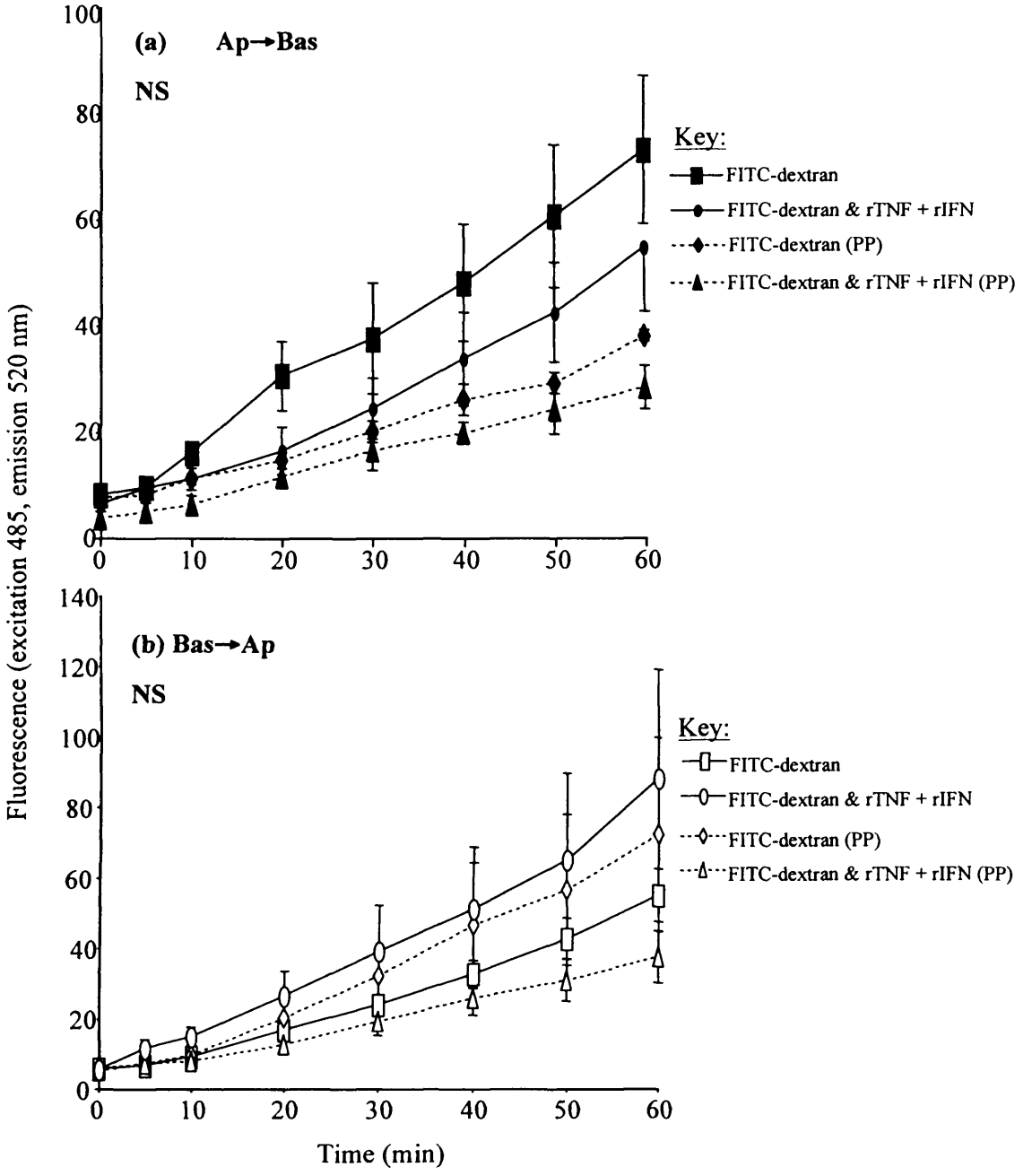

Figure 4.16 (a & b) Effect of rTNF-α (2.5 ng/mL) and rIFN-γ (10 ng/mL) on the transport of FITC-dextran across rat intestinal tissue. Panel (a) Ap→Bas, panel (b) Bas→Ap. The data shown are mean ± SEM (n> 6), and NS at t = 60 min according to one-way ANOVA.

To investigate a potential synergistic effect between TNF-α (2.5 ng/mL) and IFN-γ (10 ng/mL) they were added together as a mixture. Interestingly, there appeared to be no change in FITC-dextran transport across Peyer's patch, or non-Peyer's patch tissues in either Ap→Bas (Figure 4.16a) or Bas→Ap (Figure 4.16b) directions.

4.4 DISCUSSION

These experiments indicated that the addition of rTNF-α, rIFN-γ or rIL-2 at the lower, more physiological (pg/mL), concentrations did not influence FITC-dextran transport in either direction across rat intestinal tissue (with or without Peyer's patches), using the vertical diffusion model (Figures 4.10, 4.11 and 4.13 respectively). At higher (ng/mL) concentrations, only rIFN-γ showed an effect on FITC-dextran transport in both directions, across non-Peyer's patch tissues (Figure 4.13a and b), though this data was not significant. A concentration of 10 ng/mL was chosen in accordance with Ma *et al.,* (2004), who showed a maximum drop in TEER across Caco-2 cells at 10 ng/mL of TNF-α. IFN-γ was also used at the same concentration for comparison. For synergistic experiments, the concentration of both TNF-α and IFN-γ were chosen in accordance with Wang *et al.,* (2005). The observations at higher concentrations of rTNF-α, rIFN-γ, or at higher concentrations of both rTNF-α and rIFN-γ, were not in agreement with the literature.

High (ng/mL) concentrations of TNF-α or IFN-γ (as found in IBD diseases) can decrease the barrier function of cell monolayers within a matter of h (as measured by TEER and the transport of paracellular markers), and this occurs in a concentration- and/or time-dependent manner (Adams *et al.,* 1993; Madara and Stafford, 1996; Marano *et al.,* 1998; Youakim and Adieh, 1999; Schmitz *et al.,* 1999; Ma *et al.,* 2004; Poritz *et al.*, 2004). The ability of these cytokines to permeabilise monolayers differs between cell lines: IFN-γ has been studied in T84 cell monolayers, though TNF-α has been studied in T84, HT-29 (and its variants), and Caco-2 cell monolayers. It has no effect on T84 cells (Madara and Stafford, 1989; McKay *et al.,* 1996). Nevertheless, the permeabilising effects seen with these cytokines are reversible (Mullin and Snock, 1990; Adams *et al.,* 1993).

Some studies have suggested that the decrease in barrier properties induced by TNF-α or IFN-γ are due to them causing apoptosis (Gitter *et al.,* 2000b), however

several recent publications have shown that this is not the case. Neither TNF-α (Marano *et al.*, 1998; Smitz *et al.*, 1999; Ma *et al.*, 2004) nor IFN-γ (Youakim and Adieh, 1999; Madara and Stafford, 1996; Bruewer *et al.*, 2005) is cytotoxic to these cell lines at high concentrations. Both cytokines also work synergistically, as IFN-γ up-regulates the receptors for TNF-α (Fish *et al.*, 1999), further enhancing permeability (Bruewer *et al.*, 2005; Wang *et al.*, 2005).

Currently, the exact molecular mechanism(s) of TNF-α and/ or IFN-γ-induced TJ permeability have not been defined, though they appear to involve the redistribution of TJ proteins within the cell (see Figure 1.5). TNF-α appears to activate the cytosolic transcription factor NF-κB (Ma *et al.*, 2004), which ultimately causes the re-distribution of TJ proteins, particularly ZO-1, away from the TJ (Poritz *et al.*, 2004; Ma *et al.*, 2004). IFN-γ also decreases ZO-1 levels from the TJ, and alters the distribution of ZO-2 and occludin (Youakim and Ahdieh 1999). More recently, it has also been found to cause endocytosis of the TJ proteins: occludin, JAM-A and claudin-1 (Bruewer *et al.*, 2005; Utech *et al.*, 2005).

Though the results seen for FITC-dextran transport in the presence of cytokines were not as expected, it is important to note that the interpretation of the results obtained in the vertical diffusion system were difficult, due to the variability seen for the transport of the control FITC-dextran.

Several groups have used the Ussing chamber model, and its variants such as the vertical diffusion system, to study the GI transport of drugs (Berggren *et al.*, 2004; Wantanabee *et al.*, 2005), particularly for those that are P-gp substrates (e.g. digoxin: Ungell *et al.*, 1998; Sababi *et al.*, 2001), or the transport of paracellular markers (Pantzar *et al.*, 1994; Ghandehari *et al.*, 1997). Each has claimed reproducibility of these models. However, in these studies, a high number of experiments were needed in order to reduce the SEM error bars, due to the high degree of variability between the experiments.

Nevertheless, the rank order for FITC-dextran transport across the rat intestinal tissue at 60 min was: Ap→Bas > Bas→Ap > Ap→Bas in Peyer's patch tissue > Bas→Ap in Peyer's patch tissue (Figure 4.17). Furthermore, transport in the Ap→Bas direction at 60 min, across non-Peyer's patch tissue, was significantly higher than all other transport (Figure 4.17). The data in the literature regarding

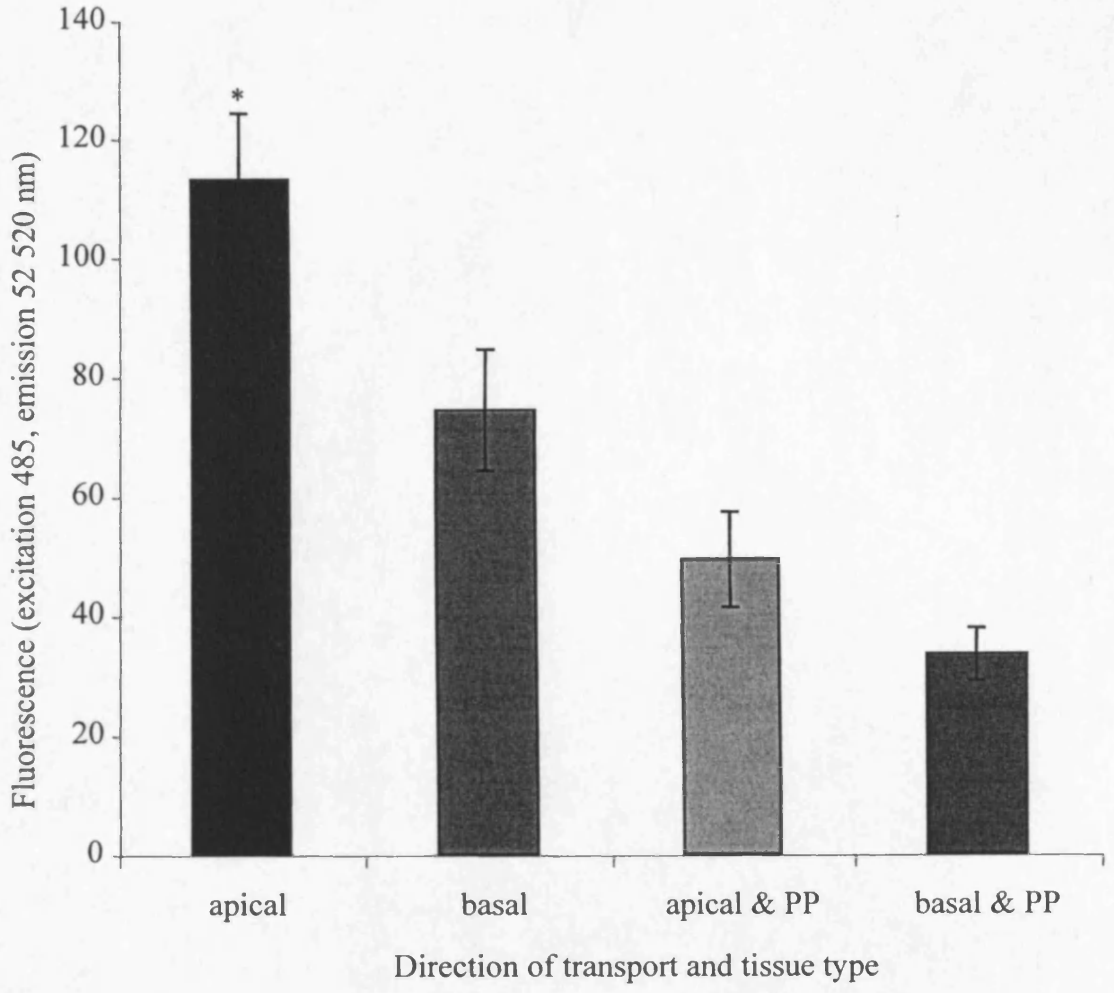

Figure 4.17 FITC-dextran transport at t = 60 min. The data shown are mean ± SEM (n > 20), and were analysed by one-way ANOVA, and Bonfeerroni post-hoc test, * = $p < 0.05$.

directional paracellular transport however are conflicting. Pantzar and colleagues (1994) have also shown the Ap→Bas transport of various paracellular markers across the intestine, including FITC-dextran (MW = 3,000 Da), is greater than Bas→Ap transport, though Nakamura and colleagues (2003) have shown increased FITC-dextran transport in the Bas→Ap direction across stripped rat colonic mucosa. A table comparing the Papp values of FITC-dextran according to the literature is given in Table 4.1. However, care should be taken when trying to make quantitative comparisons of these values, as differences in rats used (i.e. weight and species), length of fasting (if any), and method used to assay transport may affect the results obtained. Even individual components in the medium such as glucose or Ca^{2+} concentration can affect results, by altering TJ permeability. MEM tissue culture medium was used for this work in accordance with Diamanti (2004).

The studies conducted by Diamanti (2004) and those carried out in this study were essentially the same, though the Papp values for FITC-dextran transport are marginally different (see Table 4.1). This is likely to de due to a difference in rat intestinal region used (see below), different batches of animals, and the FITC-dextran used by Diamanti was also slightly larger (MW = 4,400 Da), and may have had a different fluorescent loading. Nevertheless, the Papp values observed for FITC-dextran transport observed in these studies were in-keeping with the literature which have shown transport across non-Peyer's patch tissue to be at values of 0.5 - 10 x 10^{-6} cm/s (Table 4.1). What's more, in accordance with the literature, the ileal-jejunal Ap→Bas Papp values described in these studies are greater than those reported for Ap→Bas transport across the stripped colon mucosal tissue (see Table 4.1).

It is also important to note that FITC-dextran is likely to be transported across the tissue via transcellular transcytosis mechanisms as well as paracellularly (Diamanti, 2004). Higher molecular weight FITC-dextran (MW = 10,000 Da) is commonly used as a fluid-phase marker for endocytosis (Bacic *et al.*, 2006). If time had permitted, it would have been interesting to investigate the specific mechanism of FITC-dextran transport across this tissue, perhaps with the aid of metabolic inhibitors to cease active transport mechanisms. Inhibitors of microtubule assembly (e.g. colchicines) could also be used to stop endocytosis. Knocking out these mechanisms, would have allowed their contribution towards FITC-dextran transport to be assessed.

Table 4.1 Papp values for the paracellular transport of paracellular markers across the rat intestine.

Marker	Conc^n	Method	Rat	Fasted	Region	Direction	Papp (cm/s)	Reference
FITC-dextran (4400 Da)	1 mg/mL	Perfusion (3 h)	Male Wister		Ileum	Ap→Bas	1.0×10^{-6}	(Nakamura *et*
		Ussing chamber (2 h)	(180-220 g)		Colon		0.6×10^{-6}	*al.*, 2002)
					Colon *stripped*		1.3×10^{-6}	
						Bas→Ap	1.6×10^{-6}	
FITC-dextran (4400 Da)	0.1	Vertical diffusion	Male	24 h	Rat Ileum	Ap→Bas	7×10^{-6}	(Diamanti,
	mg/mL	system (1 h)	Sprauge		*stripped*			2004)
			Dawley					
			(200-250 g)					
Mannitol (182 Da)	100 μM	Rat everted gut sacs			Jejunum	Ap→Bas	4.6×10^{-5}	(Lacombe *et al.*,
Lucifer yellow (457 Da)		(1 h)					3.9×10^{-5}	2005)
Rantidine (351 Da)							3.9×10^{-5}	
Mannitol (182 Da)	40 μM	Ussing chamber (2 h)	Male Wister	48 h	Jejunum *stripped*	Ap→Bas	9.4×10^{-5}	(Wu-Pong *et al.*,
			-					1999)
Mannitol (182 Da)			Male	no	Ileum *stripped*	Ap→Bas	5.1×10^{-6}	(Tsutsumi *et al.*,
			Sprauge					2002)
			Dawley					
			(200-300 g)					

(-) donotes where data is not available.

Viability in the vertical diffusion model

The differences in the transport of FITC-dextran between individual experiments (Figure 4.7b and c) was not due to FITC-dextran batch variation (Figure 4.2a and 4.3), nor was it due to the transport of free FITC across the tissue (Figure 4.9). FITC-dextran is a robust molecule, as its molecular weight (Figure 4.2b) and fluorescence (Figure 4.4) were not affected by storage at different temperatures. The probe was also not degraded during incubation, with rat intestinal tissue (Figure 4.8), thus only the intact polymer molecule would be available for transport across this barrier. Several factors could influence FITC-dextran transport (as described below), though great care was taken in order to control each variable.

(1) Extrinsic factors such as food and environmental stress are known to influence absorption from the small intestine. Eating produces some physiological modifications such as a decrease in gastric emptying or the stimulation of biliary secretion, which among other things affects the pH of the small intestine, and thus the results obtained. Therefore the fasting times of the animals were very important. In these studies, Sprauge Dawley rats were fasted for 23 h before each experiment, to minimise the effect of food on tissue behaviour. The animals were also kept in a comfortable environment, and were housed for one week after delivery to allow them to acclimatise before experiments. Some reports have shown that stressed rats have a morphologically different mesenteric microvasculature (Wilson and Baldwin 1998), and intestinal mucosa (Wilson and Baldwin, 1999; Baldwin *et al.,* 2006). Furthermore, for consistency, each animal used for these studies weighed between 200 – 250 g.

However, the food and environment subjected to the animals by the supplier were outside our control. A change in animal chow could have played a role in affecting the data seen in these studies. For example, exposure to different dietary antigens early in life could have important implications on the effect on the mucosal immune system of the adult rats (Yelda *et al.,* 1996).

(2) Several studies have shown that drug efflux (Sababi *et al.,* 2001) metabolism (Zhang *et al.,* 1997) and absorption (Plusquelle *et al.,* 1987; Schaiquevich *et al.,* 2002) vary between different regions of the rat intestine. Nejdfors *et al.,* (2000) have shown that mannitol permeability is higher in the rat

ileum than jejunum and colon. Nakamura and colleges (2002) have shown that FITC-dextran (MW = 4,400 Da) transport was greater across the rat ileum compared to the colon (see Table 4.1). Therefore to limit regional variation in the intestinal segments used for these studies, the first 15 cm of the each rat intestine (extending out from the stomach), was always discarded. Tissue segments (with or without Peyer's patches) were then taken from the remaining distal jejunum and ileum.

However, Peyer's patches are distributed at random throughout the ileum, and were of different size. It is important to note that these animals are outbred, and different batches of them would have had exposure to different anitgens. Of the 0.9 cm^2 tissue surface area between each donor and recipient chamber, the patches usually occupied 10 - 40 % of surface area.

(3) Differences in the viability of the tissue could also play a key role on the transport of FITC-dextran across the rat intestine. It was important to preserve the integrity of the rat intestinal tissue during preparation for the vertical diffusion chamber, by keeping it in MEM on ice. As electrical equipment supplied with the vertical diffusion system was not functioning, the LDH assay was chosen as a means to measure tissue integrity, in accordance with Diamanti (2004). Though the release of LDH seen with this assay was highly variable, and the levels of LDH released into the culture media after t = 60 min were significantly different from t = 0 min, it was considered an unnecessary experiment. Firstly there appeared to be no correlation on the rate of transport and LDH levels. Secondly, though once the animal has been sacrificed, the tissue begins to die anyway, previous reports (Grass and Sweetana, 1998; Soderholm *et al.*, 1998) have consistently shown that intestinal tissue can remain viable for 2 h, and quite often transport studies using intestinal tissue are conducted over a 1 - 2 h time-frame. Although this assay is widely used to measure viability, it is perhaps not the best for this work.

Scraping the muscle layers from the mucosal epithelium would of course result in large amounts of LDH being released into culture media from lysed cells, though in an attempt to combat this, the media was always changed from the chambers before the start of each experiment. Furthermore, as mentioned previously, the experiments in which leakage had occurred, perhaps on rare occasions from tissue laceration, or perhaps from dying tissue segments, were discarded.

CHAPTER 5:

Effect of Polymers on FITC-dextran Transport Across Rat Intestinal Tissue

Albeit rather crude, the photomicrographs taken of longtitudal sections of stripped and unstripped tissues used for these studies at x 40 magnification showed no visible lacerations in the stripped mucosal segments (Figure 4.5). This was expected as this method is routinely used for studying transport (Dickens and Weil-Malherbe in 1941; Grass and Sweetana, 1988; Wu-Pong *et al.*, 1999; Diamanti, 2004; Watanabe *et al.*, 2005). Photomicrographs (x 107 magnification) of transverse sections of stripped intestinal tissue have shown that only the mucosa (i.e. epithelia, lamina propria and mucuslaris mucosae) remains (Field *et al.*, 1971). Lastly difficulties in oxygenation of the chambers could mean that the viability of the tissue was also compromised, as this would effect the mixing of the solution in the chamber, as well.

Effect of cytokines on FITC-dextran transport, why didn't it work?

The effects rTNF-α, rIFN-γ and rIL-2 on tissue permeability were varied possibly due to the reasons described above. One limitation of the vertical diffusion model is that the duration of the study can only be conducted over an hour due to tissue viability. Permeability studies involving immortalised cell lines however can be continued for h - d. It is possible that the cytokines did have an effect on the tissue, though a 60 min incubation was not enough time in which to see an effect on TJ permeability. For example, Ma *et al.*, (2004), have shown that though NF-κB is activated in minutes in TNF-α incubated Caco-2 cells, a delay of ~ 24 h was found between this and a functional increase in TJ permeability. It is also possible, that the half-life of the cytokine was too short to have an effect. Another disadvantage of these experiments is the number of animals required, compared with rapid *in vitro* models, however, as previously mentioned this model is more physiological.

Despite the variability in FITC-dextran transport, as the vertical diffusion system had been established as a model to measure transport across rat intestinal tissue, it was decided to move forward and use this model for further studies in which the effects of polymers on transport were measured. This was mainly due to the physiology of the intestinal tissue used, which is more appropriate for these studies than would be intestinal cell monolayers. The next chapter investigates the effects of polymers on FITC-dextran transport across rat intestinal tissue.

5.1 INTRODUCTION

As rTNF-α, rIFN-γ and rIL-2 did not significantly increase the transport of FITC-dextran across rat intestinal epithelial tissue, it was decided to examine whether the polymers themselves would modify the transport rates of this paracellular marker.

As mentioned in Chapter 4 (section 4.2), recent work has demonstrated that the anionic, mucoadhesive polymer, PAcA, can permeabilise the intestine, and as a result enhance the transport of the paracellular marker sodium-fluorescein across this tissue (Kast and Bernkop-Schnürch, 2002). It has also been shown that dendrimers, particularly PAMAM dendrimers, display rapid transport rates across everted rat intestinal tissue (Wiwattanapatapee *et al.*, 2000) as well as monolayer models (El-Sayed *et al.*, 2003). Their mechanism of transport across this barrier is still unclear, and it could be by either transcellular (probably endocytosis) or paracellular pathways (if the TJ are opened).

Consequently, PAcAs and PAMAM generation 3.5 dendrimers were chosen along with alginate, HA and sHA, to study the effect of polymers on FITC-dextran transport across intestinal tissue. The vertical diffusion system was once again used as a transport model for these studies, and the rationale for the choice of polymers used for these particular experiments is given in the following paragraphs (for a review of these macromolecules see Chapter 1 sections 1.6.1 - 1.6.4).

Rationale for the choice of polymers used for transport studies

PAcA

PAcA was originally thought to enhance permeability across the intestine by chelating extracellular Ca^{2+} (Charmen *et al.*, 1990), as it acts like a weak ion exchanger and binds Ca^{2+} at neutral pH (Kriwet and Kissel, 1996). However, when polymerised into microparticles (1-10 μm in diameter), this polymer (MW = 300,000 Da) has also shown the ability to adhere to, and physically widen paracellular gaps between Caco-2 cells in monolayers (Kriwet and Kissel, 1996). As a result these microparticles increase the paracellular transport of sulforhodamine, and this effect is not due to swelling of the microparticles, nor due to cell damage (Kriwet and Kissel, 1996). Most of the polymer remains swollen in the particles, and cannot cross the monolayer due to its large size (Kriwet and Kissel, 1996). Furthermore, because

Caco-2 cells do not possess a mucus layer, the increase in permeability caused by this polymer is not due to its mucoadhesive properties. The transport of sulforhodamine across Caco-2 cells is also dependent on the side to which the microparticles are administered. Basal to apical transport of sulforhodamine was 30 times greater than that seen in the apical to basal direction (Kriwet and Kissel, 1996).

Water-soluble PAcAs (MW = 30,000 100,000 and 450,000 Da) were chosen for these studies. Besides the reported ability of PAcA to induce IFN-γ (see section 1.6.3), the specific PAcAs chosen for this work have been shown to enhance the transport of Na-Flu across guinea pig small intestinal tissue, mounted in Ussing type chambers. The increases in permeability caused by these polymers are molecular weight-dependant, with the rank order for enhancement being $PAcA_{450}$ > $PAcA_{100}$ > $PAcA_{30}$ (Kast and Bernkop-Schnürch, 2002). Thiolated, thus more mucoadhesive, forms of these polymers have also shown greater transport rates in this mucus-containing tissue, though the rank order for permeability was repeated (Kast and Bernkop-Schnürch, 2002).

PAMAM dendrimers

The potential of PAMAM dendrimers to be used for drug delivery has been demonstrated in several cell lines including Caco-2 (El-Sayed *et al.*, 2003a; El-Sayed *et al.*, 2003b; Jevprasesphant *et al.*, 2003a; Jevprasesphant *et al.*, 2003b) and Madin-Darby canine kidney (epithelial) cell monolayers (Tajarobi *et al.*, 2001), as well as in hamster microvascular endothelium (El-Sayed *et al.*, 2001).

Wiwatanapatepee and colleagues (2000) were the first to appreciate the possibility of using PAMAM dendrimers for enhancing oral drug delivery. They radioiodinated (^{125}I-labelled) anionic (generations 2.5, 3.5, 5.5) and cationic PAMAM dendrimers (generations 3 and 4), and measured their uptake and transport across the everted rat intestine. Compared to other macromolecules including PVP, HPMA, BSA and tomato lectin, PAMAM dendrimers had high serosal transfer rates (Ap→Bas) of transport into the serosal sac fluid. Although high levels of PAMAM generation 5.5, and the cationic PAMAM dendrimers, generations 3 and 4, were detected in the sac-tissue at the end of the experiment, the anionic PAMAMs were not, indicating very high transport across the tissue. The high endocytic index (EI) values (an endocytic index has been defined as the volume-equivalent of substrate cleared (μl) from the medium/mg tissue protein/h; Williams *et al.*, 1975) measured

for these molecules suggested uptake by absorptive endocytosis. This would certainly seem probable for the cationic PAMAM dendrimers, as they would bind to the cell surface non-specifically due to charge interaction.

El-Sayed *et al.*, (2003a) found further evidence for the rapid transcytosis of PAMAM dendrimers. This came from the observation that cationic dendrimers were rapidly transported across Caco-2 cells. Transport was reduced at 4 °C so they concluded that it occurred via an energy-dependent mechanism. In addition Jevprasesphant and colleagues (2004) observed gold-labelled PAMAM generation 3 dendrimers inside Caco-2 cells, confirming uptake by endocytosis. Also supporting the hypothesis that transport is at least in part by endocytosis was the fact that the endocytosis inhibitor colchicine significantly reduced the absorption of PAMAM generation 2 dendrimers in Caco-2 cells (El-Sayed *et al.*, 2002). Interestingly PAMAM dendrimers avoid efflux by the membrane efflux pump P-gp. El-Sayed *et al.*, (2003a) showed this by adding the P-gp substrate, paclitaxel, to Caco-2 monolayers, and monitoring the transport of PAMAM generation 2 dendrimers. In both Ap→Bas or Bas→Ap directions, the permeability of generation 2 dendrimers did not change.

However, it has also been shown that PAMAM dendrimers have the ability to permeabilise Caco-2 cell monolayers by opening TJ and increasing paracellular transport. PAMAM generations 1, 2, 3 and 4 decreased the TEER of Caco-2 monolayers, and increased the transport of the paracellular marker [^{14}C]mannitol (El-Sayed *et al.*, 2003a; El-Sayed *et al.*, 2003b; Jevprasesphant *et al.*, 2003a). Although it could be useful that cationic PAMAM dendrimers can allow transport via the paracellular route, it is also a potential cause for concern if the physiological barrier is destroyed, albeit transiently.

In addition, the general cytotoxicity of some dendrimers may be a concern if they were to be used to prepare oral formulations (reviewed in Duncan and Izzo, 2005). As previously mentioned (section 3.4) the cytotoxicity of cationic PAMAM dendrimers has been shown to increase in a generation-dependent manner (Malik *et al.*, 2000; El-Sayed *et al.*, 2003b) so they may not be the best option for enhancing oral drug delivery. Conversely, anionic PAMAM dendrimers were not cytotoxic towards B16F10 cells *in vitro* (Malik *et al.*, 2000) and were less cytotoxic towards

Caco-2 monolayers than cationic PAMAMs (El-Sayed *et al.*, 2003b). Interestingly, El-Sayed *et al.*, (2003b) showed that unlike other anionic PAMAM dendrimers, PAMAM 2.5 and 3.5 dendrimers caused an incubation-time dependent decline in the TEER values of Caco-2 monolayers. In addition, there was up to a 6-fold increase in mannitol permeability at non-toxic concentrations. These results can be correlated with the studies of Wiwatanapatepee *et al.*, (2000), who using the everted rat intestine, showed that the EI values of ^{125}I-labelled PAMAM generation 2.5 and 3.5 dendrimers were very low (0.6 - 0.7 µl/mg protein/h), and suggested rapid transcytosis via a fluid-phase mechanism. For these studies, it was therefore thought that PAMAM generation 3.5 dendrimers might be the most interesting, to explore the effects of polymers on permeability.

Alginates

As mentioned in Chapter 1 (section 1.6.1), alginates are widely used in drug delivery systems (i.e. in capsule coatings (as a vegetarian substitute for gelatin) and as a component of microcapsules (Gonzalez Ferreiro *et al.*, 2002; Robitaille *et al.*, 2005)). Alginate has also been used as a protein (an antigenic VP2 peptide) and drug (5-aminosalicyclic acid) carrier (Morgan *et al.*, 1995), and is well tolerated and poorly immunogenic when systemically administered to rats (Al-Shamkhani and Duncan 1995b). The fate of ^{125}I-labelled alginate when administered intravenously, subcutaneously, intraperitoneally and orally, to rats has also been examined. It was found that its distribution throughout the body was molecular weight-dependant (Al-Shamkhani and Duncan 1995b). Lower molecular weight fractions of ^{125}I-labelled alginate (MW $\leq$ 48,000 Da) were excreted in the urine, whilst larger polymer fractions remained in the circulation and did not accumulate in any organs. Orally administered alginate appeared mainly in intestinal tissue washings, thought to be due to the entanglement of the macromolecules with the glycocaylx (Al-Shamkhani, 1993). It also appeared to be degraded, as free [^{125}I]iodine was found in the urine and thyroid gland of test animals.

Early studies were interested in alginates as potential oral bioadhesive polymers to delay GI transit time, although it did not seem to fulfil its potential in this role (Al-Shamkhani, 1993). Although alginates have been developed as polymer-drug conjugates for delivery of peptides and anticancer drugs, from a drug delivery perspective, the effect alginate on transport across the small intestine has not been

well examined. It was therefore considered important to investigate this polymer in these studies.

HA

As mentioned in Chapter 1 (section 1.6.2), HA is a large hydrophilic, water-retaining polymer that is present in a variety of tissues, though it is not present in intestinal epithelial cells (Fraser, 1989). It is located in the loose connective tissue of the lamina propria, where it is synthesised by mesenchymal cells, from where it is easily mobilised (Fraser, 1989). Like alginate, HA is also being developed as a drug carrier. When conjugated to the anticancer drug Taxol®, it has been shown to be taken up into cancer cell lines (HB1-100 breast and SK-OV-3 ovarian, human) via the CD44-receptor (Luo *et al.*, 2000).

HA was specifically chosen for these studies due to its known potential to act as a mucoadhesive polymer and to promote penetration enhancement. The GI mucoadhesive properties of HA have been investigated in the rat, where it has been found to be a better bonding agent than Carbomer® (Pritchard *et al.*, 1996). Furthermore, in ophthalmology, the mucoadhesive properties of this polymer have been used to improve the residence time of drug formulations on the eye (Saettone *et al.*, 1994).

The penetration enhancement properties of HA have been demonstrated in nasal epithelial mucosa, where HA enhanced the delivery of insulin (Ryden and Edman, 1992) and vasopressin (Morimoto *et al.*, 1991). More recently, the HA has been shown to increase the absorption of the antiviral drug, acyclovir in porcine buccal and vaginal tissue, Caco-2 cell monolayers and the rat jejunum. (Sandri *et al.*, 2004). It was found that as HA molecular weight decreased, its mucoadhesive properties increased. The lowest molecular weight fraction of HA (MW = 202,000 Da), showed the best penetration enhancement properties (Sandri *et al.*, 2004).

HA is also known to play a role in the pathophysiology of disease. It has been detected in jejunal fluid, and in the inflamed colon of IBD patients (De la Motte *et al.*, 2003), as well as throughout the epithelium in patients with celiac disease (Kemppainen *et al.*, 2005). In celiac disease, it is thought that defects in the epithelial

permeability (known to be an early sign of the disease), increase the leakage of mobile, stromal, HA into the jejunal lumen. This depletes the HA levels in the villi connective tissue. As HA is such an abundant molecule in the villous stroma, and has a high capacity to bind water and expand the tissue, its loss may contribute to villous destruction and the flattening of the epithelium in this syndrome. It is also speculated that the presence of CD44-bound HA in the intestine delays and prevents the TJ formation and, thus enhances the diffusion of molecules through the intestinal epithelium in this condition (Kemppainen *et al.*, 2005). Thus, the interest in assessing its effect on FITC-dextran transport across rat intestinal tissue.

Therefore, the overall objectives of this study can be summarised as follows:

(i) First it was important to investigate the effect of the polymers on medium pH - the polymers tested have quite different pKa values.
(ii) As fluorophores often show pH- and concentration-dependence, it was important to determine the effect of both on the fluorescence output of FITC-dextran.
(iii) The effect of alginate, HA, sHA, PAcAs ($sPAcA_{30}$, $PAcA_{100}$ and $PAcA_{450}$) and PAMAM generation 3.5, on the transport of FITC-dextran across the intestinal tissue, in the vertical diffusion chamber from both the Ap→Bas and the Bas→Ap directions was then studied.
(iv) Finally, it was considered important to investigate whether the presence of Peyer's patches would influence transport.

5.2 METHODS

The preparation of rat intestinal tissue for transport experiments, along with the use of the vertical diffusion system has previously been described in Chapter 2 (section 2.3.6). Only specific details relating to the experiments carried out in this Chapter will be described below. During all experiments FITC-dextran solutions were protected from light to prevent photo-bleaching. Unless otherwise stated, all experiments were carried out in replicates of three.

5.2.1 Effect of polymers on the pH of tissue culture media

Before polymers were introduced into the vertical diffusion system, it was considered important to investigate their effect on the pH of the tissue culture

medium (MEM). This was key, not only because pH plays a basic role in cytotoxicity (Mackenzie *et al.*, 1961), but also because FITC is a pH-sensitive fluorophore (supplier information: www.sigmaaldrich.com, accessed 12/03/2002). The pH of MEM containing dissolved polymers (1 mg/mL) was therefore measured.

5.2.2 Effect of pH on FITC-dextran fluorescence

The effect of pH on the fluorescence-output of FITC-dextran was investigated using citric acid-sodium citrate buffers at pH 5.5, or 6.5, and phosphate buffer at pH 7.4. Each buffer was prepared according to recipes from Dawson *et al.* (2002) (as described below), and was used to make calibration curves (1 – 0.001 mg/mL) from a FITC-dextran stock solution (1 mg/mL in appropriate buffer). All dilutions were prepared in eppendorf tubes and then the solutions were pipetted into black 96-well plates (50 μL/well) and read in the fluorescence plate reader as previously described (section 2.3.6). The data obtained were plotted as concentration (mg/mL) against fluorescence.

To make citric acid-sodium citrate buffers, a 0.1 M citric acid monohydrate ($C_6H_8O_7$) solution (21 mg/mL in 10 mL ddH_2O), and a 0.1 M trisodium citrate dihydrate ($C_6H_5O_7Na_3$) solution (29 mg/mL in 20 mL ddH_2O) were prepared. Each solution was mixed to give a pH 5.4 and pH 6.2 buffer (see Table 5.1). The pH of these solutions was read using the pH-meter, and the solutions were adjusted to pH 5.5 and pH 6.5 using NaOH (0.1 M).

Phosphate buffer (Na_2HPO_4 - NaH_2PO_4) was prepared in a similar fashion, using a 0.2 M solution of Na_2HPO_4 ($2H_2O$: 35.61 mg/mL in 5 mL of ddH_2O), and a 0.2M solution of NaH_2PO_4 (71.64 mg/mL in 2 mL in ddH_2O). Both Na_2HPO_4 and NaH_2PO_4 solutions were mixed (4.05 mL and 0.95 mL respectively) to give a pH 7.4 buffer. The pH of this solution was checked using the pH meter.

Table 5.1 Recipe for citric acid-sodium citrate buffer

PH	0.1 M citric acid (mL)	0.1 M trisodium citrate (mL)
5.4	2.55	7.45
6.2	0.80	9.20

5.2.3 Effect of polymers on FITC-dextran transport across rat intestinal tissue using the vertical diffusion system

To examine the effect of polymers on FITC-dextran transport, a 1 mg/mL solution of each polymer was made with MEM containing FITC-dextran (0.1 mg/mL). In some cases solutions were made 12 h in advance of an experiment and were kept in the fridge (4 °C) overnight, to allow polymers (HA, sHA, $PAcA_{450}$ and alginate) to dissolve in the tissue culture medium.

Prior to each experiment, the tissue was prepared, and the vertical diffusion system was set up as previously described (Chapter 2, section 2.3.6). To start the experiment, MEM was removed from each chamber, and the apical and basal compartments were immediately replenished with either fresh MEM, or polymer - containing MEM (depending on whether Ap→Bas or Bas→Ap transport was being investigated).

All solutions were pre-warmed (37 °C) before they were added to the tissue. Samples (25 μL) were then collected from the recipient chambers at 5 - 10 min intervals from t = 0 - 60 min, and were treated as previously described in Chapter 2 (section 2.3.6). It is important to note that the total volume was maintained by the addition of an equal volume of fresh MEM at each sample time.

5.3 RESULTS

5.3.1 Effect of polymers on MEM pH

Addition of FITC-dextran, alginate, HA, $sPAcA_{30}$ and PAMAM generation 3.5 dendrimers to MEM caused little change in the pH (all 1 mg/mL). A range of pH 7.0 - 8.0 was observed (Table 5.2) with alginate causing the greatest decrease (pH 7.04) and PAMAM 3.5 causing the greatest increase (pH 7.97). The higher molecular weight PAcA polymers ($PAcA_{100}$ and $PAcA_{450}$) were more acidic in the culture media, and reduced the pH to 6.43 and 6.36 respectively.

5.3.2 Effect of pH on FITC-dextran fluorescence

A linear concentration-dependent increase in FITC-dextran fluorescence was seen at all pHs (Figure 5.1). However, fluorescence output was highly dependent on pH. It was greatest at pH 7.4, and decreased at lower pHs. For example at 1 mg/mL, fluorescence output was reduced by 47 % at pH 6.5, and by 86 % at pH5.5, compared to pH 7.4.

Table 5.2 Effect of polymers on tissue culture media pH.

Polymer dissolved in MEM (1 mg/mL)	**pH**
MEM only	7.42
FITC-dextran	7.55
Alginate	7.04
HA	7.70
$sPAcA_{30}$	7.55
$PAcA_{100}$	6.42
$PAcA_{450}$	6.36
PAMAM 3.5	7.97

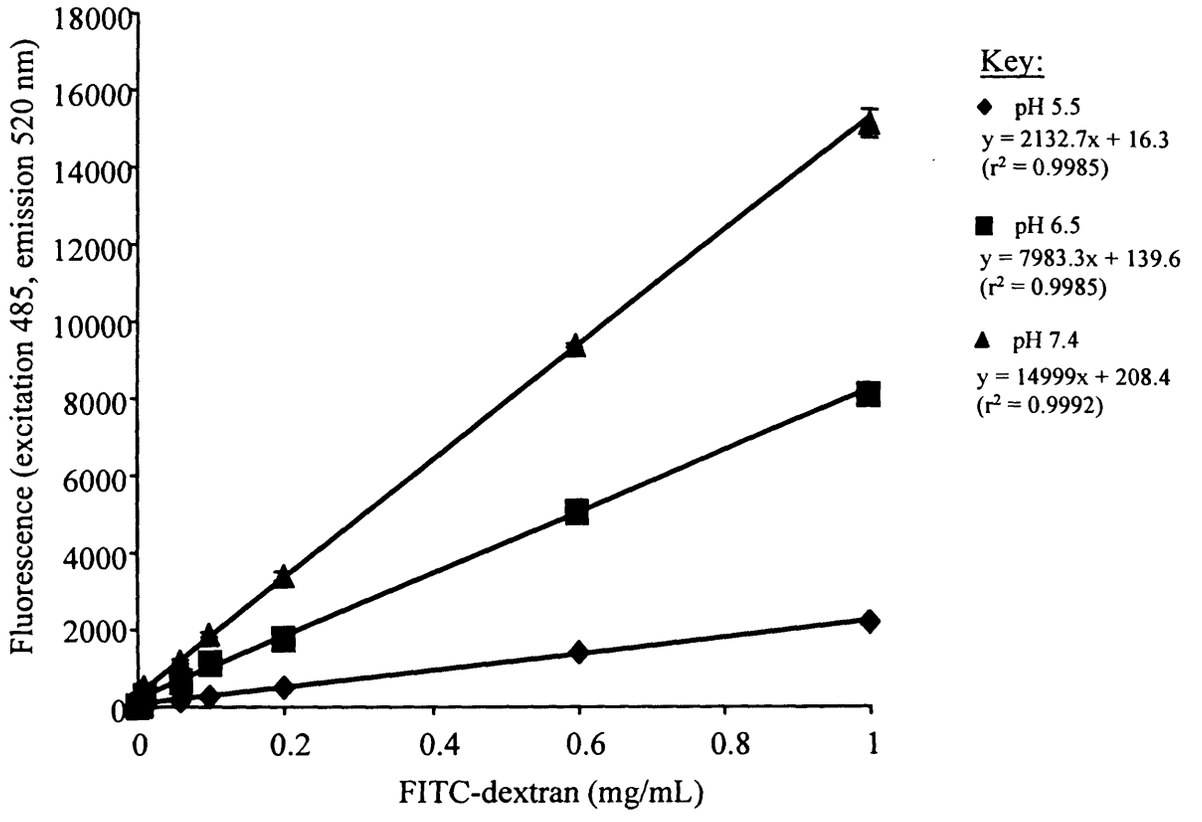

Figure 5.1 Fluorescence output of FITC-dextran (MW = 4,000 Da) in different pH buffers.

5.3.3 Effect of polymers on FITC-dextran transport across rat intestinal tissue

Ap→Bas transport and Bas→Ap transport across non-Peyer's patch tissue

In control experiments FITC-dextran transport with or without polymers (1 mg/mL) was linear over time (t = 0 - 60 min), and in this set of experiments the rate of FITC-dextran transport across the rat intestinal tissue was lower than that seen previously in Chapter 4 (Figure 4.7a). A 5 min lag phase in FITC-dextran transport was seen for Ap→Bas and Bas→Ap transfer across tissue with or without Peyer's patches (Figure 5.2). The Papp values of transport across non-Peyer's tissue were 0.5 x 10^{-6} for transport in the Ap→Bas direction, and 1.0 x 10^{-6} for transfer in the Bas→Ap direction.

Alginate (Figure 5.3a), HA (Figure 5.3b) and sHA (Figure 5.3c) did not enhance FITC-dextran transport in the Ap→Bas direction across tissue without Peyer's patches. Instead, these polymers appeared to reduce it. When PAcA was used, the Ap→Bas transport of FITC-dextran appeared to be dependent on PAcA molecular weight. The highest molecular weight PAcA ($PAcA_{450}$) had no effect on FITC-dextran transport (Figure 5.3d), whilst $PAcA_{100}$ reduced it (Figure 5.3e). At t = 60 min a 62 % decrease in fluorescence was seen for FITC-dextran transport in the presence of $PAcA_{100}$, compared to the control FITC-dextran (Figure 5.3e). In contrast, the smaller molecular weight PAcA in sodium salt form ($sPAcA_{30}$) increased FITC-dextran transport in the Ap→Bas direction as an increase (of 16 % at 60 min) in fluorescence was seen (Figure 5.3f). This data however was not significant. When the effect of PAMAM generation 3.5 dendrimers on FITC-dextran transport was measured, like other polymers, it appeared to reduce Ap→Bas transport (Figure 5.3g).

As $sPAcA_{30}$ appeared to enhance Ap→Bas transport across non-Peyer's patch tissue, it was decided to also measure the effect of this polymer on FITC-dextran transport in the Bas→Ap direction. For comparison, alginate and HA were also chosen for this work. Alginate (Figure 5.4a) and HA (Figure 5.4b) caused a significant reduction in FITC-dextran transport across non-Peyer's patch tissue in the Bas→Ap direction. Interestingly, $PAcA_{30}$ also reduced transport in this direction (Figure 5.4c).

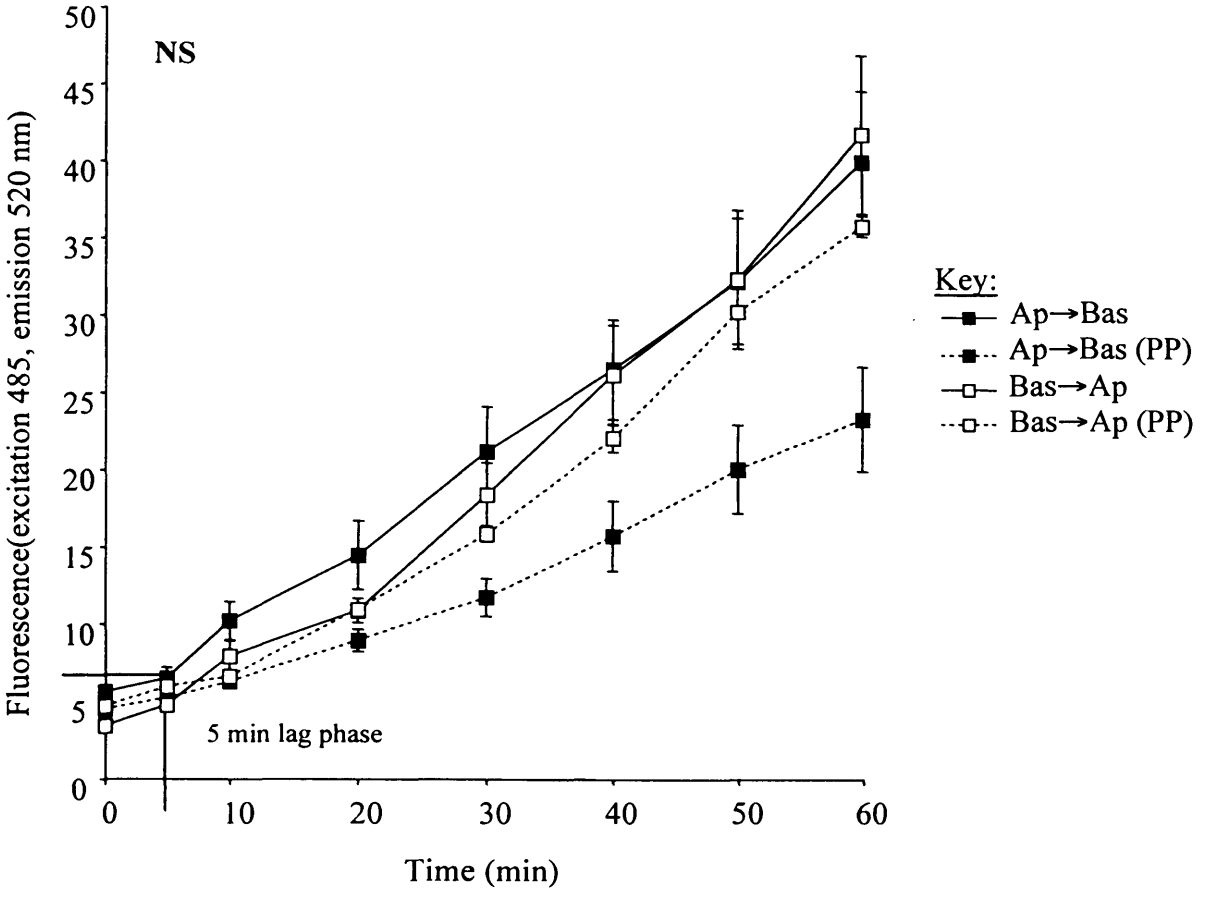

Figure 5.2 Ap→Bas and Bas→Ap FITC-dextran transport across rat intestinal tissue with or without Peyer's patches. The data shown are mean ± SEM (n > 11), and NS at t = 60 min according to one-way ANOVA.

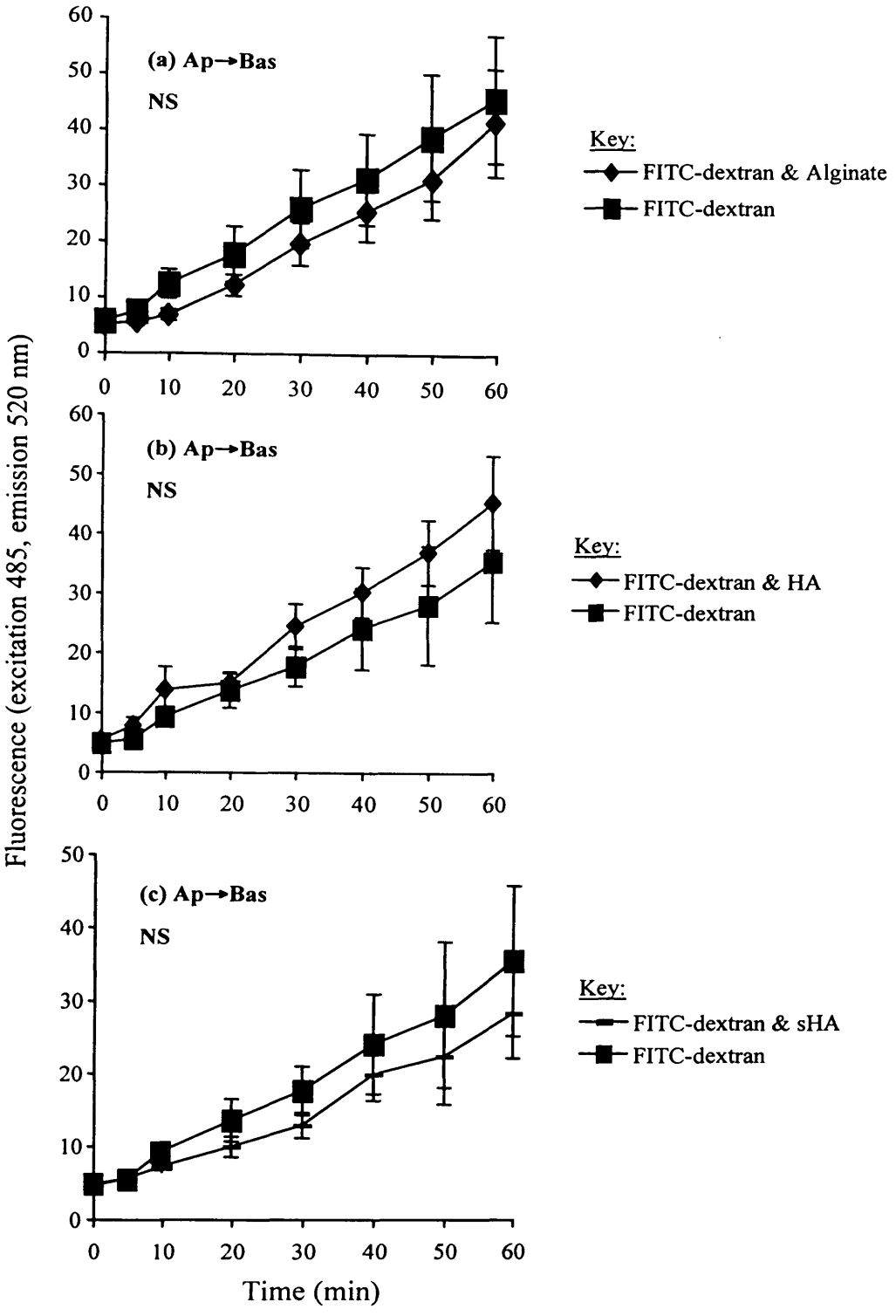

Figure 5.3 (a, b & c) Effect of polysaccharides (1 mg/mL) on Ap→Bas FITC-dextran transport across rat intestinal tissue. Panel (a) alginate, panel (b) HA, panel (c) sHA. The data shown are mean ± SEM (n > 6), and NS at t = 60 min according to two-tailed t-test.

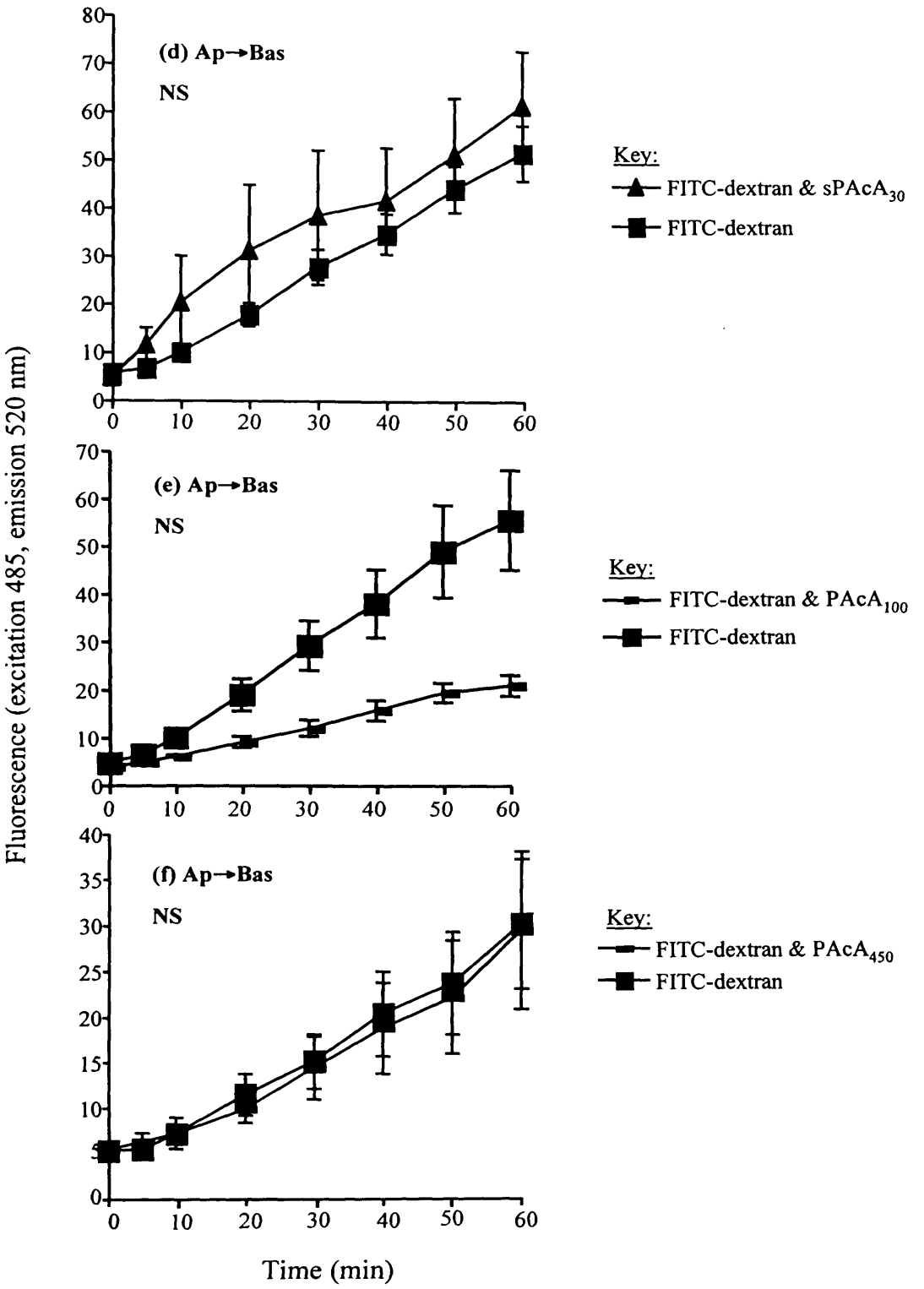

Figure 5.3 (d, e & f) Effect of PAcAs (1 mg/mL) on Ap→Bas FITC-dextran transport across rat intestinal tissue. Panel (d) $sPAcA_{30}$, panel (e) $PAcA_{100}$, panel (f) $PAcA_{450}$. The data shown are mean ± SEM ($n > 6$), and NS at $t = 60$ min according to two-tailed t-test.

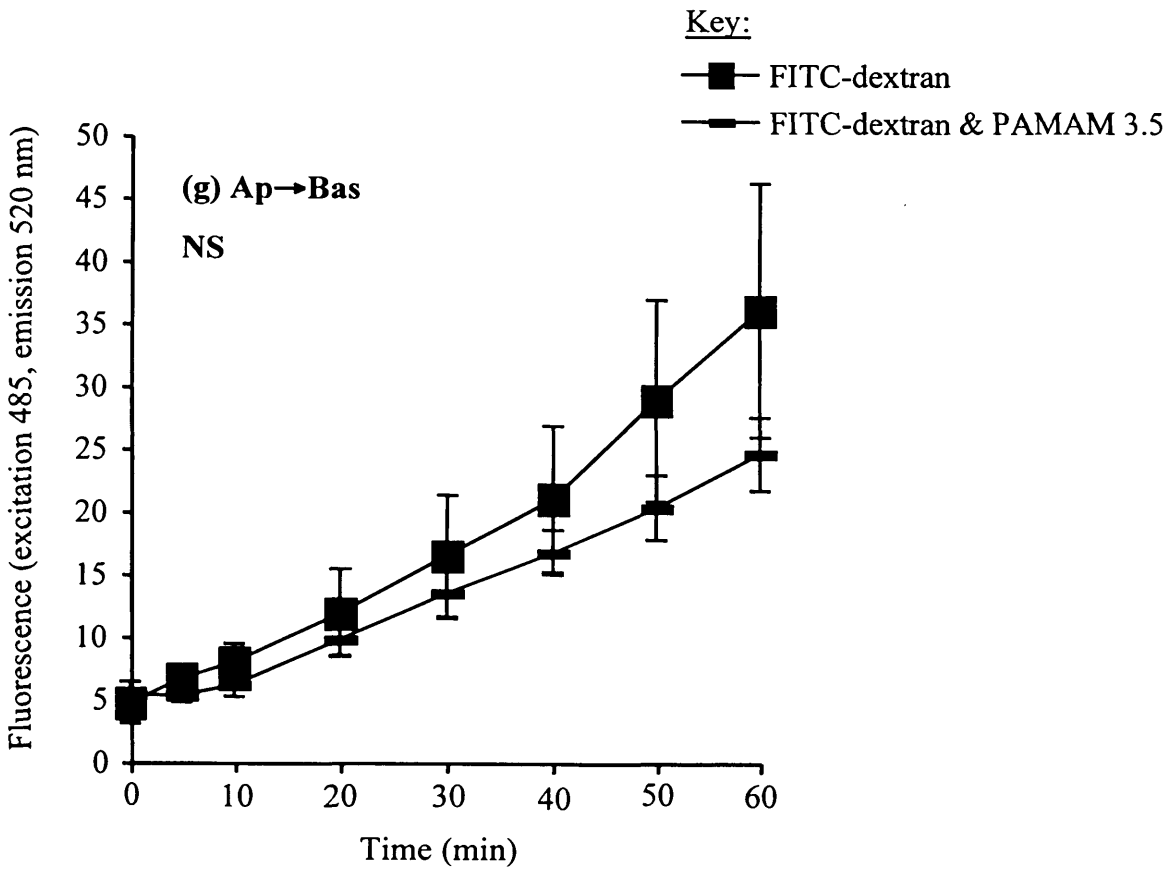

Figure 5.3 (g) Effect of PAMAM generation 3.5 dendrimers on Ap→Bas FITC-dextran transport across rat intestinal tissue. The data shown are mean ± SEM ($n > 6$), and NS at $t = 60$ min according to two-tailed t-test.

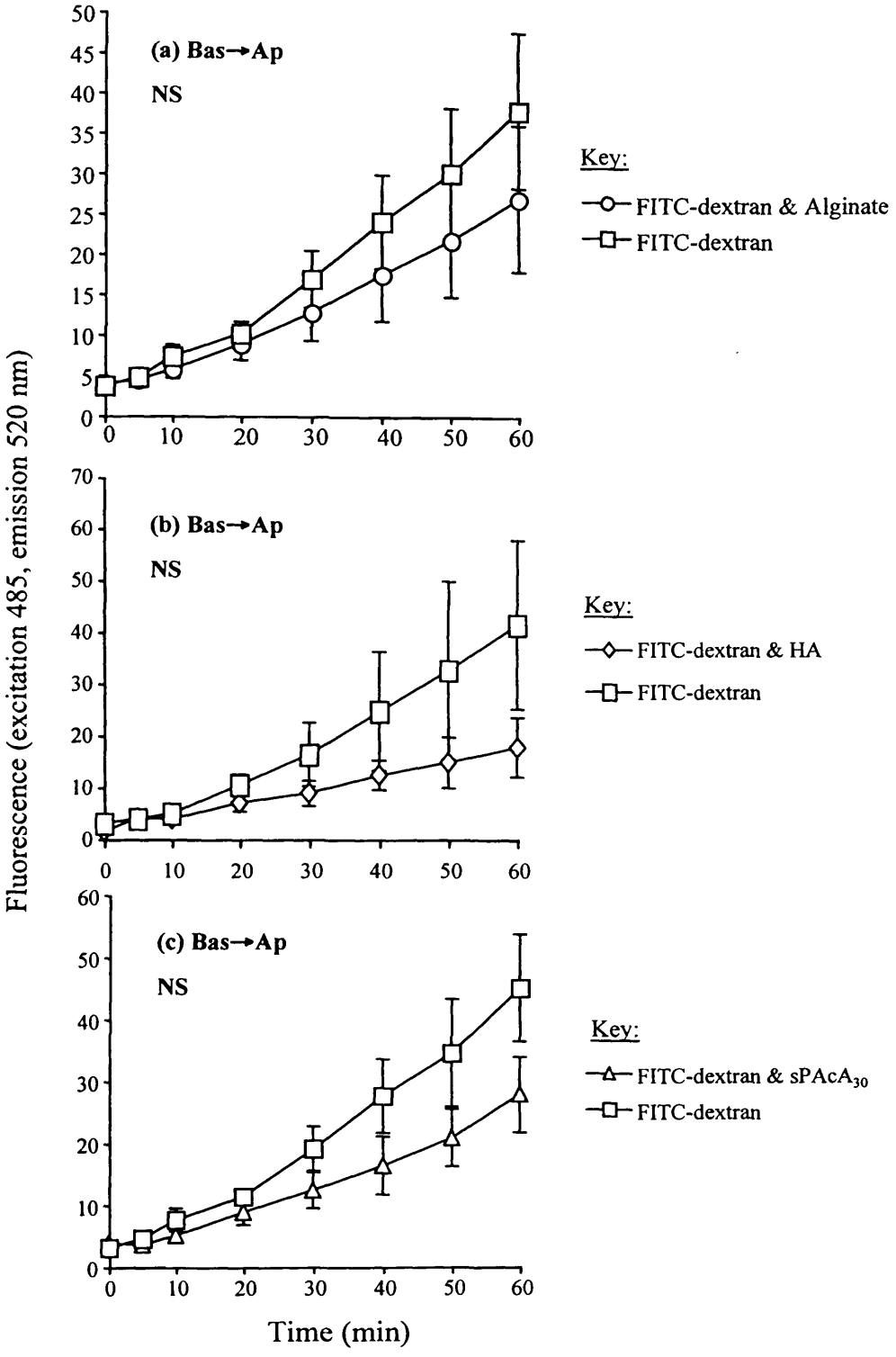

Figure 5.4 (a, b & c) Effect of polymers on Bas→Ap FITC-dextran transport across rat intestinal tissue containing Peyer's patches. Panel (a) alginate, panel (b) HA, panel (c) $sPAcA_{30}$. The data shown are mean ± SEM ($n > 3$), and NS at $t = 60$ min according to two-tailed t-test.

Ap→Bas transport and Bas→Ap transport across tissue with Peyer's patches

The control transport of FITC-dextran across Peyer's patch tissue was lower than that seen for transport across tissue without Peyer's patches (see Figure 5.2). The Papp value for Ap→Bas transport across tissue without Peyer's patches was 0.5 x 10^{-6}. For Bas→Ap transport across this tissue, the Papp value was 1.0 x 10^{-6}. The transport of FITC-dextran in the presence of all polymers increased linearly over time. Addition of $sPAcA_{30}$ (Figure 5.5a), HA (Figure 5.5b) and alginate (Figure 5.5c) all reduced FITC-dextran transport. Ap→Bas FITC-dextran transport with $sPAcA_{30}$ was 33 % less than that of the control (FITC-dextran only) at t = 60 min, and this is in contrast with the observations made in non-Peyer's patch tissue where this polymer appeared to enhance FITC-dextran transport. For HA and alginate, Ap→Bas transport was 25 % and 41 % lower than the control respectively at 60 min.

Bas→Ap transport of FITC-dextran across Peyer's patch tissue with $sPAcA_{30}$ (Figure 5.6a), HA (Figure 5.6b) and alginate (Figure 5.6c) was also significantly reduced.

5.4 DISCUSSION

It would seem that no one has previously examined the effect of polymers, on the transport of FITC-dextran in any intestinal model. As mentioned in the introduction, previous studies investigating the effect of polymers on GI permeability have used Na-Flu (Kast and Bernkop-Schnürch, 2002), mannitol (El-Sayed *et al.*, 2003a; El-Sayed *et al.*, 2003b; Jevprasesphant *et al.*, 2003a; Wu-Pong *et al.*, 1999; Tsutsumi *et al.*, 2002; Lacombe *et al.*, 2004), rhodamine (Kriwet and Kissel, 1996), lucifer yellow (Lacombe *et al.*, 2004) and in some cases PEG (Artursson *et al.*, 1993; Ghandehari *et al.*, 1997) as substrates.

As previously mentioned, FITC-dextran might cross the intestinal epithelial barrier by paracellular or transcellular mechanisms (Figure 5.7), and thus polymer enhancement of FITC-dextran transport could theoretically occur by (1) polymers stimulating endocytosis, (2) polymers opening TJ, via cytokine release, or through interactions with the apical cell membrane (Figure 5.7). However the addition of polymers might also inhibit FITC-dextran transport if they bind to either the cell membrane, or FITC-dextran itself, and block its transport across the tissue. They could also act as a competitive inhibitor for FITC-dextran endocytosis, or could alter

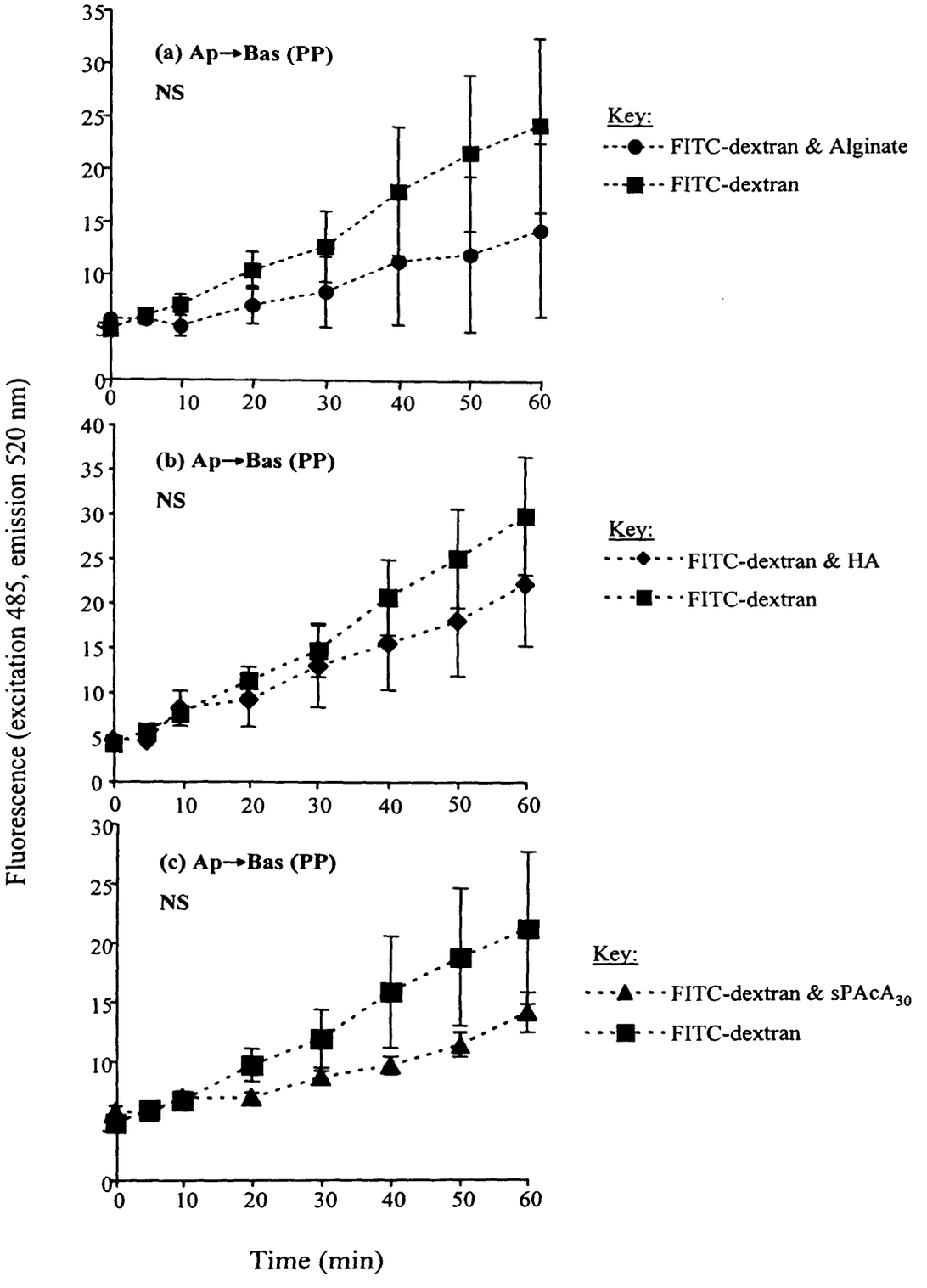

Figure 5.5 (a, b & c) Effect of polymers on Ap→Bas FITC-dextran transport across rat intestinal tissue containing Peyer's patches. Panel (a) alginate, panel (b) HA, panel (c) $sPAcA_{30}$. The data shown are mean ± SEM ($n > 3$), and NS at $t = 60$ min according to two-tailed t-test.

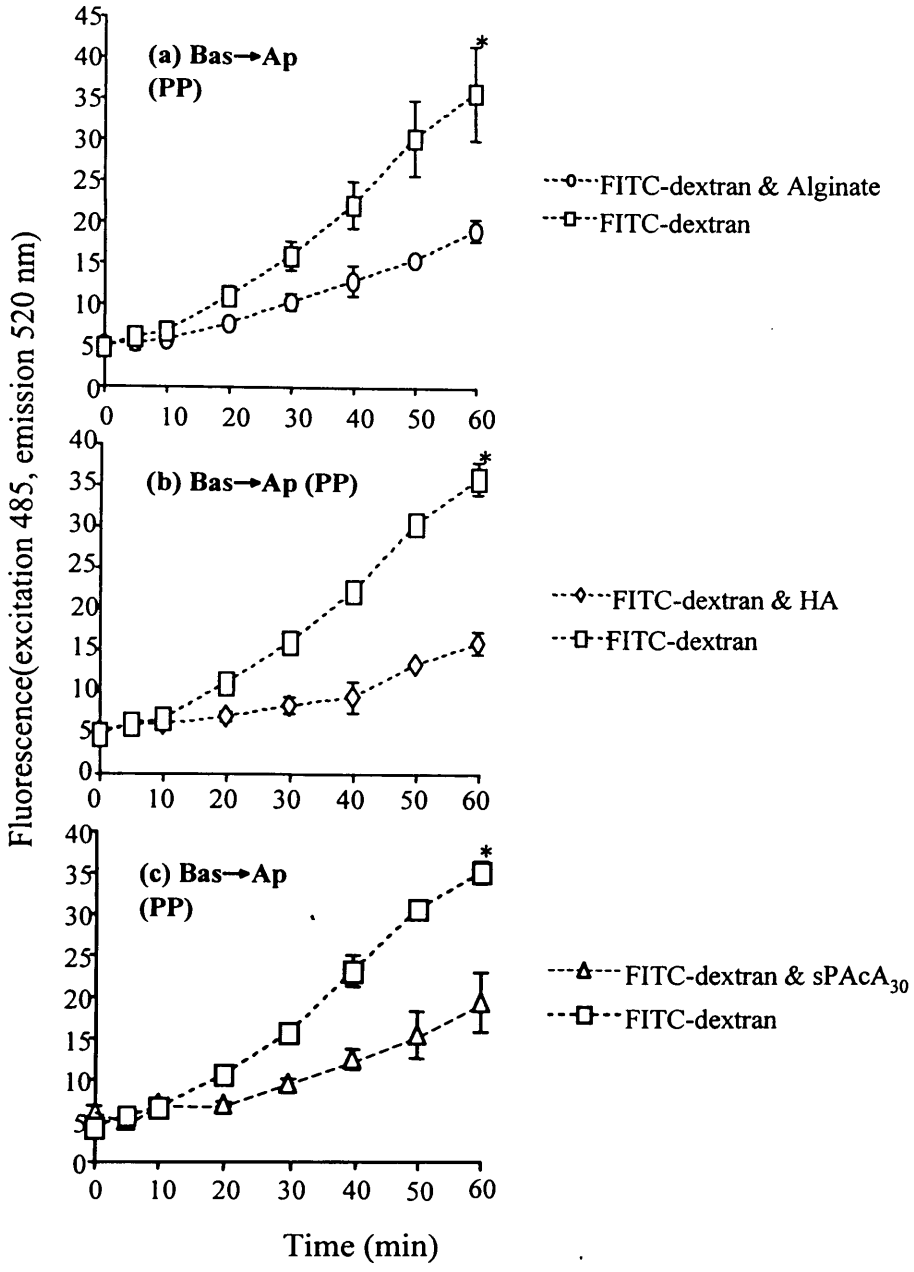

Figure 5.6 (a, b & c) Effect of polymers on Bas→Ap FITC-dextran transport across rat intestinal tissue containing Peyer's patches. Panel (a) alginate, panel (b) HA, panel (c) $sPAcA_{30}$. The data shown are mean ± SEM (n = 3). * = $p < 0.05$.

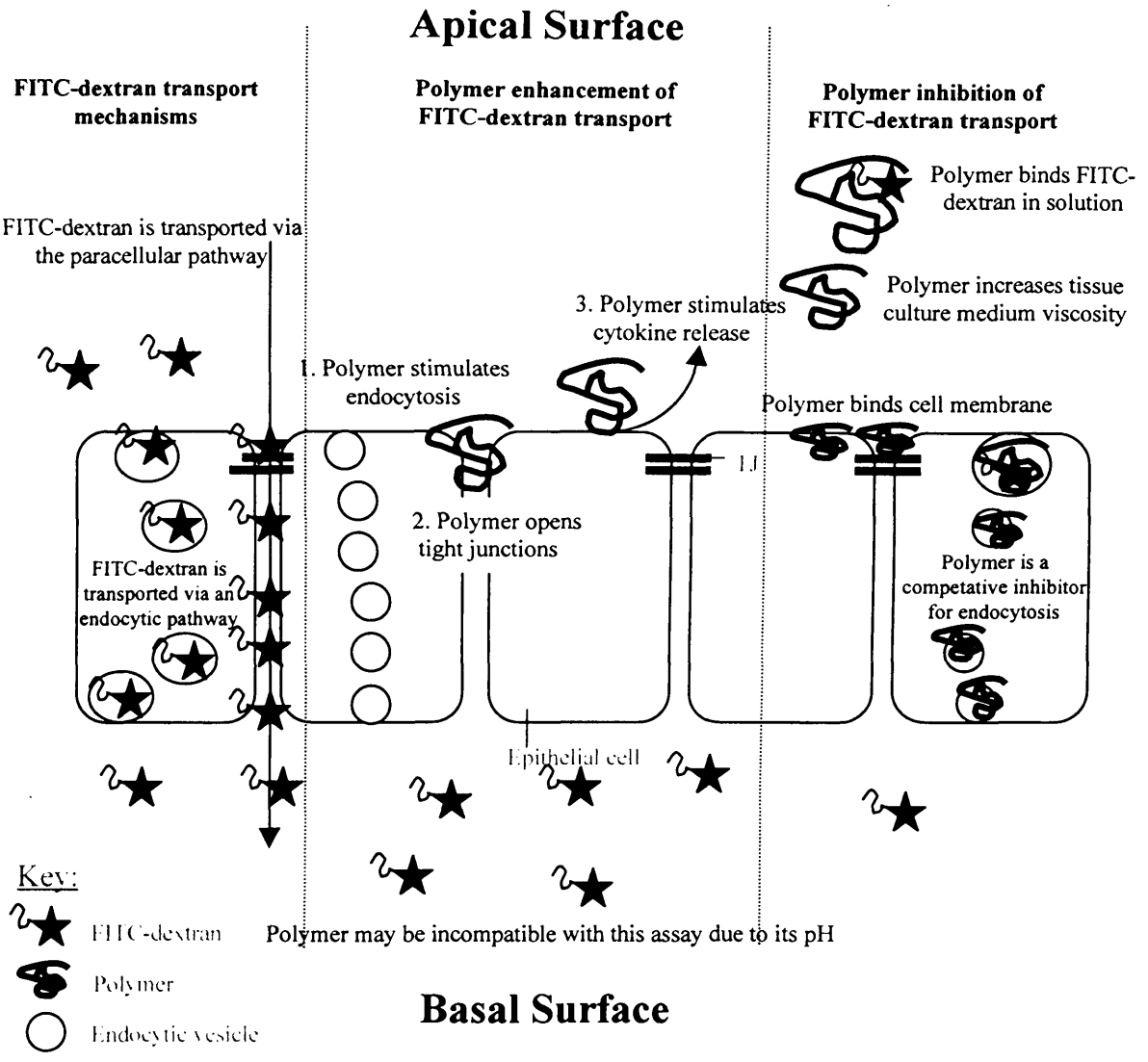

Figure 5.7 Schematic showing the possible effects of polymers on FITC-dextran transport across rat intestinal tissue.

the diffusion kinetics of FITC-dextran across the tissue by increasing the viscosity of the medium in the donor chambers of the vertical diffusion system.

Interestingly, the control transport (Papp) rates for FITC-dextran without the addition of polymer observed in these experiments were lower than those seen previously in Chapter 4. This is likely to be due to the fact that different animal batches were used. It is also probable that an improvement in the method used to remove the muscle layers from the mucosa, resulted in a more intact tissue, as with practice the time taken to prepare the tissue for the diffusion chamber was reduced.

Also in contrast to Chapter 4, the Ap→Bas transport of FITC-dextran across the tissue was not greater than the rate of Bas→Ap transport (Figure 5.2). Similarly however, the transport of FITC-dextran across Peyer's patch tissue was lower than across tissue without Peyer's patches.

When polymers were added to the vertical diffusion system, their effect on FITC-dextran transport was first investigated only in the Ap→Bas direction, and only in non-Peyer's patch tissue. The results obtained from these studies are summarised in Table 5.2. With the exception of HA (Figure 5.3b) and $sPAcA_{30}$ (Figure 5.3d) the other polymers (alginate, sHA, $PAcA_{100}$, $PAcA_{450}$, and PAMAM generation 3.5 dendrimers) appeared to decrease the transport of FITC-dextran (Figure 5.3a, c, e, f and g). As $sPAcA_{30}$ and HA were the only polymers that increased transport, they were selected for further studies to investigate their effect on FITC-dextran transport in both the Bas→Ap direction across non-Peyer's patch tissue, as well as in both (Ap→Bas and Bas→Ap) directions across tissue containing Peyer's patches. Although alginate did not enhance Ap→Bas FITC-dextran transfer, it was decided to use this polymer as a negative reference control.

Disappointingly however, in the further studies none of the polymers tested ($sPAcA_{30}$, HA, or alginate) enhanced the transport of FITC-dextran in any direction or tissue model (Figure 5.4, 5.5 and 5.6). Even though HA and $sPAcA_{30}$ did enhance transport in the Ap→Bas direction in non-Peyer's patch tissue, inhibition was seen in the Bas→Ap direction (see Table 5.2).

Possible mechanisms of polymer-induced effects

As described above, there are a number of factors to consider when interpreting

Table 5.2 Summary of the effect of polymers on FITC-dextran transport across rat intestinal tissue.

Polymer	**Non-Peyer's patch tissue**		**Peyer's patch tissue**	
	Ap→Bas	**Bas→Ap**	**Ap→Bas**	**Bas→Ap**
Alginate	↓	↓	↓	↓
HA	↑	↓	↓	↓
sHA	↓	ND	ND	ND
$PAcA_{30}$	↑	↓	↓	↓
$PAcA_{100}$	↓	ND	ND	ND
$PAcA_{450}$	unchanged	ND	ND	ND
PAMAM 3.5	↓	ND	ND	ND

ND -not determined

these results (see Figure 5.7). It was shown that several of the polymers caused changes in medium pH at the concentrations used (Table 5.2), and this could potentially influence the fluorescence output of FITC-dextran, as well as cell viability and TJ integrity. In respect of the potential mechanisms of action of the polymers (shown in Figure 5.7) it is interesting to compare these data with the literature.

Polymer-induced pH effects

Although, the MEM tissue culture medium used for this work contains Earle's salts and a high sodium bicarbonate buffer (2.2 g/L) to minimise pH fluctuations (Eagle, 1959), as seen previously in RPMI and DMEM culture media (containing 10 % FBS; see Table 3.2), $PAcA_{100}$, $PAcA_{450}$ and PAMAM generation 3.5 dendrimers were still able to alter the medium pH; in the range pH 6 – 8 (Table 5.2). As FITC is a pH-sensitive fluorophore, in theory this could affect the interpretation of the results observed. FITC-dextran exhibits a maximal fluorescence at pH 8 (supplier information; www.sigmaaldrich.com, accessed 12/03/2002), and as shown earlier (Figure 5.1), as the pH becomes more acidic fluorescence output decreases. This raises the question, could the apparent inhibitory affects seen for $PAcA_{100}$ $PAcA_{450}$ and PAMAM generation 3.5 in some experiments be an artefact?

Compared to FITC-dextran, which exhibits properties of an expandable coil in solution (Granath 1958), and is small enough to pass through TJ of the rat intestine, the large molecular mass of $PAcA_{100}$ and $PAcA_{450}$, means that they are unlikely to be transported across the tissue via the TJ pathway. However, the pH changes in the MEM tissue culture media caused by these and other dissolved polymers may have had an affect on the fluorescence output of FITC-dextran in the recipient chamber. In order to determine the extent of this effect, the pH of the MEM in the recipient chambers should have been measured at the end of each experiment. Unfortunately however, this important control was not measured at the time making it difficult to determine the effects of polymers on FITC-dextran transport.

However, as discussed previously (in section 5.1), PAMAM generation 3.5 dendrimers have been reported to decrease the TJ permeability in Caco-2 monolayers at non-toxic concentrations (El-Sayed *et al.*, 2003b), and to transverse rat everted intestinal sacs via an extremely efficient pathway; the EI value of which suggests that

polymer in the tissue culture medium would have had an effect in the recipient chamber. As the pH of PAMAM 3.5 in MEM was approximately pH 8 (Table 5.3), then the transport of FITC-dextran measured across the tissue could have been over-estimated.

Polymer cytotoxicity

It is also possible that the polymer effects observed for FITC-dextran transport could also be due to polymer-induced cytotoxicity. The transport of FITC-dextran across the rat intestinal tissue by endocytic pathways would be decreased if the energy supply were compromised. Conversely, a decrease in viability that leads to TJ opening/breakdown, would allow more FITC-dextran to pass the epithelial barrier. As it was previously shown that the IC_{50} values of these polymers were greater than 1 mg/mL during the 1 h incubation with B16F10 cells (see Chapter 3), it can be assumed that the polymers would not be cytotoxic in the system. Again, an important control here would have been to measure the pH of the medium in the recipient chambers.

TEER is usually used to measure the changes in the permeability of epithelial barriers, in conjunction with/or the transport of paracellular markers. However, as mentioned above TEER is reduced as tissue viability decreases. The permeation-enhancing effects of PAcAs described by Kast and Bernkop-Schnürch, (2002) and Kriwet and Kissel (1996) have solely been measured using the above methods. The cytotoxic effects of PAcA were not measured in these papers.

Possible transport mechanisms for $sPAcA_{30}$ and HA

It is interesting to consider why $sPAcA_{30}$ and HA had and effect on FITC-dextran transport only in the Ap→Bas direction across non-Peyer's patch tissue, particularly as P-gp is largely located on the apical membrane. The variability in transport observed when using this model has been previously described (in Chapter 4), though the experiments conducted here were more reproducible (possibly due to the reasons described above). The data shown are n = 6 ± SEM. Nevertheless, the transport of the control, FITC-dextran, did not show the same trend as seen in Chapter 4 (Figure 4.16). It is possible that the increases in the transport observed with $sPAcA_{30}$ and HA are an artefact, as the data are non-significantly different to the control.

It is also possible that enhanced transport seen with $sPAcA_{30}$ could be due to activation of the sodium-glucose transporter on the apical membrane of intestinal epithelial cells, caused by the presence of extra sodium ions in the tissue culture medium compared to the control (sodium enhances polymer solubility). When active, this transporter has been shown to increase TJ permeability due to the phosphorylation of myosin light chain kinase, and contraction of the perijunctional actinomycin ring (reviewed in Nusrat *et al.,* 2000). However, sHA did not have an effect on the TJ permeability. Therefore, the effect of sPAcA on FITC-dextran transport across rat intestinal tissue could be due to some other physiochemical properties.

The molecular weight, geometry and surface charge or pKa of polymer molecules are also features that govern whether they can physically permeabilise TJ. Clearly the effect of polymer molecular weight on FITC-dextran transport has been demonstrated in these studies with PAcA, though the results observed were in contrast with Kast and Burnkop-Schnurch, (2002), and the results observed with PAcA microparticles (MW = 300,000 Da) Krewet and Kissel (1996).

As it is not clear what effect the polymers are having on FITC-dextran transport from this work, and that none of the polymers significantly enhanced transport across the rat intestinal tissue, it was decided to move forward and to measure the transport of polymers themselves across the tissue.

CHAPTER 6:

Synthesis and Characterisation of $PAcA_{30}$-OG, and PAMAM 3.5-OG Conjugates, and Studies on their Transport Across Rat Intestinal Tissue, and Uptake by $Caco\text{-}2_{BBe}$ Cells

6.1 INTRODUCTION

The studies in Chapter 5 showed some evidence of increased Ap→Bas transport of FITC-dextran across rat intestinal tissue in the presence of HA and $sPAcA_{30}$, but unexpectedly, not in the presence of PAMAM generation 3.5 dendrimers. In fact in many experiments the polymers tested inhibited transport. It was therefore considered important to try and monitor the transport of the polymers themselves across the rat intestinal tissue, instead of simply looking at their effect on a paracellular marker. Though to do this, it was first necessary to label $sPAcA_{30}$ and PAMAM generation 3.5 dendrimers with a fluorescent dye, and Oregon green (OG) was chosen as the fluorophore. The rationale for methods used to synthesise, purify and characterise polymer-OG conjugates are given below.

Rationale for the choice of fluorescent dye

Many fluorescent dyes are available for conjugation (a list can be seen on the Molecular Probes website: http://probes.invitrogen.com/handbook/tables/0726.html (accessed 23/6/2006)), but few have the functionality to react with the carboxylic acid groups on the chosen polymers, to form amide bonds. These dyes typically have amine groups and include BODIPY FL, the dialkylamino-, hydroxyl- and methoxy-coumarins, fluoresein, Oregon green-cadaverine (OG_{cad}) and rhodamine. The OG fluorophore was preferred for this work, as it has previously been used to label polymers such as PEI (MW = 25,000 Da), and PAMAM generation 2, 3 and 4 dendrimers (Seib *et al.*, 2006), PEG-dendrons (Xyloyiannis *et al.*, 2003; Berna *et al.*, 2006), polymethacrylates (Dubruel *et al.*, 2004), and HPMA copolymers (Jensen *et al.*, 2001). Conjugation to this fluorophore has then enabled the intracellular trafficking of these polymers to be studied, using both confocal scanning laser microscopy and flow cytometry techniques. Moreover, OG was considered a better fluorophore than fluorescein, as fluorescein is pH-sensitive (see Chapter 5, Figure 5.1), and has a high rate of photobleaching (Haugland, 2002). Being a fluorinated analogue of fluorescein, OG (developed by Molecular Probes), has matching absorption (494 nm) and emission (520 nm) spectra, but it is more pH- and photo-stable (Haugland, 2002). Though many forms of OG are commercially available, OG_{cad} was chosen for these studies, as cadaverine posseses the primary reactive amine group.

Rationale for the choice of conjugation chemistry

In order to label the polymers with OG_{cad}, the carbodiimide coupling reagent, 1-ethyl-3(3-dimethylaminopropyl) carbodiimide hydrochloride (EDC) was used. EDC mediates the formation of stable amide bonds between the polymer carboxylate groups and the amine group on OG_{cad}, by modifying the carboxylic acid groups into active ester groups. The reactive esters then bind OG_{cad} by aminolysis (reviewed in Hermanson, 1996).

Several carbodiimides such as DIC; Woodward's reagent K; N,N'-carbonyldiimidazole; dicyclohexy carodiimide (DCC); cyclohexyl -3-(2-morpholinoethyl) carbodiimide (CMC); and EDC, and are commercially available, for conjugation, though few are soluble in water. Fortunately, CMC, DCC and EDC, are water soluble, and can therefore be directly added to a reaction without prior dissolution in organic solvent. Each of these reagents works in a similar fashion, though the reactive complexes formed by these molecules can be subject to hydrolysis (Hoare and Koshland, 1967; reviewed in Hermanson, 1996). Consequently, if the target amine does not find the active carboxylate before it hydrolyses, the desired coupling cannot occur.

To increase the stability of the active intermediate *N*-hydroxysulphosuccinimide (sulpho-NHS) can be used. Sulpho-NHS esters are soluble in water and in the presence of amine nucleophiles, which can attack at the carbonyl group of the ester, the N-hydroxysulfo-succinimide group rapidly leaves, creating a stable amide linkage with the amine (reviewed in Hermanson, 1996). The concentration of sulfo-NHS used in a reaction is normally much greater than the concentration of the target molecule, so the reaction preferentially can proceed through a longer-lived intermediate.

The EDC/sulfo-NHS reaction was preferred for this study, as the use of these reagents for polymer-OG_{cad} conjugation has been well characterised (Jenson *et al.*, 2001; Berna *et al.*, 2006; Izzo, 2005). A schematic representation of this reaction is given in Figure 6.1. Unlike EDC, DCC is normally used as a coupling agent for organic (particularly peptide) synthesis in organic solvent (Delmonte *et al.*, 1999), and not to perform biomolecular conjugations. It also has the disadvantage of being a waxy solid that is difficult to remove from a bottle (reviewed in Hermanson, 1996). CMC is not normally used for polymer conjugation purposes, and has been shown to

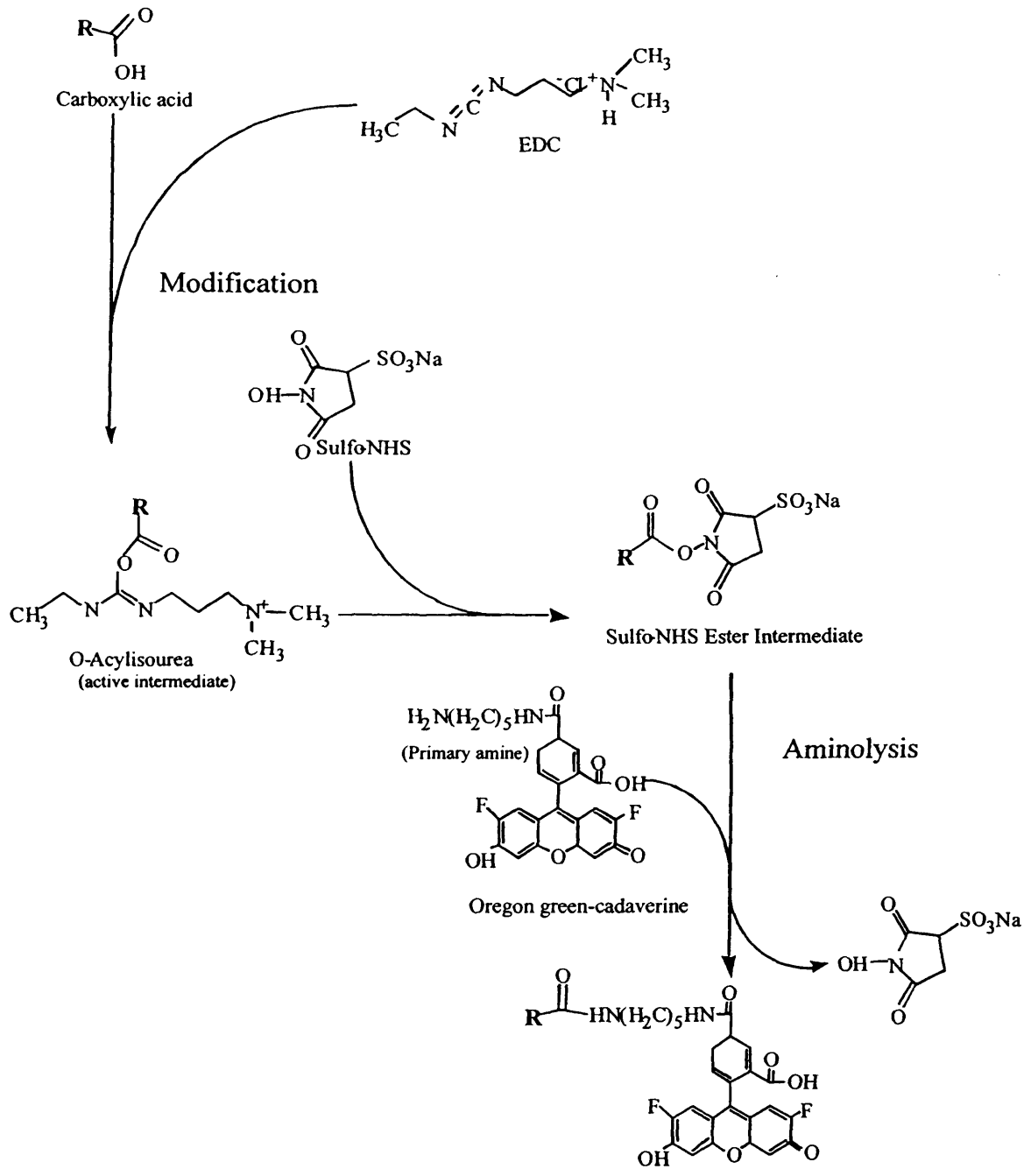

Figure 6.1 Reaction scheme for polymer (R) conjugation to OG_{cad} using EDC and Sulfo-NHS coupling reagents

Reaction scheme adapted from Hermanson, (1996)

react with phenols, alcohols, and other nucleophils to quench coupling reactions (reviewed in Hermanson, 1996).

Optimising the reaction conditions and characterisation

It was important to optimise OG_{cad}-polymer conjugation, and silica-based thin layer chromatography (TLC) was used to monitor the reaction over time. Although many protocols seem to assume that all the probe will be bound, it is essential to purify the product well, and to calculate the bound and free OG_{cad}. Dialysis was first used for purification, and then a commercially available PD-10 desalting column was used to characterise the product. The large polymer-OG_{cad} molecules elute first from the column (in the void volume), and the smaller OG_{cad} molecules elute later (for the theory of GPC see Chapter 2, section 2.3.8). The eluted fractions can then be analysed using fluorescence.

Though conjugates could be purified using PD-10 chromatography, dialysis was preferred, as it can be used more easily to purify larger volumes of conjugate from reaction mixtures. Moreover, as the reagents and the isourea by-products from the conjugation reaction were all water-soluble, they could be easily removed by this method.

Once purified all products were finally lyophilised (a process also known as freeze-drying). This method is useful for drying materials that are sensitive to heat, or have unstable structures (reviewed in Tang *et al.*, 2004). The primary mechanism for lyophilisation is sublimination, whereby ice is directly converted into water vapour, without passing through the intermediary stage of a liquid (reviewed by Franks, 1997). This is achieved via a vacuum, which lowers pressure to around 1 milibar (as opposed to atmospheric pressure, of 1017 milibars), causing water molecules to be drawn out of the sample into a condenser that converts the moisture into liquid and drains it away.

Ultraviolet-visible (UV-Vis) spectroscopy was used to determine the total OG content in each product, using the Beer-Lambert law equation (see equation 1, section 6.2.4), to find the molar absorption coefficient (ε) of OG_{cad}. This value is the absorbance of a molar concentration of OG_{cad} with a 1 cm path-length, at a 494 nm (the excitation wavelength of OG_{cad}). PD-10 column chromatography was then used

to calculate the free OG content in each sample, and fluorescence spectroscopy was used to determine the concentration-dependence of the fluorescence yield.

Assessing polymer transport and polymer uptake

To monitor the transport of OG-labelled polymers across the rat intestinal tissue (with or without Peyer's patches), the vertical diffusion chamber was used (Chapters 4 and 5).

In parallel, the uptake of the polymers into cells (thus to give an idea if they were being taken up by endocytosis), was determined using flow cytometry and Caco-2_{BBe} cells were chosen as a model. Caco-2_{BBe} cells differ from standard Caco-2 cells, as they are a brush-border expressing ($_{BBe}$) phenotype (Peterson and Mooseker, 1992). However, it takes several weeks in culture for these cells to fully differentiate, and in order to polarise, they need to be grown as a monolayer on filters. For flow cytometry experiments however, Caco-2_{BBe} cells were grown in 6-well plates for 2 d, and thus would not be a fully mature Caco-2_{BBe} phenotype.

In summary the specific aims of this chapter were to:

(i) Synthesise and characterise $PAcA_{30}$-OG and PAMAM 3.5-OG conjugates.
(ii) Study the transport of the conjugated polymers across intestinal tissue in the vertical diffusion chamber.
(iii) Study the uptake of the polymers by the Caco-2_{BBe} cells to see if there was any evidence of endoytic capture.

6.2 METHODS

6.2.1 Conjugation of Oregon green-cadaverine to polymers

Synthesis of $sPAcA_{30}$-OG_{cad}

$sPAcA_{30}$ (supplied as 40 % weight in H_2O) was weighed (439 mg) into a foil-wrapped, round-bottomed glass flask containing a magnetic flea, and ddH_2O (2 mL) was added. The flask stoppered, and the solution was stirred to mix the polymer. EDC (366.5 mg) and sulfo-NHS (415.0 mg) were added as a solid to a give 1 molar equivalent of each reagent. The reaction was stirred for a few moments (~ 10 sec), before 1.91×10^{-5} moles of OG_{cad} were added. This was estimated to label 1 % of the polymer. The solution was left to stir for 3 h at room temperature, and the reaction

was monitored on an hourly basis using TLC as described below (section 6.2.2).

Synthesis of PAMAM 3.5-OG

PAMAM generation 3.5 dendrimers (supplied as 10 % weight in methanol) were weighed (2.2 g) into a glass flask (covered with foil), and a stream of nitrogen was used to evaporate the methanol from the polymer. Double distilled water (3 mL) was then added and the solution was stirred using a magnetic flea. PAMAM generation 3.5 dendrimers have 64 terminal -COOH groups, so enough EDC (6.7 mg) and sulfo-NHS (7.6 mg) was added to activate each group. The amount of OG_{cad} added (1 μL of 5 mg/mL OG_{cad} in ddH_2O) was calculated to give a ratio of 1 OG_{cad} per dendrimer. Once EDC, sulfo-NHS and OG_{cad} had been added, the reaction was left to stir for 22 h at room temperature, and TLC was again used to monitor OG-conjugation (see section 6.2.2)

6.2.2 TLC method

Silica-covered TLC plates (with fluorescent indicator: UV_{254}) approximately 4 x 6 cm in size were used, and samples were applied at the origin using a capillary tube. Free OG_{cad} (5 mg/mL in ddH_2O) was used as a control, and samples of reaction mixture were spotted onto the plate and dried using a hair drier on a cool setting. The plates were placed into a small 250 mL glass beaker, containing ~15 mL of methanol, used as the running phase. The beaker was then covered and the TLC ran for approximately 5 min, or until the solvent had travelled 3/4 the way up the plate. The plates were then removed, and the solvent front marked. Again a hair dryer was used to dry the plates, before they were viewed under a UV-lamp. The fluorescent spots (i.e. free and bound OG) were noted. Polymer-bound OG begins to appear at the origin and the reaction times were optimised to give minimum free OG_{cad}. At the end of each reaction, polymers were purified by dialysis as described below.

6.2.3 Purification and lyophilisation of polymer-OG conjugates

Dialysis

The polymer-OG reaction mixture was placed into a dialysis tube (membrane molecular weight cut-off = 2,000 Da), which was sealed at both ends using dialysis clips. This was then placed into a 5 L conical flask containing of ddH_2O (5 L), and was protected from light with a bin liner. The flask was placed on a magnetic stirrer,

and a magnetic bead was used to stir the water and slowly rotate the bag. The water was changed from the flask a total of seven times over two days.

PD-10 column chromatography

Each column was equilibrated with 10 mLs of PBS before use. Samples (0.5 mL containing 25 μL of reaction mixture in PBS) were then added to the columns, and were eluted with 0.5 mL fractions of PBS. Each eluted fraction (0.5 mL) was collected into eppendorf tubes, and 200 μL of each was pipetted into black 96-well plates. All plates were then read in the fluorescence plate reader as previously described (Chapter 2, section 2.3.6).

Lyophilisation

The dialysed polymer conjugates were placed into foil-wrapped plastic tubes, and were snap-frozen using liquid nitrogen (-196 °C) at atmospheric pressure. This is important to prevent shrinkage of the sample during the lyophilisation process. Tongs were used to remove samples from the liquid nitrogen, and the lids of the tubes were quickly removed and replaced with tin foil (secured with tape), that was pierced several times with a needle. Samples were then placed into the lyophilisor, and were dehydrated for 48 h.

Once lyophilised, the OG-labelled polymers were then placed into labelled, foil-wrapped plastic containers, sealed with parafilm, and kept in the freezer until use.

6.2.4 Characterisation of polymer-OG conjugates

Using UV/Vis spectroscopy to determine total OG content

First, to check the molar extinction coefficient of OG_{cad}, 1 mg was weighed into plastic bijous (covered with foil), and was dissolved in 1 mL PBS (pH 7.4). This solution was then diluted with PBS to a concentration of 2.0×10^{-7} moles/L. It was then pipetted (1 mL) into 1 cm^3 quartz cuvette, and read spectrophotometrically at 494 nm, against a reference cuvette containing only PBS (1 mL).

To estimate the OG content of each polymer-OG conjugate, the lyophilised conjugates were first weighed (1 mg) into plastic bijous (covered with foil), and were dissolved in 1 mL with PBS (pH 7.4). These solutions were also read spectrophotometrically at 494 nm against PBS. Assuming that the extinction of

OG_{cad} is the same as polymer bound-OG, the total OG content was calculated as follows:

(1) $[OG] = A/\varepsilon$

Where [OG] is the concentration of OG in moles/L, A is the absorbance of the sample at 494 nm, and ε is molar absorption coefficient of OG in moles/L.

The weight % of OG in each polymer-OG conjugate was calculated by first converting [OG] into an mg/mL value ([OG] x OG_{cad} MW (496.47 Da)). The following equation was then used:

(2) OG/P x 100 = total polymer-bound OG (weight %)

Where OG is the concentration of OG in mg/mL, and P is the mg/mL concentration of the polymer dissolved in PBS.

6.2.5 Analysis of polymer-OG_{cad} transport across rat intestinal tissue using the vertical diffusion system

Rat intestinal tissue was prepared, and the vertical diffusion system was set up as described in Chapter 2, section 2.3.6. MEM was removed from both the donor and recipient chambers of each diffusion cell, and was immediately refilled with fresh, pre-warmed (37 °C) MEM (1.5 mL), or MEM containing polymer ($PAcA_{30}$-OG or PAMAM 3.5-OG) conjugates (1 mg/mL). Samples of media (25 μL) were collected from the recipient chambers at 10 min intervals, from t = 0 - 60 min, and were placed into black 96-well plates (covered with foil). All plates were read in the fluorescence plate reader as previously described (chapter 2, section 2.3.6).

6.2.6 Flow cytometry analysis of polymer-OG uptake by Caco-2_{BBe} cells

For flow cytometry experiments, Caco-2_{BBe} cells were incubated with $PAcA_{30}$-OG or PAMAM 3.5-OG (1 mg/mL in HBSS), for 10 min intervals (from 0 – 60 min), at either 37- or 4 °C.

In experiments conducted at 37 °C, Caco-2_{BBe} cells were seeded into 24-well plates (2.5 x 10^5 cells/500 μL/well), with DMEM containing 4500 mg/L glucose and

phenol red (see table 2.1). All experiments were carried out in duplicate (two wells/time point). Seeded plates were placed into the incubator, and were allowed to grow for 48 h. Following this, the plates were removed from the incubator, and the media was quickly aspirated from the t = 60 min wells. The wells were washed once with pre-warmed (37 °C) PBS (pH 7.4), to remove dead cells and DMEM media. HBSS media (0.5 mL) containing either PAMAM 3.5-OG, or $PAcA_{30}$-OG conjugates (1 mg/mL) was then added, and the plates were returned to the incubator. At 10 min intervals the process was repeated for t = 50 min, 40 min etc, until the end of the incubation at t = 0 min.

For experiments carried out at 4 °C, the procedure was essentially the same. Each plate (seeded with two wells/time point) was placed on ice 30 min prior to the addition of HBSS (0.5 mL) containing polymer-OG conjugates (1 mg/mL). Plates were kept on ice in the cold room (4 °C) throughout the experiment.

Samples of cells were treated the same irrespective of incubation temperature (37 °C and 4 °C). The plates containing cells were immediately placed on ice, and transferred to the cold room (37 °C). The incubation medium was removed from the cells, and they were washed 3 times using ice-cold PBS (1 mL/well). Caco-2_{BBe} cells were then removed from the wells, using a rubber cell scraper, and were pipetted into labelled, foil-wrapped, 25 mL centrifudge tubes. All tubes were kept on ice until they were transferred to the chilled (4 °C) centrifuge. They were spun at 1000 g for 5 min, and the pellets were resuspended in 200 μL of ice-cold PBS. To break up aggregates of cells, a 1 mL syringe with a 23 G needle was used. Then the cell suspensions were placed into labelled Falcon tubes, kept on ice and protected from light until assay by flow cytometry.

During flow cytometry, the cell-associated fluorescence of each sample was measured for a minimum number of counts (40,000 cells) and the data were expressed as the geometric mean of each sample compared to the gated control cells (Caco-2_{BBe} in HBSS only). The experiments were carried out in triplicate, and the data are plotted as incubation time (min) against fluorescence.

6.3 RESULTS

6.3.1 Synthesis and characterisation of polymer-OG conjugates

For $PAcA_{30}$, TLC showed that the majority of OG_{cad} had bound to the polymer after 3 h (Figure 6.2). However, for PAMAM 3.5, OG conjugation was much slower, and the optimised conjugation time was 22 h (Figure 6.4). In both cases, PD-10 analysis confirmed that $PAcA_{30}$- (Figure 6.3) and PAMAM 3.5- (Figure 6.5) OG conjugates had been fluorescently labelled as florescence was seen with the polymer in the void volume. The free OG_{cad} still present in the reaction mixture was eluted later (Figure 6.3a and Figure 6.5a). PD-10 analysis performed after dialysis showed that all free OG_{cad} had been removed from the $PAcA_{30}$-OG (Figure 6.3b) and PAMAM 3.5-OG (Figure 6.5b) conjugates.

Using the molar extinction coefficient estimated for OG_{cad} (41,500 moles/L), the total OG content of the $PAcA_{30}$-OG and PAMAM 35-OG conjugates was calculated using the UV/Vis spectra of each polymer (Figure 6.6a and 6.6b respectively). The molar OG content of each conjugate, as well as the % free OG present, were calculated and the results are shown in Table 6.1.

The fluorescence spectrum of $PAcA_{30}$-OG (Figure 6.7a) and PAMAM 3.5-OG (Figure 6.7b) (1 mg/mL), showed the difference in the fluorescence-loading of each polymer. At 494 nm, the fluorescence intensity of $PAcA_{30}$-OG was 0.30 arbitrary units, compared to 0.17 arbitrary units for PAMAM 3.5-OG.

Using the data shown in Table 6.1, the mg/mL concentration of PAMAM 3.5-OG required, to give an equivalent amount of OG as in 1 mg/mL of $PAcA_{30}$-OG. Therefore, for every 1.00 mg/mL of $PAcA_{30}$-OG used, a concentration of 2.06 mg/mL of PAMAM 3.5-OG was required to give a comparable amount of fluorescence. These concentrations were used for vertical diffusion work.

6.3.2 Polymer-OG transport across rat intestinal tissue in the vertical diffusion system

$PAcA_{30}$-OG transport across tissue without Peyer's patches

When $PAcA_{30}$-OG transport was measured across rat intestinal tissue without Peycr's patches, a 5 min lag phase in both Ap→Bas and Bas→Ap transfer was seen (Figure 6.8a), followed by a linear increase with time. Interestingly, the transport of

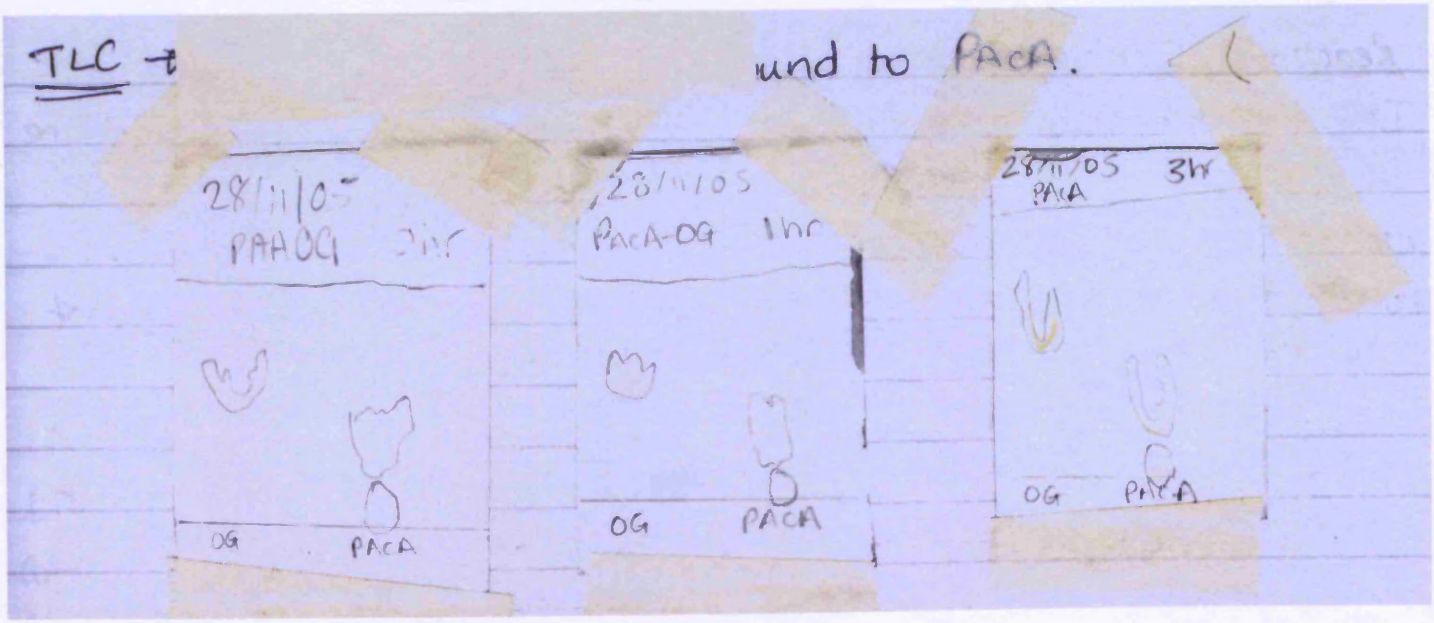

Figure 6.2 TLC plates used to monitor the conjugation of $sPAcA_{30}$ to OG_{cad}

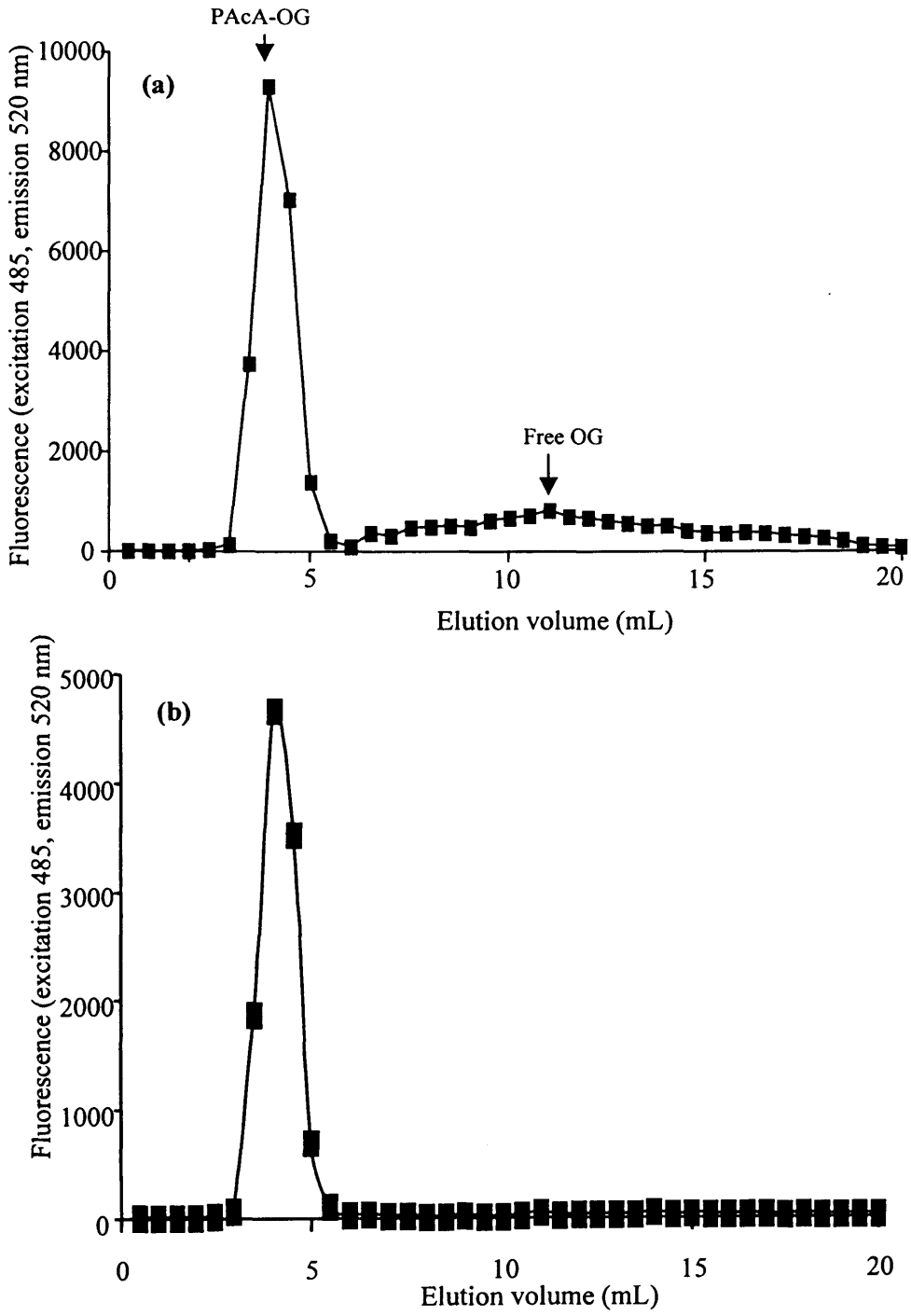

Figure 6.3 (a & b) PD-10 column chromatography elution profile of $PAcA_{30}$-OG before (panel a) and after (panel b) purification by dialysis.

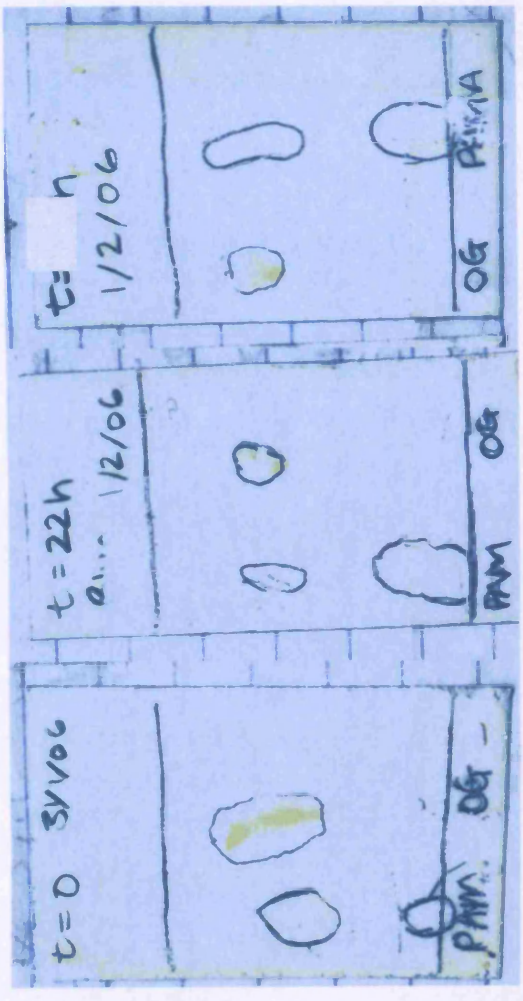

Figure 6.4 TLC used to monitor the conjugation of PAMAM 3.5 to OG_{cad}

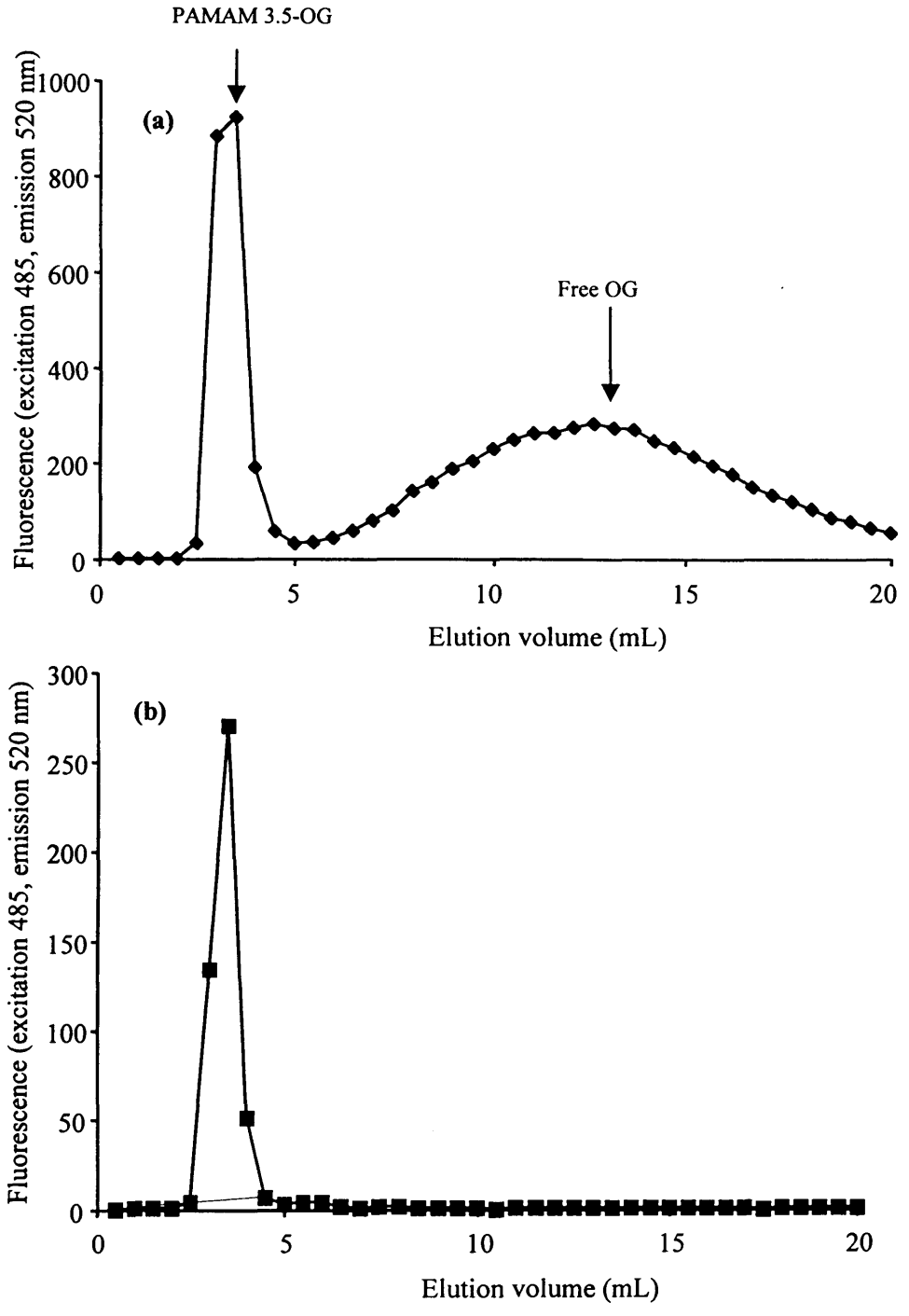

Figure 6.5 PD-10 column chromatography elution profile of PAMAM 3.5-OG before (panel a) and after (panel b) purification by dialysis.

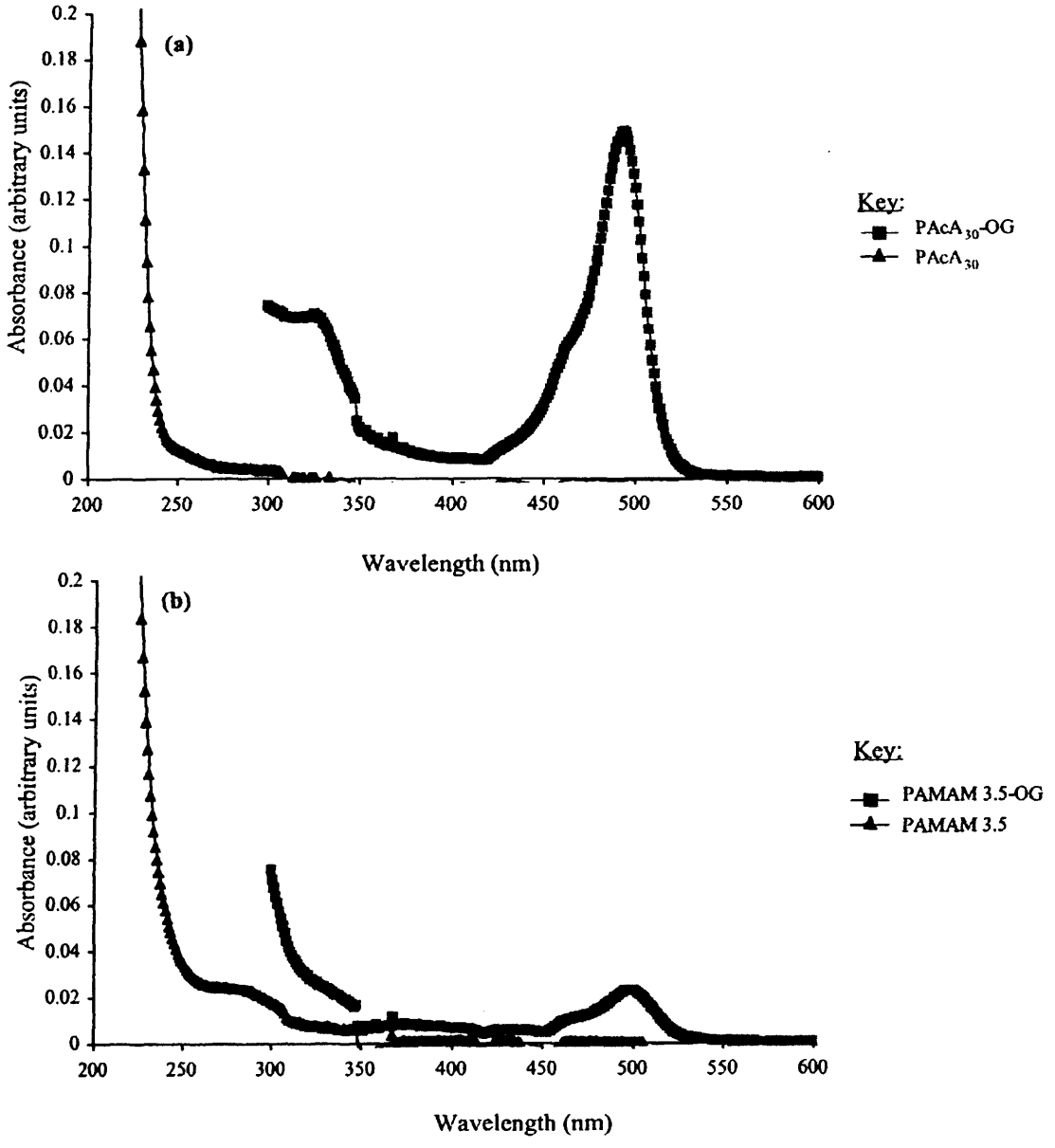

Figure 6.6 (a & b) UV/Vis spectrum for $PAcA_{30}$-OG (0.5 mg/mL; panel a) and PAMAM 3.5-OG (1 mg/mL; panel b). The absorbance of unconjugated $sPAcA_{30}$ and PAMAM 3.5 were also measured for comparison. The data shown are n = 1.

Table 6.1 Characteristics of polymer-OG conjugates.

Conjugate	Polymer MW (g/mol)	Batch name	Batch size (mg)	Total OG (wt %)	Molar Ratio
$PAcA_{30}$-OG	30,000	kpog9	102.0	0.16	10.2
PAMAM 3.5-OG	12,931	kppam5	60.0	0.02	0.007

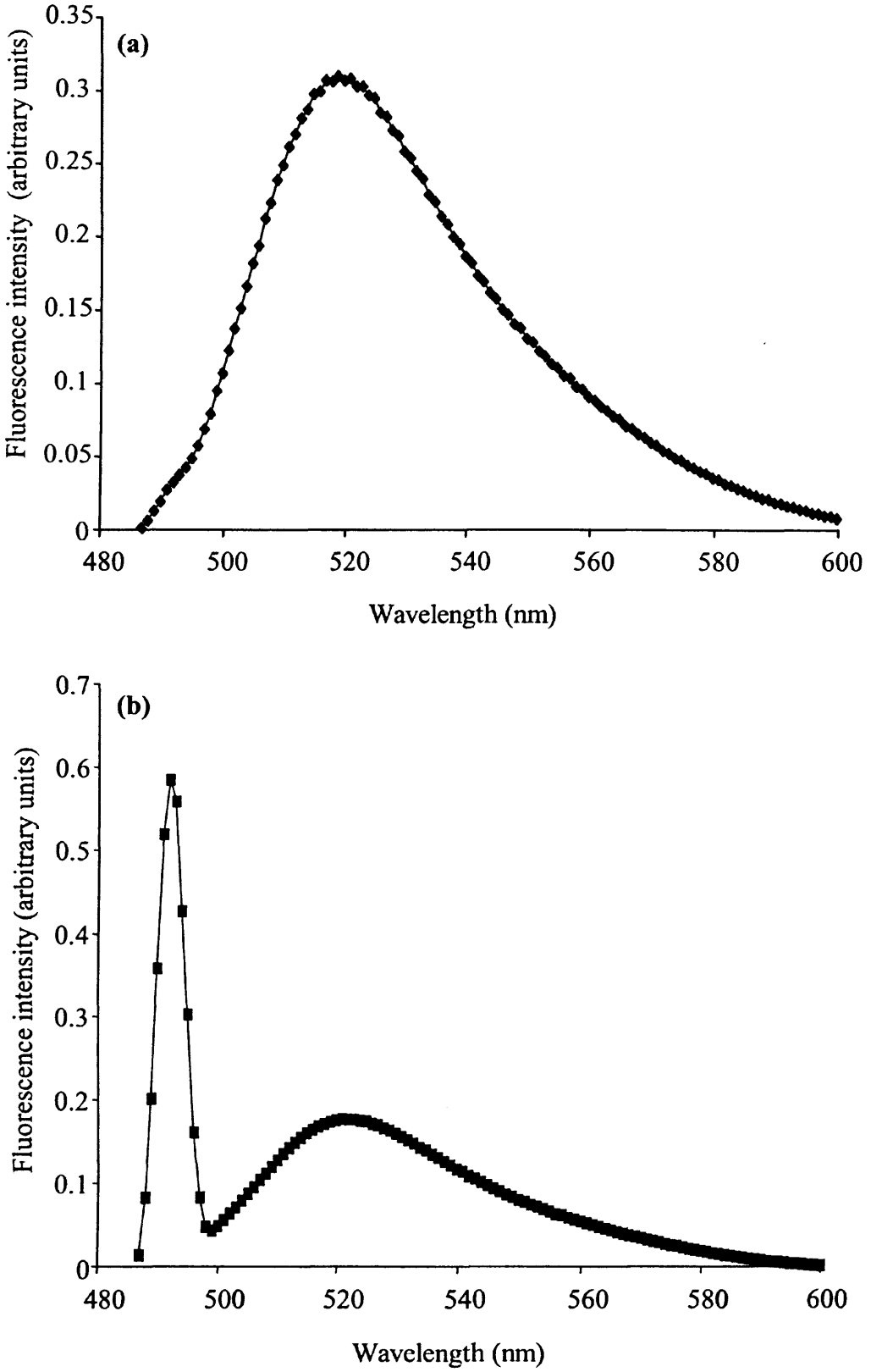

Figure 6.7 (a & b) Fluorescence spectrums of $PAcA_{30}$-OG (panel a) and PAMAM-OG (panel b). The concentration of each polymer-OG conjugate was 1 mg/mL in PBS.

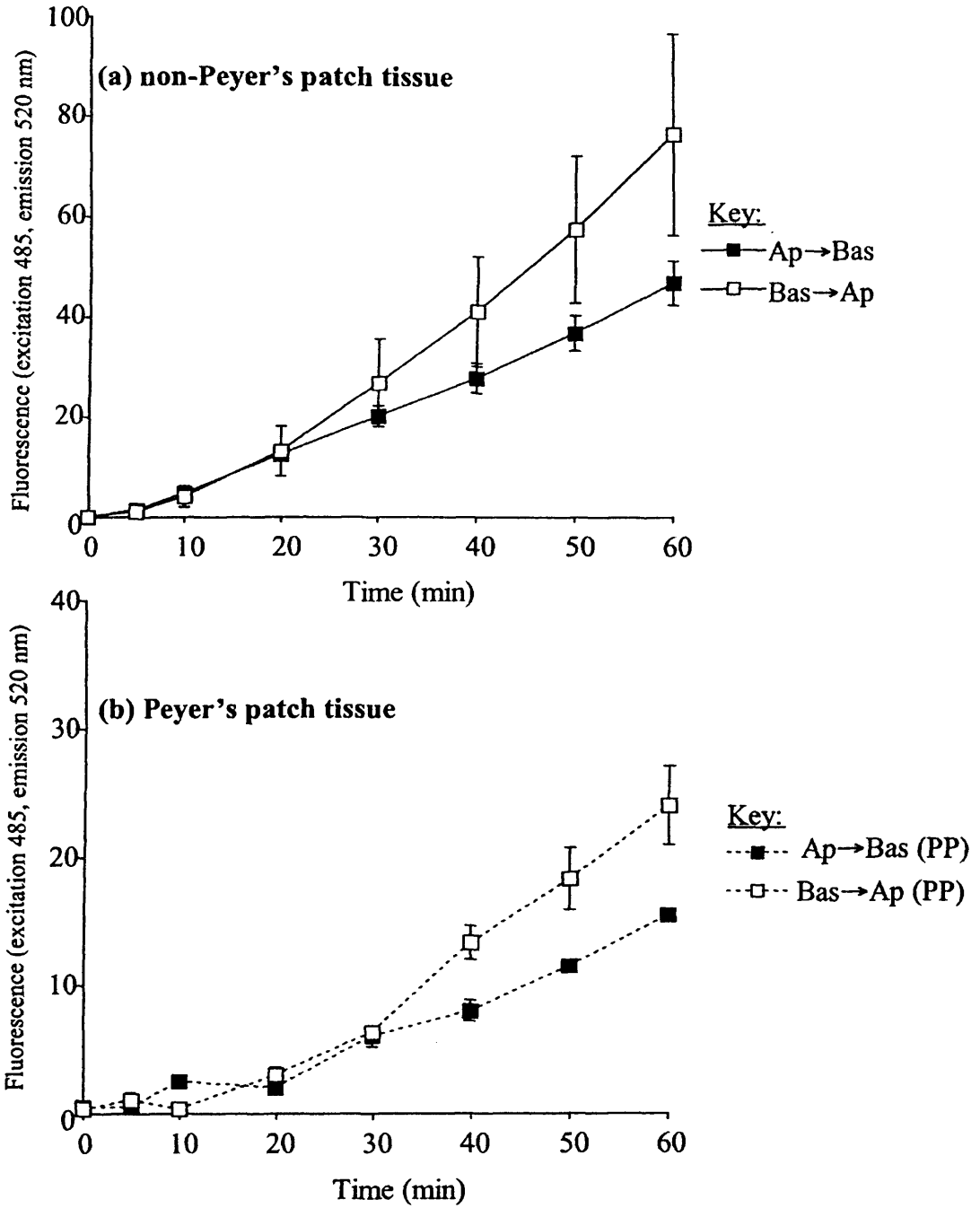

Figure 6.8 (a & b) Transport of $PAcA_{30}$-OG conjugates (1.00 mg/mL) across rat intestinal tissue (panel a), or rat intestinal tissue containing Peyer's patches (panel b). The data shown are n = 4 ± SEM.

the polymer in both directions was then over-lapping until t = 20 min, at which a greater rate of Bas→Ap transport was seen. At t = 60 min, the Bas→Ap transport of $PAcA_{30}$-OG was 63 % greater than transported in the Ap→Bas direction.

$PAcA_{30}$-OG transport across Peyer's patch tissue

The Ap→Bas and Bas→Ap transport of $PAcA_{30}$-OG_{cad} across rat intestinal tissue with Peyer's patches (Figure 6.8b) was lower than that seen across non-Peyer's patch tissue (Figure 6.8a). A 20 min lag phase in $PAcA_{30}$-OG_{cad} transport was seen for transport in both directions across this tissue, and the rate of transport remained parallel until t = 30 min. From t = 30 – 60 min, $PAcA_{30}$-OG transport was greater in the Bas→Ap direction.

PAMAM 3.5-OG transport across tissue without Peyer's patches

Although the concentration of PAMAM 3.5-OG (mg/mL) required to give an equivalent amount OG as in 1 mg/mL of the $PAcA_{30}$-OG conjugate was calculated, the fluorescence output of PAMAM 3.5-OG seen in the vertical diffusion system was relatively lower. Nevertheless, the transport of the polymer across tissue without Peyer's patches increased with time, but to a lesser extent than $PAcA_{30}$-OG. Transport was also greater in the Bas→Ap direction (Figure 6.9a). A ten min lag-phase in transport was seen for Ap→Bas transfer, whilst Bas→Ap transport occurred in a stepwise fashion.

PAMAM 3.5-OG transport across Peyer's patch tissue

No difference in the Ap→Bas or Bas→Ap transport of PAMAM 3.5-OG was seen across tissue containing Peyer's patches (Figure 6.9b). Instead, transport in both directions was overlapping. At t = 60 min Bas→Ap transport was marginally greater than Ap→Bas.

Stability of OG-conjugates during incubation in the vertical diffusion chamber

Small amounts of free OG (6 %) were found in the $PAcA_{30}$-OG stock solution (1 mg/mL) at t = 0 min (Figure 6.10a). Only a 1 % increase in the level of free OG, compared to the stock solution, was found in the donor chamber of the vertical diffusion system at the end of the incubation (t = 60 min) (Figure 6.10b). Highest

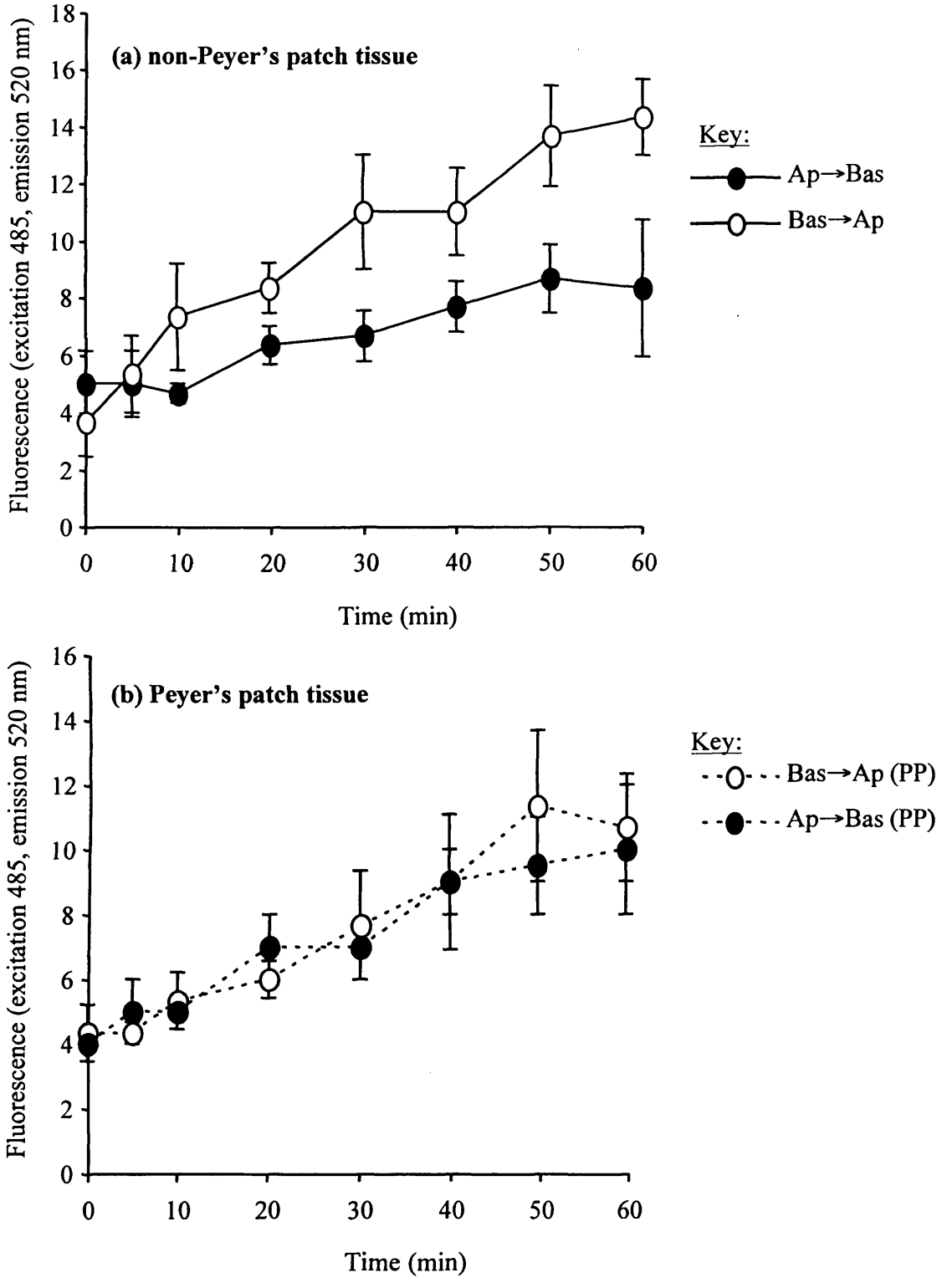

Figure 6.9 (a, b & c) Transport of PAMAM 3.5-OG conjugates (2.06 mg/mL) across rat intestinal tissue (panel a), or rat intestinal tissue containing Peyer's patches (panel b). The data shown are n = 4 ± SEM.

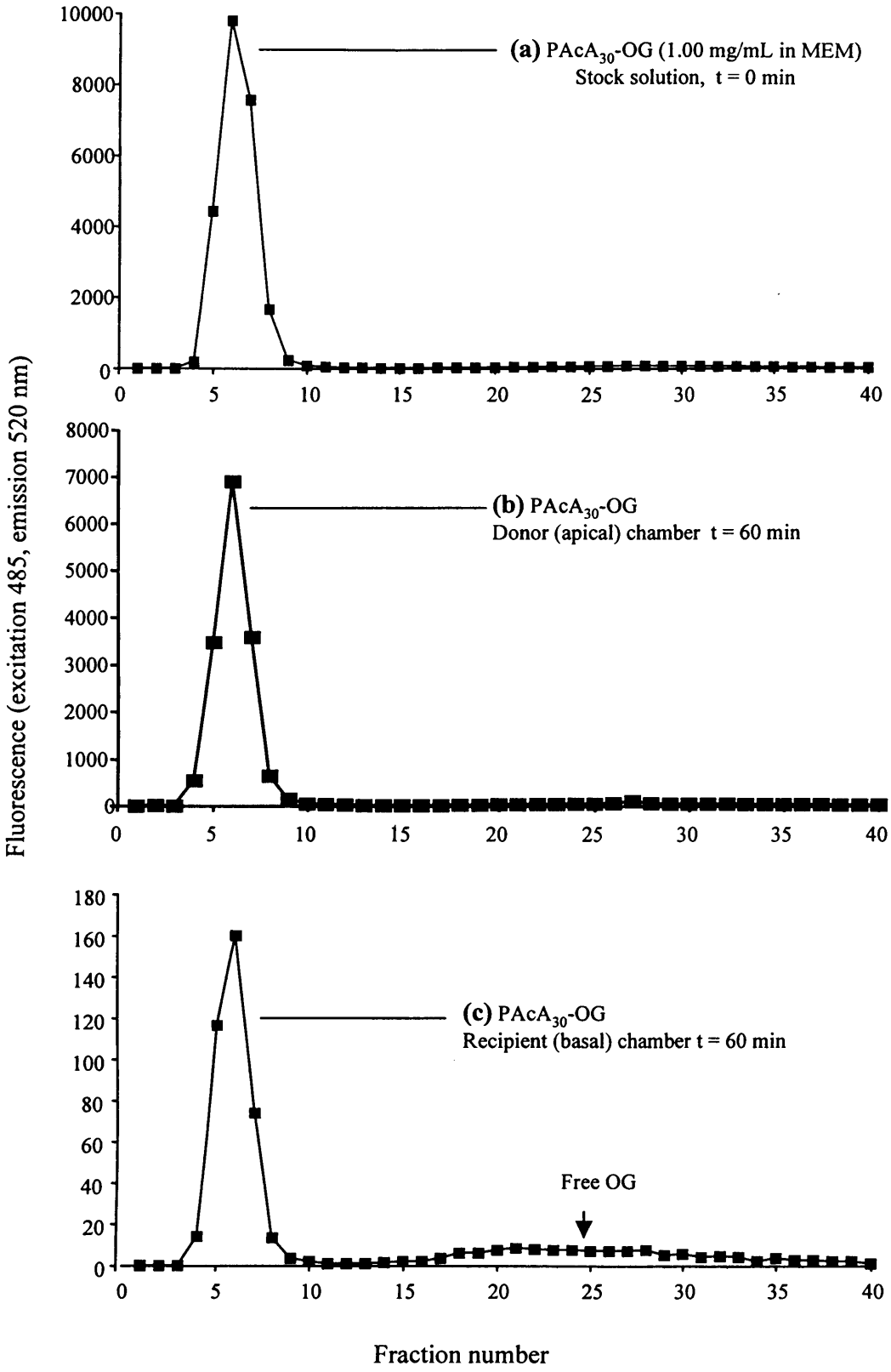

Figure 6.10 (a, b & c) PD-10 column chromatography elution profiles for PAcA30-OG stock solution at t = 0 min (panel a), or from the donor chamber (panel b) or recipient chamber (panel c) at t = 60 min.

amounts of free OG (26 %) were seen in the recipient chamber at t = 60 min (Figure 6.10c).

For PAMAM 3.5-OG conjugates, the fluorescence-output of the stock solution was lower than seen for $PAcA_{30}$-OG (Figure 6.11a). A small amount of free OG was found in the stock solution at t = 0 min (7 %), as well as in the donor chamber at 60 min (8 %) (Figure 6.11b). Over half the fluorescence found in the donor chamber at t = 60 min was due to free OG (56 %) (Figure 6.11c).

It is important to note, that during storage, the PAMAM 3.5-OG conjugates appeared to take up water, and adhered to the plastic container in which they were held. They were therefore not used for flow cytometry studies.

6.3.3 $PAcA_{30}$-OG_{cad} uptake by Caco-2_{BBe} cells

The up-take of $PAcA_{30}$-OG (1 mg/mL in HBSS) into Caco-2_{BBe} cells increased with time (t = 0 - 60 min), though the increase in cell-associated fluorescence was not linear (Figure 6.12a). Only marginally lower levels of cell-associated fluorescence were seen for cells incubated with $PAcA_{30}$-OG at 4 °C.

In some experiments it was decided to measure the uptake of FITC-dextran as this polymer had been used for transport studies in previous chapters (see Chapters 4 and 5). For cells incubated with this polymer, a general increase in cell-associated fluorescence was seen at both 37 °C and at 4 °C, over time. There was little difference in cell associated fluorescence at these two temperatures.

6.4 DISCUSSION

To measure the transport of $sPAcA_{30}$, and PAMAM generation 3.5 dendrimers across rat intestinal tissue, as well as to track the uptake of these molecules by Caco-2_{BBe} cells, each polymer was fluorescently labelled with OG_{cad} using EDC/sulfo-NHS coupling reactions. For PAMAM generation 3.5 dendrimers, the conjugation reaction was carried out as described by Izzo (2004), though there currently appears to be no data on the conjugation of OG_{cad} to PAcA in the literature. All the same, (see Figure 6.1) the reactions for both polymers were optimised. Calculations were made to give a 1.0 mole % OG-loading for $PAcA_{30}$, and a 1.5 mole % OG-loading for PAMAM generation 3.5 dendrimers (one OG unit per dendrimer).

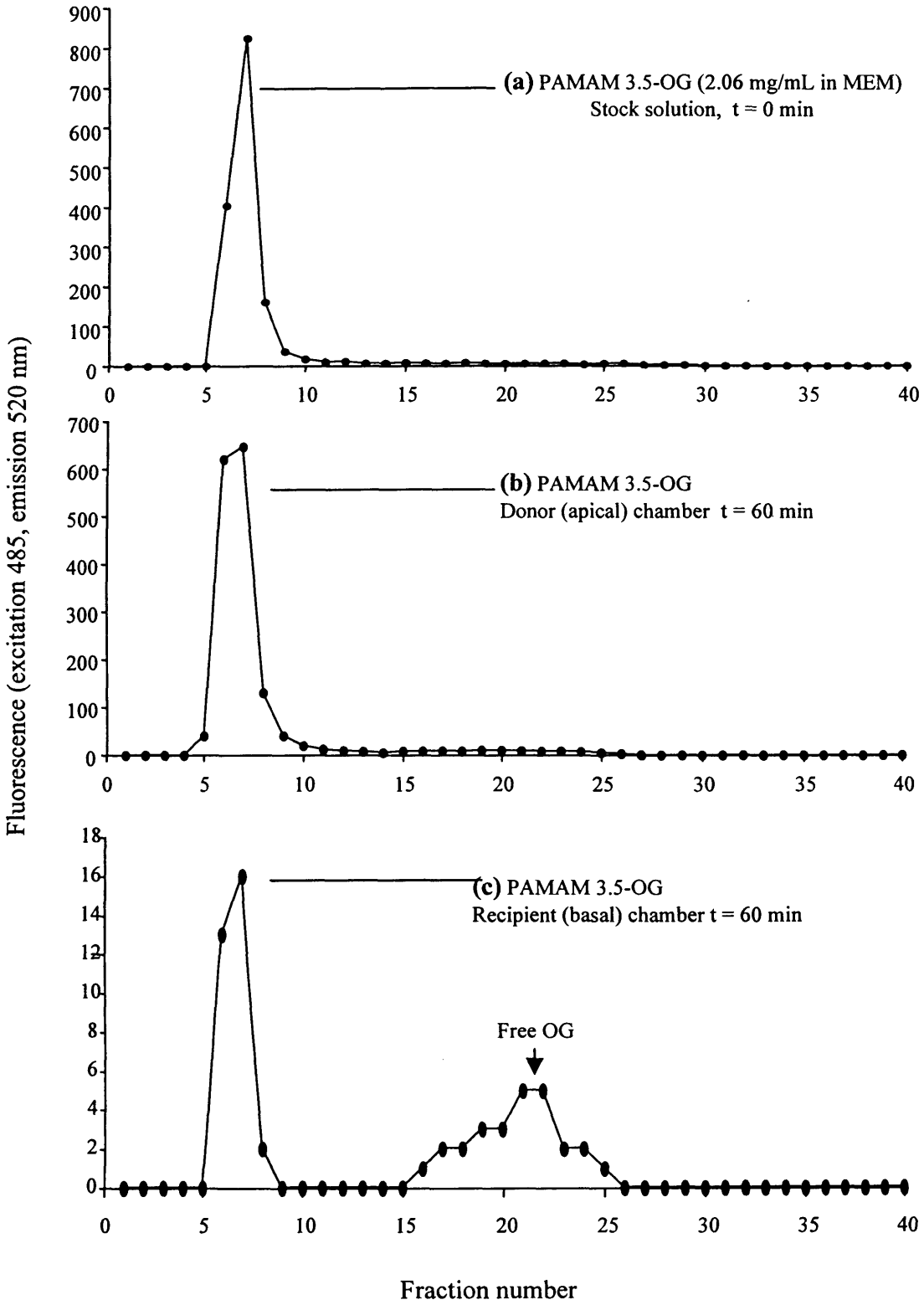

Figure 6.11 (a, b & c) PD-10 column chromatography elution profiles for PAMAM-OG stock solution at t = 0 min (panel a), or from the donor chamber (panel b) or recipient chamber (panel c) at t = 60 min.

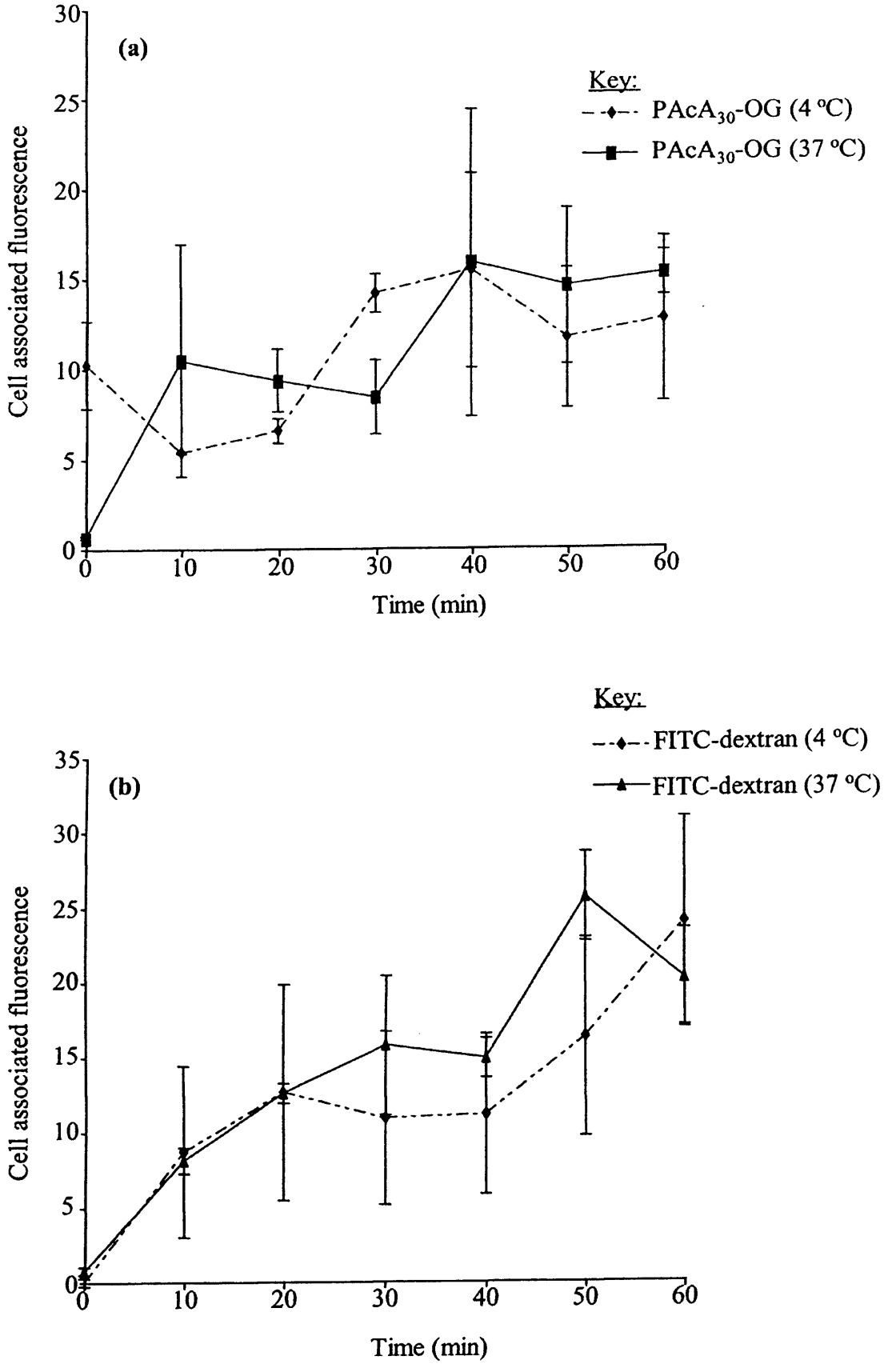

Figure 6.12 (a & b) Uptake of $PAcA_{30}$-OG (1 mg/mL; panel a), and FITC-dextran (1 mg/mL; panel b) by Caco-2_{BBe} cells over 60 min. The data shown are n =3 ± SEM.

Though the conjugation of $sPAcA_{30}$ and PAMAM 3.5 dendrimers was successful, and a relatively small amount of free OG remained in the dialysed polymers (Figure 6.2b and 6.4b respectively, and Table 6.1), the amount of polymer-bound OG according to UV/Vis analysis was not as had been calculated (Table 6.1). Nevertheless, using the UV/Vis spectrums of each polymer, the quantity of PAMAM 3.5-OG required to match the OG content in 1 mg/mL of $PAcA_{30}$-OG was calculated. The required quantity of PAMAM 3.5-OG was found to be double (2.06 mg/mL) that of $PAcA_{30}$-OG (1 mg/mL), and these polymer concentrations were used for transport studies.

Possible mechanisms of polymer transport

The transport of polymers across cellular barriers depends upon their size, charge and lipophilicity. Although an in-depth study on the exact mechanisms of $PAcA_{30}$-OG and PAMAM 3.5-OG transport was not possible here due to time constraints, the vertical diffusion system served to measure the permeation of the fluorescent polymers across rat intestinal tissue, whilst flow cytometry was used to assess whether the polymers were taken up by endocytosis.

In the vertical diffusion system, the transfer of both polymers was greater in the Bas→Ap direction across rat intestinal tissue with or without Peyer's patches, and this observation is in accordance with the literature. For example Kriwet and Kissel (1996) have shown that basally applied microparticles of PAcA enhance the transport of sulforhodamine in Caco-2 cells by 30 x compared to microparticles applied apically. It was suggested that this result was due to the chelation of extracellular Ca^{2+}. El-Sayed *et al.*, (2003b) have shown that the transport of PAMAM 3.5 dendrimers across Caco-2 cells is greater in the Bas→Ap direction. For PAMAM generation 2 dendrimers, studies with the P-gp substrate paclitaxel, have shown that the greater rate of Bas→Ap transport is not likely to be due to efflux by this protein from the apical cell surface where it resides.

Furthermore, the observations made here differ from those seen previously in Chapter 5, where it was found that $sPAcA_{30}$, but not PAMAM 3.5 seemed to enhance FITC-dextran transport only in the Ap→Bas direction. However, it is important to note that these results are not inconsistent as they measure different parameters.

Unlike PAMAM 3.5, which is globular and approximately 4.5 nm in size (Wiwatanepatepee *et al.,* 2000), the hydrodynamic radius of $PAcA_{30}$ is not known. Still, it can be expected to be large, as the polymer is linear and has a high molecular weight. Therefore the transport of $PAcA_{30}$-OG is likely to have been limited to the endocytic pathway, and this was reflected in the transport pattern seen from vertical diffusion chamber experiments (Figure 6.8). A slow lag-time in $PAcA_{30}$-OG transport was seen in transport in both Ap→Bas and Bas→Ap directions across tissue with or without Peyer's patches (Figure 6.8). This was followed by a linear increase in fluorescence in the recipient chamber. Some of this fluorescence (26 %) was due to the transport of free OG. Indeed, a similar transport pattern has been seen for numerous water soluble, neutral, hydrophilic polymers such as ^{125}I-labelled PVP, ^{125}I-labelled poly(N-vinylpyrrolidone-co-maleic anhydride) (NVPMA) (Pat_ *et al.,* 1994), and ^{125}I-labelled HPMA copolymers (Cartilidge *et al.,* 1986), when measured across the rat intestine using the everted gut sac model. These polymers were taken up by fluid-phase endocytosis.

In contrast to the above, anionic NVPMA (Pat_ *et al.,* 1994) and to a greater extent anionic PAMAM generation 2.5 and 3.5 dendrimers (Wiwatanapatepee *et al.,* 2000) have shown greater transport rates across rat intestinal tissue, though this was not the case in the studies conducted here. The transport of PAMAM 3.5-OG across rat intestinal tissue was relatively low compared to that seen for $PAcA_{30}$-OG. Hardly any PAMAM 3.5-OG was transported across the rat intestinal tissue during the 60 min incubation, and PD-10 analysis showed that a large percentage of the fluorescence (56 %) found in the recipient chamber was that of free OG (Figure 6.11). PAMAM 3.5-OG was less stable during the 60 min incubation with the rat intestinal tissue than $PAcA_{30}$-OG. It was also not stable during storage (-20 °C), and this may explain the low fluorescence output of the polymer compared to $PAcA_{30}$-OG in the experiments conducted (Figures 6.9 and 6.11). The instability of this polymer could have been the result of improper storage. When received from the manufacturers, the polymer was kept under nitrogen gas, however after having been conjugated to OG it was not. Nevertheless the polymer was kept for only a short time under these conditions (1 week) before it appeared to stick to the container it was held in.

It was because of this, that flow cytometry was not conducted with the PAMAM 3.5-OG dendrimers. However, it would have been interesting to do this, as

in theory it is possible that the polymers were being recycled by the tissue. Wiwatanapatepee *et al.*, (2000) have shown that these polymers have a low rate of accumulation in rat intestinal tissue, and Xyloxiannis (2004) has shown that dendritic hybrid polymers (PEG-poly(ester) dendrons) can be rapidly exocytosed from cells, after internalisation, in a similar manner to naturally recycled macromolecules such as the transferrin receptor (Dautry-Varsat *et al.*, 1983). It would have been interesting to have tested this theory using this polymer.

Nevertheless, flow cytometry was conducted with $PAcA_{30}$-OG conjugates, and also with FITC-dextran (MW = 4,000 Da). For $PAcA_{30}$-OG-incubated cells, at both -4 and 37 °C only a small difference in cell associated fluorescence was seen (Figure 6.12a). Therefore it can be concluded that $PAcA_{30}$-OG was binding to the cells, and little was being taken up by endocytosis. Similar results were also seen when the cells were incubated with FITC-dextran (Figure 6.12b). However, the fluorescence of FITC is pH-dependent (see Figure 5.1), and thus if the polymer was endocytosed, the fluorescence would drop as the pH inside the vesicles descreased (i.e. when endosomes become lysosomes).

However the results from flow the cytometry experiments were difficult to interpret, and contradict the results observed in the vertical diffusion system, which suggest both $PAcA_{30}$-OG (Figure 6.8) and FITC-dextran (Chapter 4) were being taken up by rat intestinal tissue by endocytosis. This was probably due to the nature of the cells used. If time had allowed it would have been beneficial to have repeated this study using a different cell line. The problems of using Caco-2_{BBe} cells for this work were: (i) Firstly, as mentioned in the introduction to this chapter, Caco-2_{BBe} cells require several weeks in culture in order to differentiate into mature, brush-border expressing enterocyte monolayers. They should also be grown on filters. If time had permitted, it would have been good to have grown these cells in this manner, and to have investigated polymer transport (in parallel to the vertical diffusion system), using fluorescence microscopy, and the measurement of TEER. (ii) Secondly, as the cells were clumped together, and had to be separated using a needle, the cells were likely to have been damaged. This could be seen during flow cytometry, as a high number of small granular particles (broken cells) were picked up by the laser, and appeared on the dot plot for each sample ran. They were gated around the population of viable cells, though it should be noted however that in most

around the population of viable cells, though it should be noted however that in most cases this population was difficult to distinguish.

In summary, a simple schematic diagram depicting the possible cellular transport mechanisms it was thought $PAcA_{30}$-OG and PAMAM 3.5-OG would exploit is given in Figure 6.13. PAcA with its large hydrodynamic radius, linear structure and high molecular weight, is limited to the transport across the tissue via endocytic mechanisms. If indeed taken up by the cells, the fate of the polymer would then be targeted to lysosomes for degradation, or to be exocytosed (transcytosis). PAMAM 3.5-OG dendrimers could be transported across the tissue paracellularly or transcellularly (in accordance with literature, see Chapter 5 for review), or could be recycled. Flow cytometry suggests they are binding (most probably non-specifically) to the cells membrane.

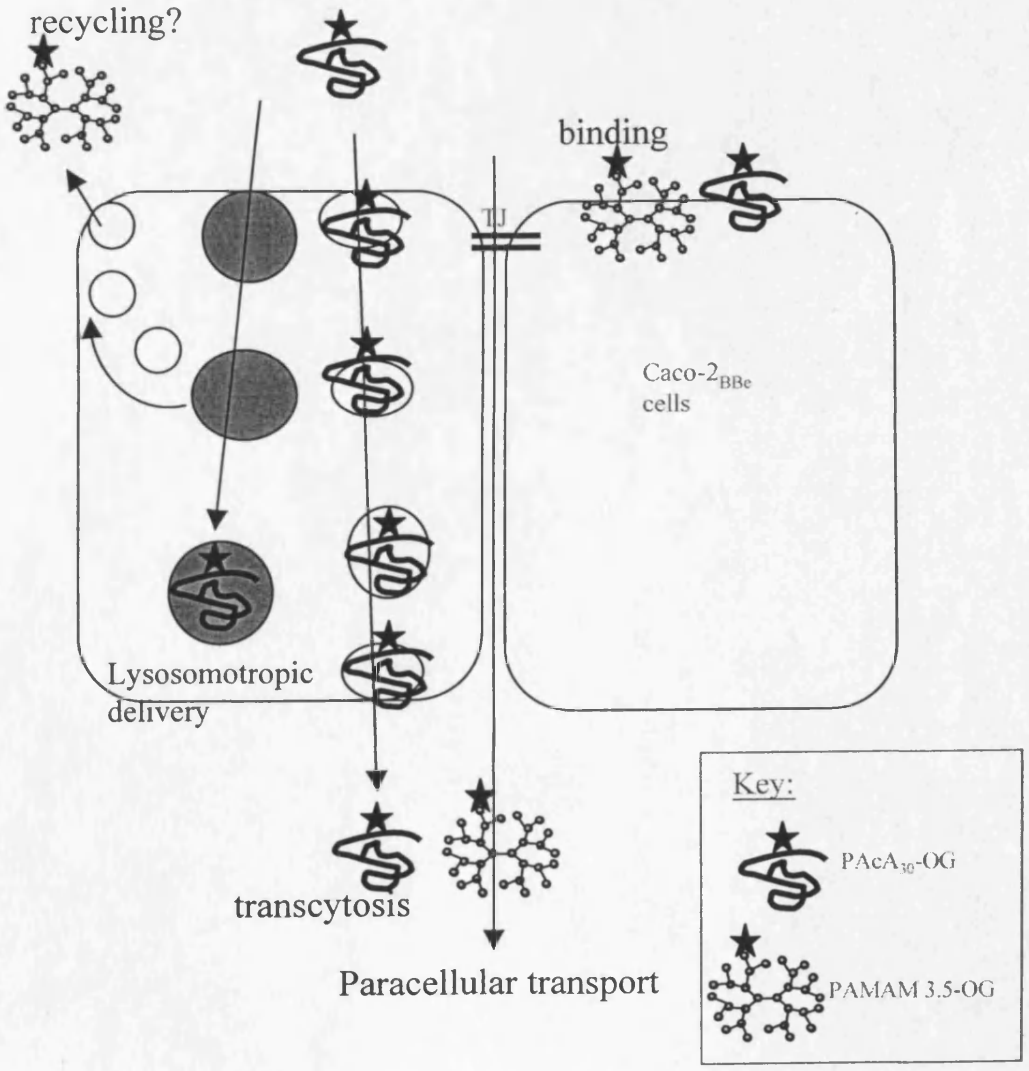

Figure 6.13 Schematic diagram showing the possible polymer transport mechanisms of polymer-OG conjugates.

CHAPTER 7:

General Discussion

7.1 General comments

The columnar cells lining the GI tract (epithelial cells), the vasculature (endothelial cells), and not least the blood brain barrier provide a significant obstacle limiting effective oral bioavailability and drug delivery. These tissues constitute not only a physical barrier, but also a biochemical one, due to the presence of cytochrome p450 drug metabolising enzymes (e.g. CYP3A), and ABC efflux transporters such as P-gp. Moreover, oral delivery via the GI tract is also hampered by pH, extracellular enzymes, mucus and luminal fluid, making this region the most daunting for delivery.

The last four decades of research have sought to design 'safe' drug delivery systems, such as particulate or soluble carriers (Table 7.1) that can efficiently overcome these barriers, to deliver therapeutic doses of poorly absorbed (low molecular) drugs and macromolecules, particularly peptides and proteins. In parallel, research has been ongoing to develop polymer therapeutics for use as biologically active polymeric drugs, polymer-protein conjugates and polymer-drug conjugates. Since 1990 a growing number of such systems have entered routine clinical use (Duncan, 2003; Duncan, 2006). The initial aim of this project was to identify *biologically active* soluble polymers (some are even approved as excipients) that might be tailored (molecular weight and chemical characteristics) so that they would quickly promote significant local paracellular or transcellular drug delivery.

Reflections on the results observed during this study

A library of linear (alginate, HA, sHA, PAcAs) and dendritic (PAMAM) polymer architectures were chosen for these studies, in the hope that they would facilitate improved transient FITC-dextran transfer, across rat intestinal tissue. Each polymer selected was anionic, and was chosen based on information gleamed from the literature (as reviewed in Chapter 5, section 5.1). They were either (i) able to induce cytokine release from cells *in vitro* (i.e. alginate, HA, PAcAs), (ii) mucoadhesive (HA, PAcA), (iii) able to enhance paracellular transport across epithelial barriers (HA, PAcA, PAMAM dendrimers), or (iv) in the case of PAMAM dendrimers, can also transverse both epithelial and endothelial barriers by extremely rapid and efficient mechanisms (Wiwatanapatepee *et al.*, 2000; El-Sayed *et al.*, 2003a; El-Sayed *et al.*, 2003b).

Table 7.1 Carriers currently used for drug delivery

Particle-type carriers	**Soluble carriers**
Liposomes	Plasma proteins
Lipid particles	Peptides
Microspheres	Polysaccharides
Nanoparticles	Monoclonal antibodies
Polymeric micelles	
Polymeric systems such as PEI that complex DNA (polyplexes)	

Initially it was thought these polymers would interact with rat intestinal tissue at the cellular level, and increase FITC-dextran transfer directly, perhaps by inhibiting P-gp or physically widening TJ (Figure 7.1). It was also hoped that they would trigger local biochemical changes, caused by the modulation of Ca^{2+} concentration or the release of cytokines and/ or chemokines (Figure 7.1). Indeed, these polymers could also enhance transcytosis, and could certainly be used to permeabilise endothelial barriers as well (Figure 7.1). It is important to note that to date, no studies have systemically investigated the ability of acknowledged polymeric drug delivery systems to modulate permeability, by eliciting local cytokine release, and from this point of view, the scope of this project was very novel.

Although in many ways the results obtained in this study were negative, in that they did not highlight particular polymers that might be further optimised as permeabilising agents, able to promote transient oral delivery, each series of experiments did produce interesting data highlighting the opportunities and challenges of research in this difficult, but important field.

Cytotoxicity experiments showed that the polymers chosen for this work were non-toxic at concentrations up to 1 mg/mL. When incubated with various cell lines (DU937, RAW 246.7 and B16F10), the non-toxic concentrations of polymers did not induce TNF-α, IFN-γ or IL-2 release, except for HA, and the positive cytotoxic control, PEI (Chapter 3). In the vertical diffusion chamber, rTNF-α, rIFN-γ or rIL-2 added at physiological levels did not show any effects on the transport of FITC-dextran, whilst at non-physiological concentrations (ng/mL) rIFN-γ appeared to enhance it, however this effect was not significant (Chapter 4). Likewise, at concentrations of 1 mg/mL, polymers did not significantly enhance FITC-dextran transport across rat intestinal tissue in the vertical diffusion system (Chapter 5), though $sPAcA_{30}$ and HA showed a slight increase. When fluorescently labelled, $sPAcA_{30}$ seemed to be transported across the tissue by transcellular mechanisms in the vertical diffusion system (Chapter 6).

Although the polymers used in this study did not appear to enhance permeability, it also appears that no significant progress has been made in the drug delivery field over the last four years either.

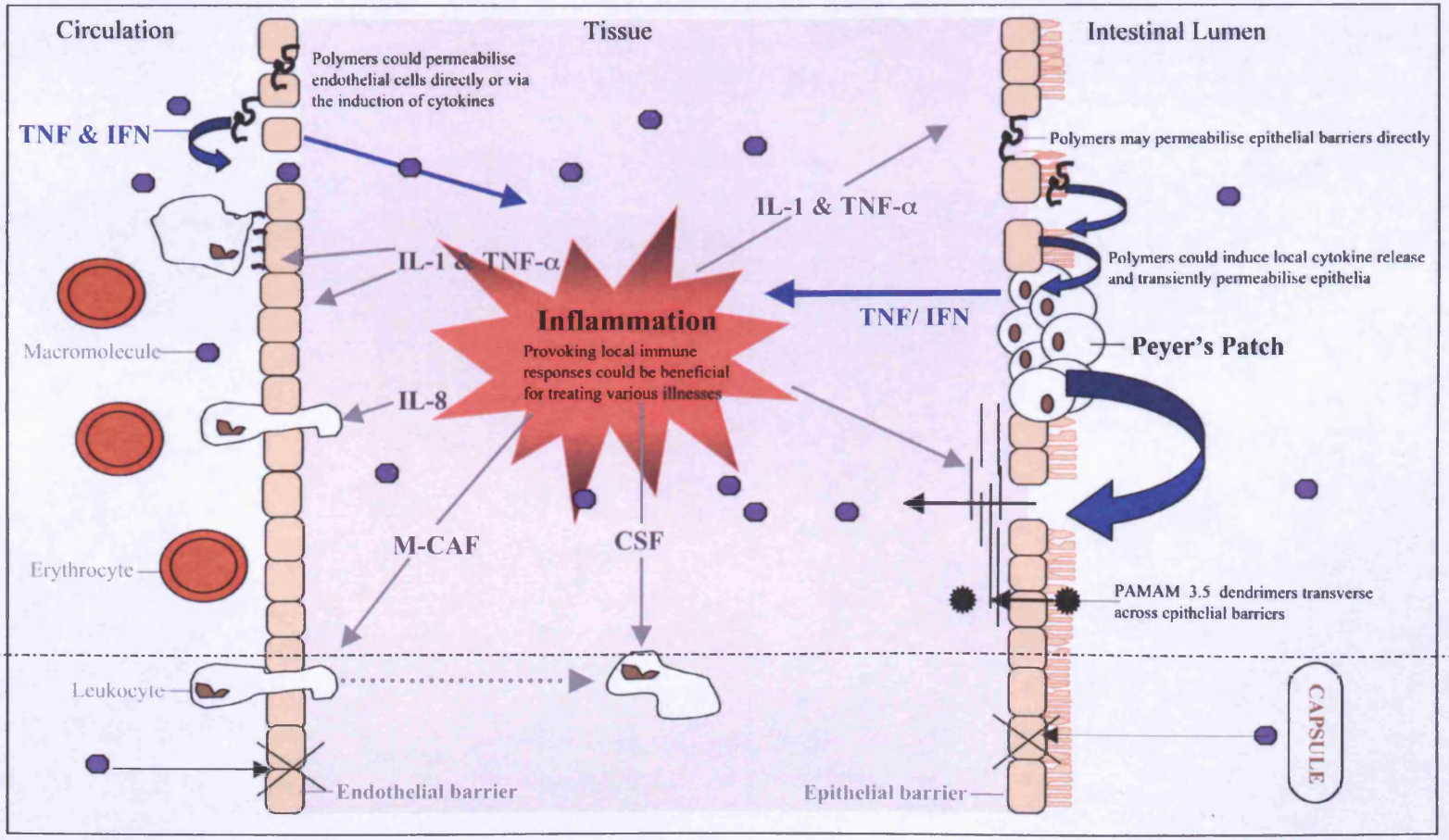

Figure 7.1 Schematic diagram showing the general aims of this thesis

Progress in identifying agents able to permeabilise cellular barriers

Over the last four years the most interesting studies investigating methods to improve permeability across cellular barriers (intestine, blood-brain barrier, eye) have involved the use of TJ permeation enhancers, such as fatty acids (reviewed in Cano-Cebrian *et al.*, 2005), and more recently toxins such as zonula occludin toxin (Zot) (Motlekar *et al.*, 2006), and clostridium perfringens enterotoxin (Kondoh *et al.*, 2006), or thiolated polymers such as trimethylated chitosan (Thanou *et al.*, 2001). The effects of these molecules are reversible. Methods previously used to increase permeability include the use of fatty acids, calcium chelators, surfactants and bile salts, which can also operate by opening TJs (i.e. calcium chelators, fatty acids and some bile salts), or by increasing the fluidity of the cell membrane (i.e. surfactants, medium chain fatty acids and other bile salts). Nonetheless, the use of all the above is often linked to toxicity, and as yet, no single permeation enhancer is effective for the delivery of macromolecules. As such they are not widely used in oral formulations.

7.2 Thoughts regarding methods used and future experiments

Use of vertical diffusion chamber

Most of the research carried out on absorption-enhancing compounds, have been limited by the use of models that are non-physiological i.e. cell monolayers. Though Caco-2 and other cell lines are adequate for initial screening tests, they are poor predictors of *in vivo* performance. In much the same way, models that use isolated tissues such as the vertical diffusion chamber, are also poor predictors of *in vivo* performance for a variety of reasons including a lack of blood flow and luminal fluid. However they provide a method that is one step closer to the *in vivo* system.

In transport experiments the control rate of FITC-dextran transfer in the vertical diffusion system was highly variable (see Chapter 4 and Chapter 5), thus it was difficult to decipher differences in the transport of this marker mediated by the polymers or cytokines that were added (Chapter 4 and Chapter 5). This factor raises the question; is the vertical diffusion system a useful model for measuring transport?

The variability seen in the vertical diffusion system was largely due to variations in the animals used (see Chapter 4, section 4.4 for full discussion). Like man, Sprauge Dawley rats are outbred and thus (unlike cell monolayer models), the vertical diffusion chamber accounts for differences between individuals. However, this method is fraught with difficulties as discussed in Chapter 4 (section 4.4).

It would have been interesting to have used another transport model, such as the everted gut sac method for this work as a comparison, however from the results observed in these studies, this would have been unnecessary.

Evaluation of cytokine release - technical challenges

The difficulty in testing for the release of cytokines is that their half-life is so short (min). They may also bind to the polymers used, or the polymers may bind to the immunoglobulins in the ELISA plates, thus interfering with the assays (Chapter 3). Furthermore, there is also the possibility that the polymer stocks could contain LPS, and this could lead to false-positive results. However, when trying to test for contamination, the polymers interfered with the LAL assay. It is also difficult to know which cell lines to use for these studies. Cells that are directly involved in the immune response i.e. leukocytes are the main cytokine producers, thus with this in mind, some transport experiments were conducted with Peyer's patch containing tissues. It was thought that the T- and B-cells held in the patches would be more responsive to the cytokines used for these studies (Chapter 4). However, no increase in FITC-dextran transport was seen across these tissues (Chapter 4 and Chapter 5).

It is also difficult to know which cytokines to select and test for. A better way to test for cytokine release would have been to use cytokine arrays, modified ELISA assays, in which the release of several cytokines could have been depicted from a single sample of culture media from the polymer-incubated cells (www.RnDSystem.com). Not only could this be used to measure the release of a range of cytokines from the cells, but it could also be used to measure the induction of cytokine release over more time points. On another note, gene profiling could also have been used to investigate the responses of the cells towards the polymers investigated. It would also have been interesting to also examine the effect of these polymers on other leukocytes such as T- and B-cells as found in Peyer's patches.

7.3 Will the use of biologically active polymers ever be safe enough??

Cytokines generally modulate the permeability of cells by affecting the cellular distribution of TJ proteins (see Figure 1.4). Great interest has been focused on the structure and cellular regulation of TJ in the last few years (as reviewed in Chapter 1, section 1.5.1), and a more in-depth knowledge of this physical barrier has recently come to light. TNF-α (Chapter 1, section 1.7.3) and IFN-γ (Chapter 1, section 1.7.2)

both decrease (among others) the levels of ZO-1 from the TJ, and in doing so, reversibly decrease the TEER in Caco-2 and other intestinal cell lines, in a matter of h (as discussed in Chapter 4, section 4.4). The production of either cytokine is known to be elicited by polymers such as alginate, HA and PAcA from cells *in vitro* (Table 1.2).

Taking this data into account, not only did the idea of using these molecules to transiently enhance drug delivery seem plausible, but it was also thought that polymers capable of inducing them could be used to improve anticancer or antiviral therapies. Indeed, provoking a *local* cytokine cascade, would limit the toxicity problems observed with intravenous administration of cytokines such as IL-2 (Chapter 1, section 1.7.1).

However, caution has to be taken when working with immunologically active molecules. Only recently (on the 13th March, 2006), a clinical trial in London, with the superagonist monoclonal antibody, TGN 14 12, served only to underline the difficulty in working with medicines that may tip the delicate balance of the host's immune system. Six healthy volunteers became violently ill, suffering multiple organ failure, and were admitted to intensive care only minutes after receiving an injection of the drug. TGN 14 12 was developed by TeGenero (Germany) to fight autoimmune disease (i.e. multiple sclerosis, rheumatoid arthritis) and leukaemia (www.tegenero.com). It functions by binding the CD28 receptor on T-cells, causing T-cell proliferation, without the involvement of the TCR as is required for natural T-cell activation (see Chapter 1, section 1.2.2, Figure 1.3).

In mice, rats, rabbits and monkeys, TGN 14 12 has demonstrated the ability to stimulate T-cell proliferation without apparent toxicity. In the human clinical trial, a flood of cytokines released by activated T-cells, was thought to be responsible for the drugs toxicity (reviewed by Bhattacharya and Coghlan, 2006). As mentioned earlier (Chapter 1, section 1.1.1), a similar fate occurred during Phase I clinical trials with DIVEMA in the 1960's.

7.5 Final thoughts

As an increasing number of therapeutic molecules are becoming available with time (especially protein and peptide drugs through advancements in genetic engineering), there is an impending need to find new ways to transiently permeabilise endothelial and epithelial barriers. The benefits for drug delivery via

this method include (i) the abolishment of injections, leading to increased patient compliance, (ii) cheaper drug manufacturing costs, as they would not need to be produced under strict sterile conditions, and (iii) a decreased need for trained professionals to administer them. Therefore, the design of novel permeation enhancers would be advantageous for the biomedical industry.

However, much research has to be made on trying to identify safe ways to permeabilise these barriers transiently. Although the polymers chosen for this study showed no inherent biological activity regarding cytokine release (except for HAs), or the ability to modulate FITC-dextran transport across rat intestinal tissue, evidence in the literature suggests otherwise, and it was difficult to validate the hypothesis of this work with the models used here. Perhaps the experiments conducted here need refining i.e. longer incubation times could be used, and different models could be employed.

As this project bridges several disciplines and the possibility of further studies are endless. I am sure with time a new class of successful biologically active polymeric drugs will be found.

BIBLIOGRAPHY

A

Abbas, A. K., Lichtman, A. H., Pober, J. S. (2000). *Cellular and Molecular Immunology.* (4th Ed.). London, UK: Saunders.

Adams, R. B., Planchon, S. M. and Roche, J. K. (1993). "IFN-γ modulation of epithelial barrier function." *J Immunol* **150**(6): 2356-63.

Aggarwal, B. B., Samanta, A. and Feldmann, M. (2000). "TNF-α." In Oppenheim, M. F., Feldman, M., Durum, S. K., Hirano, T., Vilcek, J. and Nicola, N. A. (Eds.), *Cytokine Reference: A compendium of Cytokines and Other Mediators of Host Defence:* 414-434. London, UK: Academic Press.

Agnholt, J. and Kaltoft, K. (2001). "In situ activated intestinal T cells expanded *in vitro*-without addition of antigen-produced IFN-γ and IL-10 and preserve their function during growth." *Exp Clin Immunogenet* **18**(4): 213-25.

Agnholt, J., Dahlerup, J. F., Buntzen, S., Tottrup, A., Nielsen, S. L. and Lundorf, E. (2003). "Response, relapse and mucosal immune regulation after infliximab treatment in fistulating Crohn's disease." *Aliment Pharmacol Ther* **17**: 703-10.

Ahdieh, M., Vandenbos, T. and Youakim, A. (2001). "Lung epithelial barrier function and wound healing are decreased by IL-4 and IL-13 and enhanced by IFN-γ." *Am J Physiol* **281**(6): C2029-38.

Al-Shamkhani, A. (1993). "Evaluation of alginates as a soluble drug delivery system for oral and systemic use." *Thesis (PhD).* Cardiff University.

Al-Shamkhani, A. and Duncan, R. (1995a). "Synthesis, controlled release properties and antitumour activity of alginate-cis-aconityl-daunomycin conjugates." *Int J Pharm* **122**(1): 107-19.

Al-Shamkhani, A. and. Duncan, R. (1995b). "Radioiodinaton of alginate via covalently-bound tryosinmide allows monitoring of its fate *in vivo*." *J Bioact Compat Polym* **10**: 4-13.

Anderle, P., V. Rakhmanova, V., Woodford, K., Zerangue, N. and Sadee, W. (2003). "Messenger RNA expression of transporter and ion channel genes in undifferentiated and differentiated Caco-2 cells compared to human intestines." *Pharm Res* **20**(1): 3-15.

Andersson, L., Davies, J., Duncan, R., Ferruti, P., Ford, J., Kneller, S., Mendichi, R., Pasut, G., Schiavon, O., Summerford, C., Tirk, A., Veronese, F. M., Vincenzi, V., Wu, G. (2005). "Poly(ethylene glycol)-poly(ester-carbonate) block copolymers carrying PEG-peptidyl-doxorubicin pendant side chains: synthesis and evaluation as anticancer conjugates." *Biomacromolecules* **6**(2): 914-26.

Ando-Akatsuka, Y., Saitou, M., Hirase, T., Kishi, M., Sakakibara, A., Itoh, M., Yonemura, S., Furuse, M. and Tsukita, S. (1996). "Interspecies diversity of the occludin sequence: cDNA cloning of human, mouse, dog, and kangaroo-rat homologues." *J Cell Biol* **133**(1): 43-7.

Anlar, S., Capan, Y. and Hincal, A. A. (1993). "Physico-chemical and bioadhesive properties of polyacrylic acid polymers." *Pharmazie* **48**(4): 285-7.

Artursson, P., Edman, P., Ericsson, J. L. (1987). "Macrophage stimulation with some structurally related polysaccharides." *Scand J Immunol* **25**(3): 245-54.

Artursson, P., A. Ungell, L. and Lofroth, J. E. (1993). "Selective paracellular permeability in two models of intestinal absorption: cultured monolayers of human intestinal epithelial cells and rat intestinal segments." *Pharm Res* **10**(8): 1123-9.

B

Balda, M. S., Anderson, J. M., Matter, K (1996). "The SH3 domain of the tight junction protein ZO-1 binds to a serine protein kinase that phosphorylates a region C-terminal to this domain." *FEBS Lett* **399**: 326-32.

Balda, M., S., and Matter, Karl. (2000). "The tight junction protein ZO-1 and an interacting transcription factor regulate ErbB-2 expression." *EMBO J* **19**(9): 2024-33.

Balda, M. S., Garret, M. D and Matter, K. (2003). "The ZO-1-associated Y-box factor ZONAB regulates epithelial cell proliferation and cell density." *J Cell Biol* **160**(3): 423-32.

Baldwin, A. L., Primeau, R. L. and Johnson, W. E. (2006). "Effect of noise on the morphology of the intestinal mucosa in laboratory rats." *J Am Assoc Lab Anim Sci* **45**(1): 74-82.

Barthe, L., Woodley, J. F., Kenworthy, S. and Houin, G. (1998). "An improved everted gut sac as a simple and accurate technique to measure paracellular transport across the small intestine." *Eur J Drug Metab Pharmacokinet* **23**(2): 313-23.

Barthe, L., Woodley, J. and Houin, G. (1999). "Gastrointestinal absorption of drugs: methods and studies." *Fundam Clin Pharmacol* **13**(2): 154-68.

Bastias, J., Wei, M. X., Huynh, R., Chaubet, F., Jozefonvicz, J. and Crepin, M. (2002). "Anti-proliferative and antitumoral activities of a functionalized dextran (CMDBJ) on the 1205 L-U human tumor melanoma cells." *Anticancer Res* **22**(3): 1603-13.

Bazzoni, F., Gatto, L., Lenzi, L., Vinante, F., Pizzolo, G., Zanolin, E. and De Gironoli, M. (2000). "Identification of novel polymorphisms in the human TNFR1 gene: distribution in acute leukemia patients and healthy individuals." *Immunogenetics* **51**(2): 159-63.

Bazzoni, G., Martinez-Estrada, O. M., Orsenigo, F., Cordenonsi, M., Citi, S. and Dejana, E. (2000). "Interaction of junctional adhesion molecule with the tight junction components ZO-1, cingulin, and occludin." *J Biol Chem* **275**(27): 20520-6.

Bazzoni, G., Martinez-Estrada, O. M., Mueller, F., Nelboeck, P., Schmid, G., Bartfai, T., Dejana, E. and Brockhaus, M. (2000). "Homophilic interaction of junctional adhesion molecule." *J Biol Chem* **275**(40): 30970-6.

Bentolia, A., Vlodavsky, I., Ishai-Micheal, R., Kovalchuk, O., Haloun, C., Domb, A. J. (2000). "Poly(N-acrly amino acids): a new class of biologically active polyanions." *J Med Chem* **43**(13): 2591-600.

Berggren, S., Hoogstraate, J., Fagerholm, U. and Lennernas, H. (2004). "Characterisation of jejunal absorption and apical efflux of ropivacaine, lidocaine and bupivacaine in

the rat using in situ and in vitro absorption models." *Eur J Pharm Sci* **21**: 553-60.

Berna, M., Dalzoppo, D., Pasut, G., Manunta, M., Izzo, L., Jones, A. T., Duncan, R. and Veronese, F. M. (2006). "Novel monodisperse PEG-dendrons as new tools for targeted drug delivery: synthesis, characterization and cellular uptake." *Biomacromolecules* 7(1): 146-53.

Berntzen, G., Flo, T. H., Medvedev, A., Kilaas, L., Skjak-Break, G., Sundan, A. and Espevik, T (1998). "The tumour necrosis factor-inducing potency of uronic acid polymers is increased when they are covalently linked to particles." *Clin Diagn Lab Immunol* **5**(3): 355-60.

Bhattacharya, S. and Coghlan, A. "Catestrophic immune response may have caused drug trial horror." *New Scientist* **189**(2544): 10-11.

Bielinska, A. U., Kukowska-Latallo, J. F. and Baker, J. R. Jr (1997). "The interaction of plasmid DNA with polyamidoamine dendrimers: mechanism of complex formation and analysis of alterations induced in nuclease sensitivity and transcriptional activity of the complexed DNA." *Biochim Biophys Acta* **1353**(2): 180-90.

Billau, A. and Vandenbroek, K. (2000). "IFN-γ." In Oppenheim, M. F., Feldman, M., Durum, S. K., Hirano, T., Vilcek, J., Nicola, N. A. (Eds.), *Cytokine Reference: A Copendium of Cytokines and Other Mediators of Host Defence*: 641-688. London, UK: Academic Press.

Blanchere, M., Saunier, E., Mestayer, C., Broshuis, M. and Mowszowicz, I. (2002). "Alterations of expression and regulation of transforming growth factor beta in human cancer prostate cell lines." *J Steroid Biochem Mol Biol* **82**(4-5): 297-304.

Boeckle, S., Fahrmeir, J., Roedl, W., Ogris, M. and Wagner, E. (2006). "Melittin analogs with high lytic activity at endosomal pH enhance transfection with purified targeted PEI polyplexes." *J Control Release* **112**(2): 240-8.

Bogwald, J., Gouda, I., Hoffman, J., Larm, O., Larsson, R. and Seljelid, R. (1984). "Stimulatory effect of immobilized glycans on macrophages in vitro." *Scand J Immunol* **20**(4): 355-60.

Boniface, K., Bernard, F. X., Garcia, M., Gurney, A. L., Lecron, J. C. and Morel, F. (2005). "IL-22 inhibits epidermal differentiation and induces proinflammatory gene expression and migration of human keratinocytes." *J Immunol* **174**(6): 3695-702.

Borchard, G. and Junginger, H. E. (2001). "Modern drug delivery applications of chitosan." *Adv Drug Deliv Rev* **52**(2): 103.

Bouer, R., Barthe, L., Philibert, C., Tournaire, C., Woodley, J. and Houin, G. (1999). "The roles of P-glycoprotein and intracellular metabolism in the intestinal absorption of methadone: in vitro studies using the rat everted intestinal sac." *Fundam Clin Pharmacol* **13**(4): 494-500.

Boussif, O., Lezoualch, F., Zanta, M. A., Mergny, M. D., Scherman, D., Demeneix, B. and Behr, J. P. (1995). "A versatile vector for gene and oligonucleotide transfer into cells in culture and in vivo: polyethylenimine." *Proc Natl Acad Sci USA* **92**(16): 7297-301.

Boyce, D. E., Thomas, A., Hart, J. and Harding, K. (1997). "Hyaluronic acid induces tumour necrosis factor-α production by human macrophages in vitro." *Br J Plast Surg* **50**: 362-8.

Braegger, C. P., Nicholls, S., Murch, S.H., Stephens, S., and MacDonald, T.T. (1992). "Tumour necrosis factor-α in stools as a marker of intestinal inflammation." *Lancet.* **339**(8785): 89-91.

Brayden, D., Jepson, M. A. and Baird, A. W. (2005). "Keynote review: intestinal Peyer's patch M cells and oral vaccine targeting." *Drug Discov Today* **10**(17): 1145-57.

Breslow, D. S., Edwards, E. I., Newburg, N. R. (1973). "Divinyl ether-maleic anhydride (pyran) copolymer used to demonstrate the effect of molecular weight on biological activity." *Nature* **246**(5429): 160-2.

Breslow, D. S. (1976). "Biologically active synthetic polymers." *Pure and Appl Chem* **46**: 103-113.

Bromberg, L. and Alakhov, V. (2003). "Effects of polyether-modified poly(acrylic acid) microgels on doxorubicin transport in human intestinal epithelial Caco-2 cell layers." *J Control Release* **88**(1): 11-22.

Bruewer, M., Luegering, A., Kucharzik, T., Parkos, C. A., Madara, J. L., Hopkins, A. M. and Nusrat, A. (2003). "Proinflammatory cytokines disrupt epithelial barrier function by apoptosis-independent mechanisms." *J Immunol* **171**(11): 6164-72.

Bruewer, M., Utech, M., Ivanov, A. I., Hopkins, A. M., Parkos, C. A. and Nusrat, A. (2005). "IFN-γ induces internalization of epithelial tight junction proteins via a macropinocytosis-like process." *FASEB J* **19**(8): 923-33.

Burger, W. C. and Stahmann, M. A. (1951). "The combination of lysine polypeptides with tobacco mosaic virus." *J Biol Chem* **193**(1): 13-22.

Butler, G. B. (1960). "133rd Meeting of the Amercian Chemical Society, San Francisco, California" *Polym Sci* **48**: 279.

C

Cartilidge, S. A., Duncan, R., Lloyd, J. B., Rejmanova, P. and Kopecek, J. (1986). "Soluble crosslinked N-(2-hydroxypropyl)methacrylamide copolymers as potential drug carriers. 1. Pinocytosis by rat visceral." *J Control Release* **3**: 55-66.

Cano-Cebrian, M. J., Zornoza, T., Granero, L. and Polache, A. (2005). "Intestinal absorption enhancement via the paracellular route by fatty acids, chitosans and others: a target for drug delivery. *Curr Drug Deliv* **2**(1): 9-22.

Chakravortty, D. and Kumar K. S. (1999). "Modulation of barrier function of small intestinal epithelial cells by lamina propria fibroblasts in response to lipopolysaccharide: possible role in TNF-alpha in inducing barrier dysfunction." *Microbiol Immunol* **43**(6): 527-33.

Charman, W. N., Christy, D. P., Geunin, E. P., and Monkhouse, D. C. (1990). "Interaction between calcium, a model divalent cation, and range of poly(acrylic acid) resins as a function of solution pH." *Drug Dev Ind Pharm* **17**: 271-280.

Chen, H. T., Neerman, M. F., Parrish, A R., Simanek, E. E. (2004). "Cytotoxicity, heamolysis and acute in vivo toxicity of dendrimers based on melamine, candidate vehicles for drug delivery." *J Am Chem Soc* **126**: 10044-8.

Chen, W., Tomalia, D. A. and Thomas, J. L. (2000). "Unusual pH-dependent polarity changes in PAMAM dendrimers: evidence for pH-responsive conformational changes." *Macromolecules* **23**: 9169-72.

Chiou, W. L. (1994). "Determination of drug permeability in a flat or distended stirred intestine. Prediction of fraction dose absorbed in humans after oral administration." *Int J Clin Pharmacol Ther* **32**(9): 474-82.

Choi, E-M., Hwang, J-K. (2002). "Enchancement of oxidative response and cytokine production by yam mucopolysaccharide in murine peritoneal macrophage." *Fitoteripia* **73**: 629-36.

Christensen, N. D., Reed, C. A., Culp, T. D., Hermonat, P. L., Howett, M. K., Anderson, R. A., Zaneveld, L. J. (2001). "Papillomavirus microbial activities of high molecular-weight cellulose sulfate, dextran sulfate and polystyrene sulfate." *Antimicrob Agents Chemother* **45**(12): 3427-32.

Claes, P., Billiau, A., De Clercq, E., Desmyter, J., Schonne, E., Vanderhaeghe, H. and De Somer, P. (1970). "Polyacetal carboxylic acids: a new group of antiviral polyanions." *J Virol* **5**(3): 313-20.

Cohen, C. J., Shieh, J. T., Pickles, R. J., Okegawa, T., Hsieh, J. T. and Bergelson, J. M. (2001). "The coxsackievirus and adenovirus receptor is a transmembrane component of the tight junction." *Proc Natl Acad Sci USA* **98**(26): 15191-6.

Colgan, S. P., Morales, V. M., Madara, J. L., Polischuk, J. E., Balk, S. P. and Blumberg, R. S. (1996). "IFN-γ modulates CD1d surface expression on intestinal epithelia." *Am J Physiol* **271**(1 Pt 1): C276-83.

Collett, A., Walker, D., Sims, E., He, Y-L., Speers, P., Ayrton, J., Rowland, M. and Warhurst, G. (1997). "Influence of morphometric factors on quantitation of paracellular permeability of intestinal epithelia in vitro." *Pharm Res* **14**(6): 767-73.

Cowan, J. D., Von Hoff, D. D., Neuenfeldt, B., Mills, G. M. and Clark, G. M. (1984). "Predictive value of trypan blue exclusion viability measurements for colony formation in a human tumor cloning assay." *Cancer Drug Deliv* **1**(2): 95-100.

D

Dautry-Varsat, A., Ciechanover, A. and Lodish, H. F. (1983). "pH and the recycling of transferrin during receptor-mediated endocytosis." *Proc Natl Acad Sci USA* **80**(8): 2258-62.

Davis, F. F. (2002). "The origin of pegnology." *Adv Drug Del Rev* **54**: 457-458.

Dawson, R. M. C., Elliot, W. H., Elliot, W. H. and Jones, K. M. (2002). *Data for Biochemical Research*. Oxford, UK: Oxford University Press.

De Clercq, E. and. De Somer, P. (1969). "Prolonged antiviral protection by interferon inducers (34291)." *Proc Soc Exp Biol Med* **132**(2): 699-703.

De Duve, C., De Barsy, T., Poole, B., Trouet, A., Tulkens, P. and Van Hoof, F. (1974). "Commentary. Lysosomotropic agents." *Biochem Pharmacol* **23**(18): 2495-531.

De la Motte, C. A., Hascall, V. C., Drazba, J., Bandyopadhyay, S. K., and Strong, S. A. (2003). "Mononuclear leukocytes bind to specific hyaluronan structures on colon mucosal smooth muscle cells treated with polyinosinic acid:polycytidylic acid: inter-alpha-trypsin inhibitor is crucial to structure and function." *1: Am J Pathol.* **163**(1): 121-33.

De Maeyer, E. and De Maeyer-Guignard, J. (1998). "Interferon-γ". In Sluis-Mire, A. and Thorpe, R. (Eds.), *Cytokines.* London, UK: Academic Press.

De Somer, P., De Clercq, E., Billiau, A., Schonne, E., and Claesen, M. (1968a). "Antiviral activity of polyacrylic and polymethacrylic acids. I. Mode of action in vitro." *J Virol* **2**(9): 878-885.

De Somer, P., De Clercq, E., Billiau, A., Schonne, E., and Claesen, M. (1968b). "Antiviral activity of polyacrylic and polymethacrylic acids II. Mode of action in vivo." *J Virol* **2**(9): 886-893.

Delong, R., Stephenson, k., Loftus, T., Fisher, M., Alahari, S., Nolting, A., Juliano, R.L. (1997). "Characterization of complexes of oligonucleotides with polyamidoamine starburst dendrimers and effects on intracellular delivery." *J Pharm Sci* **86**(6): 762-4.

Di Filippo, F., Cavaliere, F., Garinei, R., Anza, M., Di Angelo, P., Psaila, A., Piarulli, L., Callopoli, A., Bruno, P., Di Filippo, S., and Priore, F. (2004). "TNF-α-based isolated hyperthermic limb perfusion (HILP) in the treament of limb recurrent melanoma: update 16 years after its first clinical application." *J Chemother* **16**(5): 62-5.

Diamanti, P. (2004). "Examining polymers as a means to overcome the small intestinal barrier and improve the oral delivery of P-glycoprotein substrates." *Thesis (PhD).* Cardiff University.

Diamantstein, T., W. Keppler, W., Blitsein-Wilinger, E. (1976). "Suppression of the primary immune response in vivo to sheep red blood cells by B-cell mitogens." *Immunology* **30**(3): 401-7.

Dickens, F. and Weil-Malherbe, H. W. (1941). "Metabolism of normal tumour tissue. The metabolism of intestinal mucus membrane." *Biochem J* **35**(7): 7-15.

Donaruma, L. G. (1975). Synthetic biologically active polymers. *Prog Polym Sci* A. D. Jenkins. New York, Pergamon press. **4:** 1-25.

Dubruel, P., Christiaens, B., Rosseneu, M., Vandekerckhove, J., Grooten, J., Goossens, V. and Schacht, E. (2004). "Buffering properties of cationic polymethacrylates are not the only key to successful gene delivery." *Biomacromolecules* **5**(2): 379-88.

Duncan, R. (1997). "Polymer therapeutics for tumour specific delivery." *Chem Ind* 7: 262-4.

Duncan, R. (2003). "The dawning era of polymer therapeutics." *Nat Rev Drug Discov* **2**: 347-60.

Duncan, R., and Izzo, L. (2005). "Dendrimer biocompatibility and toxicity." *Adv Drug Deliv Rev* **57**(15): 2215-37.

Duncan, R. "Polymer conjugates as anticancer nanomedicines." *Nat Rev Cancer* **6**(9): 688-701.

E

Eagle, H. (1959). "Amino acid metabolism in mammalian cell cultures." *Science* **130**: 432-7.

Ebnet, K., Schulz, C. U., Meyer, Z., Brickwedde, M. K., Pendl, G. G. and Vesweber, D. (2000). "Junctional adhesion molecule interacts with the PDZ domain-containing proteins AF-6 and ZO-1." *J Biol Chem* **275**(36): 27979-88.

Eggermont, A. M., Schraffordt Koops H., Klausner, J. M., Lienard, D., Kroon, B. B., Schlag, P. M., Ben-Ari, G. and Lejeune, F. J. (1997). "Isolated limb perfusion with tumour necrosis factor alpha and chemotherapy for advanced extremity soft tissue sarcomas." *Semin Oncol* **24**(5): 547-55.

El-Sayed, M., Kiani, M. F., Naimark, M. D., Hikal, A. H. and Ghandehari, H. (2001). "Extravasation of poly(amidoamine) (PAMAM) dendrimers across microvascular network endothelium." *Pharm Res* **18**(1): 23-8.

El-Sayed, M., Ginski, M., Rhodes, C. and Ghandehari, H. (2002). "Transepithelial transport of poly(amidoamine) dendrimers across Caco-2 cell monolayers." *J Control Release* **81**: 355-65.

El-Sayed, M., Rhodes, C. A., Ginski, M. and Ghandehari, H. (2003a). "Transport mechanism(s) of poly(amidoamine) dendrimers across Caco-2 cell monolayers." *Int J Pharm* **265**(1-2): 151-7.

El-Sayed, M., Ginski, M., Rhodes, C., Ghandehari, H. (2003b). "Influence of surface chemistry of poly(amidoamine) dendrimers on Caco-2 monolayers." *J Bioact Compat Polym* **18**: 7-22.

Emery, S., Abrams, D. I., Cooper, D. A., Darbyshire, J. H., Lane, H. C., Ludgren, J. D., Neaton, J. D., and the ESPIRIT Study Group (2002). "The evaluation of subcutaneous Proleukin® (IL-2) in a randomised international trial: rationale, design, and methods of ESPIRT." *Control Clin Trials* **23**: 198-220.

Engert, A., Martin, G., Amlot, P., Wijdenes, J., Diehl, V. and Thorpe, P. (1991). "Immunotoxins constructed with anti-CD25 monoclonal antibodies and deglycosylated ricin A-chain have potent anti-tumour effects against human Hodgkin cells in vitro and solid Hodgkin tumours in mice." *Int J Cancer* **49**(3): 450-6.

Espevik, T., Otterlei, M., Skjak-Break, G., Ryan, L., Wright, S. D., Sundan, A. (1993). "The involvement of CD14 in stimulation of cytokine production by uronic acid polymers." *Eur J Immunol* **23**: 225-261.

F

Fais, S. (1991). "Lymphocyte traffic and adhesion molecules in the gut." *Ital J Gastroenterol* **23**(6): 395.

Fanning, A. S., Jameson, B. J., Jesaitis, L. A., and Anderson, J. M. (1998). "The tight junction protein ZO-1 establishes a link between the transmembrane protein occludin and the actin cytoskeleton." *J Biol Chem.* **273**(45): 29745-53.

Fanning, A. S., Mitic, L. L., Anderson, J. M. (1999). "Transmembrane proteins in the tight junction barrier." *J Am Soc Nephrol* **10**(6): 1337-45.

Fellay, B., Chofflon, M., Juillard, C., Paunier, A-M., Landis, T., Roth, S. and Gougeon, M.-L. (2001). "Beneficial effect of co-polymer 1 on cytokine production by CD4 T cells in multiple sclerosis." *Immunology* **104**: 383-91.

Feltz, E. T. and Regelson, W. (1962). "Ethylene maleic anhydride copolymers as viral inhibitors." *Nature* **196**: 642-5.

Fernandez, L. E., Valiente, O. G., Mainardi, V., Bello, J. L., Velez, H., Rosado, A. (1989). "Isolation and characterization of an antitumor active agar-type polysaccharide of Gracilaria dominguensis." *Cabohydr Res* **190**(1): 77-83.

Field, M., Fromm, D. and McColl, I. (1971). "Ion transport in rabbit ileal mucosa. I. Na and Cl fluxes and short-circuit current." *Am J Physiology* **220**(5): 1388-96.

Fields, J. E., Asculai, S. S., Johnson, J. H., Johnson, R. K. (1982). "Carboxyimamidate, a low-molecular-weight polyelectrolyte with antitumor properties and low toxicity." *J Med Chem* **25**(9): 1060-4.

Fihn, B. M. and Jodal, M. (2001). "Permeability of the proximal and distal rat colon crypt and surface epithelium to hydrophilic molecules." *Pflugers Arch* **441**(5): 656-62.

Finlay, G. J., Wilson, W. R. and Baguley, B. C. (1986). "Comparison of in vitro activity of cytotoxic drugs towards human carcinoma and leukaemia cell lines." *Eur J Cancer Clin Oncol* **22**(6): 655-62.

Fischer, D., Li, Y., Alemeyer, B., Krieglstein, J. and Kissel, T. (2003). "In vitro cytotoxicity testing of polycations: influence of polymer structure on cell viability and hemolysis." *Biomaterials* **24**: 1121-31.

Fish, S. M., Proujansky, R. and Reenstra, W. W. (1999). "Synergistic effects of interferon gamma and tumour necrosis factor alpha on T84 cell function." *Gut* **45**(2): 191-8.

Flo, T., Ryan, L., Skjak-Break, G., Ingalls, R. R., Sundan, A., Golenbock, D. T. and Espevik, T. (2000). "Involement of CD14 and beta2-integrins in activating cells with soluble and particulate lipopolysaccharides and mannuronic acid polymers." *Infect Immun* **68**(12): 6770-6.

Flo, T., Ryan, L., Latz, E., Takeuchi, O., Monks, B. G., Lien, E., Halaas, O., Akira, S., Skjak-Braek, G., Golenbock, D. T. and Espevik, T. (2002). "Involvement of toll-like receptor (TLR) 2 and TLR4 in cell activation by mannuronic acid polymers." *J Biol Chem* **277**(33): 35489-95.

Fogh, J., Fogh, J. M. and Orfeo, T. (1977). "One hundred and twenty-seven cultured human tumor cell lines producing tumors in nude mice." *J Natl Cancer Inst* **59**(1): 221-6.

Franks, F. (1998). "Freeze-drying of bioproducts: putting principles into practice." *Eur J*

Pharm Biopharm **45**(3): 221-9.

Fraser, J. R. and Laurent, T. C. (1989). "Turnover and metabolism of hyaluronan." *Ciba Found Symp* **143**: 41-53; discussion 53-9, 281-5.

Fridkis-Hareli, M., Santambrogio, L., Stern, J. N. H., Fugger, L., Brosnan, C. and Strominger, J. L. (2002). "Novel synthetic amino acid copolymers that inhibit autoantigen-specific T cell responses and suppress experimental autoimmune encephalomyelitis." *J. Clin. Invest.* **109**: 1635-43.

Furuse, M., Itoh, M., Hirase, T., Naqafuchi, A., Yonemura, S., Tsukita, S. and Tsukita S. (1994). "Direct associations of occludin with ZO-1 and its possible involvement in the localization of occudin at tight junctions." J *Cell Biol* **127**(6 Pt 1): 1617-26.

Furuse, M., Sasaki, H., Fujimoto, K. and Tsukita, S. (1998). "A single gene product, claudin-1 or 2, reconstitutes tight junction strands and recuits occuldin in fibroblasts." *J.Cell Biol* **143**: 391-401.

G

Garcia de Galdeano, A., Boyano, M. D., Smith-Zubiaga, I. and Canavate, M. L. (1996). "B16F10 murine melanoma cells express interleukin-2 and a functional interleukin-2 receptor." *Tumour biology* **17**(3): 155-67.

Ghandehari, H., Smith, P. L., Ellens, H., Yeh, P. Y. and Kopecek, J. (1997). "Size-dependent permeability of hydrophilic probes across rabbit colonic epithelium." *J Pharmacol Exp Ther* **280**(2): 747-53.

Giantonio, B. J., Hochster, H., Blum, R., Wiernik, P. H., Hudes, G. R., Kirkwood, J., Trump, D. and Oken, M. M. (2001). "Toxicity and response evaluation of the interferon inducer poly ICLC administered at low dose in advanced renal carcinoma and relapsed or refractory lymphoma: a report of two clinical trials of the Eastern Cooperative Oncology Group." *Invest New Drugs* **19**(1): 89-92.

Gitter, A. H., Bendfeldt, K. Schmitz, H., Schulzke, J. D., Bentzel, C. J. and Fromm, M. (2000a). "Epithelial barrier defects in HT-29/B6 colonic cell monolayers induced by tumor necrosis factor-alpha." *Ann N Y Acad Sci* **915**: 193-203.

Gitter, A. H., Bendfeldt, K., Schulzke, J. D. and Fromm, M. (2000b). "Leaks in the epithelial barrier caused by spontaneous and TNF-alpha-induced single-cell apoptosis." *FASEB J* **14**(12): 1749-53.

Godbey, W. T., Wu, K. K. and Mikos, A. G. (1999). "Tracking the intracellular path of poly(ethylenimine)/DNA complexes for gene delivery." *Proc Natl Acad Sci USA* **96**(51): 5177-81.

Gonzalez-Mariscal, L., Islas, S., Contreras, R. G., Garcia-Villegas. M. R., Betanzos, A., Vega, J., Diaz-Quinonez, A., Martin-Orozco, N., Ortz-Navarrete, V., Cereijide, M. and Valdes, J. (1999). "Molecular characterization of the tight junction protein ZO-1 in MDCK cells." *Exp Cell Res* **248**(1): 97-109.

Gonzalez-Mariscal, L., Betanzos, A., Nava, P. and Jaramillo, B. E. (2003). "Review Tight Junction proteins." *Prog Biophys Mol Biol* **81**: 1-44.

Goodell, E. M., Ottenbrite, R. M. and Munson, A. E. (1978). "Polymaleic anhydride:

effects on the immune system and Friend leukemia disease of mice." *J Reticuloendothel Soc* **23**(3): 183-93.

Goricha, D. and Duncan, R. (2001). "Do polymers interact with cells to stimulate cytokine release?" *Thesis (MPharm IV)*, Cardiff University.

Goto, M., Masuda, S., Saito, H., Inui, K. (2003). "Decreased expression of P-glycoprotein during differentiation in the human intestinal cell line Caco-2." *Biochem Pharmacol* **66**(1): 163-70.

Gottardi, C. J., Arpin, M., Fanning, A. S. and Louvard, D. (1996). "The junction-associated protein, zonula occludens-1, localizes to the nucleus before the maturation and during the remodeling of cell-cell contacts." *Proc Natl Acad Sci USA* **93**(20): 10779-84.

Gotze, K. S., Keller, U., Rose-John, S. and Peschel, C. (2001). "gp130-stimulating designer cytokine Hyper-interleukin-6 synergises with murine stroma for long-term survival of primitive human hematopoietic progenitor cells." *Exp Heamatol* **29**: 822-32.

Granath, K. A. (1958). "Solution properties of branched dextrans." *J Colloid Science* **13**(4): 308-28.

Grass, G. M. and Sweetana, A. (1988). "In vitro measurement of gastrointestinal tissue permeability using a new diffusion cell." *Pharm Res* **5**(6): 372-6.

Green, M. and Stahmann, M. A. (1953). "Inhibition of mumps virus multiplication by a synthetic polypeptide." *Proc Soc Exp Biol Med* **83**(4): 852-8.

Greene, C. M., McElvaney, N. G., O'Neil, S. J. and Taggart, C. (2004). "Secretory leucoprotease inhibitor impairs Toll-like receptor 2- and 4- medated responces in monocytic cells." *Am Soc Microbiol* **72**(6): 3684-7.

Gros, L., Ringsdrof, H., and Schupp, H. (1981). "Polymeric Antitumor Agents on a Molecular and on a Celluar Level?" *Angew Chem.* **20**: 305-25.

Grose, R., Werner, S., Kessler, D., Tuckermann, J., Huggel, K., Durka, S. and Reichardt, H. M. (2002). "A role for endogenous glucocorticoids in wound repair." *EMBO Rep* **3**(6): 575-82.

Gum, J. R. Jr., Hicks, J. W., Toribara, N. W., Rothe, E. M., Lagace, R. E., and Kim, Y. S. (1992). "The human MUC2 intestinal mucin has cysteine-rich subdomains located both upstream and downstream of its central repetitive region." *Biol Chem* **267**(30): 21375-83.

H

Han, X., Fink, M. P. and Delude, R. L. (2002). "Proinflammatory cytokines cause NO*-dependant and -independant changes in expression and localisation of tight junction proteins in intestinal epithelial cells." *Shock* **19**(3): 229-37.

Hanauske, A. R., Melink, T. J., Harman, G. S., Clark, G. M., Craig, J. B., Koeller, J. M., Boldt, D. H., Kantor, B., Kisner, D. L., Orczyk, G. *et al.* (1988). "Phase I clinical trial of carbetimer." *Cancer Res* **48**(18): 5353-7.

Haque, T., Chen, H., Ouyang, W., martoni, C., Lawuyi, B., Urbanska, A. M. and Prakash, S. (2005). "Superior cell delivery features of poly(ethylene glycol) incorporated alginate, chitosan, and poly-L-lysine microcapsules." *Mol Pharm* **2**(1): 29-36.

Harris, M. J. and Chess, R. B. (2003). "Effect of pegylation on pharmaceuticals." *Nat Rev Drug Discovery* **2**: 214-221.

Haskins, J., Gu, L., Wittchen, E. S., Hibbard, J. and Stevenson, B. R. (1998). "ZO-3, a novel member of the MAGUK protein family found at the tight junction, interacts with ZO-1 and occludin." *J Cell Biol* **141**(1): 199-208.

Haugland, R. P. (2002). *Handbook of Fluorescent and Molecular Probes and Research Products*. Oregon, USA: Molecular Probes Inc.

Hauri, H. P., Roth, J., Sterchi, E. E. and Lentze, M. J. (1985). "Transport to cell surface of intestinal sucrase-isomaltase is blocked in the Golgi apparatus in a patient with congenital sucrase-isomaltase deficiency." *Proc Natl Acad Sci USA* **82**(13): 4423-7.

Heald, K. A., Jay, T. R. and Downing, R. (1994). "Assessment of the reproducibility of alginate encapsulation of pancreatic islets using the MTT colorimetric assay." *Cell Transplant* **3**(4): 333-7.

Heming, T. A., Tuazon, D. M., Dave, S. K., Chopra, A. K., Peterson, J. W. and Bidani, A. (2001). "Post-transcriptional effects of extracellular pH on tumour necrosis factor-α production in RAW 246.7 and J774 A.I cells." *Clin Sci* **100**: 259-266.

Hermanson, G. T. (1996). *Bioconjugate techniques*. London, UK: Academic Press Inc.

Hidalgo, I. J., Kato, A. and Borchardt, R. T. (1989). "Binding of epidermal growth factor by human colon carcinoma cell (Caco-2) monolayers." *Biochem Biophys Res Commun* **160**(1): 317-24.

Hilgendorf, C., Spahn-Langguth, H., Regardh, C., Lipka, E., Amidon, G.L. and Langguth, P. (2000). "Caco-2 versus Caco-2/HT29-MTX co-cultured cell lines: Permesbilities via diffusion, inside-and outside-directed carrier-medicated transport." *J Pharm Sci* **89**: 63-75.

Hilgers, A. R., Conradi, R. A. and Burton, P. S. (1990). "Caco-2 cell monolayers as a model for drug transport across the intestinal mucosa." *Pharm Res* 7(9): 902-10.

Hillery, A. M., Lloyd, A. W. and Swarbick, J. (2001). "Drug delivery the basic concepts." In Hillery, A. M., Lloyd, A. W. and Swarbrick, J. (Eds.), *Drug Delivery and Targeting: for Pharmacists and Pharmaceutical Scientists*. London, UK: Taylor Francis.

Hoare, D. G. and Koshland, D. E. Jr. (1967). "A method for the quantitative modification and estimation of carboxylic acid groups in proteins." *J Biol Chem* **242**(10): 2447-53.

Hodge-Dufour, J., Noble, P. W., Horton, M.R., Boa, C., Wysoka, M., Burdick, M. D., Strieter, R. M., Trinchieri, G. and Pure, E. (1997). "Induction of IL-12 and chemokines by hyaluronan requires adhesion-dependent priming of resident but not elicited macrophages." *J Immunol* **159**(5): 2492-500.

Hodnett, E. M. and Tai, J. T. H. (1974). "Polymeric anions and biological activities. Effects on intramuscular and intraperitoneal Walker carcinoma 256 of the rat." *J Med Chem* **17**(12): 1335-7.

Hoogstraate, A. J., Cullander, C., Nagelkerke, J. F., Senel, S., Verhoef, J. C., Junginger, H. E. and Bodde, H. E. (1994). "Diffusion rates and transport pathways of fluorescein isothiocyanate (FITC)-labelled model compounds through buccal epithelium." *Pharm Res* **11**(1): 83-9.

Horie, T., Awazu, S., Itakura, Y. and Fuwa, T. (2001). "Alleviation by garlic of antitumor drug-induced damage to the intestine." *J Nutr* **131**(3s): 1071S-4S.

Hosoya, K. I., Kim, K. J. and Lee, V. H. (1996). "Age-dependent expression of P-glycoprotein gp170 in Caco-2 cell monolayers." *Pharm Res* **13**(6): 885-90.

Hug, M. J., Sheppard, D. N. and Li, H. (2004). "Transepithelial measurements using the Ussing chamber." *J Cyst Fibros* **3**(2): 123-6.

Hughes, S. E. (1996). "Functional characterisation of the spontaneously transformed human umbilical vein endothelial cell line ECV304: use in an in vitro model of angiogenesis." *Exp Cell Res* **225**(1).

Hunt, J. A., Flanagan B. F., Mclaughlin P. J., Strickland I., and Williams D. F. (1996). "Effect of biomaterial surface charge on the inflammatory response: evaluation of cellular infiltration and TNF alpha production." *J Biomed Mater Res* **31**(1): 139-44.

I

Ishibashi, K-I., Miura, N. N., Adachi, Y. and Ohno, N. (2001). "Relationship between solubility of Grifolan, a fungal 1,3-β-D-glucan, and production of tumour necrosis factor by macrophages in vitro." *Biosci Biotechnol Biochem* **65**(9): 1993-2000.

Islas, S., Vega, J., Ponce, L. and Gonzlez-Mariscal, L. (2002). "Nuclear localization of the tight junction protein ZO-2 in epithelial cells." *Exp Cell Res* **274**(1): 138-48.

Ito, M., Kodama, M., Masuko, M., Yamaura, M., Fuse, K., Uesugi, Y., Hirono, S., Okura, Y., Kato, K., Hotta, Y., Honda, T., Kuwano, R., and Aizawa, Y. (2000). "Expression of coxsackievirus and adenovirus receptor in hearts of rats with experimental autoimmune myocarditis." *Circ Res* **86**(3): 275-80.

Itoh, M., Furuse, M., Morita, K., Kubota, K., Saitou, M. and Tsukita, S. (1999). "Direct binding of three tight junction-associated MAGUKs, ZO-1, ZO-2 and ZO-3 with the COOH termini of claudins." *J Cell Biol* **147**(6): 1351-63.

Izzo, L. (2004). "Intracellular trafficking of polymeric mimetics designed for gene and oligonucleotide therapeutics." *BBSRC Report.* Cardiff University.

J

Jahr, T. G., Ryan, L., Sundan, A., Lichenstein, H. S., Skjak-Break, G. and Espevik, T. (1997). "Induction of tumour necrosis factor production from monocytes stimulated with mannuronic acid polymers and involvement of lipopolysaccharide-binding protein, CD14, and bacterial/permeability-increasing factor." *Infect Immun* **65**(1): 89-94.

James, A. M., Ambrose, E. J. and Lowick, J. H. (1956). "Differences between the

electrical charge carried by normal and homologous tumour cells." *Nature* **177**(4508): 576-7.

Jatzkewitz, H. (1954). "[Incorporation of physiologically-active substances into a colloidal blood plasma substitute. I. Incorporation of mescaline peptide into polyvinylpyrrolidone]." *Hoppe Seylers Z Physiol Chem* **297**(3-6): 149-56.

Jensen, K. D., Kopeckova. P., Bridge, J. H. and Kopecek, J. (2001). "The cytoplasmic escape and nuclear accumulation of endocytosed and microinjected HPMA copolymers and a basic kinetic study in Hep G2 cells." *AAPS Pharm Sci* **3**(4): E32.

Jevprasesphant, R., J. Penny, J., Attwood, D. and D'Emaunuele, A. D. (2003a). "Engineering of dendrimer surfaces to enhance transepithelial transport and reduce cytotoxicity." *Pharm Res* **20**(10): 1543-50.

Jevprasesphant, R., Penny, J., Attwood, D., McKeown, N. B. and D'Emanuele, A. D. (2003b). "The influence of surface modification on the cytotoxicity of PAMAM dendrimers." *Int J Pharm* **252**(1-2): 263-6.

Jevprasesphant, R., Penny, J., Attwood, D. and D'Emanuele, A. D. (2004). "Transport of dendrimer nanocarriers through epithelial cells via the transcellular route." *J Control Release* **97**: 259-67.

Joost, J. O. and Feldman, M. (2001). "Introduction to the role of cytokines in innate host defense and adaptive immunity." In Joost, J. O., Feldman, M. Durum, S. K., Hirano, T., Vilcek, J. and Nicola, N. A. (Eds.), *Cytokine Reference: A Compendium of Cytokines and other Mediators of Host Defense*: 3-20. London, UK: Academic Press.

Jorgensen, J. H. and Lee, J. C. (1978). "Rapid diagnosis of gram-negative bacterial meningitis by the Limulus endotoxin assay." *J Clin Microbiol* **7**(1): 12-7.

Junginger, H. E., Hoogstraate, J. A. and Verhoef, J. A. (1999). "Recent advances in buccal drug delivery and absorption-*in vitro* and *in vivo* studies." *J Control Release* **62**(1-2): 149-59.

K

Kabanov, V. A. (2004). "From Synthetic Polyelectrolytes to Polymer-Subunit Vaccines." *Polymer Science Ser A.* **46**(5): 451-70.

Kannan, S., Kolhe, P., Raykova, V., Gilbatec, M., Kannan, R. M. and Lieh-Lai, M. (2004). "Dynamics of cellular entry and drug delivery by dendritic polymers into human lung epithelial carcinoma cells." *J Biomater Sci Polym Ed* **15**(3): 311-30.

Kast, C. E. and Bernkop-Schnurch, A. (2002). "Influence of the molecular mass on the permeation enhancing effect of different poly(acrylates)." *S.T.P. Pharma Sciences* **12**(6): 351-56.

Kawaguchi, H., Akazawa, Y., Watanabe, Y., and Takakura, Y. (2005). "Permeability modulation of human intestinal Caco-2 cell monolayers by interferons." *Eur J Pharm Biopharm* **59**: 45-50.

Kean, T., Roth, S. and Thanou, M. (2005). "Trimethylated chitosans as non-viral gene delivery vectors: cytotoxicity and transfection efficiency." *J Control Release*

103(3): 643-53.

Kemppainen, T., Tammi, R., Tammi, M., Agren, U., Julkunen, R., Bohm, J., Uusitupa, M. and Kosma, V. M. (2005). "Elevated expression of hyaluronan and its CD44 receptor in the duodenal mucosa of coeliac patients." *Histopathology* **46**(1): 64-72.

Kim, H. R., Wheeler, M. A. Wilson, C. M., Iida, J., Eng, D., Simpson, M. A. Mccarthy, J. B. and Bullard, K. M. (2004). "Hyaluronan Facilitates Invasion of Colon Carcinoma Cells in Vitro via Interaction with CD44." *Cancer Res* **64**: 4569-76.

Kishimoto, T. (2005). "IL-6: from laboratory to bedside." *Clin Rev Allergy Immunol* **28**(3): 177-86.

Kiyono, H. and Fukuyama, S. (2004). "NALT-versus Peyer's-patch-mediated mucosal immunity." *Nat Rev Immunol* **4**(9): 699-710.

Knowles, D. M. (2001). "Biology of non-Hodgkin's lymphoma." *Cancer Treat Res* **104**: 149-200.

Kodaira, Y., Nair, S. K., Wrenshall, L. E., Giboa, E. and Platt, J. L. (2000). "Phenotypic and functional maturation of dendritic cells mediated by heparan sulfate." *J Immunol* **165**(3): 1599-604.

Korovkin, B. F., Eshina, E. F. and Predtechenskii, A. N. (1963). "[Colorimetric method of determining serum lactic dehydrase (lactate dehydrogenase) and its use in clinical practice]." *Lab Delo* **9**: 17-20.

Kotze, A. F., Luessen, H. L., De Luessen, B. J., De Boer, B. G., Verhoef, J. C. and Junginger, H. E. (1997). "N-trimethyl chitosan chloride as a potential absorption enhancer across mucosal surfaces: in vitro evaluation in intestinal epithelial cells (Caco-2)." *Pharm Res* **14**(9): 1197-202.

Kotze, A. F., Thanou, M. M., Luebetaen, H. L., De Boer, B. G., Verhoef, J. C. and Junginger, H. E. (1999). "Enhancement of paracellular drug transport with highly quaternized N-trimethyl chitosan chloride in neutral environments: in vitro evaluation in intestinal epithelial cells (Caco-2)." *J Pharm Sci* **88**(2): 253-7.

Kreitman, R. J., Chaudhary, V. K., Kozak, R. W., FitzGerald, D. J., Waldman, T. A. and Pastan, I. (1992). "Recombinant toxins containing the variable domains of the anti-Tac monoclonal antibody to the interleukin-2 receptor kill malignant cells from patients with chronic lymphocytic leukemia." *Blood* **80**(9): 2344-52.

Kriwet, B. (1996). "Polyacrylic acid microparticles widen the intercellular spaces of Caco-2 cell monolayers: an examination by confocal laser scanning microscopy." *Eur J Pharm Biopharm* **42**(4).

Kondoh, M., Takahashi, A., Fujii, M., Yagi, K. and Watanbe, Y. (2006). "A novel strategy for a drug delivery system using a claudin modulator." *Bio Pharm Bull* **29**(9): 1783-89.

Kubala, L., Ruzickova, J., Nickova, K., Sandula, J., Ciz, M. and Lojek, A. (2003). "The effect of (1-3)-β-D-glucans, carboxymethylglucan and schizophyllan on human leukocytes in vitro." *Carbohydr Res* **338**: 2835-2840.

Kunath, K., Von Harpe, A., Fischer, D., Petersen, H., Bickel, U., Voigt, K. and Kissel, T. (2003). "Low-molecular-weight polyethylenimine as a non-viral vector for DNA delivery: comparison of physicochemical properties, transfection efficiency and in vivo distribution with high-molecular-weight polyethylenimine." *J Control Res* **89**(1): 113-25.

L

Lacombe, O., Woodley, J., Solleux, C., Delbos, J. M., Boursier-Neyret, C. and Houin, G. (2004). "Localisation of drug permeability along the rat small intestine, using markers of the paracellular, transcellular and some transporter routes." *Eur J Pharm Sci* **23**(4-5): 385-91.

Lanza, R. P., Jackson, R., Sullivan, A., Ringeling, J., McGarth, C., Kuhtreiber, W. and Chick, W. L. (1999). "Xenotransplantation of cells using biodegradable microcapsules." *Transplantation* **67**(8): 1105-11.

Lavelle, E. C., Sharif, S., Thomas, N. W., Holland, J., and Davis, S. S. (1995). "The importance of gastrointestinal uptake of particles in the design of oral delivery systems." *Adv Drug Deliv Rev* **18**: 5-22.

Lavignac, N., Lazenby, M., Foka, P., Malgesini, B., Verpilio, I., Ferruti, P. and Duncan, R. (2004). "Synthesis and endosomolytic properties of poly(amidoamine) block copolymers." *Macromol Biosci* **4**(10): 922-9.

Lechner, F., Sahrbacher, U., Suter, T., Frei, K., Brockhaus, M., Koedel, U. and Fontana, A. (2000). "Antibodies to the junctional adhesion molecule cause disruption of endothelial cells and do not prevent leukocyte influx into the meninges after viral or bacterial infection." *J Infect Dis* **182**(3): 978-82.

Lee, K. J., Johnson, N., Castelo, J., Sinko, P. J., Grass, G, and Holme, K. (2005). "Effect of experimental pH on the in vitro permeability in intact rabbit intestines and Caco-2 monolayer." *Eur J Pharm Sci* **25**(2-3): 193-200.

Lee, N. J., Kang, N. I., Cho, W .J., Kim, S. H., Kang, K. T. and Theodorakis, E.A. (2001). "Synthesis and biological activity of medium range molecular weight polymers containing exo-3, 6-epoxy-1,2,3,6-tetrahydrophthalimido-caproic acid." *Polm Int* **50**: 1010-15.

Lee, Y. S., Chung, I. S., Lee, I. R., Kim, K. H., Hong, W. S. and Yun, Y. S. (1997). "Activation of multiple effector pathways of immune system by the antineoplastic immunostimulator acidic polysaccharide ginsan isolated from Panax ginseng." *Anitcancer Res* **17**(1A): 232-31.

Liao, J. and Ottenbrite, R. M. (1997). Biological effects of polymeric drugs. In *Controlled drug delivery challanges and strategies.* Edited by Park, K., and Washington D. C., American chemical society: 455-67.

Lin, J. H. (1996). "Bisphosphonates: a review of their pharmacokinetic properties." *Bone* **18**(2): 75-85.

Lindmark, T., Schipper, N., Lazorova, L., De Boer A. G. and Artursson, P. (1997). "Absorption enhancement in intestinal epithelial Caco-2 monolayers by sodium caprate: assessment of molecular weight dependence and demonstration of

transport routes." *J Drug Target* **5**(3): 215-23.

Liu, Y., Nusrat, A., Schnell, F. J., Reaves, T. A., Walsh, S., Pochet, M. and Parkos, C. A. (2000). "Human junction adhesion molecule regulates tight junction resealing in epithelia." *J Cell Sci* **113**(13): 2363-74.

Loty, S., Sautier, J. M., Loty, C., Boulekbache, H., Kokubo, T. and Forest, N. (1998). "Cartilage formation by fetal rat chondrocytes cultured in alginate beads: a proposed model for investigating tissue-biomaterial interactions." *J Biomed Mater Res* **42**(2): 213-22.

Lotze, M. T., Frana, L. W., Sharrow, S. O., Robb, R. J. and Rosenberg, S. A. (1985). "In vivo administration of purified human interleukin 2. I. Half-life and immunologic effects of the Jurkat cell line-derived interleukin 2." *J Immunol* **134**(1): 157-66.

Luo, Y., Ziebell, M. R. and Prestwich, G. D. (2000). "A hyaluronic acid-taxol antitumor bioconjugate targeted to cancer cells." *Biomacromolecules* **1**(2): 208-18.

M

Ma, T. Y., Iwamoto, G. K., Hoa, N. T., Akotia, V., Pedram, A., Boivin, M. A. and Said, H. M. (2004). "TNF-alpha-induced increase in intestinal epithelial tight junction permeability requires NF-kappa B activation." *Am J Physiol Gastrointest Liver Physiol* **286**(3): G367-76.

MacDonald, T. T. (2003). "The mucosal immune system." *Parasite Immunol* **25**(5): 235-46.

Mackenzie, C. G., Mackenzie, J. B. and Beck, P. (1961). "The effect of pH on growth, protein synthesis, and lipid-rich particles of cultured mammalian cells." *J Biophys Biochem Cytol* **9**: 141-56.

Madara, J. L., Stafford, J., Dharmsathaphorm, K. and Carlson, S. (1987). "Structural analysis of a human intestinal epithelial cell line." *Gastroenterology* **92**(5 Pt 1): 1133-45.

Madara, J. L. and Stafford, J. (1989). "Interferon-γ directly affects barrier function of cultured intestinal epithelial monolayers." *J Clin Invest* **83**: 724-7.

Malik, N., Evagorou, E. G. and Duncan, R. (1999). "Dendrimer-platinate: a novel approach to cancer chemotherapy." *Anticancer Drugs* **10**(8): 767-76.

Malik, N., Wiwattanapatapee, R., Klopsch, R., Lorenz, K., Frey, H., Weener, J. W., Meijer, E. W., Paulus, W. and Duncan, R. (2000). "Dendrimers: Relationship between structure and biocompatibility in vitro, and preliminary studies on the biodistribution of ^{125}I-labelled polyamidoamine dendrimers in vivo." *J Control Res* **65**: 133-148.

Manjili, M. H., Park, J-E., Facciponte, J. G., Wang, X.-Y. and Subjeck, J. R. (2006). "Immunoadjuvant chaperone, GRP170, induces 'danger signals' upon interaction with dendritic cells." *Immunol Cell Biol* **82**(2): 203.

Marano, C. W., Lewis, S. A., Garulacan, L. A., Soler, A. P. and Mullin, J. M. (1998). "Tumor necrosis factor-α increases sodium and chloride conductance across the tight junction of CACO-2 BBE, a human intestinal epithelial cell line." *J Membr*

Biol **161**(3): 263-74.

Mascarenhas, M. M., Day, R. M., Ochoa, C. D., Choi, W-I., Yu, L. and Ouyang, B. (2004). "Low molecular wieght hyaluronan from stretched lung enhances interleukin-8 expression." *Am J Respir Cell Mol Biol* **30**: 51-60.

McCarthy, K. M., Skare, I. B., Stankewich, M. D., Furuse, M., Tsukita, S., Rogers, R. A. Lynch, R. D. and Schneeberger, E. E. (1996). "Occluldin is a functional component of the tight junction." *J Cell Sci* **109**: 1031-1049.

McKay, D. M., Croitoru, K. and Perdue, M. H. (1996). "T cell-monocyte interactions regulate epithelial physiology in a coculture model of inflammation." *Am J Physiol* **270**(2) Pt 1): C418-28.

Mehvar, R. (2000). "Dextrans for targeted and sustained delivery of therapeutic and imaging agents." *J Control Release* **69**(1): 1-25.

Mellman, I. (1996). "Endocytosis and molecular sorting." *Ann Rev Cell Biol* **12**: 575-625.

Mendoza, C. E., Rosado, M. F., and Bernal, L. (2001). "The role of interleukin-6 in cases of cardiac myxoma. Clinical features, immunologic abnormalities, and possible role in recurrence." *Tex Heart Inst J* **28**(1): 3-7.

Mishima, T., Murata, J., Toyoshima, M., Fuji, H., Nakajima, M., Hayashi, T., Kato, T. and Saiki, I. (1998). "Inhibition of tumor invasion and metastasis by calcium spirulan (Ca-SP), a novel sulfated polysaccharide derived from a blue-green alga, Spirulina platensis." *Clin Exp Metastasis* **16**(6): 541-50.

Moghimi, S. M., Symonds, P., *et al.* (2005). "A two-stage poly(ethylenimine)-mediated cytotoxicity: implications for gene transfer/therapy." *Mol Ther* **11**(6): 990-5.

Monti, P., Leone, B. E., Zerbi, A., Balzano, G., Cainarca, S., Sordi, V., Pontillo, M., Mercalli, A., DiCarlo, V., Allavena, P. and Piemonti, L. (2004). "Tumor-derived MUC1 mucins interact with differentiating monocytes and induce IL-10 high IL-12 low regulatory dendritic cell." *J Immunol* **172**(12): 7341-9.

Morgan, S. M., Al-Shamkhani, A., Callant, D., Schact, E., Woodley, J. F. and Duncan, R. (1995). "Alginates as drug carriers: covalent attachment of alginates to therapeutic agents containing primary amine groups." *Int J Pharm* **122**: 121-8.

Morimoto, K., Yamaguchi, H., Iwakura, Y., Morisaka, K., Ohashi, Y. and Nakai, Y. (1991). "Effects of viscous hyaluronate-sodium solutions on the nasal absorption of vasopressin and an analogue." *Pharm Res* **8**(4): 471-4.

Morita, K., Itoh, M., Saitou, M., Ando-Akatsuka, Y., Furuse, M., Yoneda, K., Imamura, S., Fujimoto, K. and Tsukita, S. (1998). "Subcellular distribution of tight junction-associated proteins (occludin, ZO-1, ZO-2) in rodent skin." *J Invest Dermatol* **110**(6): 862-6.

Morita, K., Sasak, I. H., Furuse, M. and Tsukita, S. (1999). "Endothelial claudin: claudin-5/TMVCF constitutes tight junction strands in endothelial cells." *J Cell Biol* **147**(1): 185-94.

Moroson, H. (1971). "Polycation-treated tumor cells in vivo and in vitro." *Cancer Res*

31(3): 373-80.

Mosmann, T. (1983). "Rapid colorimetric assay for cellular growth and survival: application to proliferation and cytotoxicity assays." *J Immunol Methods* **65**(1-2): 55-63.

Motlekar, N. A., Fasano, A., Wachtel, M. S. and Youan, B. B. (2006) "Zonula occludens toxin synthetic peptide derivative AT1002 enhances in vitro and in vivo intestinal absorption of low molecular weight heparin". *J Drug Target* **133**(2): 321-9

Mrsny, R. J. (2005). "Modification of epithelial tight junction integrity to enhance transmucosal absorption." *Crit Rev Ther Drug Carrier Syst* **22**(4): 331-418.

Mulhaupt, R. (2006). "Hermann Staudinger Award 2006." *Macromol Biosci* **6**(2): 187-8.

Mullin, J. M. and Snock, K. V. (1990). "Effect of tumor necrosis factor on epithelial tight junctions and transepithelial permeability." *Cancer Res* **50**(7): 2172-6.

Mummert, M. E., Mummert, D., Edelbaum, D., Hui, F., Matsue, H. and Takashima, A. (2002). "Synthesis and surface expression of hyaluronan by dendritic cells and its potential role in antigen presentation." *J Immunol* **169**: 4322-31.

Murch, S. H., Braegger, C. P., Walker-Smith, J. A. and MacDonald, T. T. (1993). "Location of TNF-α by immunohistochemistry in chronic inflammatory bowel disease." *Gut* **34**(12): 1705-9.

N

Nafee, N. A., Ismail, F. A., Boraie, N. A. and Mortada, L. M. (2004). "Mucoadhesive delivery systems. I. Evaluation of mucoadhesive polymers for buccal tablet formulation." *Drug Dev Ind Pharm* **30**(9): 985-93.

Nakamura, K., Maitani, Y. and Takayama, K. (2002). "The enhancing effect of nasal absorption of FITC-dextran 4,400 by beta-sitosterol beta-D-glucoside in rabbits." *J Control Release* **79**(1-3): 147-55.

Nakamura, K., Takayama, K., Nagai, T. and Maitani, Y. (2003). "Regional intestinal absorption of FITC-dextran 4,400 with nanoparticles based on beta-sitosterol beta-D-glucoside in rats." *J Pharm Sci* **92**(2): 311-8.

Nathan, C. F., Horowitz, C. R., De La Harpe, J., *et al.* (1985). "Administration of recombinant interferon gamma to cancer patients enhances monocyte secretion of hydrogen peroxide." *Proc Natl Acad Sci USA* **82**: 8686-8690.

Nejdfors, P. Ekelund, M., Jeppsson, B. and Westrom, B. R. (2000). "Mucosal in vitro permeability in the intestinal tract of the pig, the rat, and man: species- and region-related differences." *Scand J Gastroenterol* **35**(5): 501-7.

Ng, M. L. and Yap, A. T. (2002). "Inhibition of human colon carcinoma development by lentinan from shiitake mushrooms (Lentinus edodes)." *J Altern Complement Med* **8**(5): 581-9.

Nishiyama, R., Sakaguchi, T., Kinugasa, T., Gu, X., MacDermott, P., Podolsky D.K. and Reinecker, H. C. (2001). "Interleukin-2 receptor beta subunit-dependent and -independent regulation of intestinal epithelial tight junctions." *J Biol Chem*

276(38): 3557-80.

Noble, P. W., Lake, F. R., Henson, P. M. and Riches, D. W. (1993). "Hyaluronate activation of CD44 induces insulin-like growth factor-1 expression by a tumor necrosis factor-alpha-dependent mechanism in murine macrophages." *J Clin Invest* **91**(6): 2368-77.

Nusrat, A., Turner, J. R. and Madara, J. L. (2000). "Molecular physiology and pathophysiology of tight junctions IV. Regulation of tight junctions by extracellular stimuli: nutrients, cytokines, and immune cells." *Am J Physiol Gastrointest Liver Physiol* **279**: G851-57.

O

Oh, K. H. and Margetts, P. J. (2005). "Cytokines and growth factors involved in peritoneal fibrosis of peritoneal dialysis patients." *Int J Artif Organs* **28**(2): 129-34.

O'Hare, K. B., Duncan, R., Strohalm, J., Ulbrich, K. and Kopecekova, P. (1993). "Polymeric drug-carriers containing doxorubicin and melanocyte-stimulating hormone: in vitro and in vivo evaluation against murine melanoma." *J Drug Target* **1**(3): 217-29.

Okhawara, Y., Tamura, G., Iwasaki, T., Tanaka, A., Kikuchi, T. and Shirato, K. (2000). "Activation and transforming growth factor-βproduction in eosinophils by hyaluronan." *Am J Resp Cell Mol Biol* **23**: 444-51.

Oppenheim, J. J. (2001). "Cytokines: past, present, and future." *Int J Hematol* **74**(1): 3-8.

Otter, W. D., Cadee, J., Gavhumende, R., De Groot, C. J., Hennink, W. E. and Stewart, R. (1999). "Short communication: Effective cancer therapy with a single injection of interleukin-2 at the site of the tumour." *Cancer Immunol Immunother* **48**: 419-420.

Otterlei, M., Ostgaard, K., Skjak-Break, G., Simsrod, O., Soon-Shiong, P. and Espevik, T. (1991). "Induction of cytokine production from human monocytes stimulated with alginate." *J Immuno Ther* **10**: 286-291.

Otterlei, M., Sundan. A., Skjak-Break, G., Ryan, L., Simsrod, O. and Espevik, T. (1993). "Similar mechanisms of action of defined polysaccharides and lipopolysaccharides: characterisation of binding and tumour necrosis factor alpha induction." *Infect Immun* **61**(5): 1917-1925.

Oude Elferink, R. P. and Paulusma, C. C. (2006). "Function and pathophysiological importance of ABCB4 (MDR3 P-glycoprotein)." *Pflugers Arch.* [epub ahead of print]

P

Pantzar, N., Lundin, S., Wester, L. and Westrom, B. R. (1994). "Bidirectional small-intestinal permeability in the rat to some common marker molecules in vitro." *Scand J Gastroenterol* **29**(8): 703-9.

Park, H., and Robinson, J.R., (1987). "Mechanisms of mucoadhesion of poly(acrylic acid) hydrogels." *Pharm Res* **4**(6): 457-64.

Parslow, T. G., Stites, D. P., Terr, A. I. and Imboden, J. B. (2001). "The immune response." In Parslow, T. G., Stites, D. P., Terr, A. I. and Imboden, J. B. (Eds.),

Medical Immunology: 6-71. San Francisco, USA: Lange Medical Books.

Pato, J., Mora, M., Naisbett, B, Woodley, J. F. and Duncan, R. (1994). "Uptake and transport of poly(N-vinylpyrrolidone-co-maleic acid) by rat small intestine cultured in vitro: Effect of chemical structure." *Int J Pharm* **104**: 227-37.

Peng, Q., Lai, D., Nguyen, T. T., Chen, V., Matsuda, T. and Hirst, S. J. (2005). "Multiple beta 1 integrins mediate enhancement of human airway smooth muscle cytokine secretion by fibronectin and type I collagen." *J Immunol* **174**(4): 2258-64.

Piccoli, M., Saito, T. and Chirigos, M. A. (1984). "Bimodal effects of MVE-2 on cytotoxic activity of natural killer cell and macrophage tumouricidal activities." *Int J Immunopharmac* **6**(6): 569-76.

Pinto, M., Appay, M-D., Simon-Assman, P., Chevalier, G., and Dracopoli, N. (1982). "Enterocytic differentiation of cultured human colon cancer cells by replacement of glucose by galactose in the medium." *Biol Cell* **44**: 193-96.

Pinto, M., Robine-Leon, S., Appay, M-D., Kedinger, M., Triadou, N., Dussaulx, E., Lacroix, B., Simon-Assmann, P., Haffen, K., Fogh, J., and Zweibaum, A. (1983). "Enterocyte-like differentiation and polarization of the human colon carcinoma cell line Caco-2 in culture." *Biol Cell* **47**: 323-30.

Plusquellec, Y. and Houin, G. (1987). "An open two-compartment model for a double site of drug absorption." *IEEE Trans Biomed Eng* **34**(1): 70-3.

Poritz, L. S., Garver, K. I., Tilberg, A. F. and Koltun, W. A. (2004). "Tumor necrosis factor alpha disrupts tight junction assembly." *J Surg Res* **116**(1): 14-8.

Pritchard, K., Lansley, A. B., Martin, G. P., Heliwell, M., Marriott, C. and Benedetti, L. M. (1996). "Evaluation of the bioadhesive properties of hyaluronan derivatives; detachment weight and mucociliary transport rate studies." *Int J Pharm* **129**: 137-145.

Pruden, E. L. and Winstead, M. E. (1964). "Accuracy control of blood cell counts with the coulter counter." *Am J Med Technol* **30**: 1-35.

Puckey, E. (2002). "An investigation into the ability of polymers to interact with cells to stimulate the release of TNF-α and IL-2." *Thesis (MPharm IV)*. Cardiff University.

R

Rafi, A., Nagarkatti, M. and Nagarkatti, P. S. (1997). "Hyaluronate-CD44 interactions can induce murine B-cell activation." *Blood* **89**(8): 2901-8.

Remie, R. (2000). "Experimental surgery." In Krinke, G. J. (Ed.), *The Handbook of Experimental Animals: The Laboratory Rat*. London, UK: Academic Press.

Richardson, S., Ferruit, P. and Duncan, R. (1999). "Poly(amidoamine)s as potential endosomolytic polymers: evaluation in vitro and body distribution in normal and tumour-bearing animals." *J Drug Target* **6**(6): 391-404.

Rietveld, I. B., Bouwman, W. G., Baars, M. W. P. L. and Heenan, R. K. (2001). "Location of the outer shell and influence of pH on carboxylic acid-functionalized poly(propyleneimine) dendrimers." *Macromolecules* **34**: 8380-8383.

Ringsdorf, H. (1975). "Structure and properties of pharmacologically active polymers." *J Polymer Sci* **51**: 135-53.

Robitaille, R., Dusseault, J., Henley, N., Desbiens, K., Labrecque, N. and Halle, J. P. (2005). "Inflammatory response to peritoneal implantation of alginate-poly-L-lysine microcapsules." *Biomaterials* **26**(19): 4119-27.

Rodriguez, P., Heyman, M., Candalh, C., Blaton, M. A. and Bouchaud, C. (1995). "Tumour necrosis factor-alpha induces morphological and functional alterations of intestinal HT29 cl.19A cell monolayers." *Cytokine* 7(5): 441-8.

Rodriguez-Ayerbe, C. and Smith-Zubiaga, I. (2000). "Effect of serum withdrawal on the proliferation of BI6F10 Melanoma Cells." *Cell Biol Int* **24**: 279-283.

Roehm, N. W., Rodgers, G. H., Hatfield, S. M. and Glasbrook, A. L. (1991). "An improved colorimetric assay for cell proliferation and viability utilizing the tetrazolium salt XTT." *J Immunol Methods* **142**(2): 257-65.

Roh, M. H., Liu, C. J., Laurinec, S. and Margolis, B. (2002). "The carboxyl terminus of zona occludens-3 binds and recruits a mammalian homologue of discs lost to tight junctions." *J Biol Chem* **277**(30): 27501-9.

Roig, T. and Vinardell, M. P. (1991). "Intestinal perfusion in vivo for the study of absorptive processes." *Comp Biochem Physiol A* **98**(1): 3-7.

Roitt, I. M. and Delves, P. J. (2001). *Roitt's Essential Immunology*. London, UK: Blackwell Publishing.

Rosenberg, S. A., Lotze, M. T., Muul, L. M., Leitman, S., Chang, A. E., Ettinghausen, S. E., Matory, Y. L., Skibber, J. M. *et al.* (1985). "Observations on the systemic administration of autologous lymphokine activated killer cells and recombinant interleukin-2 to patients with metastatic cancer." *Engl J Med* **313**: 1485.

Rubini, J. R., Rasmussen, A. F. Jr., *et al.* (1951). "Inhibitory effect of synthetic lysine polypeptides on growth of influenza virus in embryonated eggs." *Proc Soc Exp Biol Med* **76**(4): 662-5.

Ryden, L., and Edman, P. (1992). "Effect of ploymers and microspheres on the nasal absorption of insulin on rats." *Int J Pharm* **83**: 1-10.

S

Sababi, M., Borga, O. and Hultvist-Bengtsson, U. (2001). "The role of P-glycoprotein in limiting intestinal regional absorption of digoxin in rats." *Eur J Pharm Sci* **14**(1): 21-7.

Saettone, M., Monti, F. D. *et al.* (1994). "Mucoadhesive ophthalmic vehicles: evaluation of polymeric low-viscosity formulations." *J Ocul Pharmacol* **10**(1): 83-92.

Saitou, M., Furuse, M., Sasaki, H., Schulzke, J.D., Fromm, M., Takano, H., Noda, T. and Tsukita, S. (2000). "Complex phenotype of mice lacking occludin, a component of tight junction strands." *Mol Biol Cell* **11**(12).

Sakai, M., Imai, T., Ohtake, H., Azuma, H. and Otagiri, M. (1997). "Effects of absorption enhancers on the transport of model compounds in Caco-2 cell monolayers:

assessment by confocal laser scanning microscopy." *J Pharm Sci* **86**(7): 779-85.

Sandri, G., Rossi, S., Ferrari, F., Bonferoni, M. C., Zerrouk, N. and Caramella, C. (2004). "Mucoadhesive and penetration enhancement properties of three grades of hyaluronic acid using porcine buccal and vaginal tissue, Caco-2 cell lines, and rat jejunum." *J Pharm Pharmacol* **56**(9): 1083-90.

Scarpa, M., Behboo, R., Angriman, I., Termini, B., Barollo, M., Ruffolo, C., Polese, L., D'Inca, R., Sturniolo, G. C. and Amico, D. F. (2004). "The role of costimulatory molecules CD80 and CD86 and IFN-gamma in the pathogenesis of ulcerative colitis." *Dig Dis Sci* **49**(11-12): 1738-44.

Schaiquevich, P., Niselman, A. and Rubio, M. (2002). "Comparison of two compartmental models for describing ranitidine's plasmatic profiles." *Pharmacol Res* **45**(5): 399-405.

Schmitz, H., Barmeyer, C., Fromm, M., Runkel, N., Foss, H. D., Bentzel, C. J., Riecken, E. O. and Schlzke, J. D. (1999). "Altered tight junction structure contributes to the impaired epithelial barrier function in ulcerative colitis." *Gastroenterology* **116**(2): 301-9.

Schmitz, H., Fromm, M., Bentzel, C. J., Scholz, P., Detjen, K., Mankertz, J., Bode, H., Epple, H. J., Riecken, E. O. and Schulzke, J. D. (1999). "Tumor necrosis factor-alpha (TNF-α) regulates the epithelial barrier in the human intestinal cell line HT-29/B6." *J Cell Sci* **112** (1): 137-46.

Schottelius, A. J., Moldawer, L. L., Dinarello, C. A., Asadullah, K., Sterry, W. and Edwards, C. K. (2004). "Biology of tumor necrosis factor-alpha- implications for psoriasis." *Exp Dermatol* **13**(4): 193-222.

Scott, J. E. *et al.* (1999). "Hyaluronan forms specific stable teritary structures in aqueous solution: A ^{13}C NMR study." *Proc Natl Acad Sci USA* **96**: 4850-4855.

Seib, F. P. (2005). "Endocytosis and trafficking of polymer therapeutics in melanoma cells." *Thesis (PhD)*. Cardiff University.

Seymour, L. W., Ferry, D. R., Anderson, D., Hesslewood, S., Julyan, P. J., Poyner, R., Doran, J., Young, A. M., Burtles, S. and Kerr, D. J. (2002). "Hepatic drug targeting: phase 1 evaluation of polymer-bound doxorubicin." *J Clin Oncol* **20**(6): 1668-76.

Sgouras, D. and Duncan, R. (1990). "Methods for the evaluation of biocompatibility of soluble synthetic polymers which have potential for biomedical use. 1. Use of the tetrazolium-based colorimetric assay (MTT) as a preliminary screen for evaluation of in vitro cytotoicity." *J Mater Sci Mater Med:* 61-68.

Shaunak, S., Thornton, M., John, S., Teo, I., Peers, E., Mason, P., Krausz, T. and Davies, D. (1998). "Reduction of the viral load of HIV-1 after the intraperitoneal administration of dextrin 2- sulphate in patients with AIDS." *AIDS* **12**: 399-409.

Slater, E. C. and Tager, J. M. (1963). "Synthesis of Glutamate from Alpha-Oxoglutarate and Ammonia in Rat-Liver Mitochondria. V. Energetics and Mechanism." *Biochim Biophys Acta* 77: 276-300.

Smart, J. D., Kellaway, I. W. and Worthington, H. E. (1984). "An in-vitro investigation of mucosa-adhesive materials for use in controlled drug delivery." *J Pharm Pharmacol* **36**(5): 295-9.

Soderholm, J. D., Hedman, L., Artursson, P., Franzen, L., Larsson, J., Pantzar, N., Permert, J. and Olaison, G. (1998). "Integrity and metabolism of human ileal mucosa in vitro in the Ussing chamber." *Acta Physiol Scand* **162**(1): 47-56.

Son, E. H., Moon, E. Y., Rhee, D. K. and Pyo, S. (2001). "Stimulation of various functions in murine peritoneal macrophages by high mannuronic acid-containing alginate (HMA)." *Int Immunopharmacol* **1**: 147-154.

Song, J-Y., Han, S-K., Bae, K-G., Lim, D-S., Son, S-J., Jung, I-S., Yi, S-Y., and Yun, Y-S. (2003). "Radioprotective effects of ginsan, an immunomodulator." *Radiat Res* **159**: 768-774.

Sorimachi, K., Akimoto, K. *et al.* (1999). "Secretion of TNF-alpha, IL-8 and nitric oxide by macrophages activated with polyanions, and involvement of interferon-gamma in the regulation of cytokine secretion." *Cytokine* **11**(8): 571-8.

Stingele, F., Corthesy, B., Kusy, N., Porcelli, S. A., Kasper, D. L. and Tzianabos, A. O. (2004). "Zwitterionic polysaccharides stimulate T cells with no preferential V B usage and promote anergy, resulting in proctection against experimental abscess formation." *J Immunol* **172**: 1483-1490.

Sugi, K., Musch, M. W., Field, M. and Chang, E. B. (2001). "Inhibition of Na^+, K^+-ATPase by interferon gamma down-regulates intestinal epithelial transport and barrier function." *Gastroenterology* **120**(6): 1393-403.

Suzuki, M., Kobayashi, H., Kanayama, N., Nishida, T., Takigawa, M. and Tero, T. (2002). "CD44 stimulation by fragmented hyaluronic acid induces upregulation and tyrosine phosphorylation of c-Met receptor protein in human chondrosarcoma cells." *Biochim Biophys Acta* **1591**(1-3): 37-44.

T

Tajarobi, F., El-Sayed, M., Rege, B. D., Polli, J. E. Ghandehari, H. (2001). "Transport of poly amidoamine dendrimers across Madin-Darby canine kidney cells." *Int J Pharm* **215**(1-2): 263-7.

Takahashi, Y., Kondo, H., Yasuda, T., Watanabe, T., Kobayashi S. I. and Yokohama, S. (2002). "Common solubilizers to estimate the Caco-2 transport of poorly water-soluble drugs." *Int J Pharm* **246**: 85-94.

Takemoto, K. and Fabish, P. (1963). "Influence of acid polysaccharides on plaque formation by influenzae A2 and B viruses." *Proc Soc Exp Biol Med* **114**: 811-4.

Tang, X. and Pikal, M. J. (2004). "Design of freeze-drying processes for pharmaceuticals: practical advice." *Pharm Res* **21**(2): 191-200.

Termeer, C., Averbeck, M., Hara, H., Eibel, H., Herrlich, P., Sleeman, J. and Simon, J. C. (2003). "Targeting dendritic cells with CD44 monoclonal antibodies selectively inhibits the proliferation of naive CD4+ T-helper cells by induction of FAS-independent T-cell apoptosis." *Immunology* **109**(1): 32-40.

Tew, G. N., Liu, D., Chen, B., Doerksen, R. J., Kaplan, J., Carroll, P. J., Klein, M. L. and DeGrado, W. F. (2002). "De novo designs of biomimetic antimicrobial polymers." *Proc Natl Acad Sci USA* **99**: 5110-5114.

Thanou, M., Florea, B. I., Langemeyer, M. W., Verhoef, J. C. and Junginger, H. E. (2000). "N-trimethylated chitosan chloride (TMC) improves the intestinal permeation of the peptide drug buserelin in vitro (Caco-2 cells) and in vivo (rats)." *Pharm Res* **17**(1): 27-31.

Thomas, A., Harding, K. G. and Moore, K. (2000). "Alginates from wound dressings activate human macrophages to secrete tumour necrosis factor-α." *Biomaterials* **21**: 1797-1802.

Thoren, L. (1980). "The dextrans - clinical data." *Dev Biol Stand* **48**: 157-67.

Thornton, M., Barkley, L., Mason, J. C. and Shaunak, S. (1999). "Anti-Kaposi's Sarcoma and Antiangiogenic Activities of Sulfated Dextrins." *Antimicrobial Agents Chemother* **43**(10): 2528-2533.

Thorpe, R. (1998). "Interleukin-2." In Sluis-Mire, A. and Thorpe, R. (Eds.), *Cytokines*: 1-11. London, UK: Academic Press.

Tomalia, D. A., Baker, H., Dewald, M., Hall, G., Kallos, S., Martin, J., Roeck, J., Ryder, J. and Smith, P. (1985). "A new class of polymers-starburst dendritic macrmolecules." *Polym J* **17**: 117-32.

Tomalia, D. A. (1993). "Starburst™/cascade dendrimers: fundemental building blocks for a new nanoscopic chemistry set." *Aldrichim Acta* **26**: 91-101.

Tomalia, D. A. (1995). "Dendrimer maromolecules." *Sci Am* **272**: 62-6.

Tomlinson, R., Heller, J., Broccini, S. and Duncan, R. (2003). "Polyacetal-doxorubicin conjugates designed for pH-dependent degradation." *Bioconjug Chem* **14**(6): 1096-106.

Tortora, G. J., and Grabowski, S. R. (2003). "Small intestine." (10th Ed.), *Principles of Anatomy & Physiology:* 881-891. London, UK: John Wiley & Sons Inc.

Tracey, K. J., and Cerami, A. (1994). "Tumor necrosis factor: a pleiotropic cytokine and therapeutic target." *Annu Rev Med* **45**: 491-503.

Tracey, L., Spiteri, I., Ortiz, P., Lawler, M., Piris, M. A. and Villuendas, R. (2004). "Transcriptional response of T cells to IFN-alpha: changes induced in IFN-alpha-sensitive and resistant cutaneous T cell lymphoma." *J Interferon Cytokine Res* **24**(3): 185-95.

Tsutsumi, S., Tomisato, W., Takano, T., Rokutan, K., Tsuchiya, T. and Mizushima, T. (2002). "Gastric irritant-induced apoptosis in guinea pig gastric mucosal cells in primary culture." *Biochim Biophys Acta* **1589**(2): 168-80.

Tzianabos, A. O. (2000). "Polysaccharide immunomodulators as therapeutic agents: structural aspects and biologic fucntion." *Clin Microbiol Rev* **13**(4): 523-33.

U

Uhing, M. R. and Kimura, R. E. (1995). "The effect of surgical bowel manipulation and anesthesia on intestinal glucose absorption in rats." *J Clin Invest* **95**(6): 2790-8.

Ulevitch, R. J. (1993). "Recognition of bacterial endotoxins by receptor-dependent mechanisms." *Adv Immuol* **53**: 267-89.

Ungell, A. L., Nylander, S., Bergstrand, S., Sjoberg, A. and Lennernas, H. (1998). "Membrane transport of drugs in different regions of the intestinal tract of the rat." *J Pharm Sci* **87**(3): 360-6.

Ussing, H. H. and Zerahn, K. (1951). "Active transport of sodium as the source of electric current in the short-circuited isolated frog skin." *Acta Physiol Scand* **23**(2-3): 110-27.

Utech, M., A. Ivanov, I., Samarin, S. N., Bruewer, M., Turner, R. J., Mrsny, R. J., Parkos, C. A. and Nusrat, A. (2005). "Mechanism of IFN-gamma-induced endocytosis of tight junction proteins: myosin II-dependent vacuolarization of the apical plasma membrane." *Mol Biol Cell* **16**(10): 5040-52.

V

Van Der Bijl, P., Van Eyk, A. D. and Thompson, I. O. C. (1998). "Penetration of human vaginal and buccal mucosa by 4.4-kd and 12-kd fluorescein-isothiocyanate-labeled dextrans." *Oral Surg Oral Med Pathol Oral Radiol Endod* **85**: 686-91.

VanDeventer (1997). "Tumour necrosis factor and Crohn's disease." *Gut* **40**: 443-48.

Vasey, P. A., Kaye, S. B. *et al.* (1999). "Phase I clinical and pharmacokinetic study of PK1 [N-(2-hydroxypropyl)methacrylamide copolymer doxorubicin]: first member of a new class of chemotherapeutic agents-drug-polymer conjugates. Cancer Research Campaign Phase I/II Committee." *Clin Cancer Res* **5**(1): 83-94.

Veronese, F. M., Schiavon, O. *et al.* (2005). "PEG-doxorubicin conjugates: influence of polymer structure on drug release, in vitro cytotoxicity, biodistribution, and antitumor activity." *Bioconjug Chem* **16**(4): 775-84.

Vicent, M. J., Manzanaro, S., De la Fuente, J. A. and Duncan, R. (2004). "HPMA copolymer-1,5-diazaanthraquinone conjugates as novel anticancer therapeutics." *J Drug Target* **12**(8): 503-15.

W

Wagner, E., Zenke, M., Cotten, M., Beug, H., and Birnstiel, M, L. (1990). "Transferrin-polycation conjugates as carriers for DNA uptake into cells." *Proc Natl Acad Sci USA* **87**: 341-3414.

Wagner, E. (2006). "Gene delivery using polymer therapeutics." *Adv. Polym. Sci.* **192**: 135-173.

Walsh, S. V., Hopkins, A. M. and Nusrat, A. (2000). "Modulation of tight junction structure and function by cytokines." *Adv Drug Deliv Rev* **41**: 303-13.

Wan, K-W., Malgesini, B., Verpillio, I., Ferruti, P., Griffiths, P., Paul, A., Hann, A. C. and Duncan, R. (2004). "Poly(amidoamine) salt form: effect on pH-dependent membrane activity and polymer conformation in solution." *Biomacromolecules*

5(3): 1102-9.

Wang, F., Graham, W. V., Wang, Y., Witkowski, E. D., Schwarz, B. T. and Turner, J. R. (2005). "IFN-γ and TNF-α synergize to induce intestinal epithelial barrier dysfunction by up-regulating myosin light chain kinase expression." *Am J Pathol* **166**(2): 409-19.

Wang, M. J., Kuo, J. S., Lee, W. W., Haung, H. Y., Chen, W. F. and Lin, S. Z. (2006). "Translational event mediates differential production of TNF-α in hyaluronan-stimulated microglia and macrophages." *J Neurochem* **97**(3): 857-71.

Watanabe, E., Kinoshita, M., Takahashi, M. and Hayashi, M. (2004). "A possibility to predict the absobability of poorly water0soluble drugs in humans based on rat intestinal permeability assed by an in vitro chamber method." *Eu J Pharm Sci* **58**: 659-665.

Watanabe, E., Kinoshita, M., Takahashi, M. and Hayashi, M. (2005). "Prediction of absorbility of poorly water-soluble drugs based on permeability obtained through modified in vitro chamber method." *Drug Metab Pharmacokinet* **20**(6): 428-34.

Whicher, J. and Ingham, E. (1990). "Cytokine measurements in body fluids." *Eur Cytokine Netw* **1**(4): 239-43.

Whiteside, T. L. (2002). "Cytokine assays." *Biotechniques* Suppl: 4-8, 10, 12-5.

Wikman-Larhed, A. and Artursson, P. (1995). "Co-cultures of human intestinal Goblet (HT29H) and absorptive (Caco-2) cells for studies and peptide absorption." *Eur. J. Pharm Sci* **3**: 171-193.

Wild, J. S., Hyde, D. M. and Giri, S. N. (1994). "Dose and regimen effects of poly ICLC, an interferon inducer, in a multi-dose bleomycin model of interstitial pulmonary fibrosis." *Pharmacol Toxicol* **75**(1): 42-8.

Williams, K. E., Kidston, E. M., Beck, F. and Lloyd, J. B. (1975). "Quantitative studies of pinocytosis. II. Kinetics of protein uptake and digestion by rat yolk sac cultured in vitro." *J Cell Biol* **64**(1): 123-34.

Wilson, L. M. and Baldwin, A. L. (1998). "Effects of environmental stress on the architecture and permeability of the rat mesenteric microvasculature." *Microcirculation* **5**(4): 299-308.

Wilson, L. M. and Baldwin, A. L. (1999). "Environmental stress causes mast cell degranulation, endothelial and epithelial changes, and edema in the rat intestinal mucosa." *Microcirculation* **6**(3): 189-98.

Wilson, T. H. and Wiseman, G. (1954). "The use of sacs of everted small intestine for the study of the transference of substances from the mucosal to the serosal surface." *J Physiol* **123**(1): 116-25.

Wittchen, E. S., Haskins, J. and Stevenson, B. R. (1999). "Protein interactions at the tight junction. Actin has multiple binding partners, and ZO-1 forms independent complexes with ZO-2 and ZO-3." *J Biol Chem* **274**(49): 35179-85.

Wiwattanapatapee, R., Carreno-Gomez, B., Malik, N. and Duncan, R. (2000). "Anionic

PAMAM dendrimers rapidly cross adult rat intestine in vitro: a potential oral delivery system?" *Pharmaceutical Research* **17**(8): 991-997.

Wright, S. D., Ramos, R. A., Tobias, P. S., Ulevitch, R. J. and Mathison, J. C. (1990). "CD14 a receptor for complexes of lipopolysaccharides (LPS) and LPS binding protein." *Science* **249**: 1431-3.

Wu-Pong, S., Livesay, V., Dvorchick, B. and Barr, W. H. (1999). "Oligonucleotide transport in rat and human intestine ussing chamber models." *Biopharm Drug Dispos* **20**(9): 411-6.

X

Xiao, W., Hodge, D. R., Wang, L., Yang, X., Zhang, X. and Farrar, W. L. (2004). "NF-kappaB activates IL-6 expression through cooperation with c-Jun and IL6-AP1 site, but is independent of its IL6-NFkappaB regulatory site in autocrine human multiple myeloma cells." *Cancer Biol Ther* **3**(10): 1007-17.

Xyloyiannis, M. (2004). "Poly(ethylene glycol) (PEG)-poly(ester) dendritic hybrids: biocompatibility and effect of architecture on cellular pharmacokinetics." *Thesis (PhD)*. Cardiff University.

Y

Yamamoto, T., Umegae, T., Kitagawa, T. and Matsumoto, K. (2004). "Mucosal cytokine production during remission after resection for Crohn's disease and its relationship to future relapse." *Aliment Pharmacol Therapy* **19**: 671-78.

Yang, H., Soderholm, J., Larsson, J., Permert, J., Olaison, G., Lindgren, J. and Wiren, M. (1999). "Glutamine effects on permeability and ATP content of jejunal mucosa in starved rats." *Clin Nutr* **18**(5): 301-306.

Yasin, B., Pang, M., Lehrer, R. I. and Wagar, E. A. (2003). "Activity of Novispirin G-10, a noval antimicrobial peptide against Chlamydia trachomatis and vaginosis-associated bacteria." *Exp Mol Pathol* **74**: 1-6.

Yelda, S., Solie, A., Immo, R. and Erika, I. (1997). "IFN-γ enhances macromolecular transport across Peyer's patches in suckling rats: implications for natural immune responses to dietary antigens early in life." *J P G N* **24**(2): 162-9.

Youakim, A. and Ahdieh, M. (1999). "Interferon-gamma decreases barrier function in T84 cells by reducing ZO-1 levels and disrupting apical actin." *Am J Physiol* **276**(5 Pt 1): G1279-88.

Z

Zawadzki, V., Perschl, A., Rosel, M., Hekele, A. and Zoller, M. (1998). "Blockade of metastasis formation by CD44-receptor globulin." *Int J Cancer* **75**(6): 919-24.

Zhang, Q. Y., Wikoff, J., Dunbar, D., Fasco, M. and Kaminsky, L. (1997). "Regulation of cytochrome P4501A1 expression in rat small intestine." *Drug Metab Dispos* **25**(1): 21-6.

Zhang, Q., Choo, S., Everard, J., Jennings, R. and Finn, A. (2000). "Mucosal immune responses to meningococcal group C conjugate and group A and C polysaccharide vaccines in adolescents." *Infect Immun* **68**(5): 2692-7.

Zhou, X., Schmidtke, P., Zepp, F., and Meyer, C. U. (2005). "Boosting interlukin-10 production: therapeutic effects and mechanisms." *Curr Drug Targets Immune Endocar Metabol Disord* **5**(4): 465-75.

Zweibaum, A., Hauri, H. P., Sterchi, E., Chantret, I., Haffen, K., Bamat, J., and Sordat, B. (1984). "Immunohistological evidence, obtained with monoclonal antibodies, of small intestinal brush border hydrolases in human colon cancers and foetal colons." *Int J Cancer.* **34**(5): 591-8.

Zweibaum, A., Triadou, N., Kedinger, M., Augeron, C., Robine-Leon, S., Pinto, M., Rousset, M., and Haffe, K. (1983). "Sucrase-isomaltase: a marker of foetal and malignant epithelial cells of the human colon." *Int J Cancer.* **32**(4): 407-12.

Zwerina, J., Hayer, S., Tohidast-Akrad, M., Bergmeister, H., Redlich, K., Feige, U., Dunstan, C., Kollias, G., Steiner, G., Smolen, J. and Schett, G. (2004). "Single and combined inhibition of tumor necrosis factor, interleukin-1, and RANKL pathways in tumor necrosis factor-induced arthritis: effects on synovial inflammation, bone erosion, and cartilage destruction." *Arthritis Rheum* **50**(1): 277-9.

APPENDIX

PUBLICATIONS

Abstracts presented as posters

Phelps, K. D. and Duncan, R. (2004). "Investigating the use of biologically active polymers as a means of transiently permeabilising the intestinal barrier." In *Welsh School of Pharmacy Postgraduate Research Day.* **18**. Cardiff University, UK.

Phelps, K. D. and Duncan, R. (2004). "Identification of biologically active polymers as a eans to enhance drug delivery across epithelial barriers." In *J Pharm Pharmacol.* **57**(supplement 18): s-22.

See attached publication

Abstracts presented orally

Phelps, K. D. and Duncan, R (2005). "Evaluation of cytokines and polymers as a means to enhance drug delivery across epithelial barriers." In *Welsh School of Pharmacy Postgraduate Research Day.* **19**. Cardiff University, UK.

Investigating the use of Biologically Active Polymers as a Means of Transiently Permeabilising the Intestinal Barrier

K. Phelps and R. Duncan

Centre for Polymer Therapeutics, Welsh School of Pharmacy, Cardiff University, King Edward VII Avenue, Cardiff CF10 3XF, UK.

E-mail: Phelpskd@cf.ac.uk

Numerous linear, water-soluble polymers (particularly polyanions) are biologically active and can induce cytokines, such as tumour necrosis factor-alpha (TNF-α), interferon-gamma (IFN-γ) and interleukin-2 (IL-2), from cells depending on their molecular weight (MW), composition or salt form. The proinflammatory cytokines TNF-α and IFN-γ are able to permeabilise epithelial barriers by affecting the protein composition of the tight junction (Walsh et al., 2000). The aim of this work is to identify polymers that will promote enhanced drug delivery due to their inherent ability to stimulate TNF-α IFN-γ and IL-2 release, and therefore transiently permeabilise epithelial barriers. Several linear polyanions already used as excipients, including alginic acid, hyaluronic acid, sodium hyaluronate and polyacrylic acid (MW 30 kDa, 100 kDa, or 450 kDa), were chosen as the first library to investigate. Branched polymers, including polyamidoamine (PAMAM) generation 3.5 and the polycation polyethylenimine, PEI (MW 750 kDa), were also studied.

Finally, isolated rat intestine (the half cell model) was used to investigate the ability of polymers or cytokines to modulate the transport of the paracellular marker, FITC-dextran (MW 4 kDa). Initially, polymer cytotoxicity was investigated in B16F10 murine melanoma and ECV304 human endothelial-like cells using the MTT assay (Mosmann, 1983) after 1 h or 72 h incubation times. Nontoxic concentrations of polymers (0.1–100 mg/mL) were then added to DU937 human macrophage-like cells for 24 h, or to B16F10 (0.1 and 1mg/mL), or to 246.7 (1 mg/mL) murine raw monocyte/macrophage cells, for 1 h, to test their ability to induce TNF-α, IFN-γ and IL-2 release. Cytokine release was assayed using human and murine sandwich-ELISA assays. Effects of IFN-γ, TNF-α, IL-2 or polymers on apical to basal or basal to apical FITC-dextran transport, across rat jejunal tissue (with or without Peyer's patches), was measured with the vertical diffusion system (Grass & Sweetana, 1988) over 1 h. Viability of the tissue was assessed during these experiments by measuring lactate dehydrogenase (LDH) release. Polyanions showed little cytotoxicity towards B16F10 cells and ECV304 cells at 72 h except polyacrylic acid of MW 100 kDa in both cell lines, and 450 kDa in B16F10. PEI was cytotoxic even at low concentrations. Decreasing the incubation time to 1 h reduced polymer cytotoxicity (IC_{50} > 1 mg/mL) with the exception of PEI (IC_{50} 0.04 mg/mL). Highest amounts of TNF-α IL-2 and IFN-γ release from B16F10 and 246.7 cells were seen with PEI (1 mg/mL). Sodium hyaluronate induced TNF-α release (1675–2500 pg/mL) from DU937 cells in a concentration-dependent manner. In transport studies, FITC-dextran transfer was greatest in the apical to basal direction, and in the absence of Peyer's patches. Apically applied TNF-α (30, 45, 60 pg/mL) tended to enhance FITC-dextran transport in a concentration-dependent manner. The polyacrylic acids (MW 100 kDa and 450 kDa) and alginates (1mg/mL) showed no increase in apical to basal FITC-dextran transport across non-Peyer's patch tissue. Polyacrylic acid sodium salt (MW 30 kDa), appeared to induce an increase in transport.

K. Phelps would like to thank the BBSRC for funding this studentship.

Grass, G. M. and Sweetana, S. A. (1988) Pharm. Res. 5: 372–376
Mosmann, T. (1983) J. Immunol. Methods 65: 55–63
Walsh, S. V. et al. (2000) Adv. Drug Del. Rev. 41: 303–113